The design of a rectal cryoprobe.

Orpwood, R. D.

Award date:
1984

Awarding institution:
University of Bath

THE DESIGN OF A RECTAL CRYOPROBE

Submitted By

R.D. ORPWOOD

for the degree of PhD of the University of Bath

1984

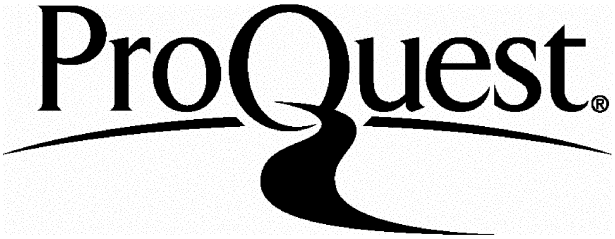

THE DESIGN OF A RSCTAL CRYOPROBE

Submitted BY

R.D. ORPWOOD

for the degree of PhD of the University of Bath

1984

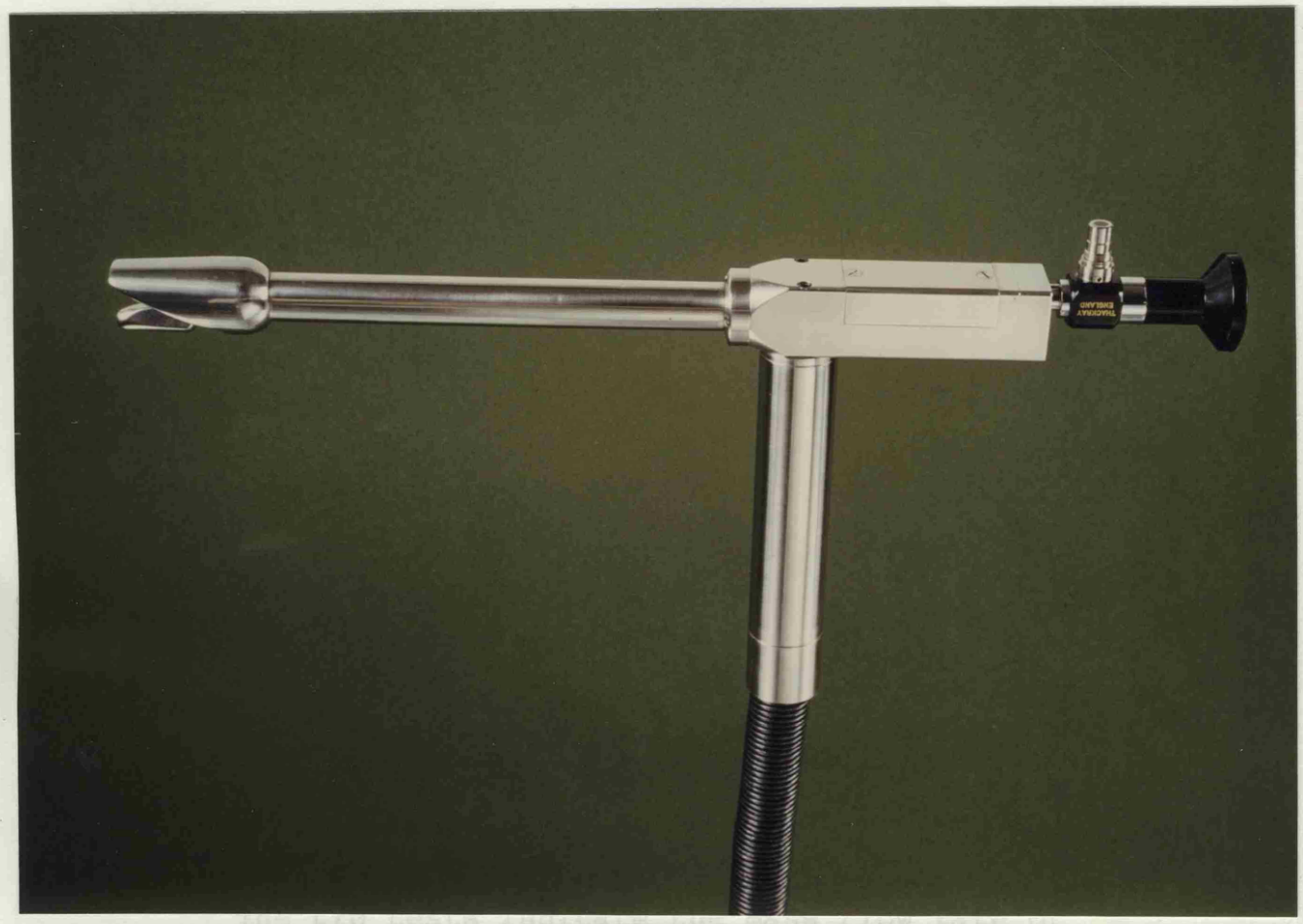

THE RECTAL CRYOPROBE

SUMMARY

This thesis describes the design and development of an instrument to destroy rectal tumours by freezing them. The work described progresses systematically from the surgical performance requirements to a complete system for operating theatre use.

A thermodynamic specification for the freezing tip is derived by using mathematical models of ice-ball growth to relate the performance of the tip to the thermal environment around it. The tip is cooled by boiling liquid nitrogen within it and a test rig is built to measure the heat flux to the tip, and allow the influence of tip variables to be explored. The final tip design incorporates a thin layer of plastic in the wall to encourage nucleate boiling. This tip design meets the specification and is also analysed using finite difference equations to describe the transient heat transfer through the tip wall.

The tip tests indicate the mass flow rate of nitrogen needed and a system to transfer the cryogen at this rate from a storage dewar is described. The liquid nitrogen is kept in film boiling (Leidenfrost) flow as this has many advantages for cryoprobe performance. The Leidenfrost flow is maintained by providing a controlled heating of the transfer pipes.

A viewer is incorporated in the probe to enable monitoring within the rectum. The viewer forms the interface between the device and the patient and an

evolutionary design technique is used. The final viewer design uses gas inflation to expand the rectum.

A supporting unit is also designed so that the whole instrument is self-contained to enable safe and effective clinical evaluation.

ACKNOWLEDGEMENTS

No piece of work is ever completed successfully by one person in isolation and I would like to express my appreciation of the many people who have helped towards the success of this project and in the production of the thesis. May I first of all thank Dr. Hylton Hardisty for his supervision and the hard work he has put in on my behalf, and also to Professor Stephen Lillicrap for his constant support and encouragement. Much of this project required careful clinical assessment and I would like to thank Mr. Ken Lloyd-Williams and his colleagues at the Royal United Hospital, Bath, for providing this support so willingly and enthusiastically.

There are always many people who provide essential support to R and D projects but who rarely receive much recognition for their assistance. In the case of this project I would particularly like to thank Mr. Simon Adams for his cheerful technical assistance and to Mr. Pete Box for his skill in turning my poor drawings into components that are always masterpieces, no matter how tightly toleranced. I would also like to thank Mr. Brian Auty and Mr. Mike Perkins for designing and developing the electronics. Thanks must also go to Mrs. Ruth Hooper for her dedication in typing the manuscript in a very limited timescale. Finally, I must give my sincere thanks and apologies to my wife, Ann, and my children for putting up with only having half a dad and husband around the house for such a long time.

Behind all work lies an aim and motivation. This acknowledgement would not be complete without a mention of my appreciation for all the many people who, in very different ways, have shown me the value and importance of positively applying technology to the benefit of society.

NOTATION

Symbols

A	Area (m^2)
BEH_n	Behaviour of design achieved at nth evolution
BEH_r	Required behaviour
c	Specific heat (J/kg. °C)
c_b	Specific heat of blood (J/kg.°C)
C_D	Drag coefficient
d	Diameter (m)
d_D	Drop diameter (m)
DES_n	Design achieved at nth evolution
E	Effective emissivity
g	Acceleration due to gravity (m/s^2)
h	Heat transfer coefficient ($W/m^2.°C$)
h_e	Specific enthalpy (J/kg)
i	Number of space intervals in finite difference equations
I	Electrical current (amp .)
k	Thermal conductivity (W/m.°C)
k_f	Thermal conductivity in frozen phase (W/m.°C)
l	Length (m)
l_T	Length of tip (m)
L	Latent heat of fusion (J/kg)
L_V	Latent heat of evaporation (J/kg)
$\dot{m}$	Mass flow rate (kg/s)
$\dot{m}_b$	Mass flow rate of blood (kg/s)

Symbols

n	Number of time intervals in finite difference equations
q'_b	Heat generation rate due to blood flow (W/m^3)
q'_m	Heat generation rate due to metabolism (W/m^3)
$\dot{q}$	Heat transfer per unit area (W/m^2)
$\dot{Q}$	Rate of heat transfer (W)
$\dot{Q}_E$	Heat dissipated by electrical heater (W)
$\dot{Q}_N$	Heat transferred to liquid nitrogen (W)
$\dot{Q}_S$	Heat transferred to environment around test rig (W)
r	Radius (m)
r_o	Radius of ice-ball (m)
r_t	Radius of probe tip (m)
r_{-15}	Radius of -15°C isotherm (m)
t	Time (sec)
T	Temperature (°C)
T_A	Air temperature (°C)
T_b	Systemic blood temperature (°C)
T_f	Temperature in ice-ball (°C)
T_o	Phase change temperature (°C)
T_N	Temperature of liquid nitrogen (°C)
T_S	Temperature of environment around test rig (°C)
T_{SH}	Temperature of probe shaft (°C)
T_t	Tip temperature (°C)
T_∞	Temperature of tissue far from probe (°C)
Δt	Time interval in finite difference equations (sec)

Symbols

ΔT	Temperature difference (°C)
ΔT_{SAT}	Temperature difference between wall and saturation temperature of nitrogen (°C)
u	Specific velocity (m/s)
U	Velocity (m/s)
U_D	Droplet velocity (m/s)
U_v	Vapour velocity (m/s)
U_{HT}	Overall heat transfer coefficient ($W/m^2.°C$)
V	Electrical potential (volts)
w	Tip wall thickness (m)
$\dot{W}$	Rate of work (W)
Δx	Space interval in finite difference equations (m)
z	Vertical co-ordinates (m)

Greek Symbols

α	Thermal diffusivity (m^2/s)
ρ	Density (kg/m^3)
σ	Stefans constant (5.669×10^{-8} W/m. $°K^4$)
ϕ	Pipe inclination (degrees)

Non-dimensional Groups

Bi	Biot number
Fo	Fourier number
Gr_d	Grashof number based on diameter
Nu_d	Nusselt number based on diameter
Pr_d	Prandtl number based on diameter
Ra	Rayleigh number

CONTENTS

SUMMARY		1
ACKNOWLEDGEMENTS		3
NOTATION		5
CHAPTER 1 - INTRODUCTION		21
1.1	Scope of Project	21
1.2	The Clinical Problem	21
1.3	Surgical Requirements	22
1.4	Design Problems	23
1.5	Design Approach	24
1.5.1	Performance aspects: the cryoprobe cooling system	24
1.5.2	Operational aspects: the patient/instrument interface	25
1.6	Structure of Thesis	26
1.7	Role of Experimental Investigations in the Cryoprobe Design	28
CHAPTER 2 - THE BIOPHYSICS OF CRYOSURGERY		29
2.1	Introduction	29
2.2	Mechanisms of Cell Death	29
2.2.1	The two main causes of cell destruction	29
2.2.2	Extra-cellular ice formation	30
2.2.3	Intra-cellular ice formation	30
2.2.4	The effect of cooling rate on cell	31

destruction
2.2.5 Effect of thawing rate on cell destruction 31
2.2.6 Extent of cell destruction 33
2.2.7 Predicted pattern of cell damage around a cryoprobe 33
2.2.8 Measured cell destruction in tissues 35
2.2.9 Conclusions about cell destruction 37
2.3 Models of Ice-ball Growth in Tissues 37
2.3.1 The need to model ice-ball growth 37
2.3.2 Basis of ice-ball model 38
2.3.3 Steady-state models of ice-ball 39
2.3.4 Temperature-time models of ice-ball growth 39
2.3.5 Numerical models of ice-ball growth 42
2.3.6 Relating ice-ball models to cell destruction 42
2.4 Conclusions 43

CHAPTER 3 - DERIVATION OF A PERFORMANCE SPECIFICATION 45
3.1 Introduction 45
3.2 Model used to Study Ice-ball Growth 45
3.2.1 Basis of model 45
3.2.2 Assumptions made 46
3.2.3 Starting point of analysis 47
3.2.4 Use of radial co-ordinates 47
3.2.5 Solution of equations 2 and 3 48
3.3 Study of Rate of Growth of Ice-ball 49
3.3.1 Application of model and results 49
3.3.2 Conclusions about ice-ball growth 50
3.4 Cell Cooling Rate Produced by Cryoprobe 55

3.4.1 Reason for study 55
3.4.2 Derivation of equation for temperature gradient 55
3.4.3 Results obtained for temperature gradient during freezing 58
3.5 Temperature Distribution Within Ice-ball 60
3.5.1 Basis of investigation 60
3.5.2 Results of temperature distribution 60
3.5.3 Position of -15°C isotherm 62
3.6 Heat Flux Through Cryoprobe 62
3.6.1 Analysis of cryoprobe heat flux 62
3.6.2 Results for cryoprobe heat flux 64
3.7 Conclusions About Cryoprobe Design From Analyses 66
3.7.1 The number of cooling tips 66
3.7.2 Cryoprobe specification 67
3.8 Experimental Measurements of Ice-ball Growth 68
3.8.1 Reasons for taking measurements 68
3.8.2 Apparatus 68
3.8.3 Method 72
3.8.4 Results 74
3.9 Conclusions 74

CHAPTER 4 - CHOICE OF COOLING SYSTEM 79
4.1 Introduction 79
4.2 History of Surgical Freezing Techniques 79
4.3 Current Techniques of Cooling 80
4.3.1 Joule-Thomson cryoprobes 80
4.3.2 Liquid nitrogen cryoprobes 82
4.4 The System Design of Joule-Thomson Cryoprobes 83

4.4.1 Transport of working fluid to freezing tip 83
4.4.2 Expansion of working fluid 85
4.4.3 Transport of working fluid away from tip 85
4.4.4 Problem of supply cylinder cooling 86
4.5 The System Design of Liquid Nitrogen Cryoprobes 88
4.5.1 Storage of cryogen 88
4.5.2 Transport of working fluid to tip 88
4.5.3 Cryoprobe thermal insulation 90
4.5.4 Flexible transfer hose 90
4.6 Comparison Between Liquid Nitrogen and Joule-Thomson Cryoprobes 91
4.6.1 Differences of tip temperature 91
4.6.2 Differences of tip heat flux 91
4.6.3 Differences of system design 94
4.6.4 Conclusions on comparisons 94
4.7 Alternative Cooling Techniques 96
4.7.1 Nitrogen probes using a Joule-Thomson expansion 96
4.7.2 Self-contained liquid nitrogen probes 97
4.7.3 Miscellaneous cryoprobes 97
4.8 Choice of System for Rectal Cryoprobes 98
4.9 Conclusions 99

CHAPTER 5 - THE BOILING BEHAVIOUR OF NITROGEN IN THE CRYOPROBE TIP 100
5.1 Introduction 100
5.2 Liquid Nitrogen Boiling Behaviour 100
5.2.1 Known pool boiling behaviour 100
5.2.2 Leidenfrost boiling 103

5.2.3 Wall temperatures that occur when cooling an object from room temperature 103

5.3 Experimental Measurement of Heat Flux in Cryoprobe Tips 106

5.3.1 Reasons for measurement 106

5.3.2 General approach used to measure heat transfer 106

5.3.3 Test rig design 107

5.3.4 Thermal analysis of test rig 107

5.3.5 Derivation of liquid nitrogen temperature in the tip 111

5.3.6 Measurements taken in tests 115

5.3.7 Test procedure 117

5.4 Results Obtained 119

5.4.1 Typical data obtained 119

5.5 Conclusions 122

CHAPTER 6 - EXPERIMENTAL INVESTIGATION OF TIP DESIGN 123

6.1 Introduction 123

6.2 Required Heat Flux 123

6.2.1 Sources of heat 123

6.2.2 Sensible and latent heat from ice-ball 125

6.2.3 Heat conducted from probe shaft 125

6.2.4 Heat transferred from surrounding tissue 126

6.2.5 Total heat flux through tip 128

6.3 Tests Used to Measure Tip Heat Flux 128

6.3.1 Aim of experimental investigations 128

6.3.2 Test procedure 128

6.4 Results of Heat Flux Measurements 129
6.4.1 Effect of nitrogen mass flow rate 129
6.4.2 Effect of input pipe position 131
6.4.3 Effect of input pipe design 134
6.4.4 Effect of tip internal configuration 134
6.5 The Boiling Curve and Tissue Cooling 139
6.5.1 Tip equilibrium temperature 139
6.5.2 The importance of tip equilibrium temperature 141
6.6 Techniques of Encouraging Nucleate Boiling in the Tip 141
6.6.1 Breaking through the film barrier 141
6.6.2 Generating a steep thermal gradient in the tip wall 143
6.7 Investigations of Plastic Tip Performance 144
6.7.1 The existence of an optimum wall thickness 144
6.7.2 Empirical investigation of optimum tip wall thickness 147
6.7.3 Effect of plastic tip on equilibrium temperature 150
6.8 Final Tip Design 150
6.9 Conclusions 153

CHAPTER 7 - ANALYSIS OF TIP HEAT TRANSFER USING FINITE DIFFERENCE TECHNIQUES 156
7.1 Introduction 156
7.2 Major Assumptions 157
7.2.1 Pool boiling heat transfer coefficients 157
7.2.2 One-dimensional heat transfer 158

7.3 Structure of Finite Difference Models 158
7.3.1 Basis of models 158
7.3.2 The finite difference equations used 158
7.3.3 Stability criteria 161
7.4 Computer Program Used to Calculate Temperature Distribution 162
7.4.1 Basic structure of program 162
7.4.2 Accommodating the cooled boundary heat transfer coefficient 162
7.4.3 Speed of computing 162
7.5 Pool Boiling Heat Transfer Coefficients 164
7.5.1 Access to heat transfer coefficients in the program 164
7.5.2 Division of the boiling curve into regions 164
7.5.3 Equations derived from boiling curve 166
7.6 Effect of Material on Cooled Surface Temperature 167
7.6.1 Description of case being modelled 167
7.6.2 Results for boundary temperature 168
7.7 Behaviour of an Infinite Sheet Cooled on Both Sides 168
7.7.1 Description of case being modelled 168
7.7.2 Results 171
7.8 Cooling Both Sides of a Sheet of Good Conductor Lined with a Layer of Poor Conductor 171
7.8.1 Outline of case being modelled 171
7.8.2 Results 174
7.9 Conclusions 177

CHAPTER 8 - THE LIQUID NITROGEN TRANSFER SYSTEM 179

8.1 Introduction 179

8.2 Overall Transfer System Design 179

8.2.1 Choice of system for the rectal probe 179

8.2.2 The need for thermal insulation around the transfer pipes 181

8.2.3 Major problems of transfer system design 181

8.3 The Operating Temperature of the Transfer System 182

8.3.1 The effect of pipe temperature on flow boiling behaviour 182

8.3.2 Choice of operating temperature for the transfer pipes 183

8.4 Advantages of Using Leidenfrost Flow 184

8.4.1 Overcoming the problem of transfer pipe insulation 184

8.4.2 Overcoming the problem of flexible transfer hose design 185

8.5 Disadvantages of Using Leidenfrost Flow 186

8.6 Conclusions 186

CHAPTER 9 - MAINTAINING LEIDENFROST FLOW IN THE TRANSFER SYSTEM 188

9.1 Introduction 188

9.2 The Effect of Pipe Internal Geometry on Leidenfrost Flow 188

9.3 The Effect of Pipe Inclination on Leidenfrost Flow 189

9.4 Acceleration of Flow Along Pipe 193

9.5 Energy Requirements to Maintain Leidenfrost Flow 195

9.6 Techniques Used to Develop Heating Systems 198

9.6.1 The two separate heating systems needed 198
9.6.2 Methods used to monitor boiling behaviour 199
9.6.3 Methods used to monitor liquid fraction 199
9.7 The Transfer Hose Heating System 201
9.7.1 The effect of pipe wall thickness 201
9.7.2 Warm vapour heating of flexible hose 202
9.7.3 Electrical heating of flexible hose 204
9.8 The Probe Shaft Heating System 207
9.8.1 Procedure used to develop the probe heater 207
9.8.2 The feed pipe used as a heating element 210
9.8.3 Feed pipe immersed in a heated liquid 210
9.8.4 Feed pipe heated by exhaust vapour 210
9.9 Conclusions 212

CHAPTER 10 - REVIEW OF CRYOSURGICAL MONITORING 214
10.1 Introduction 214
10.2 Indirect Visual Monitoring Using Endoscopes 214
10.3 Thermocouples 215
10.4 Tissue Impedance Measurements 216
10.5 Electrical Current Measurements 217
10.6 Heat Flux Measurements 218
10.7 Liquid Crystals 219
10.8 Thermography 219
10.9 Ultrasound 220
10.10 Standardised Cryosurgical Procedures 220
10.11 Choice of Technique for Monitoring Rectal Cryosurgery 221
10.12 Conclusions 221

CHAPTER 11 - AN EVOLUTIONARY DESIGN TECHNIQUE 223

11.1 Introduction 223

11.2 Outline of Standard Design Technique 223

11.2.1 Problem definition 223

11.2.2 Design specification 225

11.2.3 Creation of ideas for possible solutions 225

11.2.4 Construction and development of prototype 226

11.2.5 Factors influencing the effectiveness of the prototype 226

11.3 The Effect of Applying Standard Design Procedures to Devices with a Human Interface 227

11.3.1 The problem of compiling a complete specification 227

11.3.2 The effect of designing for a human interface on the basis of a specification 228

11.3.3 A typical result of using standard design procedures 229

11.4 The Evolutionary Design Technique 230

11.4.1 Aims of technique 230

11.4.2 Initial stages of design 230

11.4.3 Define the human interface 230

11.4.4 The first rough prototype 232

11.4.5 Trial of prototype 233

11.4.6 The evolutionary cycle 233

11.4.7 Combine the patient interface aspects of the design with the supporting features 234

11.5 The Number of Evolutionary Cycles 234

11.5.1 The iteration followed in the 234

evolutionary cycle

11.5.2 The number of cycles needed 235

11.6 Conclusions 235

CHAPTER 12 - DESIGN OF THE RECTAL VIEWER 236

12.1 Introduction 236

12.2 Operating Requirements for Rectal Viewer 236

12.3 The Telescope Used for the Rectal Viewer 237

12.4 Study of Rectal Expansion 239

12.4.1 Reasons for study 239

12.4.2 Technique used to assess degree of expansion needed 239

12.4.3 Results of expansion study 241

12.5 Application of Evolutionary Design Technique to Rectal Viewer 241

12.5.1 Human interface identification 241

12.5.2 Isolation of the human interface 242

12.5.3 Problem of applying the evolutionary technique to the rectal cryoprobe 242

12.6 Technique of Rectal Expansion 244

12.7 Viewer Designs that Attempted to Isolate a Rectal Cavity 245

12.7.1 Viewer using clear tube in cavity 245

12.7.2 Viewer with integral balloon 247

12.7.3 Viewer using Foley catheter 249

12.7.4 Device with fixed seals 252

12.8 Viewer Designs that Did Not Confine Gas 252

12.8.1 Rationale behind alternative approach 252

12.8.2 Initial designs that allowed gas escape 254

12.8.3 Final viewer design 254
12.9 Design of Anal Introducer for Viewer 257
12.10 Conclusions 257

CHAPTER 13 - COMPLETE SYSTEM DESIGN 262
13.1 Introduction 262
13.2 Integrated Cryoprobe Design 264
13.2.1 Internal arrangement of components 264
13.2.2 Rectal inflation system within cryoprobe 267
13.2.3 Materials used in the cryoprobe 269
13.3 Complete Transfer Hose Design 269
13.3.1 The structure of the transfer hose 269
13.3.2 Problems caused by third hose 269
13.3.3 Transfer hose connection to the supply unit 272
13.4 Specification of the Support Unit 272
13.5 Overall Design of the Unit Structure 275
13.6 The Liquid Nitrogen Supply System 275
13.6.1 Technique used to pump nitrogen 275
13.6.2 Improving the heat transfer from the heater 279
13.6.3 Problem of pressure switch control margin 280
13.7 Liquid Nitrogen Delivery System 282
13.7.1 Delivery system design 282
13.7.2 Remote actuation of on/off valve 286
13.7.3 Liquid fraction enhancing device 286
13.8 The Defrost System 287
13.9 The Rectal Inflation System 291

13.9.1 Basic design of inflation system 291

13.9.2 Measurement of intra-rectal pressure 291

13.10 The Viewer Light Source 292

13.11 Temperature Controllers 294

13.12 Tip Temperature Display 295

13.13 Safety Considerations in the Design 295

13.13.1 Electrical safety 295

13.13.2 Mechanical safety 296

13.14 Performance of Complete System 296

13.15 Conclusions 297

CHAPTER 14 - CONCLUSIONS AND RECOMMENDATIONS 300

14.1 Introduction 300

14.2 Cryoprobe Performance and Cell Destruction 300

14.3 Analysis of Tip Thermodynamic Behaviour 301

14.4 Liquid Nitrogen Transport 301

14.5 Human Interface Design 302

14.6 Further Development of System 303

14.7 Clinical Trials 303

14.8 Possible Areas for Future Work 305

14.9 Concluding Remarks 306

APPENDIX 1 - DERIVATION OF MODEL OF ICE-BALL GROWTH 307

APPENDIX 2 - VACUUM INSULATION OF CRYOPROBE 311

APPENDIX 3 - DERIVATION OF FINITE DIFFERENCE EQUATIONS 316

APPENDIX 4 - COMPUTER PROGRAM USED TO ESTIMATE TIP COOLING 321

REFERENCES 323

CHAPTER 1

Introduction

1.1 Scope of Project

Cryosurgery is the clinical technique of destroying unwanted living tissue by freezing. The freezing is usually carried out by means of a heat-extracting probe, known as a cryoprobe, and is at present limited in application to the surface of the body because of the need to visually monitor the growth of the frozen tissue mass, or ice-ball. The aim of the work described in this thesis is to extend the application of cryosurgery to within body cavities, and in particular the human rectum, by developing a cryoprobe that can be operated effectively within such cavities. This thesis describes and discusses the work carried out to design, develop and test the rectal cryoprobe.

1.2 The Clinical Problem

Rectal cancer is more often contracted by the elderly and major surgery using the scalpel can be particularly traumatic for such patients and can lead to much post-operative pain. Cryosurgery would have many benefits for patients of this kind (Hobbs 1980, Lloyd-Williams 1978, Osborne et al, 1978)

1. Post-operative pain following cryosurgery is far less than for surgery using the scalpel or electro-cautery (burning).

2. The bowels remain connected through to the anus and do not have to be attached to an opening made in the abdominal wall (colostomy), as is often necessary with other techniques.

4. There are no side effects such as occur with treatment using ionising radiations or cancer destroying chemicals.

The major drawback of using cryosurgery is that it is difficult at present for the surgeon to guarantee removal of all the cancerous tissue. However for elderly patients this is not so critically important and has to be weighed against the considerable trauma, at a late stage in life, of alternative treatments.

At the present moment there are no cryosurgical instruments available that can be used within body cavities such as the rectum, and the potential benefits of cryosurgery for rectal tumours cannot be realised. The objective of this project is to provide an instrument that fulfills this need.

1.3 Surgical requirements

The most relevant starting point in the design of the rectal cyroprobe is the surgical requirement. What exactly does the surgeon require of the device in order to carry out successfully the medical treatment he is following?

The consultant supervising the clinical aspects of this project was Mr. K. Lloyd-Williams, consultant

general surgeon, Bath Royal United Hospital. At the start of the project he defined the required freezing performance as follows:-

1. The cyroprobe should be able to destroy a tumour mass of roughly hemi-spherical shape and up to 3cms in diameter.
2. It should take no longer than 5 minutes to complete the freezing.

As well as these performance requirements there were also a number of basic operational requirements that were specified:-

1. The surgeon will need to place the tip of the cryoprobe accurately onto the tumour mass.
2. The surgeon will need to be able to monitor the growth of the ice-ball so that he can be sure he has destroyed all the tumour.

1.4 Design Problems

Implicit within the surgical requirements listed above are a large number of problems with regard to the design of the cryoprobe. These design problems can be divided into two major aspects:-

1. Problems of performance. What thermodynamic performance must be specified to ensure that the cryoprobe can achieve the cell destruction required in the time available? How can that performance be satisfied?
2. Problems of operation. How can the surgeon gain access to the tumour with the cryoprobe, place it

accurately and monitor its effects on the tumour cells?

This division of the design problems is an important one. The first part is a reasonably straight forward problem of designing a cooling system. It must incorporate a cooling tip of adequate freezing power together with a cryogen supply and control system. The second part is far less straightforward. It concerns the design of the interface between the device and the patient and embraces many of the problems that face the designer in the field of medical engineering. A different design approach is needed when tackling these two aspects of the design requirements and these different approaches are outlined below.

1.5 Design Approach

1.5.1 Performance Aspects: the cryoprobe cooling system

As cryosurgery has become an accepted procedure for destroying unwanted tissue, so researchers have examined the process of cell destruction by freezing and the growth of ice in tissues. However all too often in the past, the design of the cryoprobes themselves has been a very crude process. Most devices have been made to work on the basis of trial and error. Very few papers have been published which seek to relate the performance of these instruments to the desired surgical effect, or which study them as thermodynamic systems.

It was intended that the present design of the rectal cryoprobe should be far more systematic and its

performance tailored to the biological requirements as closely as possible. The necessary thermal environment for cell destruction by freezing was therefore examined and the cryoprobe thermodynamic performance related to that environment through the use of mathematical models of ice-ball growth in tissues. The derived thermodynamic specification then formed the basis of the cooling system design.

1.5.2 Operational Aspects: the patient/instrument interface

In the field of medical engineering, devices often have an intimate relationship with the human body. This may be because the device is replacing or augmenting some bodily function that has failed. It may be because the device simply has to operate in conjunction with the human body or inside it. The designer of such devices is faced with the problem that because the devices have an intimate relationship with the human body they are affected by a large number of essentially biological variables. These variables can be anatomical, physiological or psychological. When it comes to applying normal design procedures to these devices a major problem occurs when the designer tries to draw up a specification because of the large number of variables involved. Many variables will be impossible to define precisely and many will not even be obvious until a prototype has been tried out.

The operational aspects of the rectal cryoprobe design have an interface with both the patient and the

surgeon and suffer from the problems discussed above. In this project an evolutionary design technique was used to tackle these aspects of the design. This technique has been found to be effective in other areas of medical engineering design. (Orpwood, 1983)

1.6 Structure of the Thesis

The first task tackled in this project was to derive a performance specification for the rectal cryoprobe. **Chapter 2** starts by reviewing the literature on mechanisms of cell destruction and techniques of modelling ice-ball growth. One of these models is used in **Chapter 3** to relate the required thermal environment in the tumour to the thermodynamic performance of the cryoprobe. Having established a performance specification, techniques of cooling are examined and their capabilities compared to the specification. This investigation is discussed in **Chapter 4.**

One of the most important components of the cryoprobe is the freezing tip and its design is discussed in the next three chapters. **Chapter 5** describes measurement of the boiling behaviour of liquid nitrogen in the tip and these measurements are extended in **Chapter 6** to look at the effect of several tip design variables on its performance. Also discussed in **Chapter 6** is the problem of achieving a low tip operating temperature when freezing tissues. **Chapter 7** examines tip cooling in more detail using numerical models.

The tip design established can achieve the performance specification as long as it is supplied with liquid nitrogen at a specified flow rate. The next two chapters examine the design of the system used to transfer the cryogen from a storage dewar to the tip. **Chapter 8** discusses the overall design of the transfer system and recommends using Leidenfrost flow of the liquid. **Chapter 9** proceeds to examine the features needed in the transfer system to maintain this kind of flow.

All the discussions up to this point have examined the performance aspects of the cryoprobe design. The operational aspects are tackled in the next three chapters. **Chapter 10** reviews techniques of cryosurgical monitoring to see what kind of system would be most appropriate for use in the rectal cavity and recommends incorporating a telescope in the probe. **Chapter 11** describes the evolutionary design technique used to tackle the human interface aspects of the design and this technique is applied in **Chapter 12** to the rectal viewer design.

The performance aspects of the design and the operational aspects are finally combined in **Chapter 13** with a description of the total system.

1.7 Role of Experimental Investigations in the Cryoprobe Design

Throughout this thesis many experimental measurements are described. These measurements are seen as part of the overall design process in that they enable the impact of variables to be quantitatively assessed and for trends to be established. The experimental investigations are at no point intended to be complete examinations of the performance of any given components. Once an impression of the influence of variables has been gained, the design process proceeds to the next step.

CHAPTER 2

THE BIOPHYSICS OF CRYOSURGERY

2.1 Introduction

This chapter starts the process of identifying a performance specification for the cryoprobe by briefly reviewing two areas of major concern.(See Orpwood 1981).

(1) The mechanism of cell death by freezing.

(2) Techniques of mathematically modelling the growth of an ice-ball in tissues.

Both these areas are important. From an understanding of the mechanism of cell death from freezing it is possible to define the thermal environment to which the tumour cells must be exposed to kill them. By modelling the growth of the ice-ball in the tumour it is possible to identify a performance specification for the cryoprobe that enables the desired thermal environment to be generated.

2.2 Mechanisms of Cell Destruction

2.2.1 The two main causes of cell destruction

Investigations on cells and tissues frozen in vitro (i.e. in cell cultures and isolated slabs of tissue, not in living animals) have indicated two main mechanisms of cell destruction. These two mechanisms are associated with extra-cellular and intra-cellular ice crystallization respectively.

2.2.2 Extra-cellular ice formation

A possible mechanism whereby extra-cellular ice could kill cells was suggested by Lovelock (1953). This mechanism, known as the "solution effect", has become generally accepted as one of the major causes of cell death from freezing. Lovelock suggested that as the extra-cellular ice crystal grows, the extra-cellular solution becomes more concentrated and free cell water passes out of the cells down the osmotic gradient generated. This loss of water causes the cells to shrink. Eventually cell shrinkage reaches a minimum and, as the extra-cellular concentration increases further, equilibrium is maintained by solutes passing into the cell. Lethal cell damage occurs on thawing, when these extra solutes ensure a large uptake of water and cells eventually rupture.

2.2.3 Intra-cellular ice formation

Cell death from freezing is also associated with intra-cellular ice. It has been shown (Asahina 1966) that extra-cellular ice always forms first, with a concomitant concentration of extra-cellular fluid. However, at high rates of cooling, water cannot leave the cells fast enough to maintain osmotic equilibrium across the cell membrane. Osmotic equilibrium is therefore achieved by ice forming within the cells as well. The actual mechanism whereby intra-cellular ice kills cells is not fully understood, but when it occurs, cell destruction is always greater. Mazur (1963) has

demonstrated that the probability of intra-cellular ice formation is strongly dependent on the rate of cooling.

2.2.4 The effect of cooling rate on cell destruction

The effect of cooling rate on cell destruction is illustrated for several cell types in **Figure 1.** The "solution effect" occurs between temperatures of about -4°C and the eutectic point of the extra-cellular fluid, that is, about -21°C. As the cooling rate is increased the cells spend less time in this temperature range, exposed to the hypertonic extra-cellular fluid. Consequently the number of cells being killed is reduced. For even higher cooling rates, intra-cellular ice starts to form and cell destruction increases again. The critical cooling rate for minimal cell destruction depends on the cell type being frozen (Mazur, Leibo, Farrant, Chu, Hanna and Smith, 1970)

2.2.5 Effect of thawing rate on cell destruction

During thawing, much more heat is required to melt the ice than to raise its temperature to the freezing point. Consequently the tissue mass quickly warms to the freezing point and the cells are then exposed to the high extra-cellular concentrations whilst the latent heat is provided. The damaging "solution effect" is therefore prominent, especially if the thawing rate is slow.

FIGURE 1

EFFECT OF COOLING RATE ON CELL DESTRUCTION IN VITRO

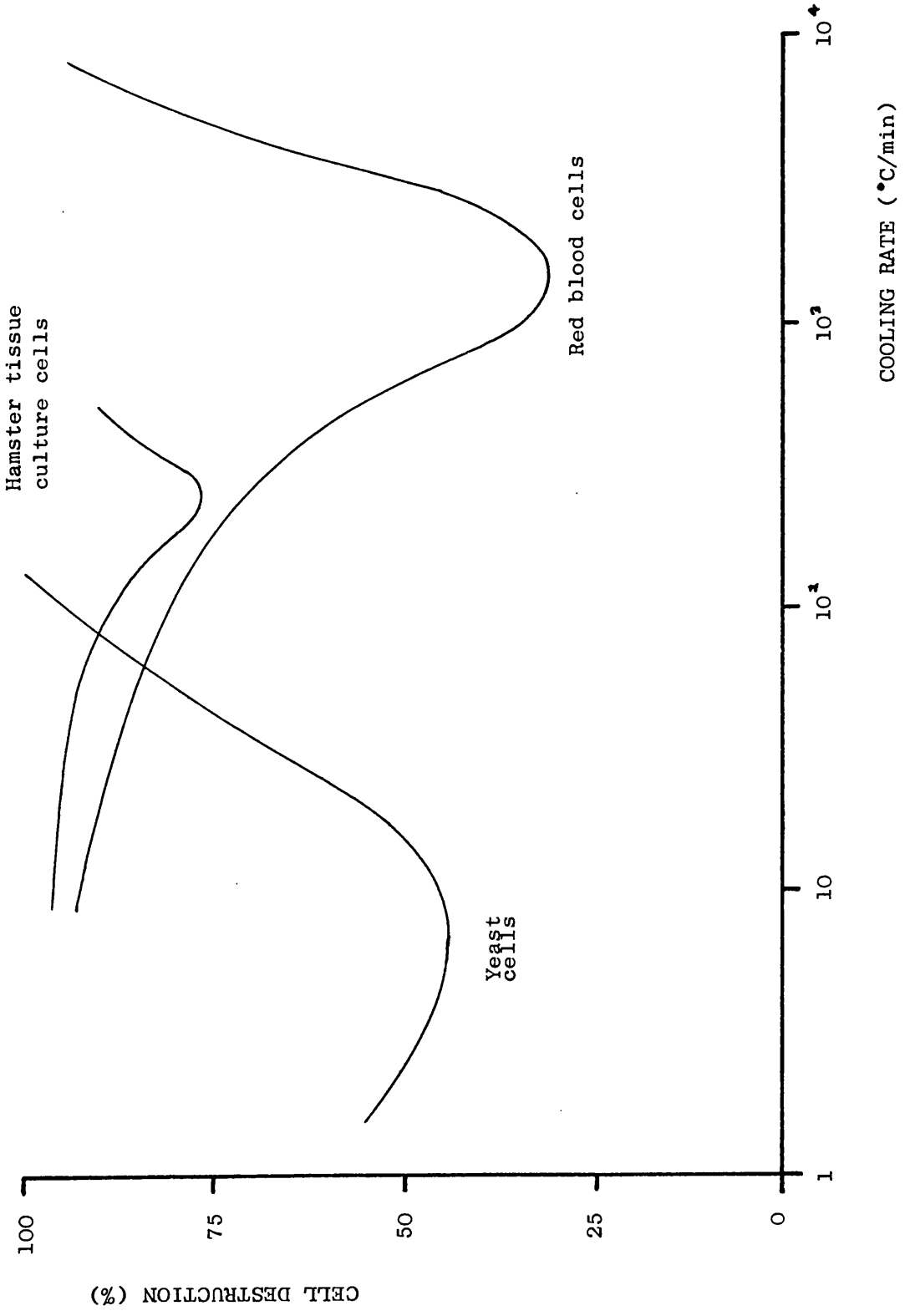

2.2.6 Extent of cell destruction

Despite the cell destroying mechanisms described above, experience shows that many cells do survive the freezing process, when the freezing is carried out in vitro (Gye et al 1949, Mazur et al 1969, Leibo et al 1970). The survival of some cells is generally regarded as being simply due to different cells being exposed to different thermal environments rather than any genetic difference favouring resistance to freezing (Ashwood-Smith 1965).

2.2.7 Predicted pattern of cell damage around a Cryoprobe

The reports of significant cell survival after freezing are rather disturbing, and it is pertinent to try and predict the pattern of cell survival around the cryoprobe using the published results discussed above. **Figure 2** shows the cooling rate experienced by cells as a function of their distance from the cryoprobe. Based on the known effects of cooling rate on cell survival, a graph of cell survival as a function of distance from the cryoprobe is shown in **Figure 3.**

These different zones of cell damage, based on the in vitro studies, were initially discussed by Farrant (1971). Cells close to the tip will be subjected to a fast cooling rate and cell death will be high following intra-cellular ice crystalisation. Further away the cooling rate will be lower and less cells will be killed. At a certain distance, cell death will reach a

FIGURE 2

COOLING RATE AT A DISTANCE FROM CRYOPROBE

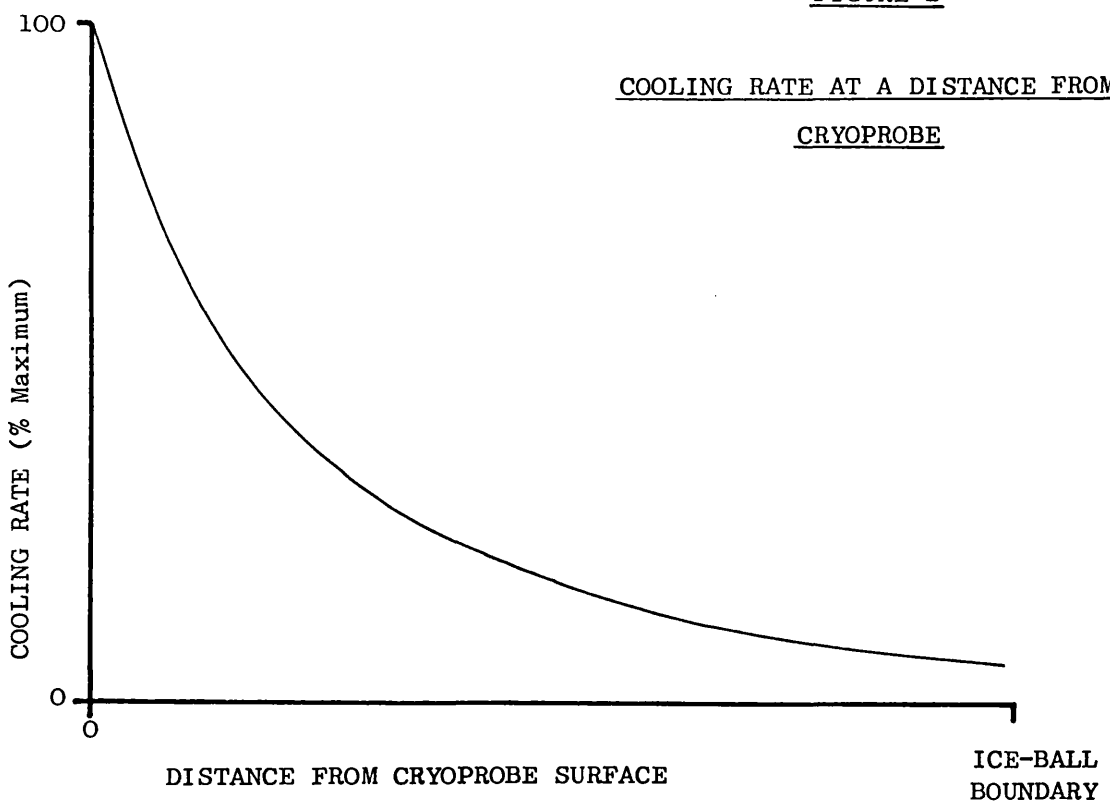

FIGURE 3

CELL DESTRUCTION AT A DISTANCE FROM CRYOPROBE

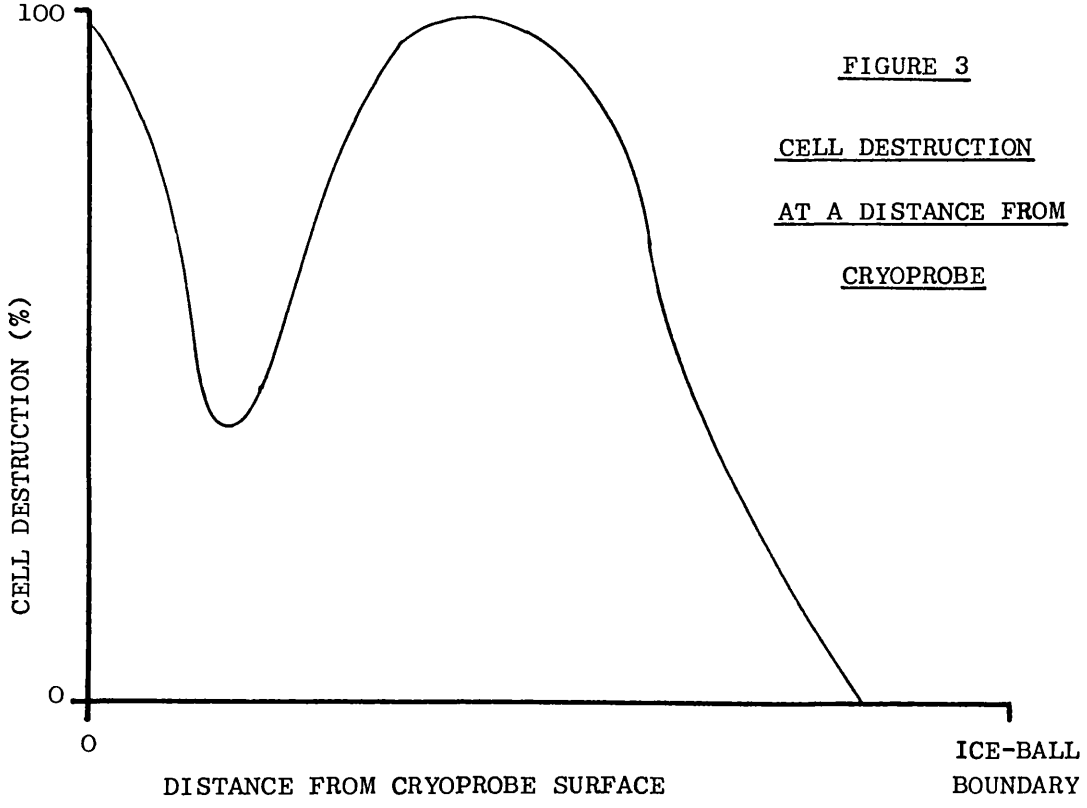

minimum but will start to rise again as the cooling rate is further reduced and the "solution effect" predominates. Finally, near the edge of the ice mass, cell death will again become low as the temperature does not drop much below 0°C and little ice crystallization will have taken place.

The postulated pattern of cell damage around a cryoprobe tip leads to three main conclusions:

(i) The zone in which most cells are killed is smaller than the size of the ice mass.

(ii) On the basis of the in vitro studies, a significant proportion of the cells would be expected to survive in the frozen volume.

(iii) The most effective freezing procedure would be a fast freeze followed by a slow thaw.

2.2.8 Measured cell destruction in tissues

The above rather unsatisfactory state of affairs appears less disturbing when the published results of in vivo experiments are studied (i.e. studies carried out on living animals). In vivo, a much greater destruction of cells occurs than would be expected from the in vitro results (Fraser and Gill 1967, Smith and Fraser 1974). Smith and Fraser (1974) took tissue sections through a region of rat liver frozen in vivo and found only a vague demarcation between live and dead cells 30 minutes after freezing, but after 48 hours

there was a well defined line. This line corresponded with the -15°C temperature contour within the ice mass. Cell temperatures within this region varied from -15°C to -70°C and the cooling rates from 30 to 100°C/min. Significant cell survival would be expected in many cell suspensions subjected to these thermal environments, but all rat liver cells frozen in vivo appeared to be killed.

Histological studies of tumour cells, both animal and human, have shown the same effect. Viable cells appeared to remain immediately after carefully controlled cryosurgery, but 48 hours later all cells within the region were dead (le Pivert et al 1975b, 1976).

The mechanism underlying the delayed destruction is not fully understood. Presumably the cell destroying mechanisms that have been elucidated in the in vitro studies do take place in living tissues following cryosurgery. However, some other process seems to occur in the subsequent few hours which kills all cells within a given region, including those that initially survived the cold insult. One possibility is that freezing damages the micro-circulation and the cells are deprived of oxygen and nutrients. The lack of oxygen eventually kills the cells (Gill et al, 1970). However, studies of sections of tissue that had been frozen in vivo show little evidence for the postulated circulatory damage (Smith et al 1978, Whittacker 1975a,b).

2.2.9 Conclusions about cell destruction

The picture that emerges from these studies is a rather confused one. There is a lot of evidence that many cells would be expected to survive being frozen during cryosurgery. However, there is conflicting evidence that when freezing is carried out on living tissues rather than cell suspensions, all cells within a certain region are killed. The conclusions arrived at from these studies and which form the basis of the rectal cryoprobe design are that:

(i) The cryoprobe tip temperature should be as cold as possible and should reach this temperature quickly so that the mean cooling rate experienced by cells within the ice mass is as high as possible.

(ii) The ice mass should be allowed to thaw on its own, rather than be heated, to allow as slow a thaw as possible.

(iii) When considering the size of ice mass that must be grown in a given time, it is the -15°C contour that is important, not the 0°C contour.

2.3 Models of Ice-ball Growth in Tissues

2.3.1 The need to model ice-ball growth

The studies discussed in Section 2.2 establish the necessary thermal environment for cell destruction. The next problem to be examined is what thermodynamic

performance of the cryoprobe must be specified in order to attain this environment. To explore this problem it is necessary to use a mathematical model of ice-ball growth. There have been a number of such studies published in the literature and these are now examined.

It is stressed that only a general review of published ice-ball models is presented in this chapter. Chapter 3 contains a more detailed discussion of the model used in this thesis to investigate ice-ball growth.

2.3.2 Basis of ice-ball model

When a cryoprobe is placed in contact with tissue and cooled, a temperature field develops in the tissue. The tissues adjacent to the probe will undergo a phase change and, as the cooling continues, this freezing front will propagate through the tissues, generating an ice-ball . Eventually a steady state will be reached where the rate at which heat is being extracted by the cryoprobe balances the rate at which heat is supplied to the tissues and the ice-ball reaches its maximum size.

The prediction of the temperature field is essentially a problem of conductive heat transfer with the added complication of a phase change. Heat is conducted from the deep body temperature at a large distance from the probe, to the probe tip itself. The model must also take into account two further sources of heat. These are the heat supplied by the blood perfusing the unfrozen tissue and the heat generated as

a by-product of metabolism.

2.3.3 Steady-state models of ice-ball

Starting from the basic differential equation of heat conduction in a solid, expressions can be derived that give the temperature distribution within the frozen and unfrozen regions. By equating the heat flux across the interface between the frozen and unfrozen tissue an expression for the steady-state ice-ball radius can be obtained (Cooper and Trezek, 1970,1971a). Barron (1968) developed this model further by taking into account the temperature dependence of tissue thermal conductivity.

2.3.4 Temperature-time models of ice-ball growth

The time taken to approach the steady-state radius of an ice-ball can be very long. For example, a 12mm diameter probe tip at -196°C will take over 20 minutes to reach 95% steady-state radius. Of much more importance to both the surgeon and the cryoprobe designer is the size of the ice-ball after a given freezing time.

The basic partial differential equation of heat conduction in solids, incorporating the phase change condition, is not analytically soluble for time-temperature fields of this kind and inevitably requires numerical solutions. Rough estimates can be produced by ignoring the blood-flow and metabolic-heat terms (Trezek and Jewett 1970). However, approximate solutions which include these terms can be found if the heat capacity

effects in both the frozen and unfrozen phases are considered to be neglegible compared to the latent heat effects (Cooper and Trezek 1971b). The result obtained, although cumbersome, does provide a means of quickly analysing the influence of the variables (See **Chapter 3** and **Appendix 1**).

The predictions from the last mentioned model compare well with numerical solutions and when compared with actual measurements have been found to be accurate to within 8% (Cooper and Petrovic 1974). A typical comparison, taken from the last mentioned study, is shown in **Figure 4**.

Another approach used by several authors to obtain an analytical solution of the time-temperature fields is to use some measured "effective" biological variables The blood flow and metabolic heat sources have been combined into an "effective" thermal conductivity of the unfrozen tissues (Eichler and Lenz 1976, Lenz and Eichler 1976). To obtain the value of this term however, the results of experimental work on the same tissue in the same animal have to be used. Boyarskii and Filippov (1979) described a method for predicting the ice-ball radius as a function of time after measuring the steady-state heat flow in the tissue. No further biological data is then required. Despite the rather approximate nature of these approaches, they apparently produce accurate predictions, provided they are related to a given tissue.

Several other approaches to the problem of

FIGURE 4

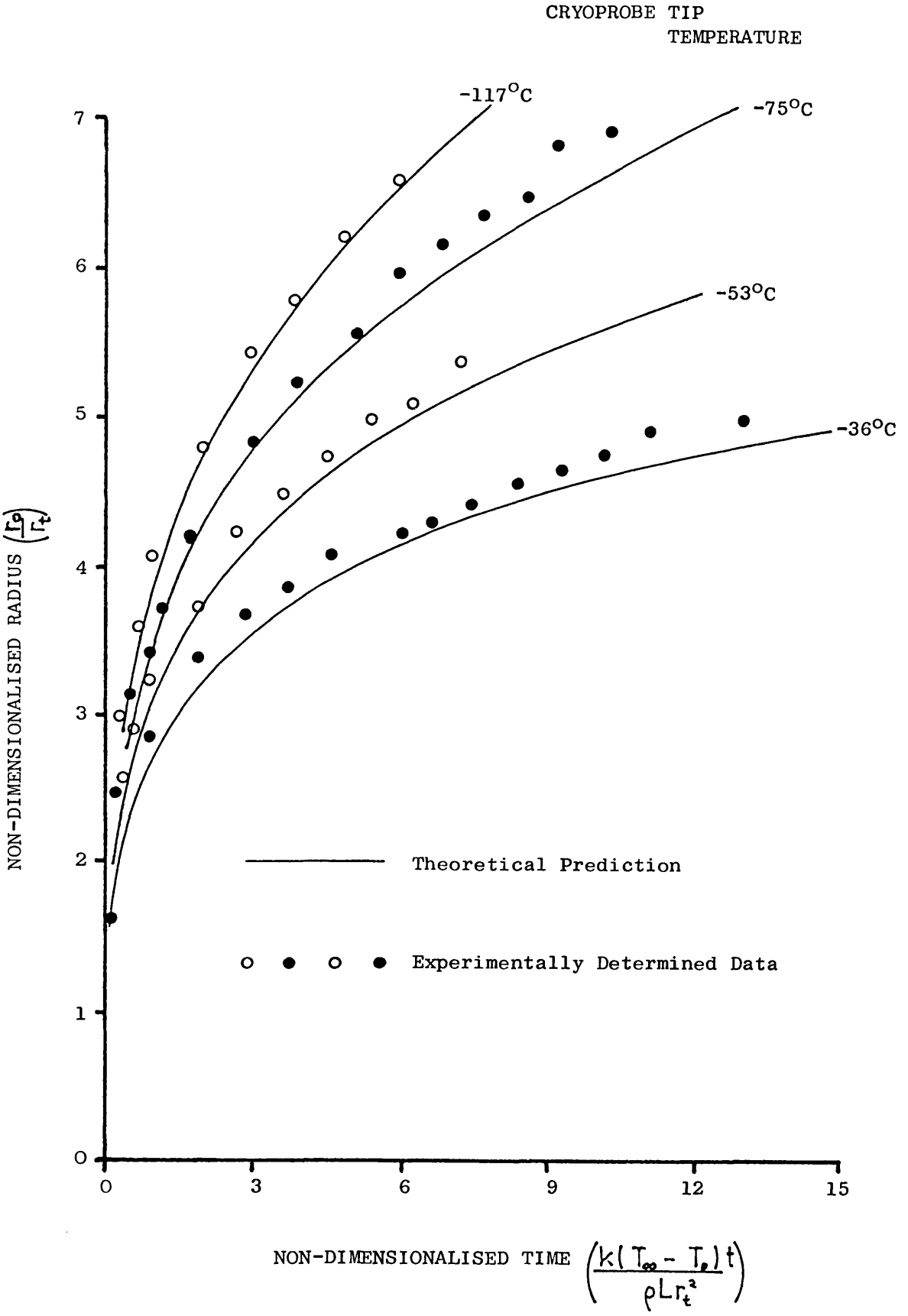

ICE-BALL GROWTH: COMPARISON BETWEEN EXPERIMENT AND THEORY (COOPER & PETROVIC, 1974)

predicting ice-ball size have been published. Warren et al (1974) used integral equations to describe the energy balances in the frozen and unfrozen regions. The temperature distributions within these regions were approximated by second degree polynomials whose coefficients were determined by reference to the boundary conditions. Hrycak et al (1975) used Newmann's solution for ice front penetration into semi-infinite slabs to model the effect of planar cryotips.

2.3.4 Numerical models of ice-ball growth

Numerical techniques are used to analyse more complicated geometries than the simple one-dimensional systems analysed above. They also have to be used if time-dependent boundary conditions are involved. A fairly comprehensive model has been described recently, by Comini et al (1976). This model uses a two-dimensional mesh and can be used to investigate temperature fields in which any shape of probe or tissue boundary is used and in which the temperature dependence of tissue properties can be taken into account. Variable tip temperatures can also be accommodated.

Other authors have produced simpler models and reduced computing time by using the "effective" parameter technique referred to earlier (Trezek and Jewett 1970).

2.3.5 Relating ice-ball models to cell destruction

Few studies have attempted to relate the effect of

the cooling profile to the lethality of the process. Cravalho (1971) included the effect of the cooling rate on cell death in his analysis. Rubinsky and Shitzer (1976) attempted to define an optimum time course of heat extraction via the cryoprobe in order to attain a constant optimal cooling rate at the ice front. The principal problem is that insufficient data is available about the optimum thermal environment for cell death. A much greater understanding of the mechanisms of cell destruction following cryosurgery will be necessary before these theoretical models of the ice-ball can be used to define the cryoprobe performance necessary to achieve complete destruction of the target area. However, enough is known from the studies discussed in Section 2.2 for the mathematical models to be used to give reasonable guidelines for cryoprobe performance.

The model developed by Cooper and Trezek (1971b) will be used in the next chapter to develop a performance specification for the rectal cryoprobe. This model is not as sophisticated as the numerical models discussed in Section 2.3.4 but it does give fairly quick predictions of the transient temperature distribution around the cryoprobe.

2.4 Conclusions

This chapter has laid the foundations for the rectal cryoprobe design by reviewing the biophysics of cryosurgery. Two main conclusions result from this review:

(i) The most effective thermal environment for cell destruction is a rapid freeze followed by a slow thaw, although when tissue is frozen in vivo, all cells cooled below -15°C are killed.

(ii) The mathematical model of ice-ball growth published by Cooper and Trezek (1971b) should enable a performance specification for the cryoprobe to be defined.

CHAPTER 3

DERIVATION OF A PERFORMANCE SPECIFICATION

3.1 Introdution

This chapter shows how the surgical requirements can be interpreted in terms of a performance specification for the rectal cryoprobe. The surgical requirements of the probe, as stated in Chapter 1, are:-

1. The maximum size of tumour tissue to be destroyed is a sphere 3 cms in diameter.
2. The freezing time should be no longer than 5 minutes.

There are three major cryoprobe variables that need to be quantified to produce a performance specification:

1. Probe tip radius.
2. Probe tip temperature.
3. Probe tip heat flux.

This chapter derives values for these variables by using a mathemathical model of ice-ball growth. Several areas are explored with this model to gain an understanding of the effect of the probe variables on the ice-ball. Whenever possible the effects predicted by the model are scrutinized from the point of view of their biological relevance.

3.2 Model Used to Study Ice-ball Growth

3.2.1 Basis of model

The model of ice-ball growth used in this study is

the Cooper and Trezek (1971b) transient model introduced in Chapter 2. Their analysis examines the case of a hemi-spherical tip placed into intimate contact with warm tissue. Their model expresses the time taken to form an ice-ball of a given radius in terms of the major variables.

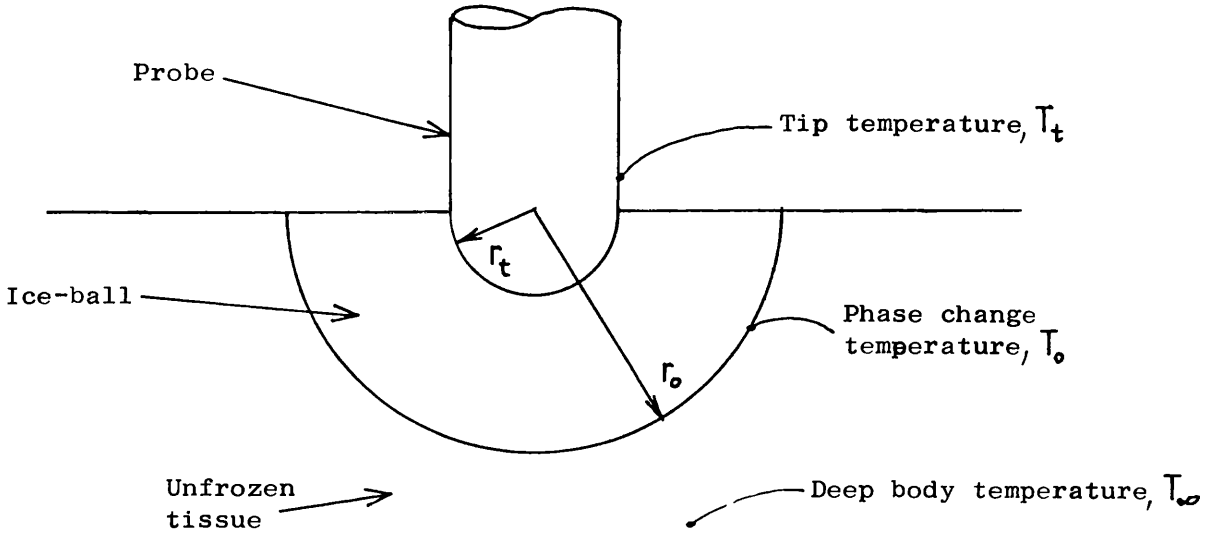

3.2.2 Assumptions made

1/. The contact surface between the probe and tissue is a hemi-sphere.

2/. The thermal resistance at the contact surface is negligible

3/. The tip temperature is constant from t=0.

4/. The thermal conductivity of tissue is not a function of its temperature.

5/. Deep body temperature is 37°C.

6/. The heat capacity effects in both the frozen and unfrozen phases are small compared to the latent heat effects (see Appendix 1 for importance of this assumption).

3.2.3 Starting point of analysis

Cooper and Trezek's analysis, in agreement with several other authors (eg. Perl 1962, Perl and Hirsch 1966, Ferro and Filippi 1978), starts from the basic partial differential equation of heat conduction in a solid incorporating two sources of heat;

1/. Heat supplied by perfusing blood,

2/. Heat supplied as a by-product of metabolism.

$$k \nabla^2 T + q'_b + q'_m = \rho c \frac{\partial T}{\partial t} \qquad (1)$$

where k = thermal conductivity

T = tissue temperature at a given point

q'_b = heat supplied by the perfusing blood

q'_m = heat supplied by metabolism

ρ = density

c = specific heat

t = time

and where $q'_b = \dot{m}_b c_b (T_b - T)$

$\dot{m}_b$ = mass flow rate of blood

c_b = blood specific heat

T_b = local blood temperature

3.2.4 Use of radial co-ordinates

The physical model being analysed is a hemispherical structure and so equation 1 is re-expressed in radial co-ordinates and applied to both

the ice-ball and the un-frozen tissue.

For the ice-ball,

$$\frac{k_f}{r^2}\frac{\partial\left(r^2\frac{\partial T_f}{\partial r}\right)}{\partial r} = \rho c_f \frac{\partial T_f}{\partial t} \qquad (2)$$

For the un-frozen tissue,

$$\frac{k}{r^2}\frac{\partial\left(r^2\frac{\partial T}{\partial r}\right)}{\partial r} + \dot{m}_b c_b (T_b - T) + q'_m = \rho c \frac{\partial T}{\partial t} \qquad (3)$$

where r represents the radial position in the field and the subscript, f, refers to the frozen tissue. The blood flow terms and metabolic heat terms are zero in the ice-ball.

3.2.5 Solution of equations 2 and 3 .

The solution of equations 2 and 3 is summarised in Appendix 1. This appendix shows that by applying the boundary conditions to these equations, the transient temperature distributions in the frozen and un-frozen are found. By applying the interface heat flux conditions, these temperature profiles can be combined and solved to provide an expression relating ice-ball radius to time.

$$t = \frac{\rho L r_t^2}{k(T_\infty - T_o)} \left\{ \frac{1}{2a^2} \ln \left[\frac{\left(a\left(\frac{r_o}{r_t}\right)^2 + (1-a)\frac{r_o}{r_t} + c\right)}{1+c} \right] \right. \qquad (4)$$

$$\left. + \frac{[1-a(1+2c)]}{2a^2 b} \ln \left[\left(a\left(2\frac{r_o}{r_t}-1\right) + b + 1\right)\left(a + b + 1\right) \right] - \left[\frac{\frac{r_o}{r_t} - 1}{a} \right] \right\}$$

where $a = \sqrt{\frac{\dot{m}_b c_b r_t^2}{k}}$ $\qquad b = \sqrt{(1-a)^2 - 4ac}$

$$c = \frac{k_f}{k}\left(\frac{T_o - T_t}{T_o - T_\infty}\right) - 1$$

and where r_o = ice-ball radius

r_t = probe radius

k_f =thermal conductivity of frozen tissue

k = thermal conductivity of unfrozen tissue

T_o = phase change temperature

T_t = probe tip temperature

T_∞ = deep body temperature

L = latent heat of fusion

t = time

$\dot{m}_b$ = mass flow rate of blood

c_b = specific heat of blood

3.3 Study of Rate of Growth of Ice-ball

3.3.1 Application of model and results

A simple program was used to calculate the value of time, t, for increasing values of ice-ball radius, r_o.

The analysis was repeated for tip temperatures ranging from -50°C to -196°C in six steps and the whole procedure repeated for tip radii, r_t, ranging from 1mm to 6mm.

The results are plotted in **Figures 5 to 7.** Each graph is for a different tip radius and plots ice-ball radius as a function of time for each of the tip temperatures. The graphs also show the steady-state radius for each case (i.e. the radius achieved at time infinity).

3.3.2 Conclusions about ice-ball growth

There are a number of interesting conclusions that can be drawn from the results shown in **Figures 5 to 7.**

1. Most of the ice-mass growth occurs during the first few minutes of the freeze. Not much is gained by freezing for more than about 5 minutes. To achieve a size of ice-ball approaching the steady-state radius, the freezing would have to be continued for at least half an hour.
2. The ice-ball radius increases approximately linearly with temperature as long as the tip is cooler than about -50°C. **Figure 8** shows ice-ball radius after a 3 minute freeze for different tip temperatures. It can be seen that although there is some tailing off of the curve, in general the lower the tip temperature, the bigger the ice-ball.

FIGURE 5

THEORETICAL ICE-BALL GROWTH USING

1mm RADIUS PROBE

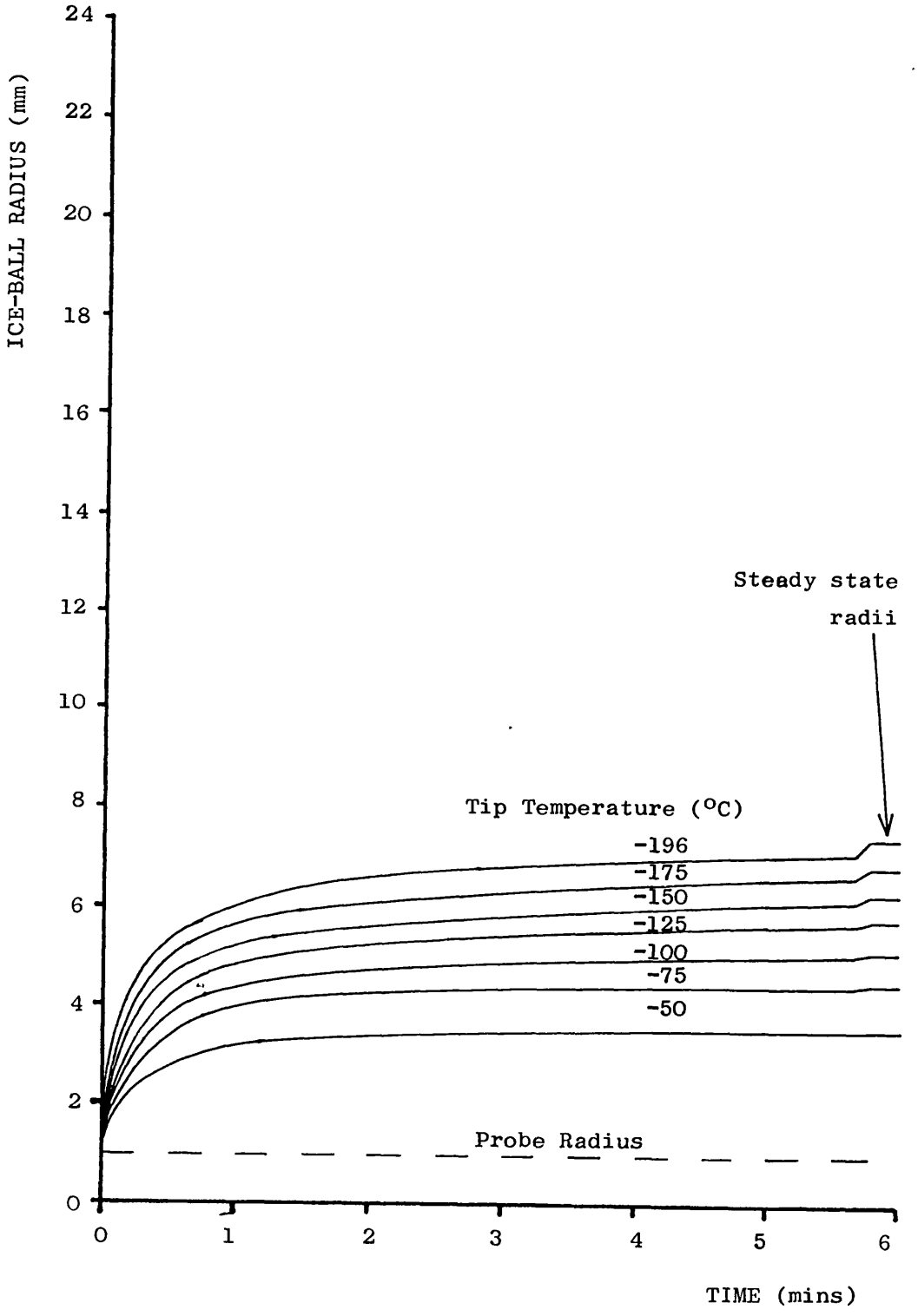

FIGURE 6

THEORETICAL ICE-BALL GROWTH USING

3mm RADIUS PROBE

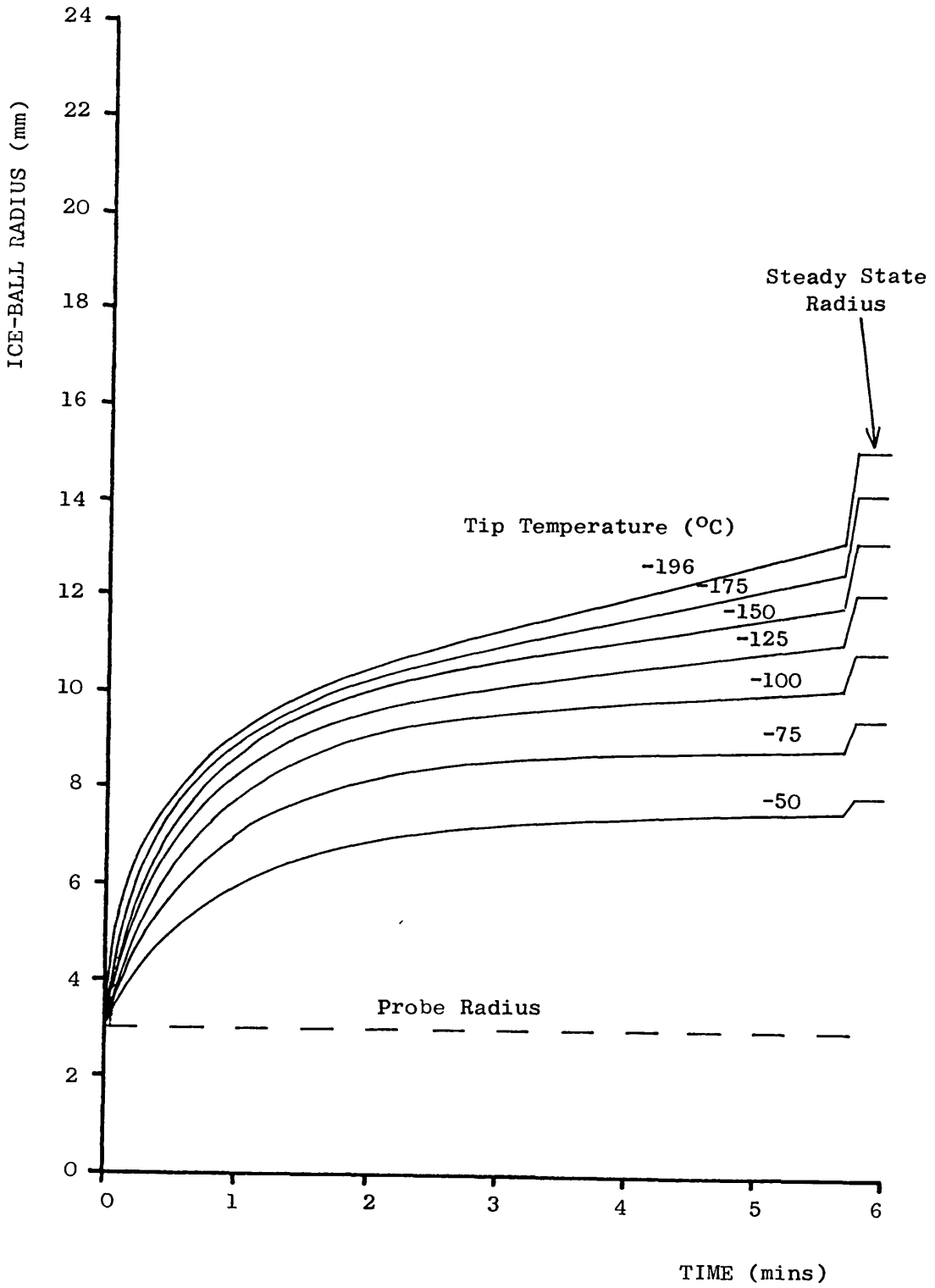

FIGURE 7

THEORETICAL ICE-BALL GROWTH USING

6mm RADIUS PROBE

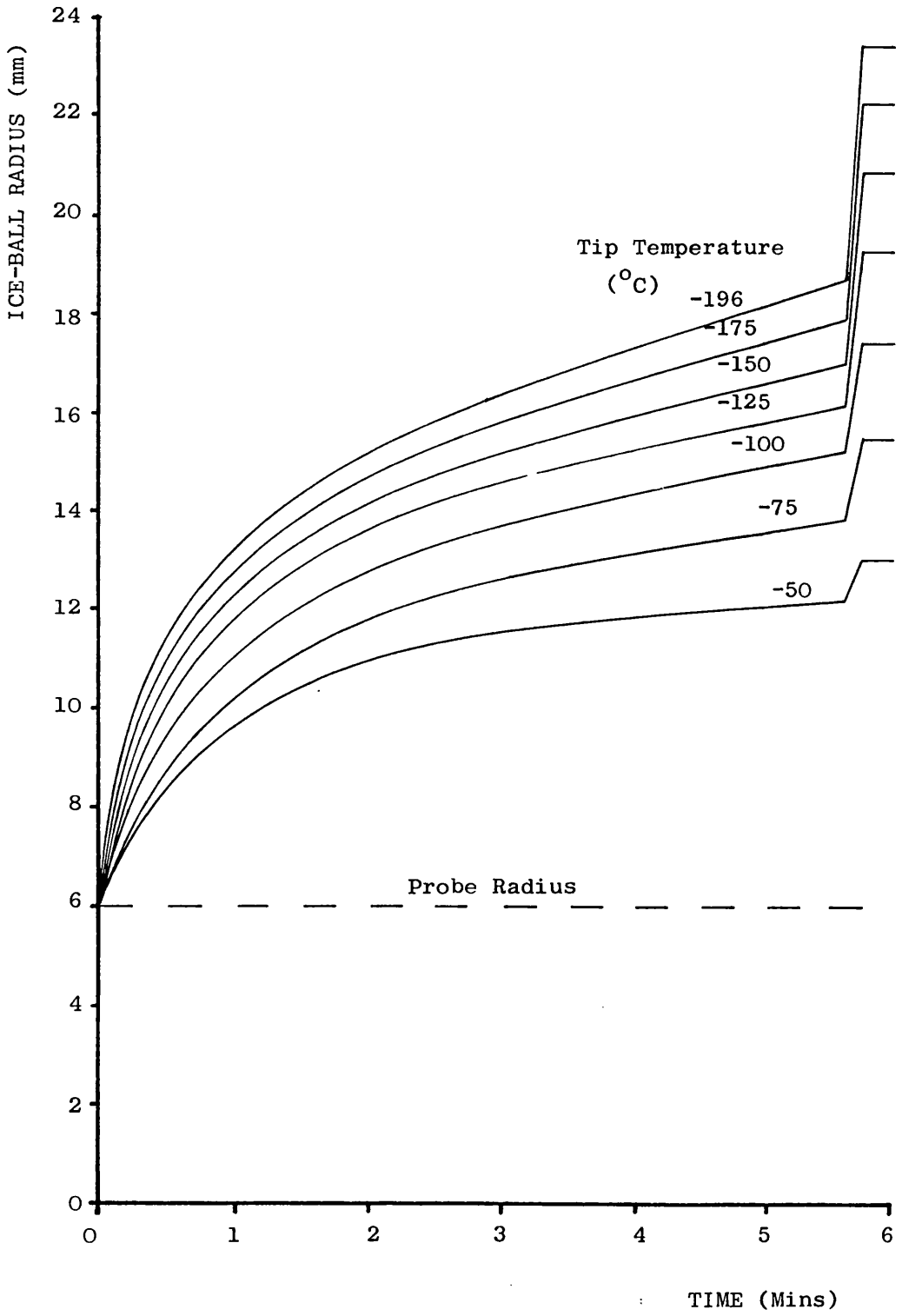

FIGURE 8

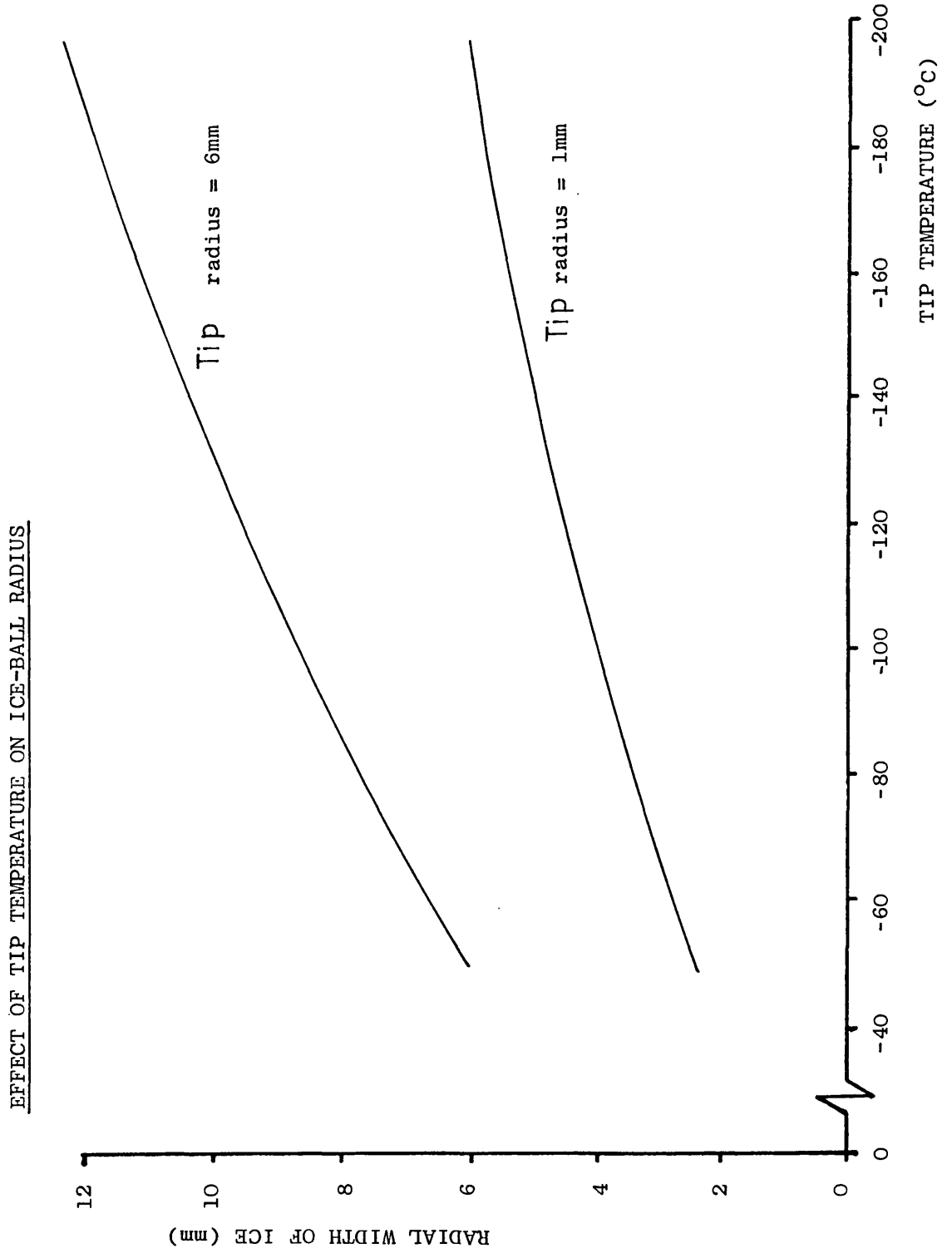
EFFECT OF TIP TEMPERATURE ON ICE-BALL RADIUS
RADIAL WIDTH OF ICE (mm)
12
10
8
6
4
2
0
Tip radius = 6mm
Tip radius = 1mm
0
-40
-60
-80
-100
-120
-140
-160
-180
-200
TIP TEMPERATURE (°C)

3. As the probe radius increases in size, the ice-mass size achieved in a given time does not go up in direct proportion. Figure 9 plots the ice-mass radius achieved as a function of the probe radius. As can be seen, the smaller probes are proportionately more efficient than the larger ones.

3.4 Cell Cooling Rate Produced By Cryoprobe

3.4.1 Reason for Study

Studies of the biological effects of freezing in vitro reviewed in Chapter 2 showed that the rate of freezing had a strong influence on cell destruction. The cooling rates experienced by cells being frozen by the rectal cryoprobe will now be examined.

3.4.2 Derivation of equation for temperature gradient

The analysis presented in this and subsequent sections is the authors work but uses expressions derived by Cooper and Trezek. In the derivation of Cooper and Trezek's model of ice-ball growth, as presented in Appendix 1, a non-dimentional expression is obtained for the temperature at any point within the frozen region.

$$\theta_f = 1 - \theta_o\left(\frac{T_o - T_t}{T_o - T_\infty}\right)\left(\frac{R_o}{R_o - 1}\right)\left(\frac{1 - R}{R}\right) \qquad (5)$$

where $\theta_f = \dfrac{T_f - T_\infty}{T_t - T_\infty}$

FIGURE 9

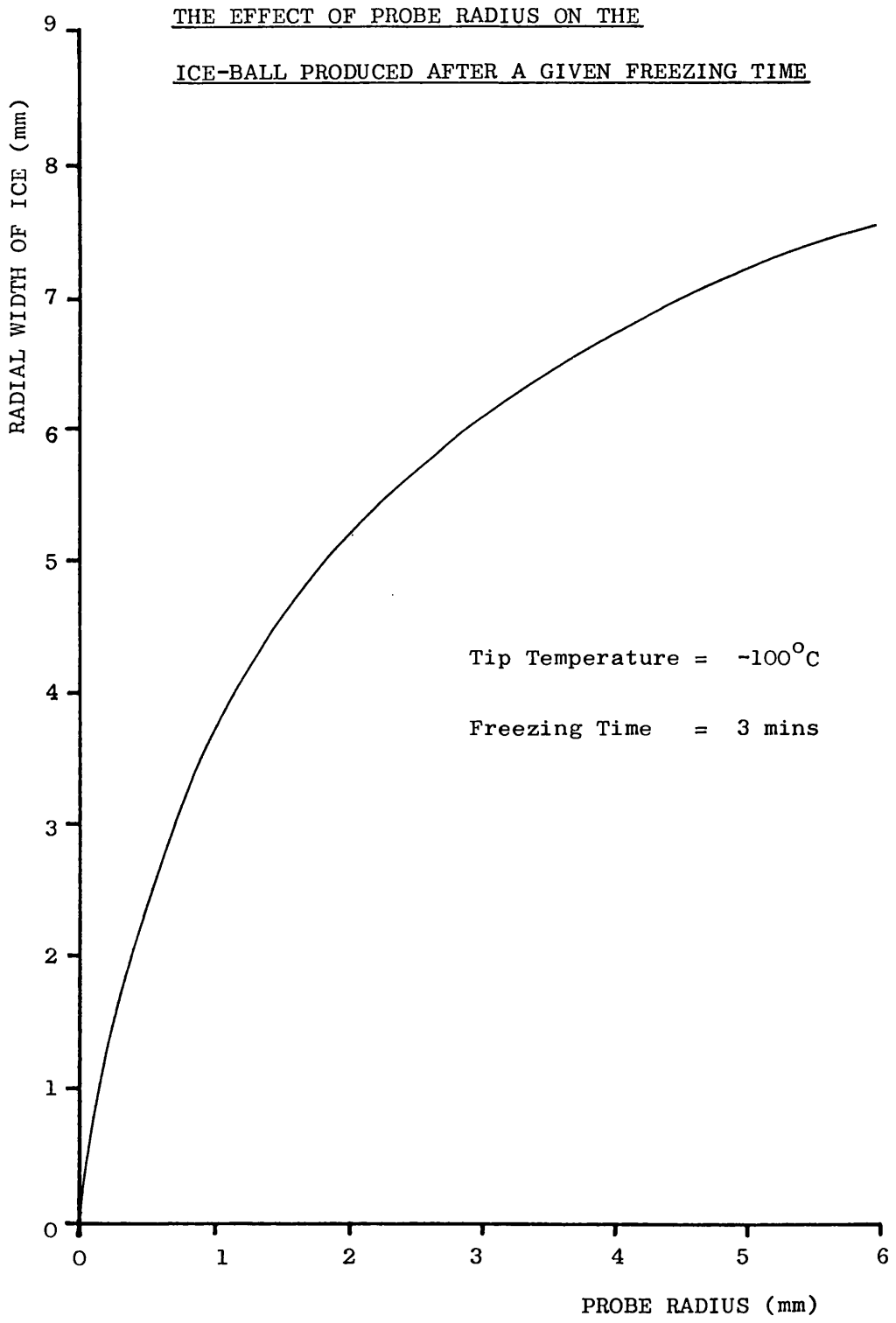
THE EFFECT OF PROBE RADIUS ON THE
ICE-BALL PRODUCED AFTER A GIVEN FREEZING TIME
RADIAL WIDTH OF ICE (mm)
0
1
2
3
4
5
6
7
8
9
PROBE RADIUS (mm)
0
1
2
3
4
5
6
Tip Temperature = -100°C
Freezing Time = 3 mins

$$\theta_o = \frac{T_o - T_\infty}{T_t - T_\infty}$$

$$R_o = \frac{r_o}{r_t} \qquad R = \frac{r}{r_t}$$

r = radial position in field

T_f = temperature in frozen phase

This temperature profile is transient in nature by virtue of the time dependance of R_o .

Differentiating with respect to τ, where $\tau = \frac{k(T_\infty - T_o)}{\rho L r_t^2} t$ (non-dimensional time)

$$\frac{\partial \theta_f}{\partial \tau} = \frac{\partial \theta_f}{\partial R_o} \times \frac{\partial R_o}{\partial \tau} = -\theta_o \left(\frac{T_o - T_t}{T_o - T_\infty}\right)\left(\frac{1}{(R-1)^2}\right)\left(\frac{1-R_o}{R_o}\right)\left(\frac{\partial R_o}{\partial \tau}\right) \qquad (6)$$

where L = latent heat of fusion

By applying the boundary conditions that relate to the frozen/unfrozen interface an expression is derived in Appendix 1 for $\frac{\partial R_o}{\partial \tau}$.

$$\frac{\partial R_o}{\partial \tau} = -\left(\frac{1 + \sqrt{\beta} R_o}{R_o} + \frac{\theta_f}{R_o(1-R_o)}\right) \qquad (7)$$

where $\beta = \frac{\dot{m}_b c_b r_t^2}{k}$

Substituting equation 7 into equation 6

(8)

$$\frac{\partial \theta_f}{\partial \tau} = \theta_o \left(\frac{T_o - T_t}{T_o - T_\infty}\right)\left(\frac{1}{R_o(R_o-1)^2}\right)\left(\frac{1-R}{R}\right)\left(1 + \sqrt{\beta} R_o + \frac{\theta_f}{(1-R_o)}\right)$$

but $$\frac{\partial T_f}{\partial t} = \frac{\partial \theta_f}{\partial \tau} \times \frac{\partial \tau}{\partial t} \times \frac{\partial T_f}{\partial \theta_f}$$

After simplifying,

$$\frac{\partial T_f}{\partial t} = \frac{-k(T_\infty - T_o)(T_o - T_t)}{\rho L r_t^2}\left(\frac{R-1}{R}\right)\left(\frac{1}{R_o(R_o-1)^2}\right)\left(1 + \sqrt{\beta}R_o + \frac{\theta_f}{(1-R_o)}\right) \quad (9)$$

Equation 9 shows that for any given ice-ball radius, R_o the maximum rate of cooling occurs when $\frac{R}{r_t}$ is as large as possible, ie. at the edge of the ice-ball.

At the edge of the ice-ball, $R = R_o$

$$\theta_f = \theta_o$$

Substituting these expressions into equation 9 and assuming $T_o = 0$.

$$\frac{\partial T_f}{\partial t} = \frac{-k T_\infty T_t}{\rho L r_t^2}\left(\frac{1}{R_o^2(R_o-1)}\right)\left(1 + \sqrt{\beta}R_o + \frac{T_\infty}{T_t(1-R_o)}\right) \quad (10)$$

3.4.3 Results obtained for temperature gradient during freezing

Equation 10 was used to examine the temperature gradient at the edge of the ice-ball as it developed. Results for a tip temperature of -196°C are plotted in Figure 10 as a graph of temperature gradient as a function of the distance from the cryoprobe. Two probe radii are used, 1mm and 6mm.

The freezing rate during the initial growth of the ice-ball is high but it rapidly drops to lower values with increasing ice-ball radius. There is not a great difference in the results obtained for the different sized probes. Therefore most cells within the ice-ball will be subjected to freezing rates that are likely to

FIGURE 10

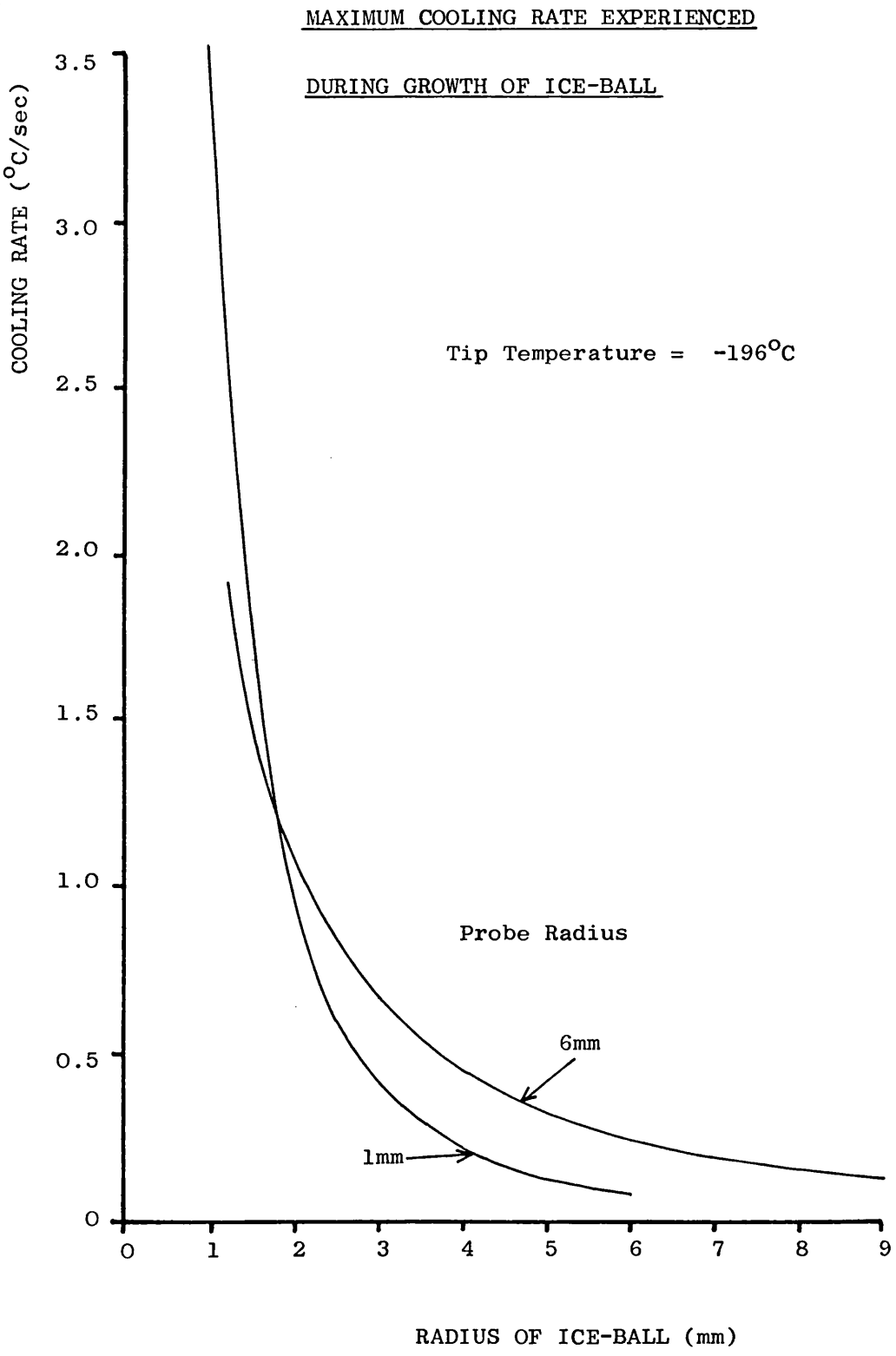
MAXIMUM COOLING RATE EXPERIENCED
DURING GROWTH OF ICE-BALL
COOLING RATE (°C/sec)
3.5
3.0
2.5
2.0
1.5
1.0
0.5
0
Tip Temperature = -196°C
Probe Radius
6mm
1mm
0
1
2
3
4
5
6
7
8
9
RADIUS OF ICE-BALL (mm)

cause extra- cellular freezing. If the cells are killed it will probably be by means of the "solution effect".

3.5 Temperature Distribution Within Ice-ball

3.5.1 Basis of investigation

Equation 5 allows the temperature distribution within the ice-ball to be calculated. Assuming the phase change temperature, T_o, is zero and simplifying.

$$T_f = T_t\left(\frac{r_o}{r_o - r_t}\right)\left(\frac{r_t - r}{r}\right) + T_t \qquad (11)$$

The investigations carried out in Section 3.2 provided results for r_o as a function of time. Substituting these results into Equation 11 allows the temperature distribution within the ice-ball to be calculated as a function of time.

3.5.2 Results of temperature distribution

Figure 11 shows the temperature distribution through an ice-ball calculated using Equation 11. The curves plotted are for a 6mm radius probe at -196°C and represent the temperature distribution at different times from the start of the freeze.

It was shown in Chapter 2, that the critical temperature to ensure cell destruction in vivo was -15°C. As can be seen from Figure 11, the -15°C isotherm is well within the visible ice-ball (the 0°C isotherm). Consequently a specification for the cryoprobe based on ice-ball size alone will considerably

FIGURE 11

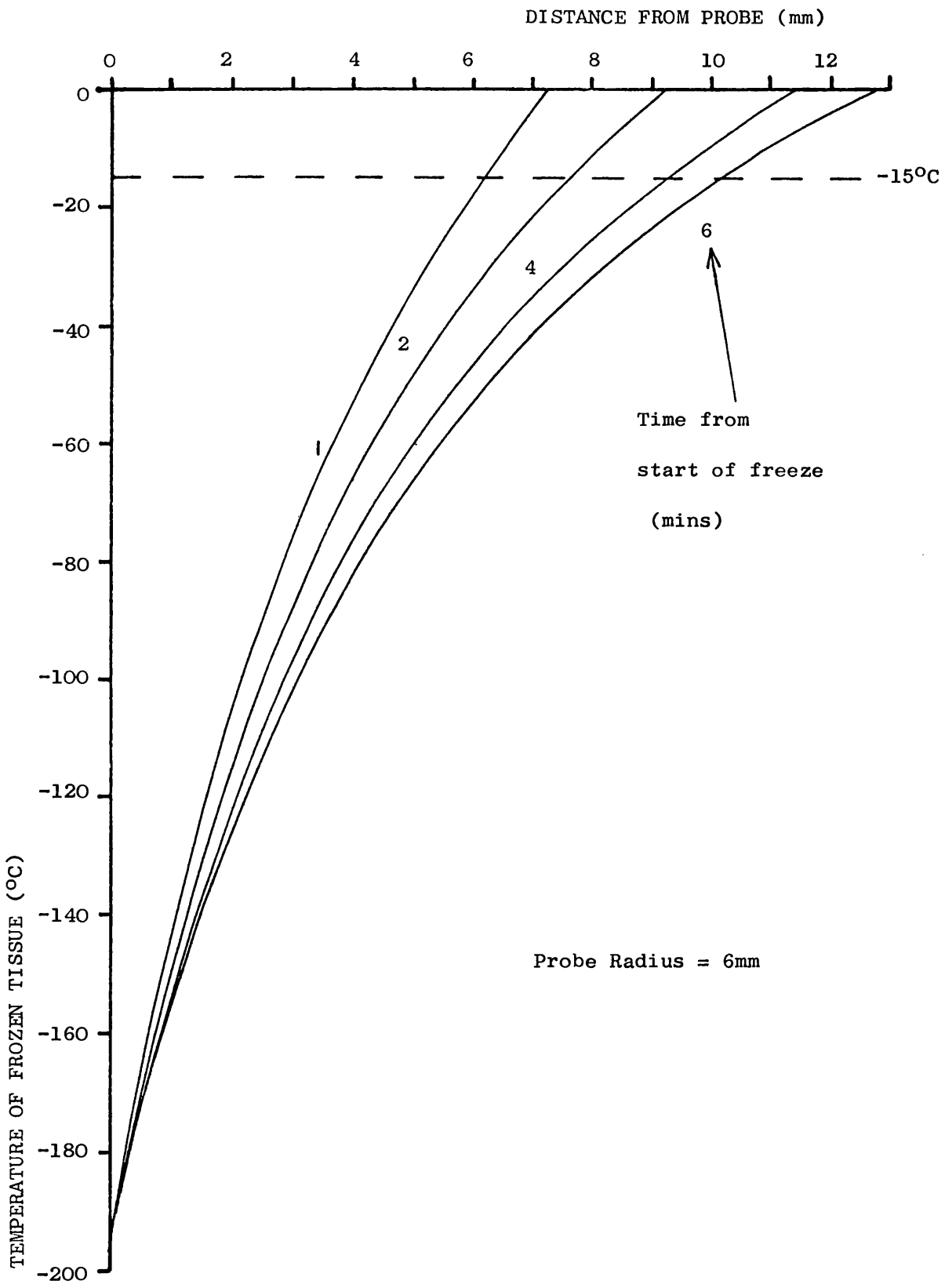

TEMPERATURE DISTRIBUTION THROUGH ICE-BALL AT DIFFERENT TIMES FROM START OF FREEZE

underestimate the cooling power needed to subject all of the tumour mass to temperatures of -15°C and lower.

3.5.3 Position of -15°C isotherm

It is important to know what fraction of the ice-ball is cooler than -15°C. Equation 11 can be rearranged to enable the radius of the -15°C isotherm to be expressed as a fraction of the ice-ball radius.

$$\frac{r_{-15}}{r_o} = \frac{1}{1 - \frac{15}{T_t}\left(\frac{r_o}{r_t} - 1\right)} \qquad (12)$$

where r_{-15} is the radius of the -15°C isotherm

The ice-ball radius, r_o , was calculated as a function of time in Section 3.2. It is possible therefore to calculate the location of the -15°C using Equation 12.

The results obtained are shown in Figure 12 where $\frac{r_{-15}}{r_o}$ is plotted as a function of tip temperature for several tip radii, after a freezing time of 5 minutes. As can be seen, a considerable portion of the ice-ball is not within the -15°C isotherm.

3.6 Heat Transfer To Cryoprobe

3.6.1 Analysis of cryoprobe heat transfer

Fouriers Law states:-

$$\dot{Q} = -kA\frac{\partial T}{\partial r} \qquad (13)$$

where $\dot{Q}$ = rate of heat transfer

FIGURE 12

POSITION OF -15°C ISOTHERM WITHIN ICE-BALL

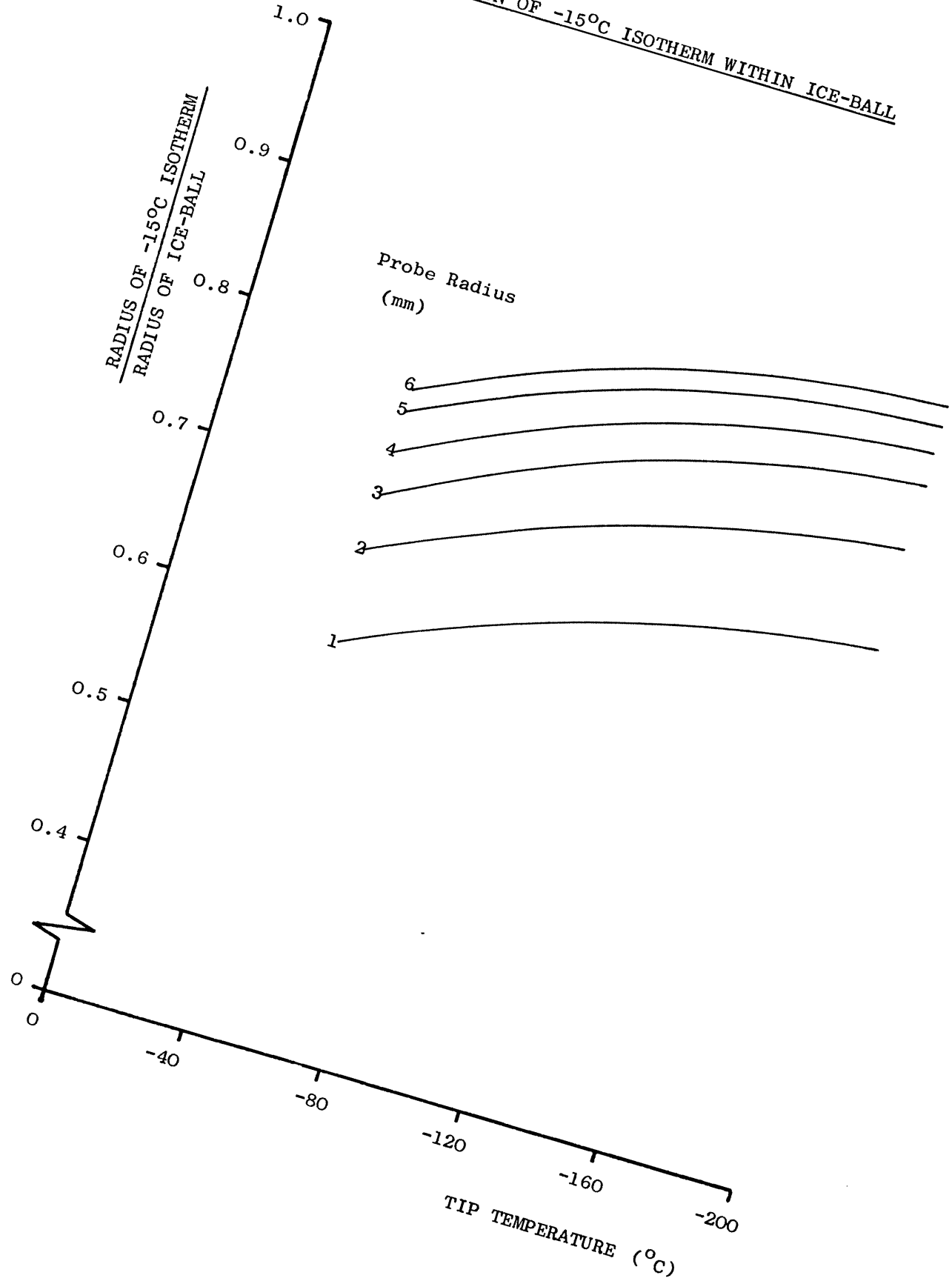

Applying Fouriers Law to the problem of heat tranfer through a hemi-spherical shell of frozen tissue:-

$$\dot{Q} = -k_f 2\pi r^2 \frac{\partial T_f}{\partial r} \qquad (14)$$

Equation 11 expressed the temperature within the ice-ball, T_f , as a function of radius, r . This equation can be differentiated to give the temperature gradient,

$$\frac{\partial T_f}{\partial r} = (T_o - T_t)\left(\frac{r_o r_t}{r_o - r_t}\right)\left(\frac{1}{r^2}\right) \qquad (15)$$

Substituting equation 15 into equation14 and assuming $T_o = 0$

$$\dot{Q} = \frac{2\pi k_f T_t r_t}{\left(1 - \frac{r_t}{r_o}\right)} \qquad (16)$$

3.6.2 Results for cryoprobe heat transfer

Equation 16 was used to calculate the maximum heat transfer through the ice-ball to the cryoprobe, for tip temperatures ranging from 0°C to -200°C, and for tip radii ranging from 1mm to 6mm. Some results are plotted in Figure 13 for 1mm and 6mm radius tips. These results will be used in defining a performance specification for the cryoprobe, and in Chapter 6 in a discussion of tip equilibrium temperatures.

FIGURE I3

HEAT TRANSFER THROUGH ICE-BALL

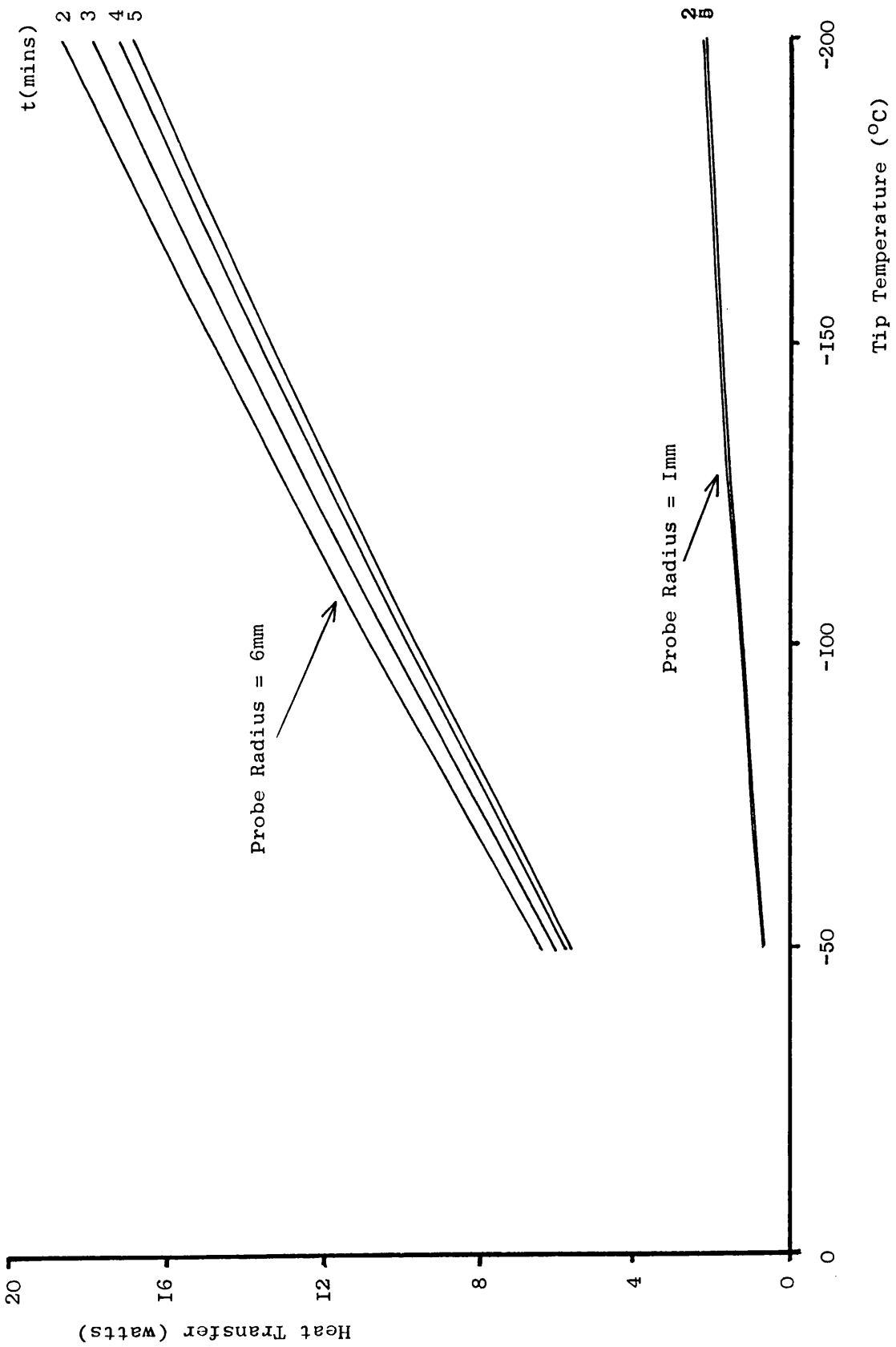

3.7 Conclusions About Cryoprobe Design From Analyses

3.7.1 The number of cooling tips

The calculations of ice-ball radius as a function of time show that smaller probes freeze more tissue for their size than large probes (see **Figure** 9). A tumour 3 cms in diameter could be more easily frozen using several small probes spread over its surface rather than one large one placed in the middle.

There are other advantages in using multi-tipped cryoprobes:-

1. Several discrete cold tips would enable an irregularly shaped tumour to be frozen more easily.

2. Several authors have suggested that a multi-tipped probe would be more effective at providing the appropriate environment for cell death (Cooper 1964, Mazur 1968). Farrant (1971) has proposed that by surrounding the target area with cold sinks, it may be possible to expose the cells uniformly to the most hazardous conditions for the cell type involved and to dispense with the need for very low cryoprobe tip temperatures.

The tumour to be destroyed will not always be large. It could vary in size from a couple of millimetres in diameter to 30mm. Consequently if a multi-tipped probe is to be used, the number of tips in use may have to vary. It would also be desirable that the tips could be placed independently of each other, to accommodate irregularly shaped tumours. If these features were incorporated it would make the cryoprobe

design, and its operation by the surgeon, very much more complicated than a single probe tip. Consequently it was decided that initially the probe should have only one tip but that the possibility of installing several tips would be investigated.

3.7.2 Cryoprobe Specification.

The theoretical results discussed in Sections 3-2 to 3-6 provide an understanding about the influence of the major probe variables on its performance. From the results obtained, a performance specification can be defined.

Section 3-3 examined the cooling rate experienced by the cells within the ice-ball. The rates obtained are initially high but decrease rapidly to below the rates needed for intracellular freezing. Consequently it is not possible using a single tip, to base the tip design on achieving intracellular freezing throughout the ice-ball.

The studies reviewed in **Chapter 2** also showed that when in vivo freezing was implemented all the cells cooled below -15°C were killed, irrespective of cooling rate. It was decided to base the probe specification on achieving this critical temperature rather than achieving a critical cooling rate. All the cells within the 3cm diameter tumour would have to be cooled below -15°C in the 5 minute freeze.

The cooling curves displayed in **Figures 5** to 7 show that ice-balls in the order of 3cms can only be

obtained in 5 minutes if the probe is larger than 4mm in radius with a tip temperature below about -125°C. Bearing in mind the location of the -15°C isotherm within the ice-ball, as shown in **Figure 12**, the actual size of ice-ball needed is nearer 17mm radius. On the basis of this information it was decided that a 6mm radius tip would be needed, and the tip temperature would need to be cooler than -150°C.

Results of heat transfer calculations for the probe are featured in **Figure 13**. A 6mm radius tip cooled below -150°C would require a tip heat flux greater than 14 watts.

3.8 Experimental Measurements of Ice-ball Growth

3.8.1 Reasons for taking measurements

The thermodynamic specification for the cryoprobe tip is crucial to the whole rectal cryoprobe design. It was therefore decided to check the theoretical predictions by measuring the growth of ice-balls in the laboratory under controlled conditions. The test rig used would also serve to assess the performance of the completed instrument.

3.8.2 Apparatus

A simple freezing tip was used for all these measurements and is illustrated in **Figure 14**. The probe was cooled by liquid nitrogen and had interchangeable tips so that the effect of tip radius on ice-ball growth could be explored.

FIGURE 14

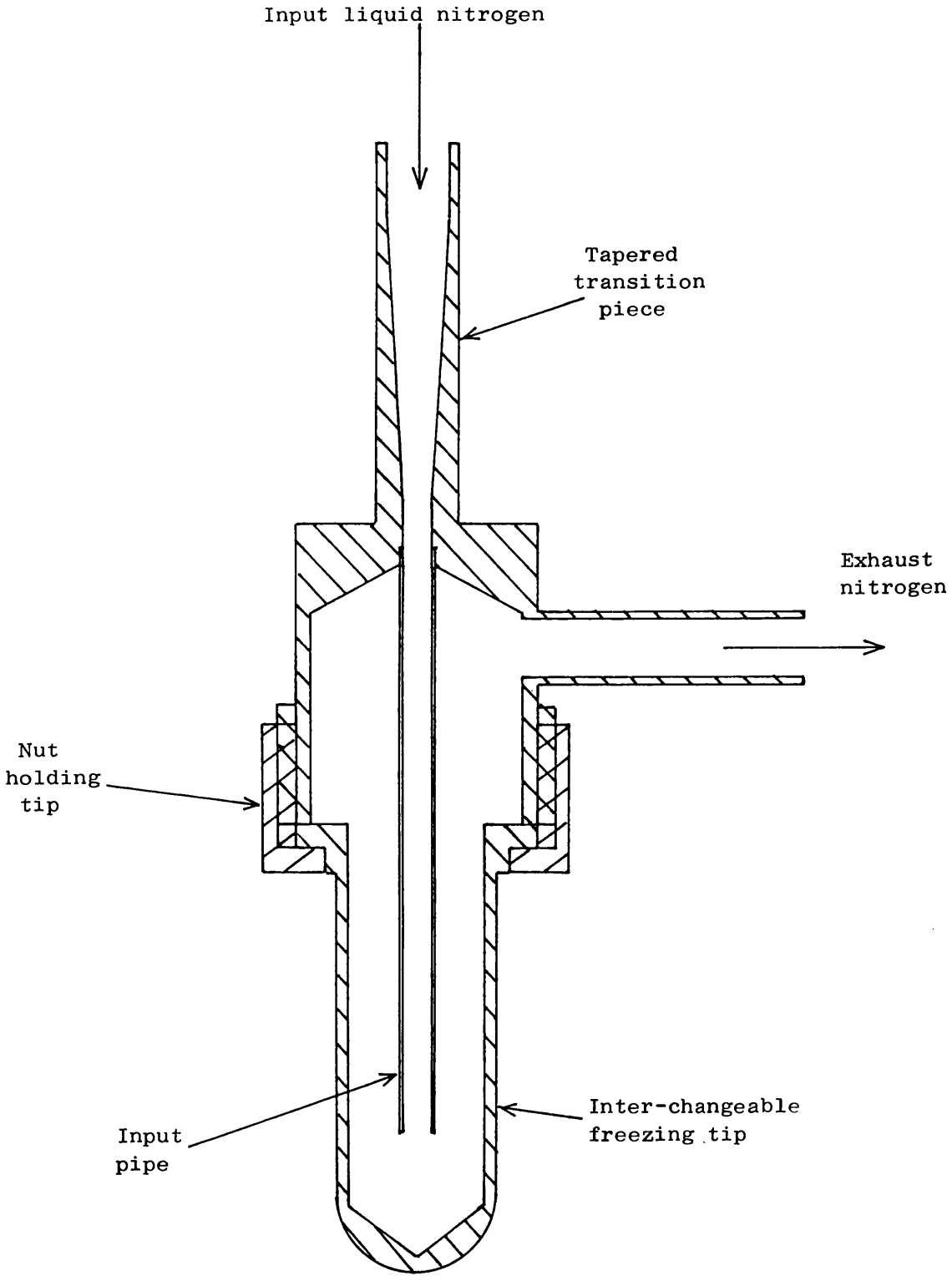

TEST TIP HOLDER

It was decided to freeze a gel solution in a small plastic tank, rather than freeze a piece of animal tissue. The gel provided a controlled medium that was homogeneous and of constant geometry. The gel form of the solution also prevented convection currents. The solution used was a 1.5% solution of gelatin in water. This forms a transparent gel at room temperatures and has a thermal conductivity similar to that of tissues (Lenz, 1961).

Measurement of the ice-ball radius as a function of time was not an easy process. Published techniques have included measurement of the ice-ball mass (Amoils 1968), and photography of the growing ice-ball, either directly (Harly and Aastrup 1972) or by means of cholesteric liquid crystals (Cooper and Petrovic 1974). Many possibilities were looked at but eventually a simple technique was used which, although suffering from some measurement errors, did provide a quick and simple technique.

The measurements were taken using the apparatus illustrated in **Figure 15.** A fine line was scribed on two perspex panels that could move either side of the perspex tank containing the gelatin. By observing through the gelatin, the operator could align the marks scribed in the perspex with the edge of the ice-ball. The perspex panels were joined and their motion controlled by a leadscrew connected to them. The leadscrew also moved a linear potentiometer, the output of which was displayed on a U.V. recorder.

FIGURE 15

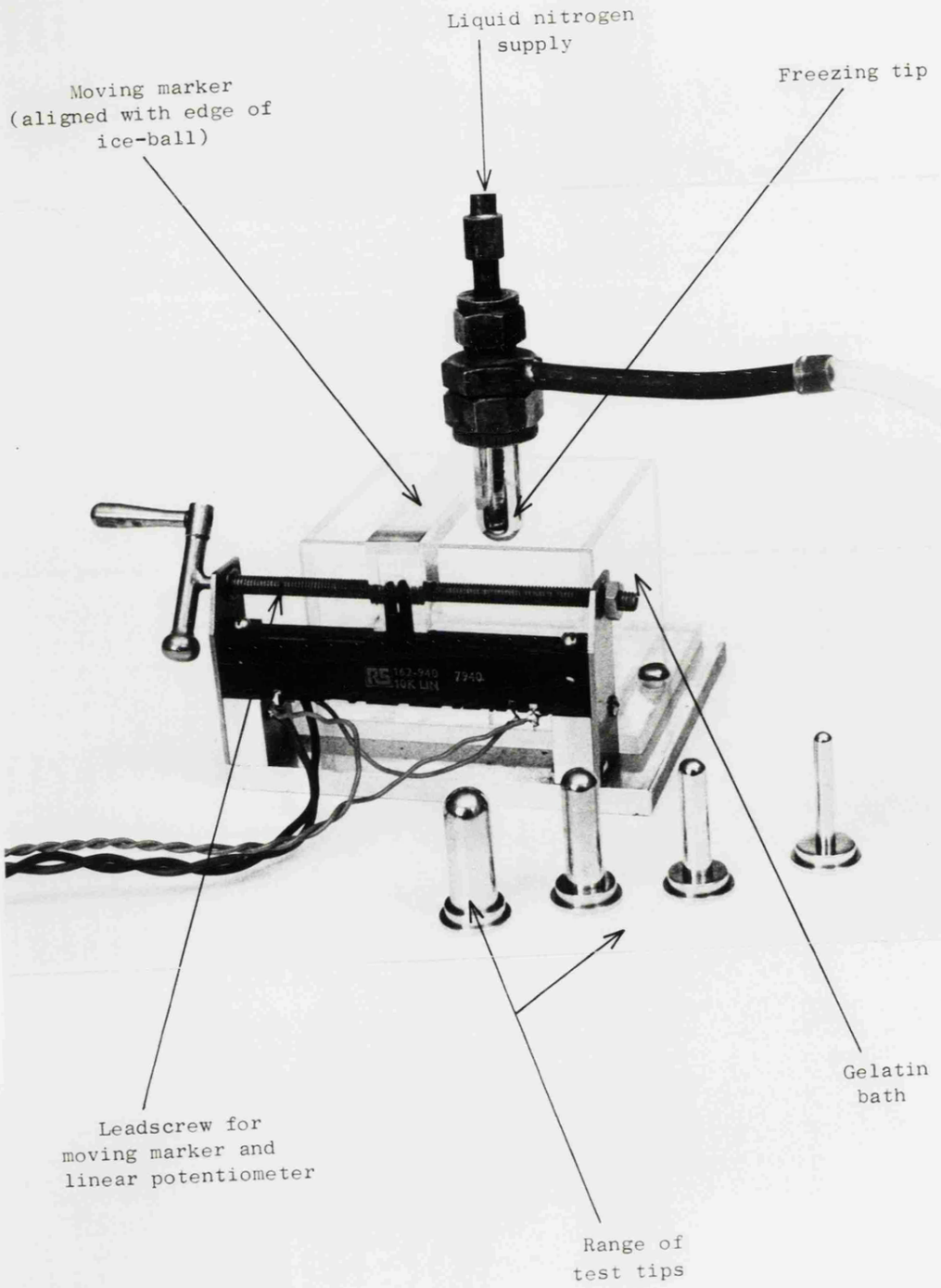

TEST APPARATUS FOR MEASURING ICE-BALL GROWTH

3.8.3 Method

The freezing tip was placed on to the gel such that the contact surface was a hemisphere. The two indicating lines were aligned with the edge of the tip and the chart recorder zeroed. The nitrogen was turned on and as the ice-ball grew in the gelatin, the two fine lines would be continuously moved to line up with its edge by turning the leadscrew. In this way a time/radius curve was obtained.

An alternative technique of monitoring ice-ball growth used a capacitance measurement. The technique looked very promising but was not explored at length because of lack of suitable apparatus. The gelatin was dissolved in a saline solution (0.9% NaCl) to make the gel electrically conductive. Once frozen, however, the gel became an electrical insulator. As the ice-ball grew, capacitance measurements were taken between the cryoprobe itself and the conductive gel near the edge of the measuring tank. One plate of the capacitor was the cryoprobe and, because the unfrozen gel was highly electrically conductive, the other plate was the gel surrounding the outside of the ice-ball (see **Figure 16**). The dielectric was the frozen and non-conductive ice-ball. As the ice-ball grew the capacitance increased and provided a measure of ice-ball size. This description is probably an over simplification of the processes taking place but was the rationale behind the test. The technique appeared promising and a

FIGURE 16

MONITORING ICE-BALL CAPACITANCE

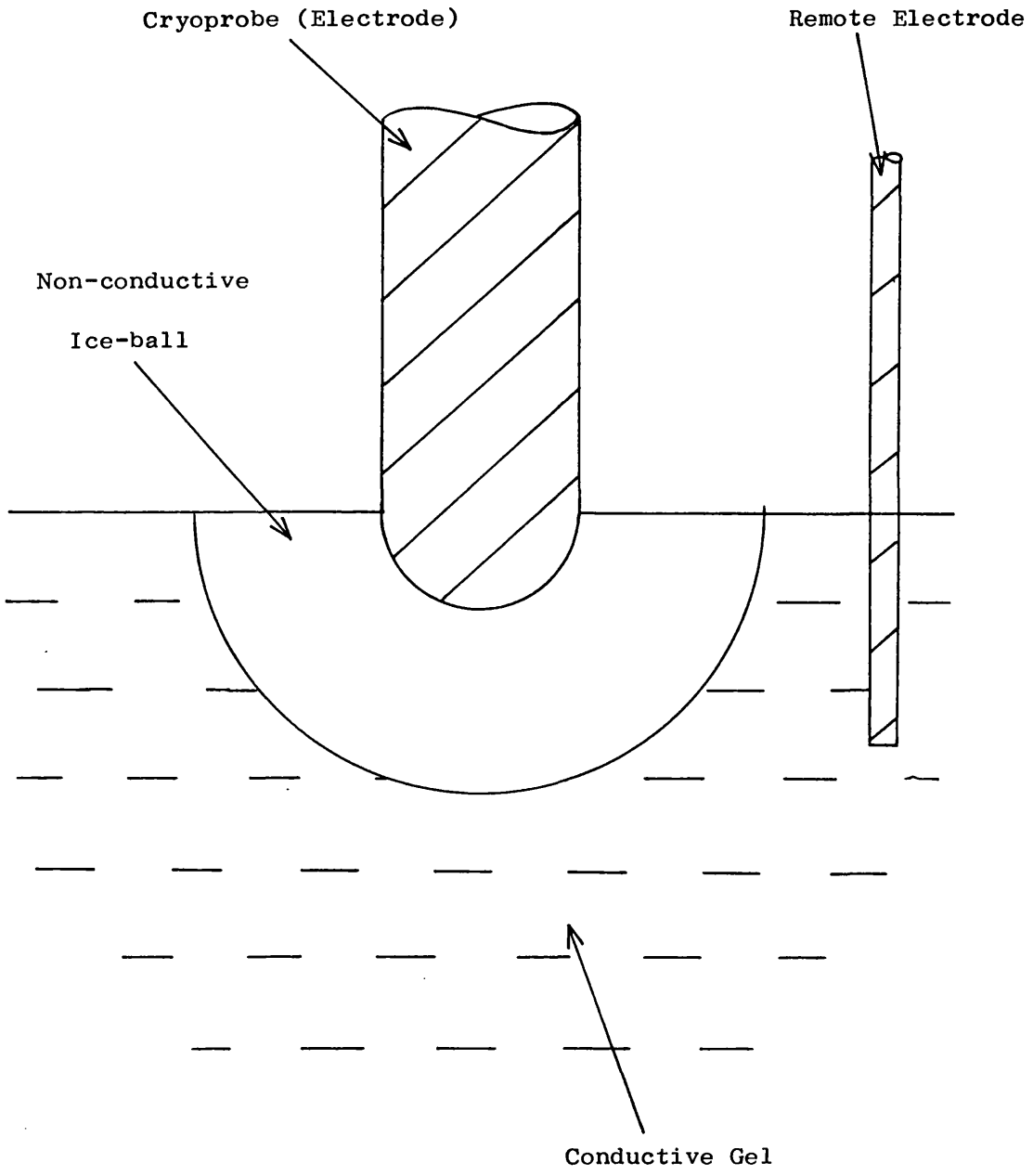

calibration curve is included in **Figure 17.** It may well be worth exploring as a means of monitoring ice-ball growth during cryosurgery as tissue also acts as a good electrical conductor until it is frozen.

3.8.4 Results

Some typical recordings obtained using the optical method are illustrated in **Figure 18.** **Figure 19** shows measured results of ice-ball radius against time for different tip radii and a comparison is made with the theoretical predictions. As can be seen the correlation is good.

Following several such experiments it was concluded that the theoretical predictions of ice-ball growth were accurate and the trends real. The predictions should provide a valid basis for the cryoprobe performance specification.

3.9 Conclusions

The rectal cryoprobe should ideally use multiple tips for freezing a tumour, but initially a single tip should be used to avoid over complication. The tip needs to meet the following specification.

1. The tip radius should be 6mm.
2. The tip temperature should be cooler than -150°C.
3. The tip heat flux should be greater than 14 watts.

Experimental measurements of ice-ball growth

FIGURE 17

CAPACITANCE OF GROWING ICE-BALL

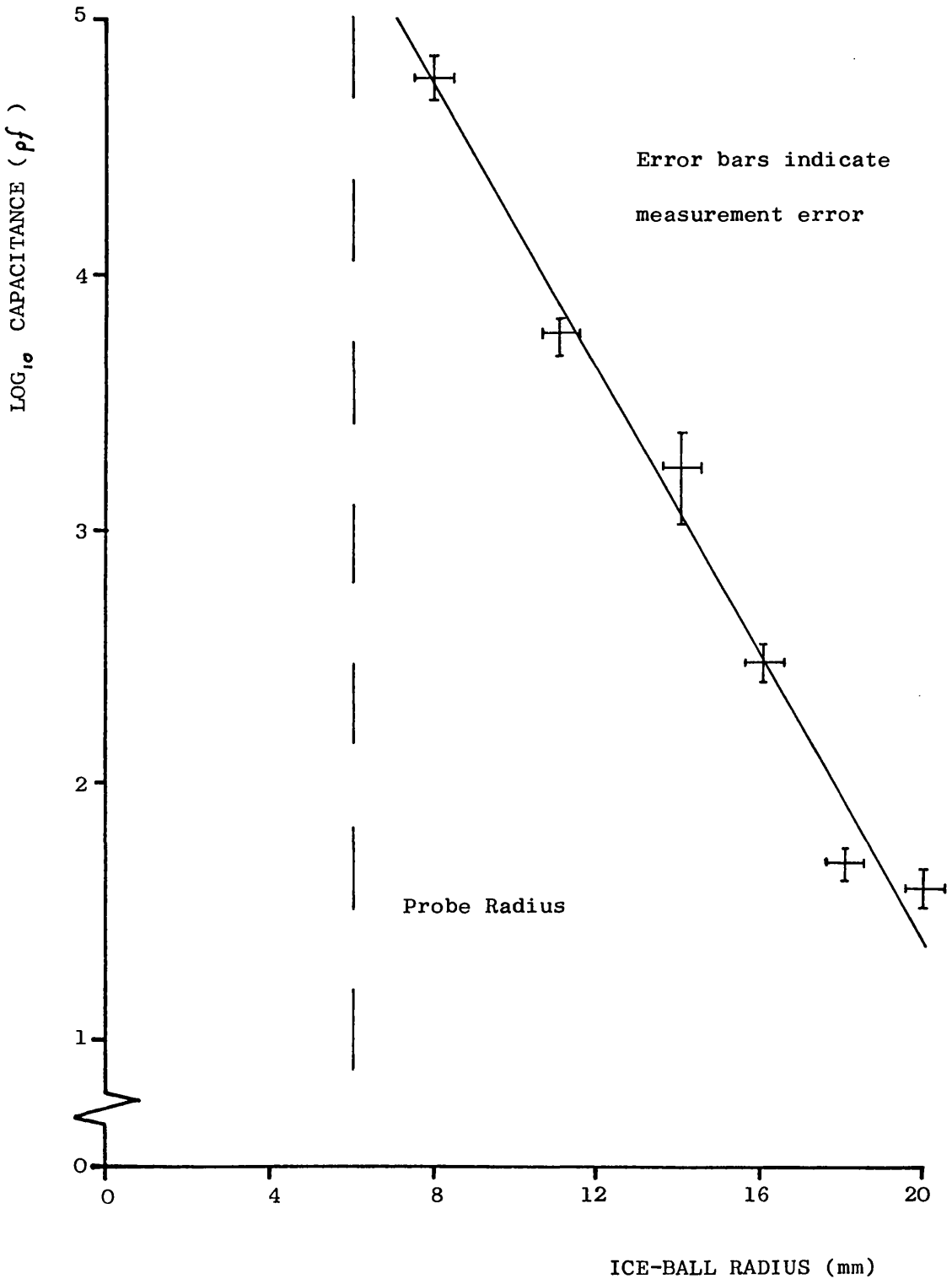

FIGURE 18

TRACING OF OUTPUT FROM ICE-BALL MEASURING RIG, TOGETHER WITH TIP TEMPERATURE

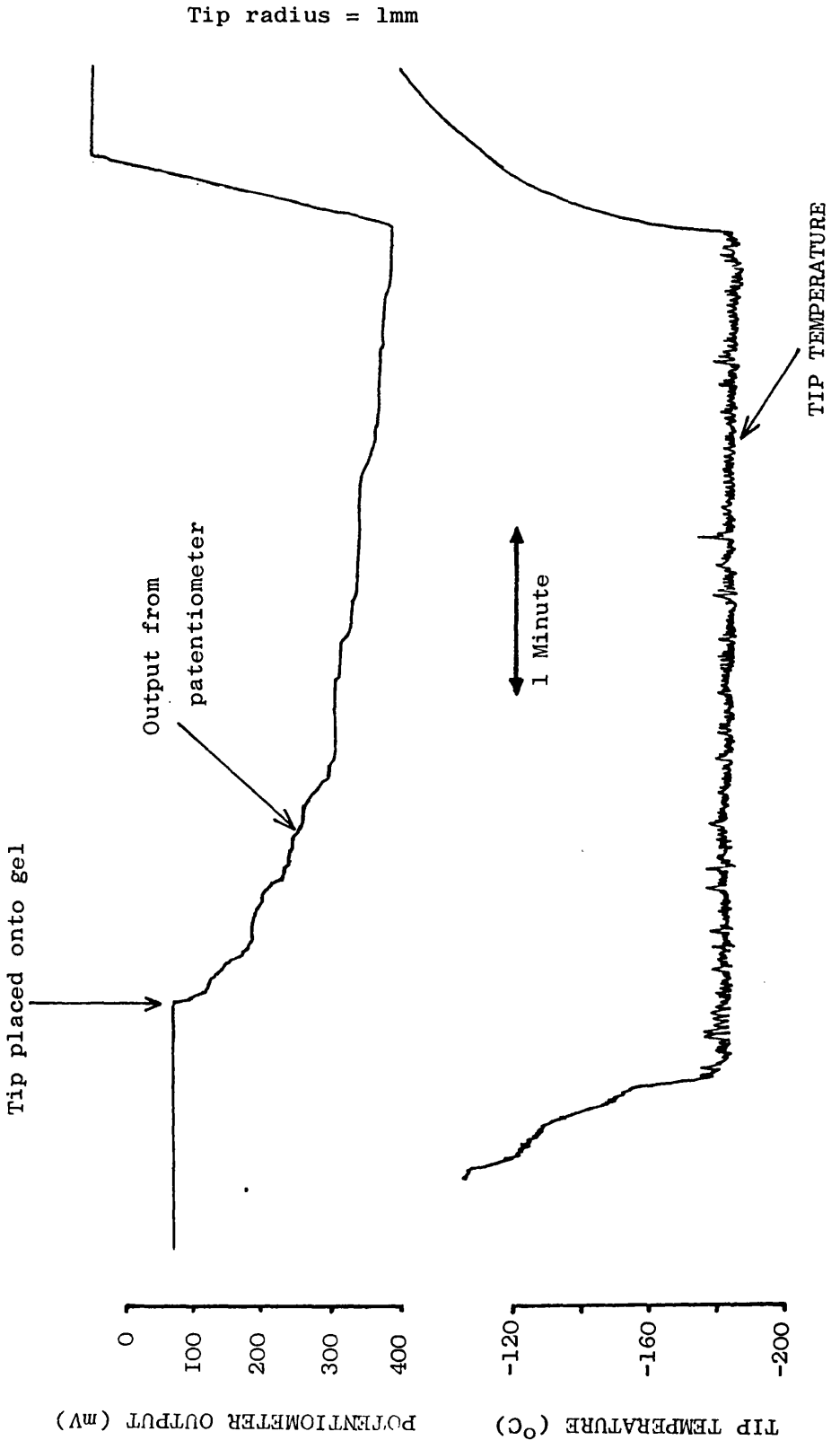

FIGURE 19

COMPARISON BETWEEN THEORY AND MEASURED RESULTS

OF ICE-BALL GROWTH

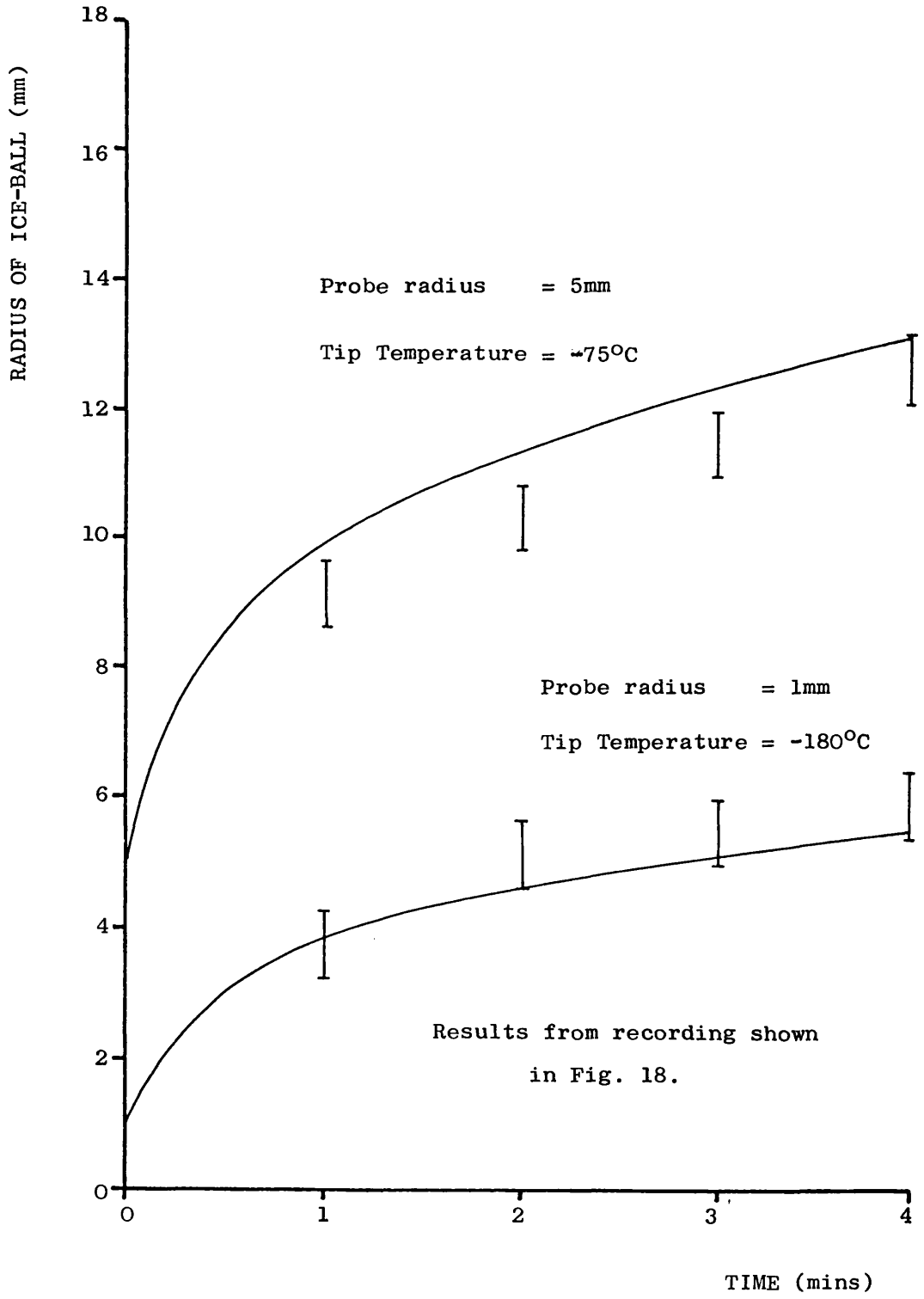

indicate that the theoretical predictions are accurate.

CHAPTER 4

CHOICE OF COOLING SYSTEM

4.1 Introduction

There are many ways of achieving the low tip temperatures needed for an effective cryoprobe. In this chapter various techniques are examined in the light of the performance specification derived in Chapter 3, to see which method would be most appropriate for the rectal cryoprobe. The two main techniques currently used, boiling liquid nitrogen and expansion of high pressure fluids, are initially examined in detail. However, other techniques that have been investigated are also reviewed, to see if they have potential for the rectal probe.

4.2 History of surgical freezing techniques

The equipment used to generate cryogenic temperatures for surgical use has, over the last 130 years, reflected the technology available at the time. Mixtures of salt and ice were used originally by Arnott in his pioneering work in 1851 (Arnott 1851). A technique used later in the 19th century was the evaporation of ether (Openchowski 1883). As liquified gases became more universally available, swabs dipped in liquid air started to be used, as well as sprays of the same fluid (White 1899). Solid carbon dioxide was also

TABLE I

TIP THERMODYNAMIC BEHAVIOUR OF SEVERAL FLUIDS COMMONLY USED IN CRYOPROBES

	N_2O	CO_2	Freon-I2	N_2
Temperature of fluid in tip (°C)	-88.5	-78.5	-29.8	-I95.8
Maximum enthalpy change in tip (kJ/kg)	I73	I7I	I2I	209

Values for fluids used in Joule-Thomson probes assume adiabatic expansion from their vapour pressure at 20°C to atmospheric pressure, along a path such as that shown in Figure 24

used, shaped in the form of a pencil (Bietti 1935). Cryoprobes with a cooling agent circulating through them did not appear until the late 1950's, when a mixture of solid carbon dioxide and acetone was used to provide a cooling source (Rowbotham et al 1959). Liquid nitrogen cryoprobes did not come into use until the work of Cooper in the early 1960's (Cooper and Lee 1961, Cooper et al 1962), and later in that decade the high pressure type of cryoprobe, utilising a Joule-Thomson expansion, came into use (Amoils 1967). These last two techniques of cooling, Joule-Thomson cryoprobes and liquid nitrogen devices are employed in the bulk of the equipment in use today.

4.3 Current Techniques of Cooling

4.3.1 Joule-Thomson cryoprobes

A major technique of cooling cryoprobes is to use a Joule-Thomson expansion of a suitable working fluid. The high pressure fluid is usually expanded within the tip itself. The low pressure exhaust fluid is then channeled back along the probe to be passed into the atmosphere. The temperature of the expanded fluid varies according to the fluid being used and **Table 1** summarises the temperatures expected for several typical fluids, assuming they are expanded adiabatically from their vapour pressure at 20°C, to atmospheric pressure. The latent heat of vapourisation at the normal boiling point is also tabulated. As can be seen the temperatures of the expanded fluids do not achieve the

low levels reached with liquid nitrogen.

The most commonly used fluid in Joule-Thomson cryoprobes is nitrous oxide (Amoils 1967, Wright 1971). This is a widely available gas in hospitals and has a high latent heat of vapourisation at its normal boiling point. A possible disadvantage of nitrous-oxide is its toxicity. It has been suspected for some time that there is a link between exposure to this anaesthetic gas and the frequency of miscarriages (Lane 1980). Consequently the large volumes of gas exhausted from the cryoprobe during use have to be piped outside. Other fluids used are carbon-dioxide (Bellows 1966, Shalimov et al 1976) and the Freons (Barron 1971).

4.3.2 Liquid nitrogen cryoprobes

Liquid nitrogen cryoprobes cool by extracting the latent heat of boiling nitrogen from tissues. They can be either open circuit or closed circuit. The open circuit devices, known as cryosprayers, simply squirt the liquid/gas mixture onto the tissue to be destroyed. They are very powerful freezers because a large surface area of tissue can be cooled to a low temperature, which means a large ice-ball can be formed. However, cryo-sprayers do suffer from problems of control. A lot of liquid can run off from the target area and cause unwanted freezing elsewhere. In addition, the cold nitrogen condenses water vapour in the air to form large foggy clouds.

The control problems associated with cryosprayers

can be overcome by using closed circuit cryoprobes. In these devices the liquid nitrogen is passed into the tip of the probe where it boils and extracts its latent heat of boiling from the tip. The tip in turn is used to conduct heat away from the tissues. The exhaust fluid from the tip is passed back along the cryoprobe to be channelled into the atmosphere at some convenient point away from the patient. Closed circuit cryoprobes are far more controllable than cryosprayers but are not as powerful because the heat transfer from the tissues to the boiling cryogen is a two step process. Heat is conducted from the tissues to the probe tip, and then transferred to the boiling liquid inside.

An elegant demonstration of the relative cooling powers of open and closed circuit cryoprobes was made by Bradley (1977). He took infra-red thermograms of ice-balls formed by these instruments for a given flow rate of nitrogen. Much larger volumes of ice were formed by the cryosprayer.

4.4 The System Design of Joule-Thomson Cryoprobes

4.4.1 Transport of working fluid to freezing tip

A typical Joule-Thomson cryoprobe system is illustrated diagramatically in **Figure 20** . The cryogen is stored in a high pressure cylinder and the fluid is passed through a pressure regulator to the cryoprobe via a flexible hose that can withstand the operating pressures (about 50 atmospheres for N_2O). In the probe the fluid is again simply transported to the tip.

FIGURE 20

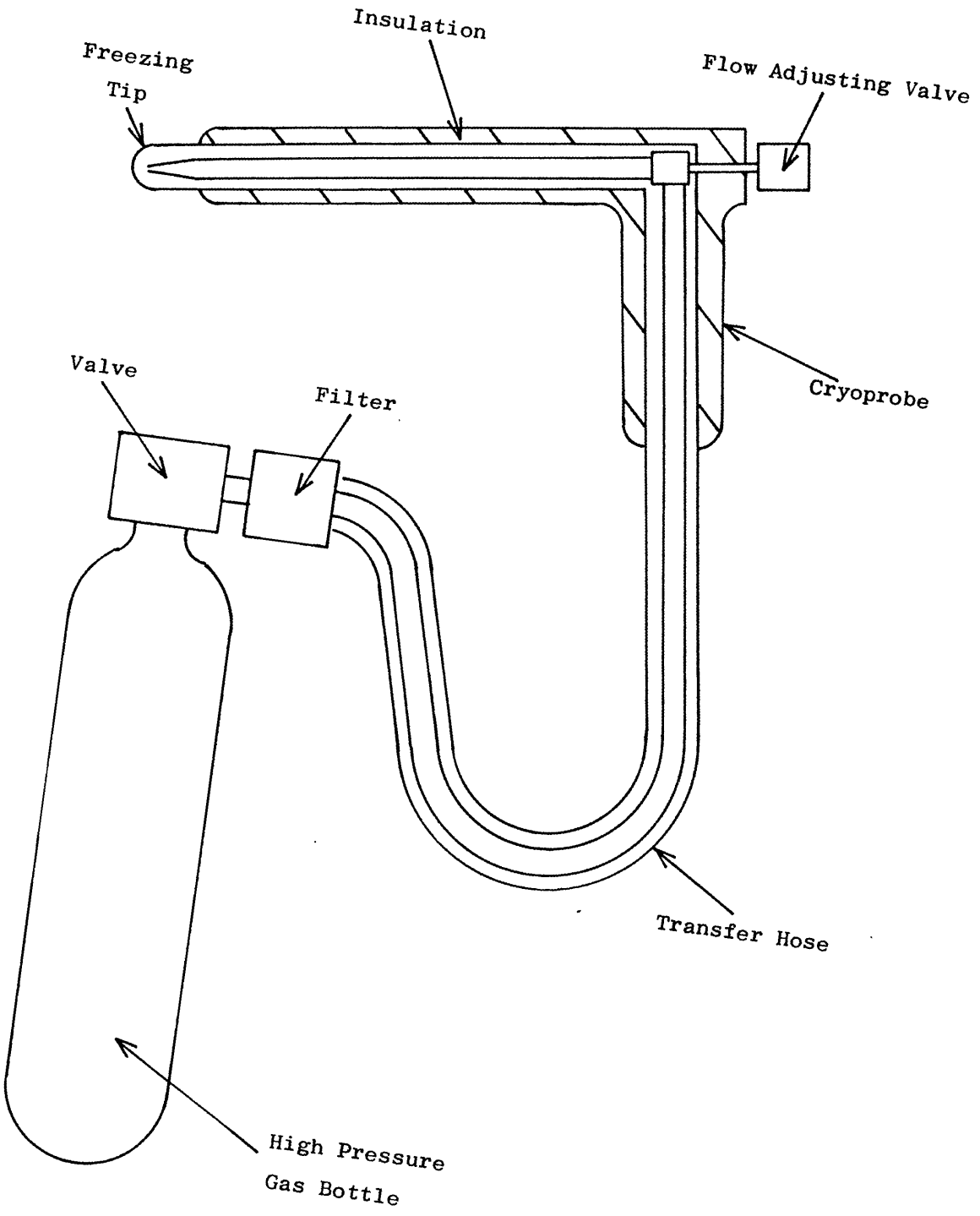

DIAGRAM OF JOULE-THOMSON CRYOPROBE SYSTEM

During its transfer from the storage bottle to the tip the fluid is at room temperature, and so no cooling of the probe and hose occurs.

4.4.2 Expansion of working fluid

In the tip the fluid is expanded through a narrow orifice. The size of the orifice has to be carefully controlled to produce the necessary pressure drop. Any change in its size can markedly affect the cryoprobe performance. The main source of problems lies with particulate matter in the cryogen supply. A filter in the line is usually used to overcome this problem. Ice crystals especially cause difficulties as any water vapour in the high pressure gas supply will crystalise as soon as the gas temperature drops below zero (Shalimov 1976).

4.4.3 Transport of working fluid away from the tip

Once the fluid has been expanded in the tip, it has to be transported back along the hose to be exhausted. However the fluid is now cold and can cool not only the tip but the rest of the cryoprobe as well. Some form of thermal insulation is needed around the shaft of the probe and its handle. A sheath of plastic normally suffices because the cooling power of the exhaust is not excessive.

The problem of probe shaft cooling can be reduced by passing the warm high pressure fluid to the tip along the outer pipe of the cryoprobe rather than the inner

one (**Figure 21**). The cold exhaust gas is then removed through the inner pipe. The warm in-coming fluid can in this way keep the casing warm. Cryoprobes with this facility can produce ice-balls that are more limited to the tip and do not spread back along the shaft (Wright 1971).

4.4.4 Problem of supply cylinder cooling

A further problem with high pressure cryoprobe systems is the cooling of the supply cylinder. This cooling is especially noticeable with small cylinders after prolonged operation when the cylinder becomes very cold and the cryoprobe performance deteriorates. The reason for this is that as gas is piped away from the cylinder, some of the remaining liquid evaporates to replace the gas removed. The heat of vapourisation for this boiling comes from the liquid phase in the supply cylinder and it cools.

The cylinder cooling would not be a significant problem if it were not for the fact that as the contents of the cylinder cool, so their pressure drops. The effectiveness of a high pressure probe is largely dependent on the gas supply pressure. The net result therefore of the cold induced pressure drop is that the cryoprobes cooling power is reduced. Some authors have suggested overcoming this problem by surrounding the high pressure cylinder with warm water (Wild 1975).

FIGURE 21

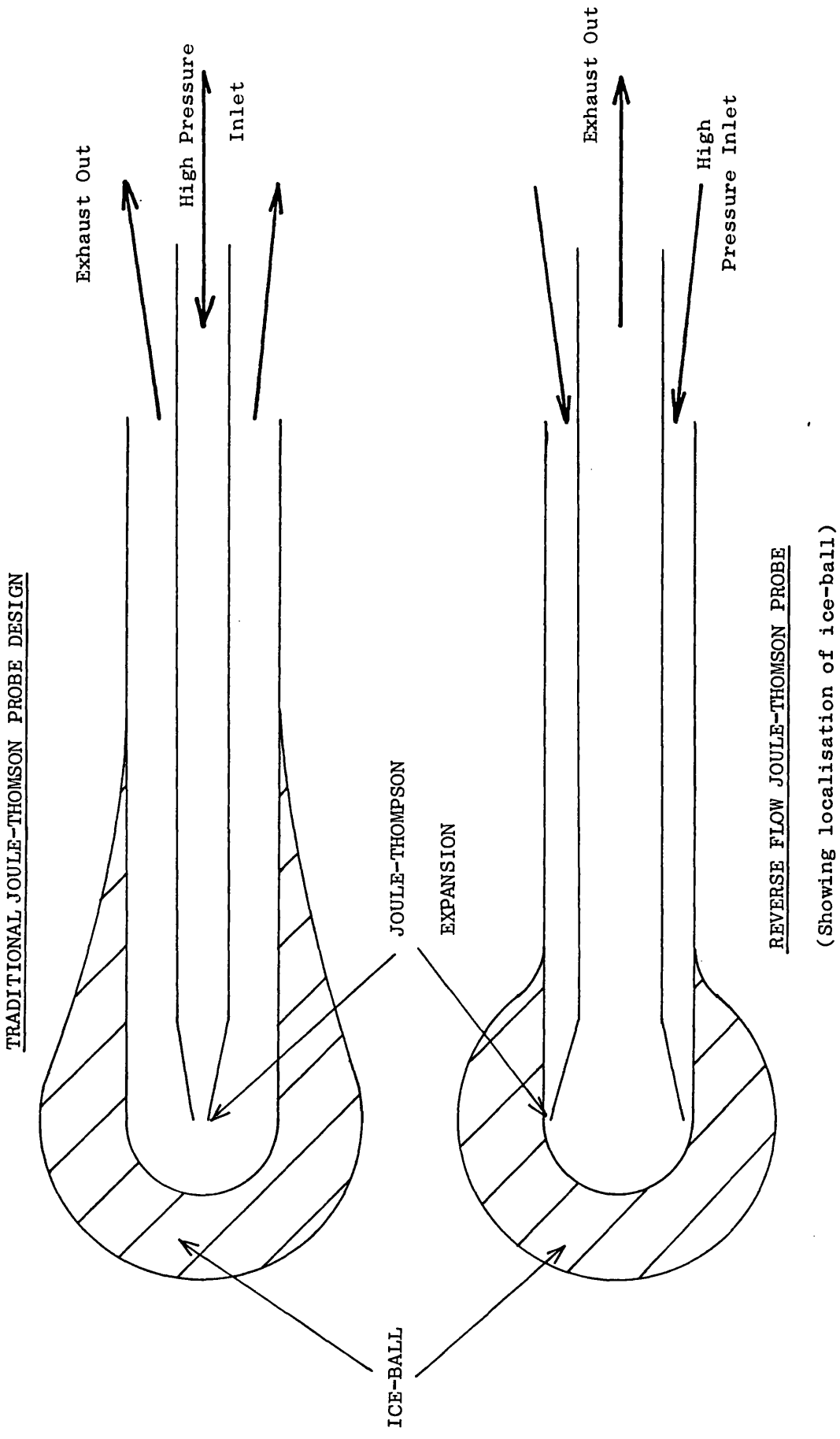
TRADITIONAL JOULE-THOMSON PROBE DESIGN
Exhaust Out
High Pressure Inlet
JOULE-THOMPSON EXPANSION
ICE-BALL
REVERSE FLOW JOULE-THOMSON PROBE
(Showing localisation of ice-ball)
Exhaust Out
High Pressure Inlet

4.5 The System Design of Liquid Nitrogen Cryoprobes

4.5.1 Storage of cryogen

Figure 22 illustrates a typical liquid nitrogen cryoprobe system. The transfer and storage problems for these devices are much more acute than for Joule-Thomson probes. The liquified gas is stored in well insulated dewars which are quite expensive. Liquid is continuously lost when the instrument is not in use.

4.5.2 Transport of working fluid to tip

The transport of the liquid from the dewar to the cryoprobe tip also causes some difficulties. All hoses, pipes and valves used on a liquid nitrogen system will initially be warm. When the liquid is turned on, substantial quantities of the cryogen will boil off during its transfer in the pipework, and this evaporation will continue until it has cooled the pipes and valves near to the boiling point of the liquid. Until the pipe cooling has taken place, the fluid reaching the tip will not have much liquid left in it, and the performance of the cryoprobe will be generally poor.

To prevent this initial reduction in performance, many liquid nitrogen devices need a pre-cool before use. The cryogen flow is turned on for a few minutes before the surgeon uses the device, in order to cool all the supply pipes. This pre-cool can take up to 15 minutes with some cryoprobes because of the incorporation of large masses of metal, such as solenoid valves, in the

FIGURE 22

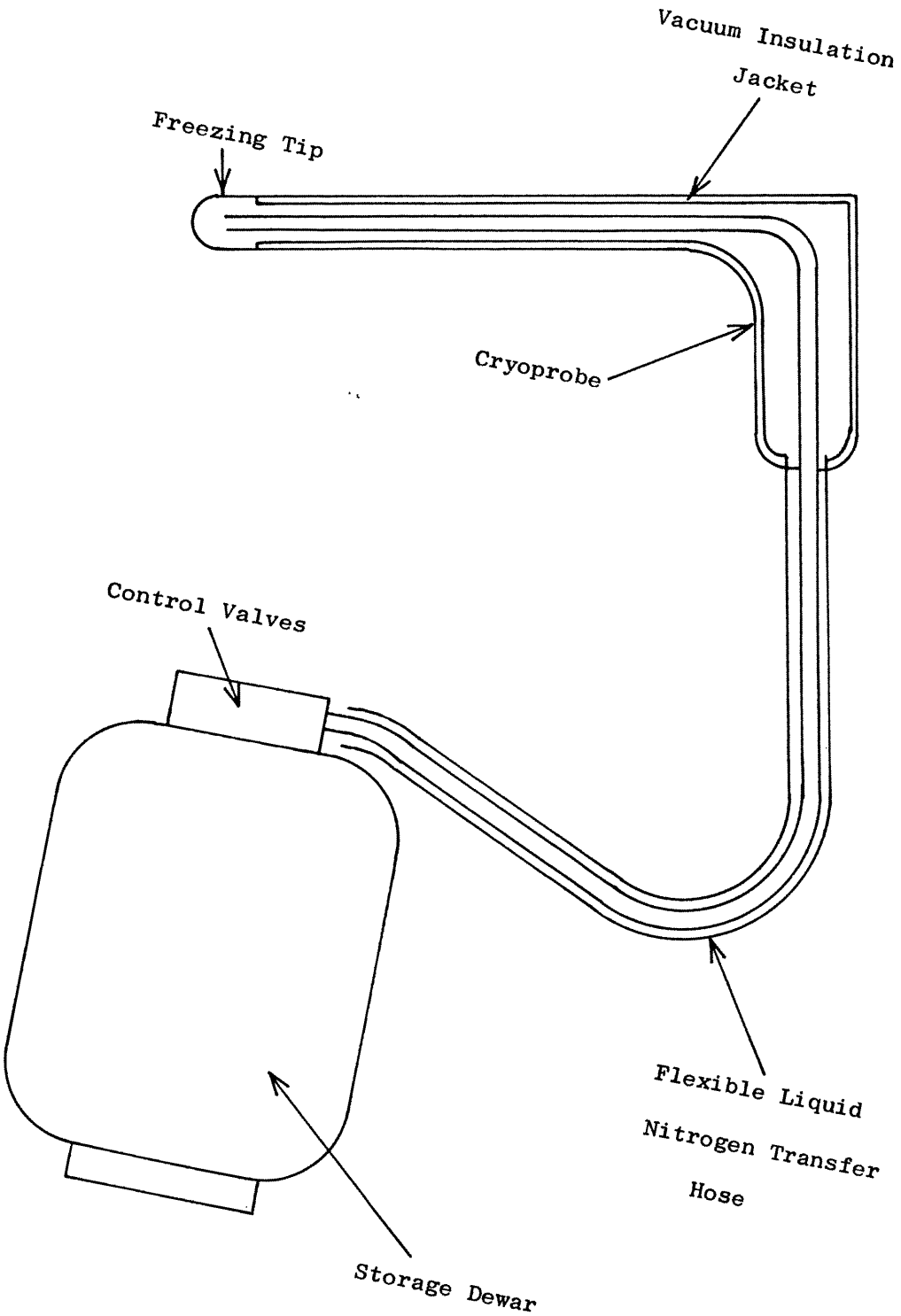

DIAGRAM OF LIQUID NITROGEN CRYOPROBE SYSTEM

supply.

4.5.3 Cryoprobe thermal insulation

Once the liquid has been boiled in the tip, the exhaust gas is piped away. The exhaust nitrogen is cold and usually the vapour/liquid mixture will have a substantial fraction of liquid. Because of this, both the exhaust pipes and the supply pipes of a liquid nitrogen probe are capable of producing a powerful cooling effect.

To make sure only the tip of the cryoprobe is cold on the outside, large amounts of thermal insulation have to be employed around the cryoprobe, usually in the form of a vacuum jacket around the cryoprobe shaft and handle. These vacuum sheaths can be unreliable. They have a small volume and the vacuum can quickly degrade following out-gassing of flux residues, etc. Some manufacturers have tried to overcome this problem by vacuum brazing their products.

4.5.4 Flexible transfer hose

A flexible transfer hose is needed to carry the cryogen from the dewars to the probe and to return the exhaust fluid. To keep this flexible after it has been cooled, it is usually made from corrugated PTFE or stainless steel. To prevent the hose from becoming too cold to the touch, it has to be wrapped in a sheath of insulating plastic. The resulting assembly can be bulky and some flexibility is inevitably lost.

4.6 Comparison between Liquid Nitrogen and Joule-Thomson Cryoprobes

4.6.1 Differences of tip temperature

The most obvious performance difference between Joule-Thomson and liquid nitrogen probes is the tip temperature that can be achieved. The fluid inside the tip of a liquid nitrogen device will be at -196°C whereas that expanded into the tip of a Joule-Thomson probe will be at a much higher temperature. A nitrous oxide probe, for example, will contain fluid around -88°C. The tip temperatures achievable with these probes will of course reflect these differences.

4.6.2 Differences of tip heat flux

The other major performance difference between Joule-Thomson and liquid nitrogen probes is the tip heat flux. Consider the tip of a simple cryoprobe and assume conditions of steady flow. Applying the steady flow energy equation to the probe tips, initially between conditions at position 2 and position 3, as shown in Figure 23 .

$$\dot{Q} - \dot{W} = \dot{m}\left[\Delta\left(h_e + \tfrac{1}{2}u^2 + gz\right)\right] \qquad (17)$$

where $\dot{Q}$ = heat flux

$\dot{W}$ = rate of work done

FIGURE 23

Liquid Nitrogen Probe

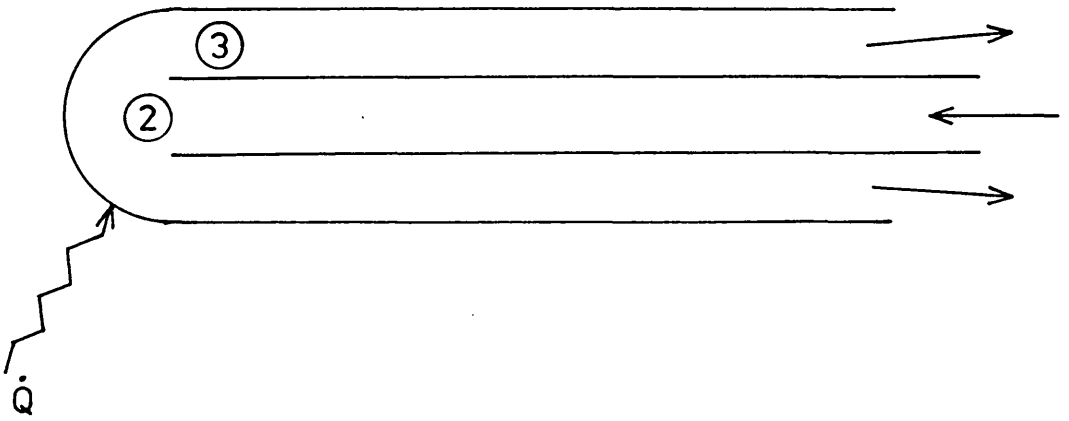

High Pressure Probe

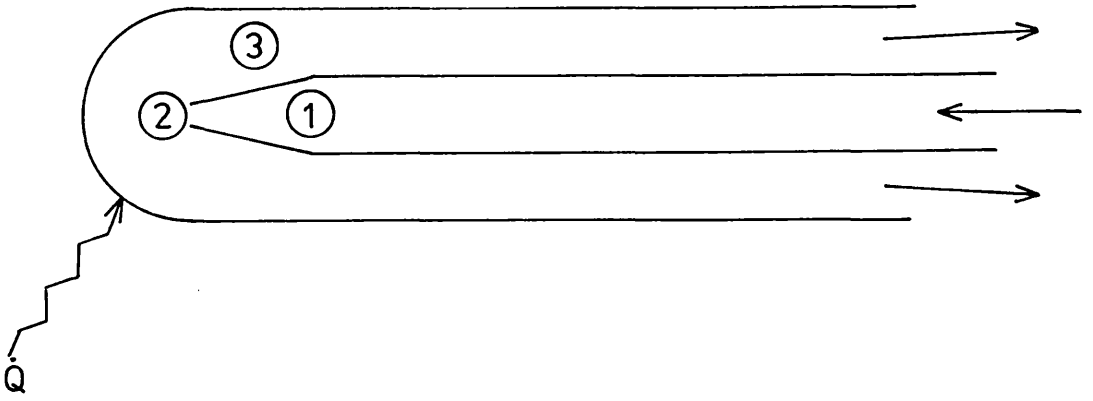

POSITIONS USED IN APPLYING THE STEADY

FLOW ENERGY EQUATION TO CRYOPROBE TIPS

$\dot{m}$ = mass flow rate

h_e = specific enthalpy

u = specific velocity

g = gravitational acceleration

z = vertical co-ordinate

For the tip, $\dot{W} = \Delta u = \Delta z = 0$

$$\therefore \quad \dot{Q} = \dot{m}(h_{e3} - h_{e2}) \qquad (18)$$

In order to compare the two types of probe it is further assumed that the same mass flow rates of cryogen are used for both the liquid nitrogen system and the Joule-Thomson system. To compare the heat fluxes possible with the two systems it is therefore necessary to compare the specific enthalpy change within the tip.

The maximum cooling performance of the two systems will be achieved when the cryogen reaching the tip is a saturated liquid. However in the Joule-Thomson probe the working fluid has to undergo a throttle to achieve a temperature reduction. To estimate the tip enthalpy change for the Joule-Thomson probe it is necessary to apply the S.F.E.E. to the throttle as well.

Applying the S.F.E.E. between position 1 and 2 of Figure 23 , and assuming an adiabatic expansion, with $\dot{W} = \Delta u = \Delta z = 0$,

$$h_{e2} = h_{e1} \qquad (19)$$

Figure 24 shows a temperature/ enthalpy diagram for nitrous oxide, a typical fluid used in Joule-Thomson probes. The enthalpy changes discussed above are indicated.

Table 1 also shows values of $(h_{e3} - h_{e1})$ for several fluids used in Joule-Thomson probes and $(h_{e3} - h_{e2})$ for nitrogen.

4.6.3 Differences of system design

The major differences of system design are as follows:

1. The transfer system in the Joule-Thomson probes has to withstand pressures of many atmospheres.
2. The liquid nitrogen probes require sophisticated cryogen storage facilities.
3. The liquid nitrogen probes require a transfer system that can withstand temperatures of -196°C, including a flexible transfer hose.
4. The liquid nitrogen systems require sophisticated thermal insulation around the probe.

4.6.4 Conclusions on comparisons

The comparison between liquid nitrogen cryoprobes and high pressure devices is therefore one of comparing tip temperature and complexity. The liquid nitrogen probes can produce very low tip temperatures but are complicated because of the need for efficient thermal insulation and the need for a flexible liquid nitrogen transfer hose. The complexity is reflected in the

FIGURE 24

TEMPERATURE/ENTHALPY DIAGRAM FOR N_2O

(data from BOC, 1975)

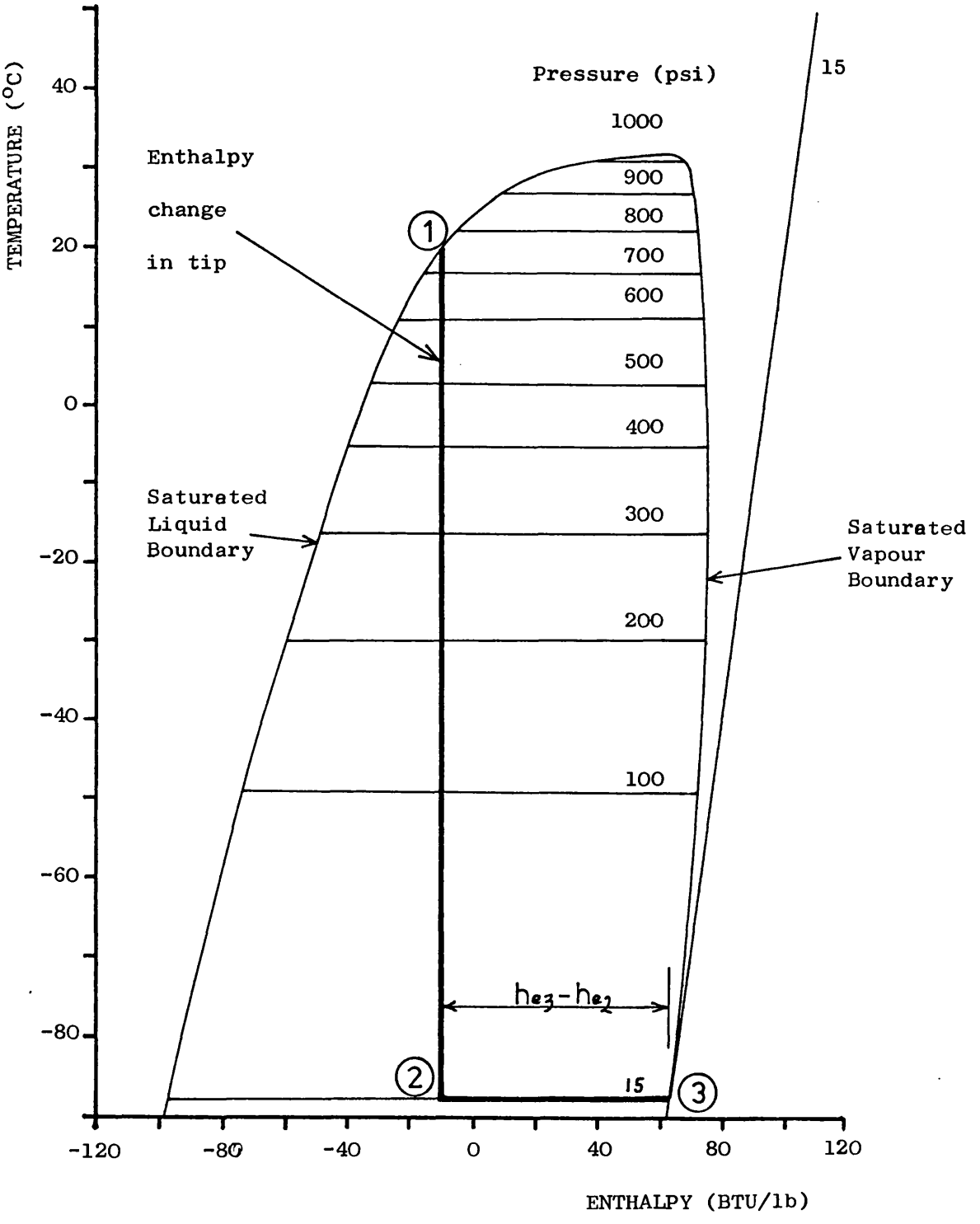

reliability and cost of these devices. High pressure probes cannot produce very low tip temperatures but are much simpler to construct, and therefore cheaper and more reliable.

4.7 Alternative Cooling Techniques

4.7.1 Nitrogen probes using a Joule-Thomson expansion

A few designers have examined a hybrid of the liquid nitrogen and Joule-Thomson probes, namely a Joule-Thomson device that uses nitrogen as the working fluid (Barron 1966, Gorlina et al 1976). In this way it is hoped to combine the advantages of a Joule-Thomson probe (no liquified gas transfer problems, no liquified gas storage needed) with the freezing power of a liquid nitrogen device. The main problem with using nitrogen gas is that there is not a large change in temperature when room temperature gas is adiabatically expanded because of its low critical point. For example an initial expansion from 150 atmospheres to 1 atmosphere cools the gas from 20°C to -8°C. A reflux regenerative heat exchanger is needed to transfer heat from the incoming high pressure fluid to the low pressure exhaust.

Boyarskii and Filippov (1978) compared standard liquid nitrogen probes with those using a Joule-Thompson expansion of nitrogen gas. They concluded that the normal liquid nitrogen cryoprobe was preferable on grounds of simplicity and reliability, but felt there were advantages in using Joule-Thomson devices where

liquid nitrogen was not easily available.

4.7.2 Self-contained liquid nitrogen probes

The problems of transferring liquid nitrogen from the dewar to the cryoprobe have been overcome in some designs by incorporating a small storage dewar on the probe itself. Borthwick (1972) described one of the early designs. This has a miniature version of a normal storage dewar hung below the cryoprobe shaft at the handle end. No pre-cool or insulated hose is needed but these advantages have to be weighed against the somewhat cumbersome nature of the device and the need to keep the dewar upright. The storage dewars usually have sufficient capacity for one freeze, and can form the handle of the probe (Verkin et al 1976a). Some designs have provision for replacing an empty dewar with a full one by simply clipping it in place (Verkin et al 1977). To conserve liquid nitrogen, a cryoprobe developed for removing tonsils had provision for returning any unused liquid back to the storage dewar from the exhaust (Komarov 1974). Several cryosprayer designs have been published which also incorporate a hand-held storage dewar (Verkin et al 1976b, Rundnya et al 1976; Murinets-Markevich et al 1975).

4.7.3 Miscellaneous Cryoprobes

The Peltier effect has been investigated as a possible way of providing cryogenic temperatures for surgical use (Crump 1967). The Peltier effect is the

cooling that results from passing an electrical current between two dissimilar metals. However the temperature reduction achieved is small and it does not appear to be an effective means of cooling.

Heat pipes have also been used to form cryoprobes. However it is difficult to achieve a high mass flow rate of cryogen using a wick for transport and the heat flux is therefore not large. Published information on one device (Zubashich 1976), which had one end immersed in liquid nitrogen and the other acting as the freezing tip, showed it not to be very powerful. The same investigator has used a heat pipe to warm the tip to defrost it, to good effect.

4.8 Choice of System for Rectal Cryoprobe

The choice of system for the rectal cryoprobe was mostly dictated by the required tip temperature. Joule-Thomson probes using fluids with a high critical point could not provide a sufficiently low temperature to generate the 30mm diameter ice-ball.

It was decided that if a liquid nitrogen probe was to be used, it would have to be a closed circuit device. Although cryosprayers are powerful freezers, there would be severe dangers if one was used within the rectum and the exhaust gas could not escape fast enough.

The major problem with the liquid nitrogen devices is the difficulty of insulating the probe casing from the low temperatures inside. With the rectal probe there was an additional insulation problem because it

was likely that the device would incorporate a viewing facility. The optics would need to be shielded from the temperature extremes. Although substantial amounts of insulation are needed, there is not a large amount of space available for it because the instrument has to be small enough in diameter to pass into the rectal cavity.

It was decided that the work would initially examine a liquid nitrogen device to see if the insulation problem could be overcome. If this proved to be impossible a Joule-Thomson probe would then be developed and some reduction in performance would have to be accepted.

4.9 Conclusions

1. The rectal cryoprobe should use boiling liquid nitrogen to cool the tip because tip temperatures cooler than -150°C are needed.
2. A closed circuit probe should be used rather than a cryosprayer.

CHAPTER 5

THE BOILING BEHAVIOUR OF NITROGEN IN THE CRYOPROBE TIP

5.1 Introduction

This chapter examines the boiling behaviour of liquid nitrogen within the tip of the cryoprobe. The tip of the cryoprobe is a crucial component, representing as it does the interface between the boiling cryogen and the tissue being destroyed. This chapter is the first of three that examine and develop the tip design.

The known boiling behaviour of nitrogen is initially discussed in relation to its use as a cooling agent in the cryoprobe. The chapter continues by describing the test procedure used to measure the tip heat flux produced by experimental tip designs, and demonstrates the dependence of the tip heat flux on tip temperature.

5.2 Liquid Nitrogen Boiling Behaviour

5.2.1 Known pool boiling behaviour

The heat flux occuring between boiling liquid nitrogen and a heating surface is strongly dependent on the heating surface temperature. Figure 25 shows the heat flux plotted as a function of the temperature difference between a heated surface and the saturated fluid, ΔT_{SAT} . The data shown are for nitrogen pool boiling (Frost 1975). The figure shows the three main

FIGURE 25

CHARACTERISTIC BOILING CURVE FOR LIQUID NITROGEN

(data from Frost, 1975)

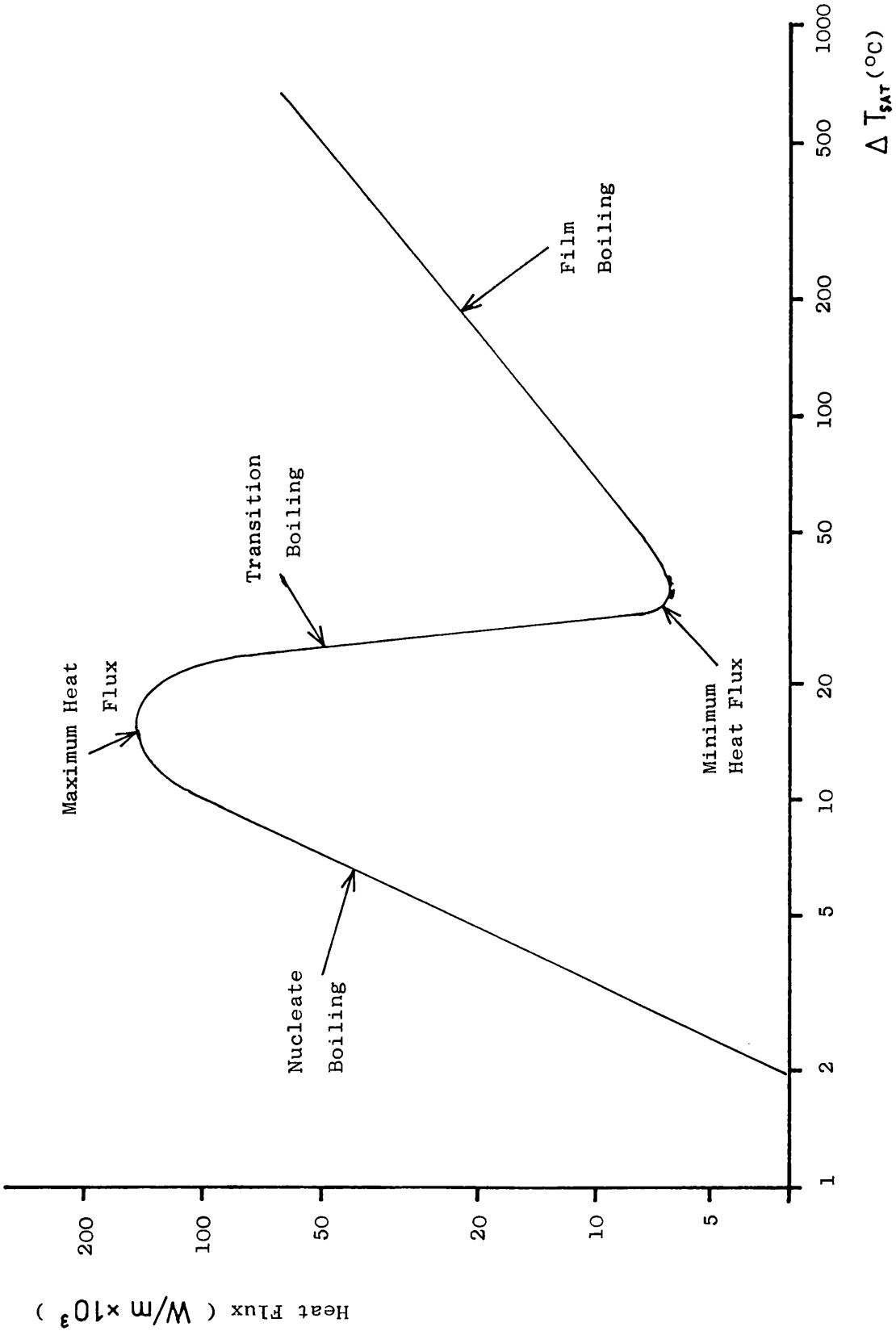

regions of the boiling curve; the nucleate boiling region, the transition boiling region and the film boiling region.

The dependence of the heat flux on the wall temperature can be explained by examining the nature of the boiling taking place in the three boiling regions. In the nucleate region the liquid wets the wall and boiling takes place by vapour bubble evolution from nucleation sites on the wall. Because the liquid wets the wall, good thermal contact is maintained between the wall and the liquid, and the heat flux is high.

As the wall temperature is increased, the vapour bubble evolution becomes more and more vigorous. This agitation causes a breaking up of the boundary film with a resultant improvement in heat transfer. The heat flux therefore rises until a maximum is reached.

In the transition boiling region, vapour bubbles are evolved from so many sites per unit area that they coalesce. Because of the relatively low thermal conductivity of vapour a barrier to efficient heat transfer is thereby formed and the heat flux is reduced. In the film boiling region, the process of coalescence becomes complete and a continuous vapour film is present between the heating surface and the liquid. The heat flux no longer drops once a stable film has been formed. It increases with increasing ΔT_{sat} but much less rapidly than in nucleate boiling.

5.2.2 Leidenfrost boiling

Figure 26 shows the nature of nitrogen boiling when flow is taking place and the liquid fraction is not close to unity. These conditions are usual in cryoprobes. Two sections of pipe are shown, one with the nitrogen in the nucleate boiling region and one with it in the stable film boiling region. In the nucleate region boiling takes place by vapour bubble formation at nucleation sites as in pool boiling. In the film boiling region the liquid breaks up into droplets and boils by vapour evolution from the droplets' surface. The vapour film separates the droplets from each other and from the pipe wall. The heat flux is low because of the thermal barrier formed by the vapour. This form of boiling is also known as Leidenfrost boiling. It is examined in much greater detail in **Chapter 9** because keeping the nitrogen in this form brings many advantages for the design of the nitrogen transfer system.

5.2.3 Wall temperatures that occur when cooling an object from room temperature

Figure 27 shows the temperature changes that occur when an object is cooled from a high temperature by liquid nitrogen, and where there are no heat sources. This is typical of the conditions that exist when using a cryoprobe, where the probe and the transfer pipes are initially at room temperature before the nitrogen flow

FIGURE 26

NATURE OF NITROGEN FLOW BOILING IN TWO SECTIONS OF PIPE, ONE COLD AND THE OTHER WARM

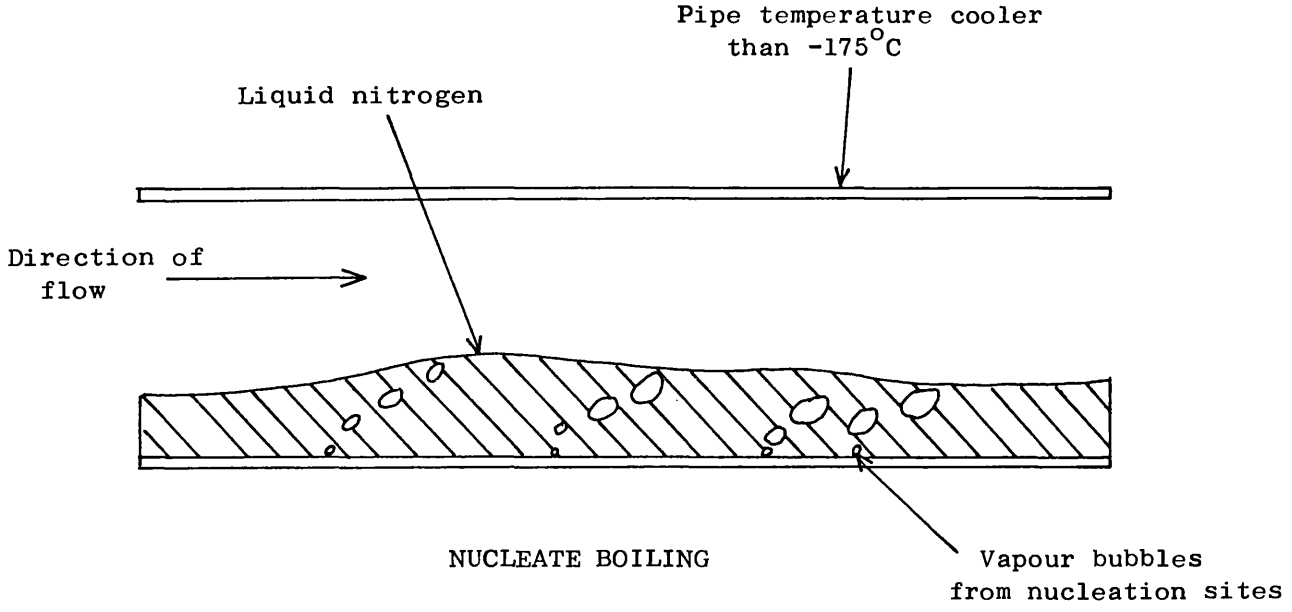

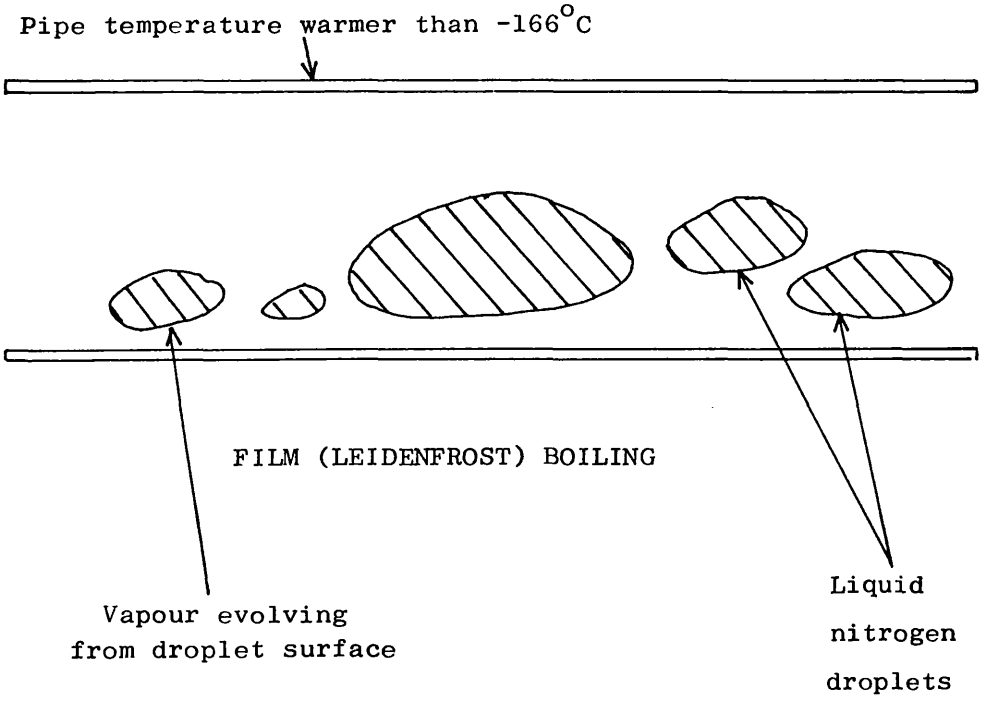

FIGURE 27

TEMPERATURE CHANGES EXPECTED FROM NITROGEN BOILING CURVE

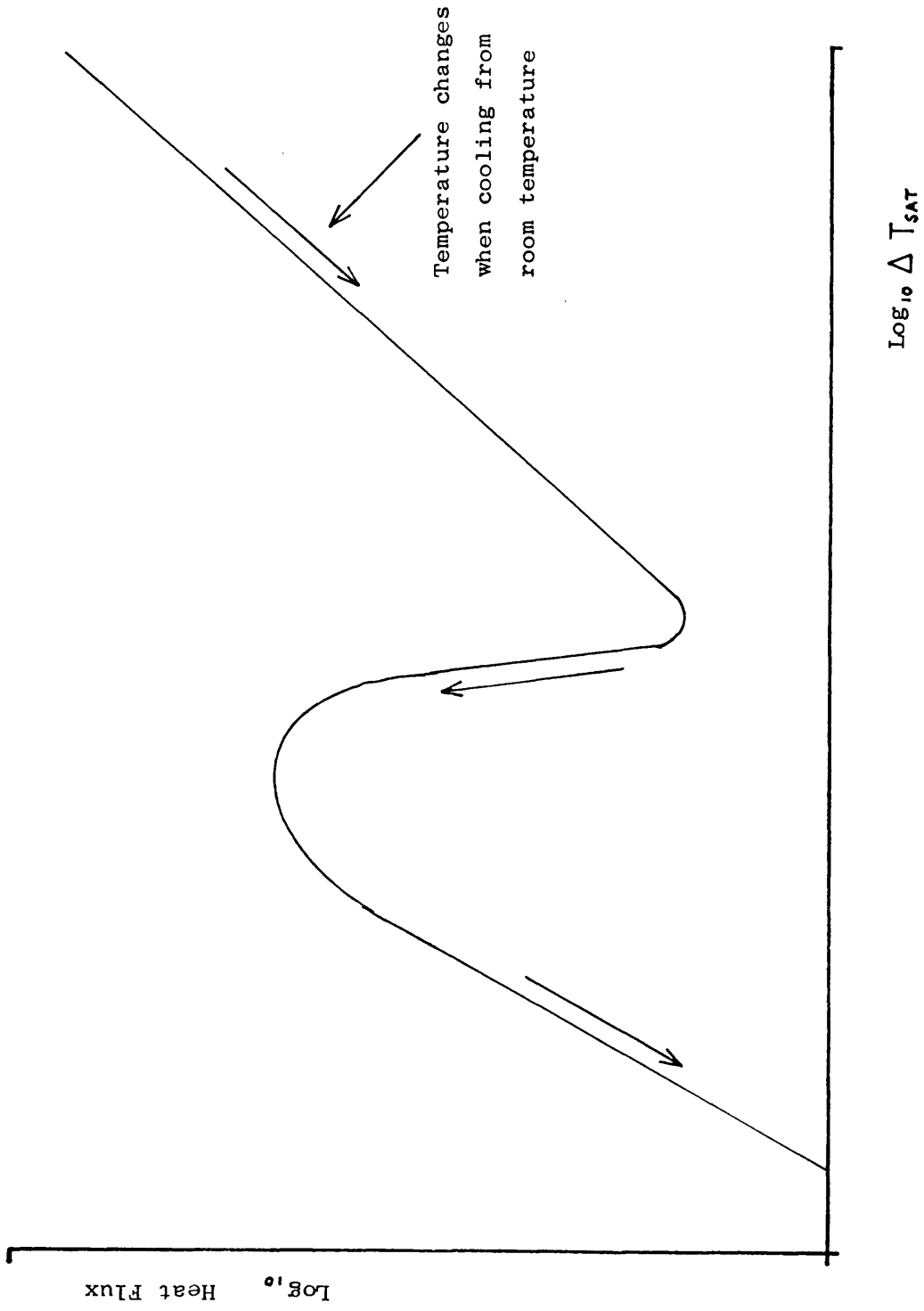

is turned on. The nitrogen will initially be undergoing film boiling and the heat transferred to the cryogen from the object will cause it to cool. The temperature of the object will decrease steadily until the minimum heat flux is reached. The heat flux isn't being controlled so it will rise as the temperature of the object takes the boiling into the transition and the nucleate regions. The large increase in heat flux causes a sudden increase in the cooling rate and the temperature of the object rapidly decreases.

5.3 Experimental Measurement of Heat Flux in Cryoprobe Tips

5.3.1 Reasons for measurement

It was assumed that the liquid nitrogen boiling beahviour in the cryoprobe tip would be similar to that described in the last section. However the cryogen flow through the tip was complicated and so it was necessary to measure the heat flux to provide quantitative data for the design of the tip.

5.3.2 General approach used to measure heat transfer

The general approach used to measure the heat transfer to an experimental tip was as follows. The tip was thermally isolated from its surroundings and heated in a controlled manner whilst passing liquid nitrogen through it. From a simple heat balance, once steady-state conditions were achieved, the heat flux and the internal heat transfer coefficient could be

calculated.

5.3.3 Test rig design

Figure 28 illustrates the test rig that was designed and built for the heat transfer measurements. The heating coil was permanently fixed inside the polycarbonate body and a test tip, constructed in stainless steel, could be slid inside the heating coil former. Before each test tip was installed in this way, it was coated with heat sink compound on the outside to improve the thermal contact between the tip and the heating coil. The position of the input pipe could be altered by sliding it through its 'O'-ring seal.

The whole rig was immersed in a constant temperature environment so that the heat transferred between the tip and the environment could be measured and accounted for in the experiments. Either a liquid nitrogen bath or a constant temperature water bath were used. The water bath was far easier to manage than the bath of liquid nitrogen, but the test was much less sensitive because of the large temperature difference between the tip and the environment.

5.3.4 Thermal analysis of test rig

Consider Figure 29, which is a diagrammatic representation of the test rig. At steady-state the heat extracted by the boiling liquid nitrogen is balanced by the heat supplied by the electrical heater and the heat conducted from the constant temperature

FIGURE 28

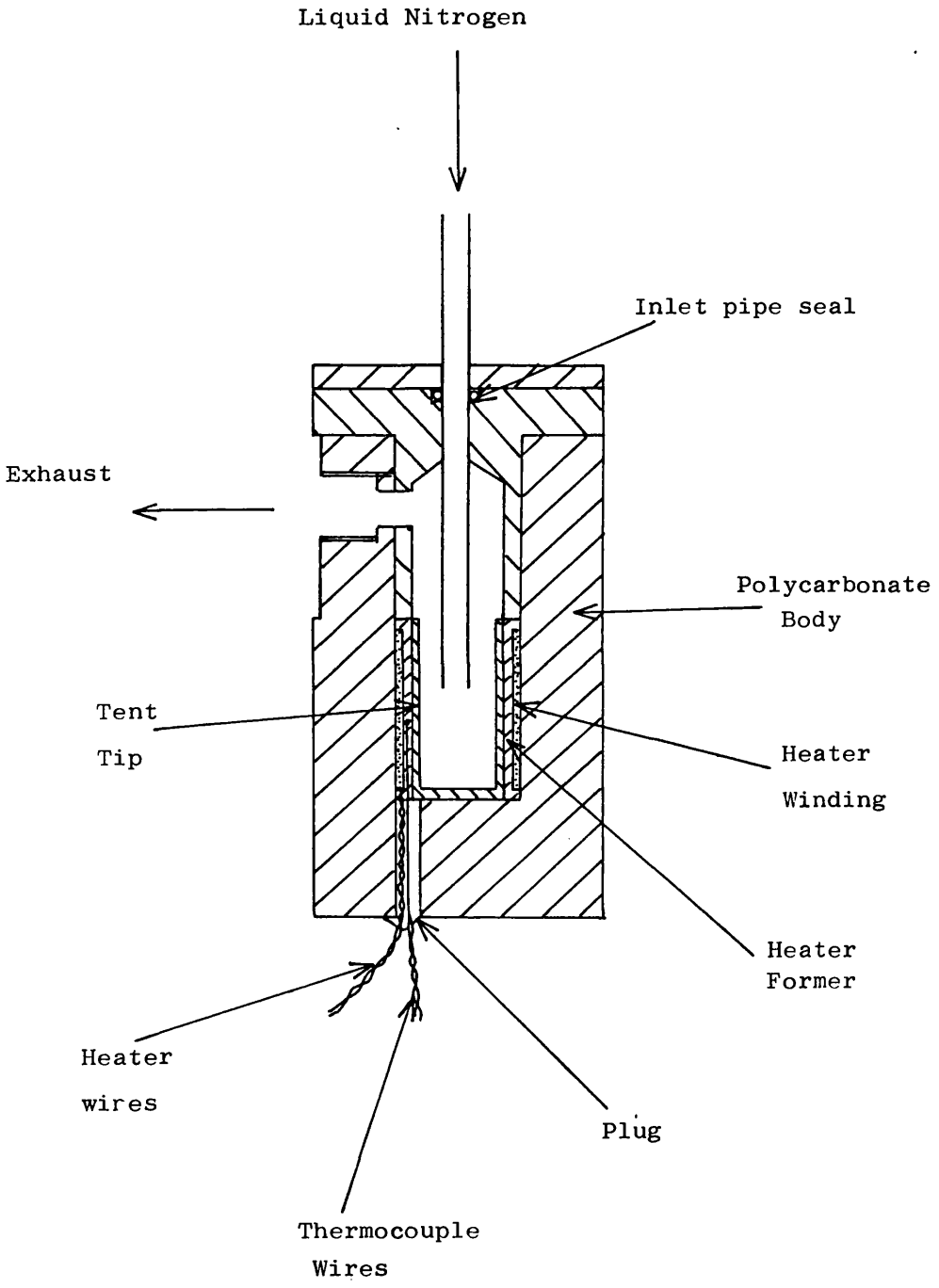

SECTION THROUGH TIP HEAT FLUX MEASURING TEST RIG

FIGURE 29

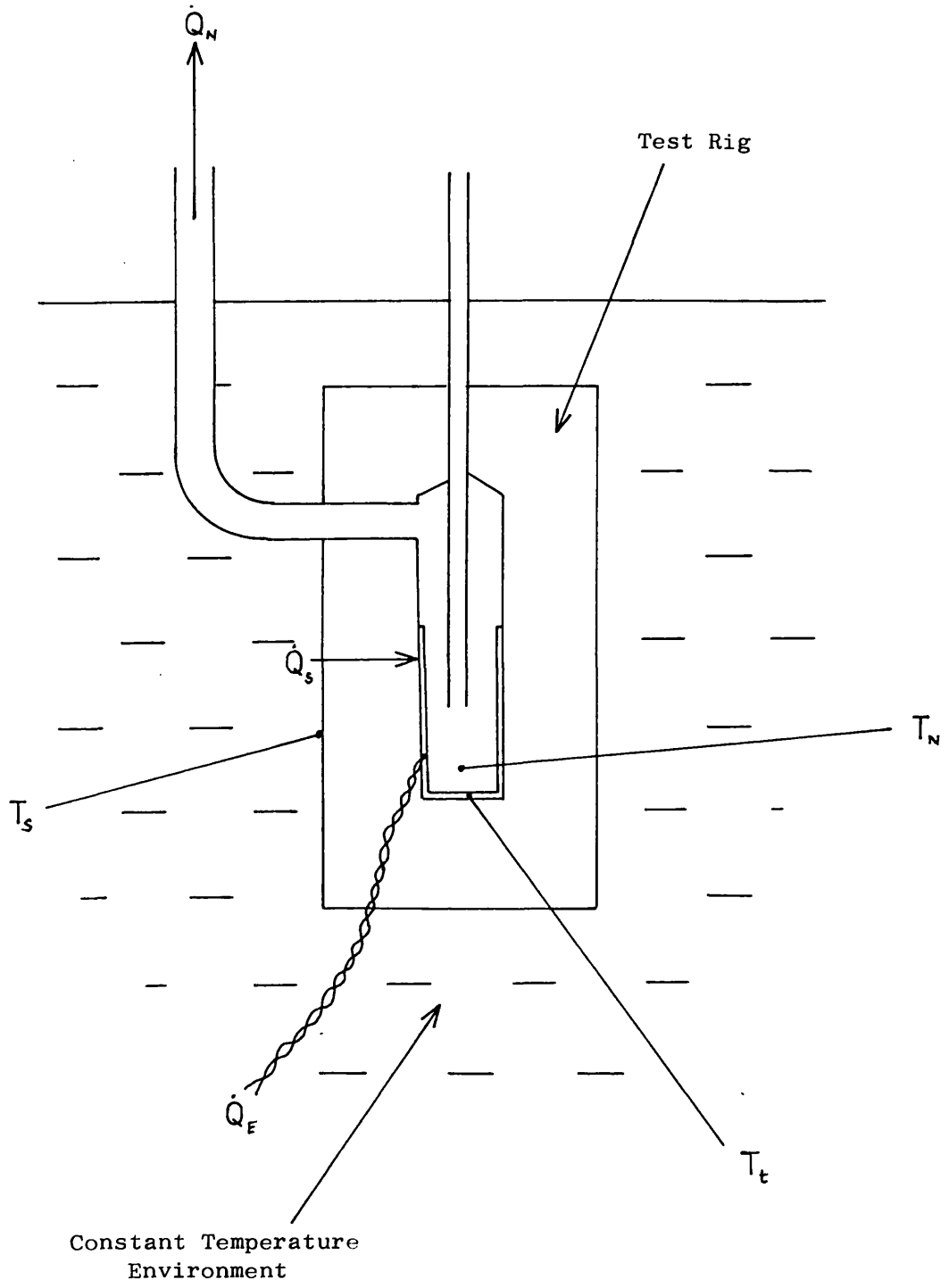

DIAGRAM OF TIP TEST RIG FOR ANALYSIS

environment.

h = tip internal heat transfer coefficient ($W/m^2°C$)

T_t = tip temperature (°C)

T_N = liquid nitrogen temperature (°C)

T_s = temperature of environment (°C)

A = internal surface area (m^2)

Heat transferred to nitrogen = $\dot{Q}_N = hA(T_t - T_N)$

Heat dissipated from tip by heater = $\dot{Q}_E = VI$

Heat transferred to tip from environment = $\dot{Q}_s = K(T_s - T_t)$

where K = constant of proportionality for this rig and a given environment.

$$\dot{Q}_N = \dot{Q}_E + \dot{Q}_s$$

For the heat flux,

$$\dot{Q}_N = VI + K(T_s - T_t) \qquad (20)$$

For the heat transfer coefficient,

$$h = \frac{VI + K(T_s - T_t)}{A(T_t - T_N)} \qquad (21)$$

In order to measure K, the constant of proportionality for the environmental heat gain, a series of measurements were taken with the liquid nitrogen turned off. The tip temperature was measured for a given power dissipation in the heating coil, once steady conditions had been achieved. This measurement was repeated for several values of heater power.

Then $$0 = \dot{Q}_E + \dot{Q}_S$$

$$= VI + K(T_s - T_t)$$

$$K = \frac{VI}{(T_t - T_s)} \qquad (22)$$

The value of K was obtained from a plot of VI against $(T_t - T_s)$. As can be seen from **Figure 30** a good linearity was obtained over the range of temperatures used.

5.3.5 Derivation of liquid nitrogen temperature in the tip

The value of T_N is obviously essential to the analysis described above. The driving pressure generated in the supply dewar was of course higher than ambient, so the temperature of the incident nitrogen in the tip would be higher than the static pool surrounding the test rig. **Figure 31** shows a plot of the boiling point of liquid nitrogen as a function of pressure up to 15 psi. It proved to be difficult to measure T_N and it could not be estimated from the pressure in the supply dewar as there was a significant pressure drop between the dewar and the tip.

T_N was eventually derived by considering the heat balance for the test rig. Consider **Figure 32** which shows a section through the wall of the test rig. The temperature distribution across the wall is shown for increasing values of heat dissipation from the electrical heater, $\dot{Q}_E$. As the nitrogen flowing

FIGURE 30

GRAPH TO DETERMINE CONSTANT OF PROPORTIONALITY FOR ENVIRONMENTAL HEAT GAIN FROM TIP TEST RIG WHEN IN LIQUID NITROGEN

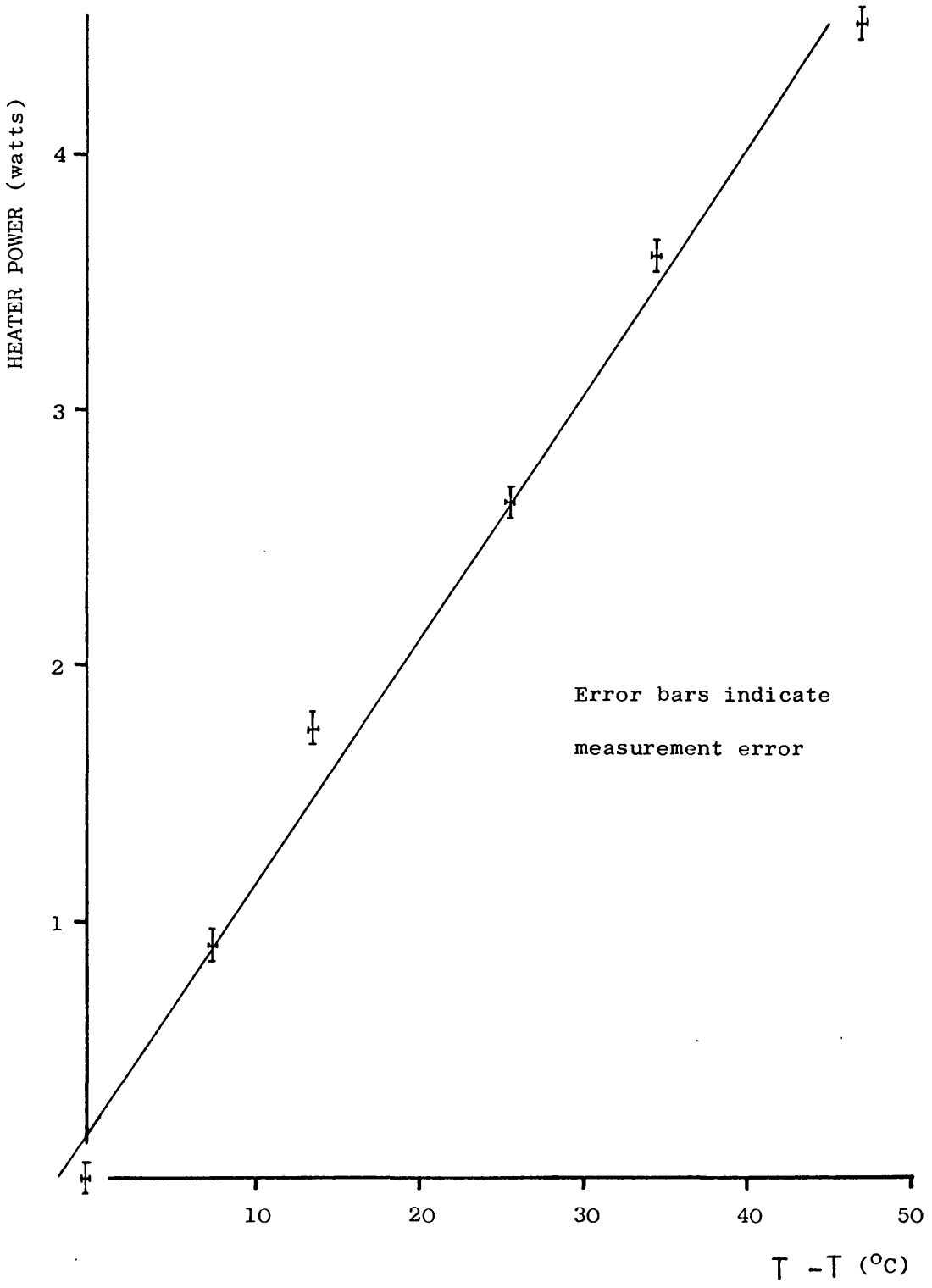

FIGURE 31

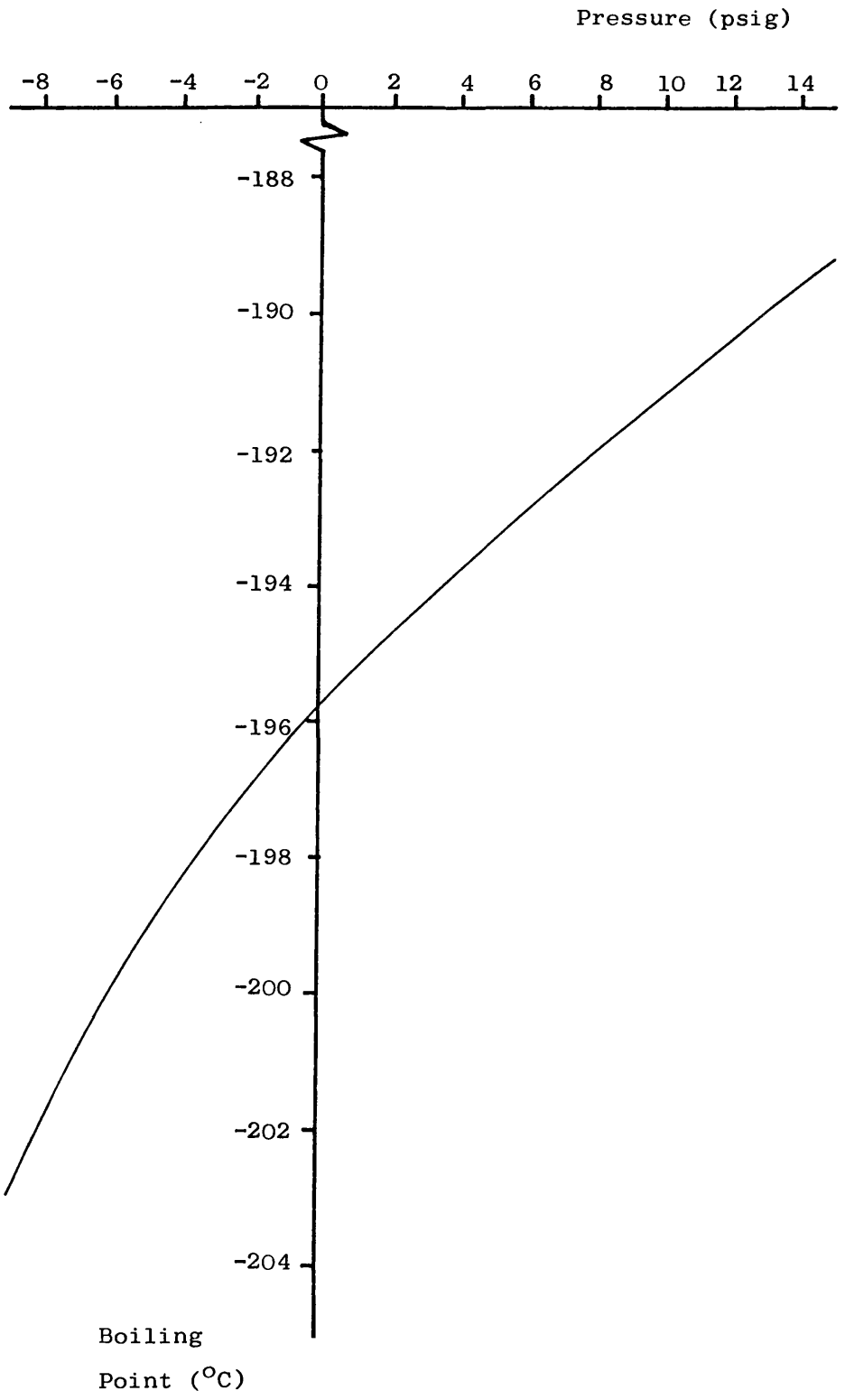

CHANGE OF LIQUID NITROGEN BOILING POINT WITH PRESSURE

FIGURE 32

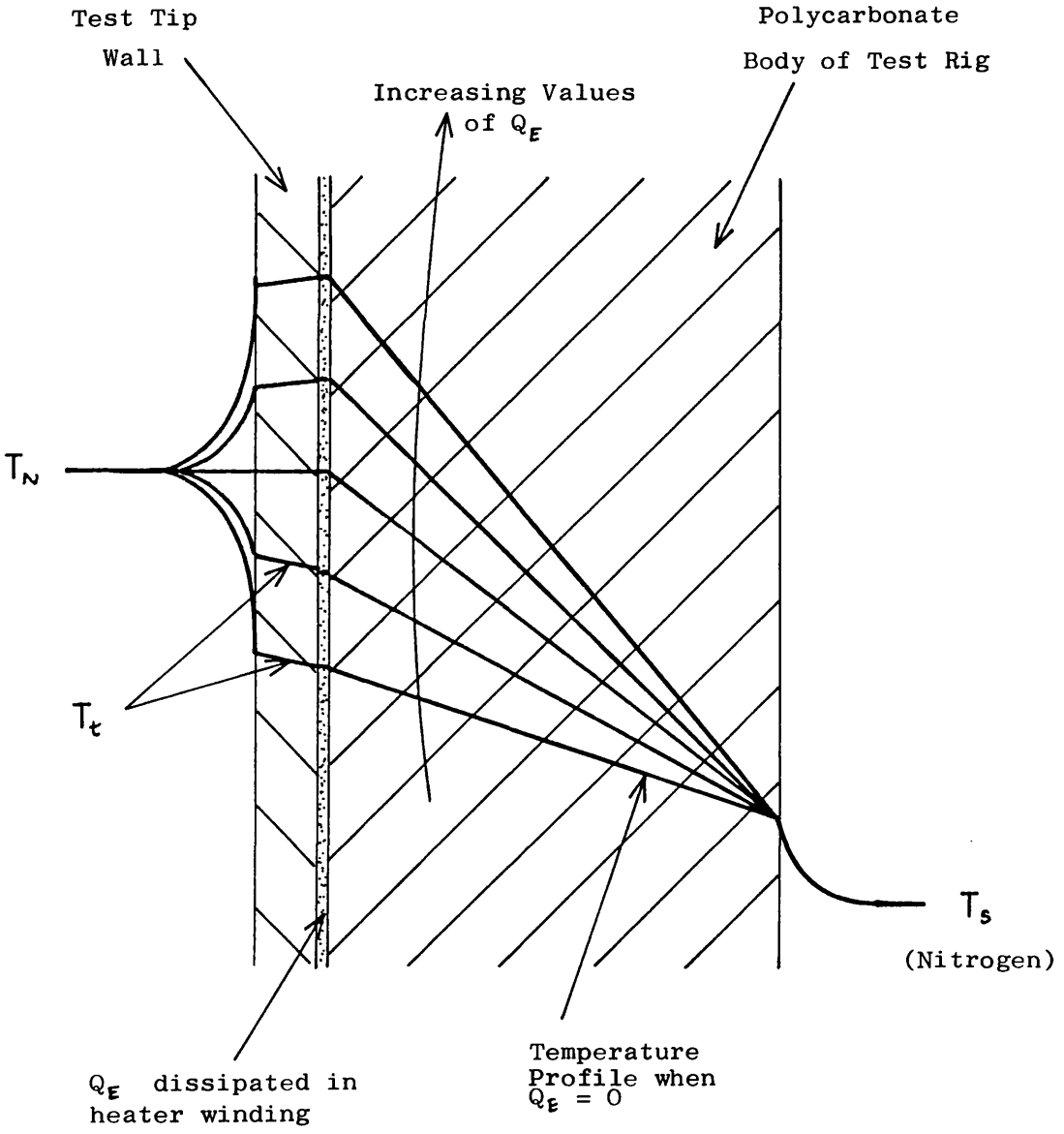

SECTION THROUGH TEST RIG WALL SHOWING TEMPERATURE PROFILES FOR INCREASING POWER DISSIPATED IN THE HEATER (Test Rig Immersed In Liquid Nitrogen Bath)

through the tip is at a higher pressure than the static pool surrounding the rig, the nitrogen temperature, T_N, is greater than the environmental temperature, T_s. As the value of $\dot{Q}_E$ is increased the tip temperature, T_t, also increases. At a given value of $\dot{Q}_E$, the tip temperature equals the nitrogen temperature. Considering the energy balance for the rig for these conditions, no heat is being transferred from the tip to the nitrogen so the heat supplied by the heater must equal the heat gained by the environment,

$$\text{i.e.} \quad \dot{Q}_E + \dot{Q}_s = 0$$

T_N was therefore derived for each test by plotting $(\dot{Q}_E + \dot{Q}_s)$ against T_t. The value of T_N was equal to T_t when $(\dot{Q}_E + \dot{Q}_s) = 0$. Figure 33 shows a typical plot.

5.3.6 Measurements taken in tests

Temperatures were measured using copper/copper-nickel thermocouples and a Comark digital thermometer with a 0.05°C resolution. A multichannel U.V. recorder was also used to record the analogue output from the thermometer when it was necessary to observe transient temperature changes. The digital thermometer could also be connected to a multichannel automatic switching unit so that a number of thermocouples could be rapidly scanned. The temperature of the tip was measured from a thermocouple embedded in the heating coil former and

FIGURE 33

DERIVATION OF NITROGEN TEMPERATURE IN TIP

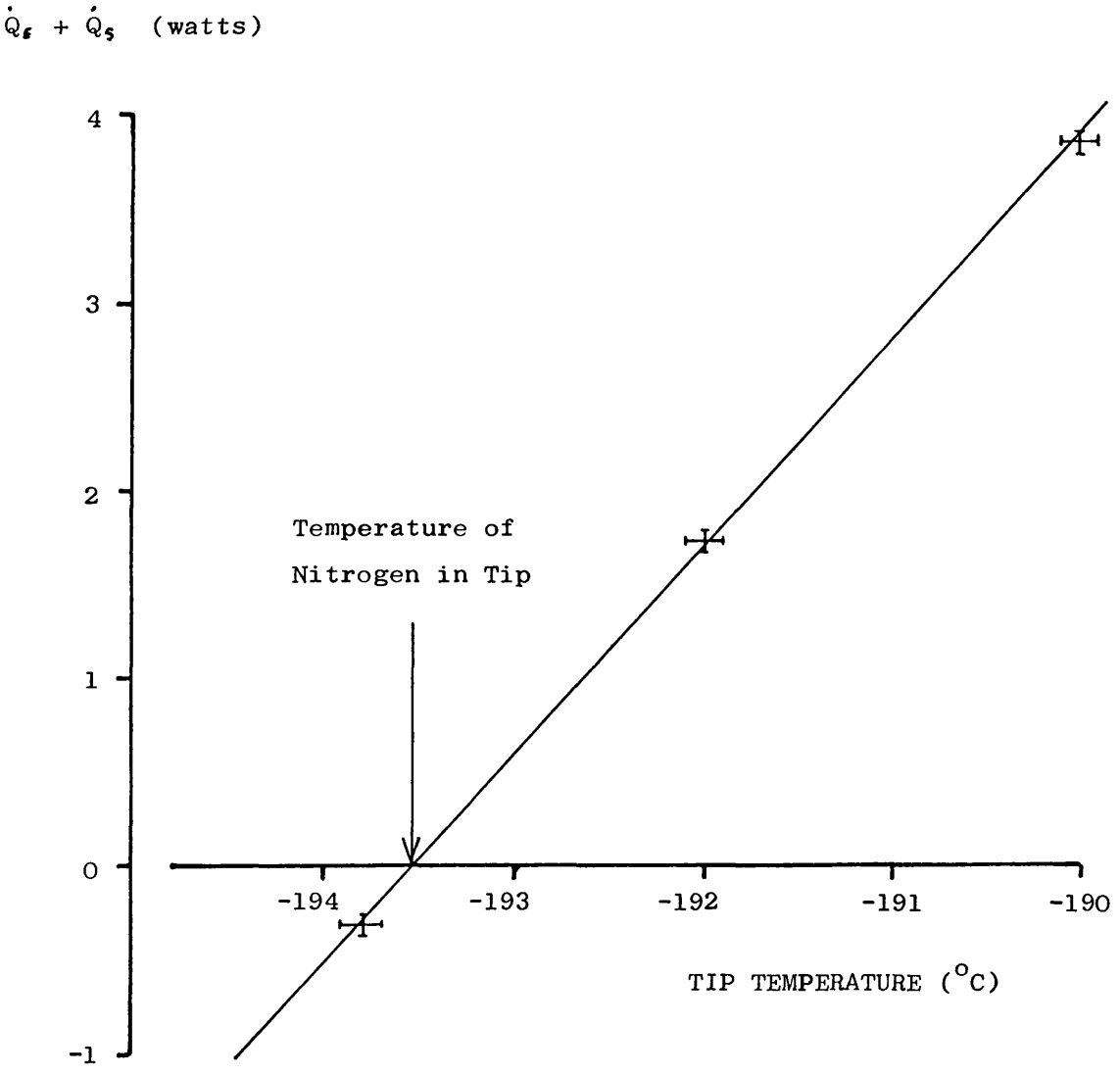

ERROR BARS REPRESENT READING ERROR

the environmental temperature from a thermocouple in the bath. These were the main temperatures measured.

The mass flow rate through the tip was measured by passing the exhaust nitrogen through a 2 metre coil of pipe in a constant temperature water bath to warm it to a known temperature. The volume flow rate was then measured by an accurate float flow meter. The nitrogen temperature was monitored by a thermocouple just prior to the flow meter.

All the measuring equipment was housed in a purpose made test rack as shown in **Figure 34.** This had many additional features to those described above. It was used both for the tip tests and for the test described later on for the transfer hoses.

The power supply for the heating coil was again purpose made with accurate analogue meters for both voltage supplied and current passing through the coils. The supply could dissipate a maximum of 30 Watts.

5.3.7 Test procedure

The test rig, containing the particular tip under test, was placed in the constant temperature bath and left for about 15 minutes to thermally equilibrate. During this equilibrating period the liquid nitrogen would also be turned on and the various feed and exhaust pipes were also allowed to reach an equilibrium temperature. Readings of T_t, T_s and I were then taken for increasing values of V until T_t approached 0°C. The readings were then repeated for decreasing values of V.

FIGURE 34

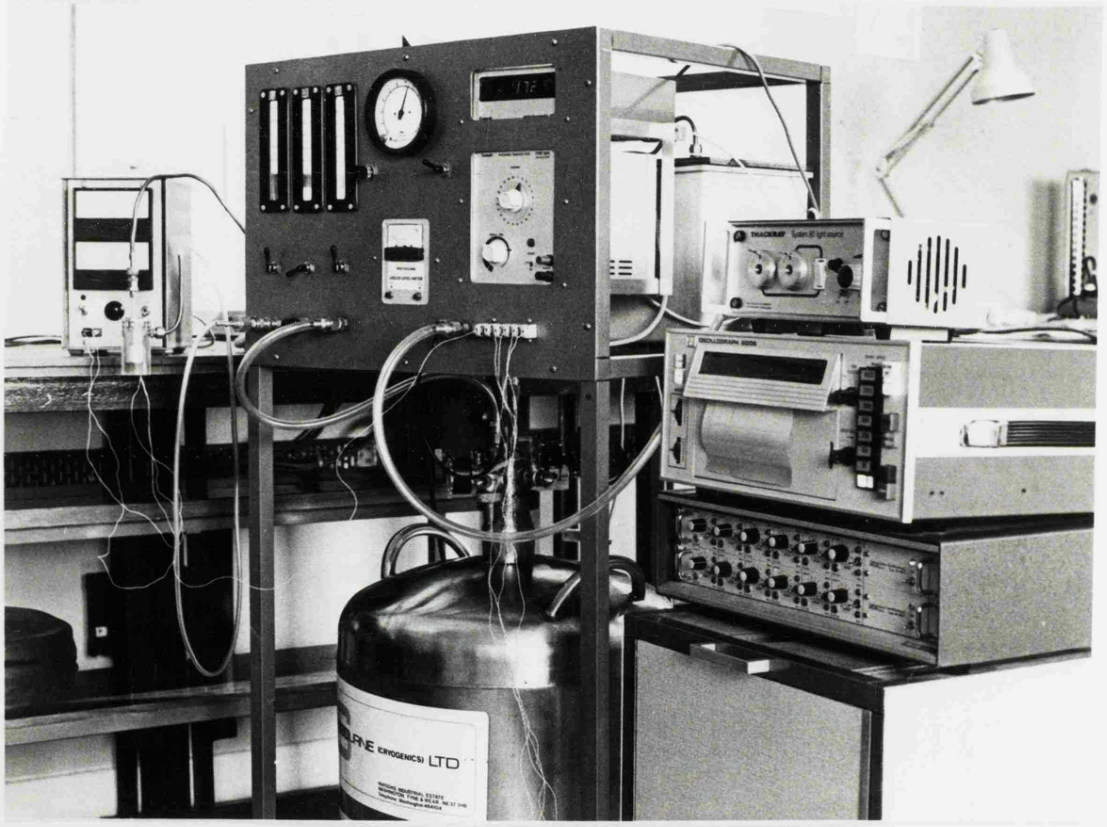

TEST EQUIPMENT USED FOR EXPERIMENTAL MEASUREMENTS

The temperatures were of course allowed to stabalize before readings were taken.

5.4 Results Obtained

5.4.1 Typical data obtained

As the amount of power dissipated in the heating coil was increased, so the tip temperature increased. However, a point was reached when the tip temperature suddenly increased by over 100°C. Further increases in power dissipation produced further smaller increases in tip temperatures.

On reducing the power to the heater the tip temperature became cooler again but along a different path. The temperature dropped steadily until the heater power was almost back to zero, when the tip temperature suddenly dropped close to the boiling point again.

Typical data, in the form of the heat transferred to the liquid nitrogen as a function of tip temperature are plotted in **Figure 35** . **Figure 36** shows the same data superimposed on a possible nitrogen boiling curve to explain the results obtained. In these tests the heat transferred to the nitrogen is controlled, because the heat dissipated in the heating coil is controlled. At point A any further increase in $\dot{Q}$ can only be accommodated by a change from nucleate to film boiling and so the temperature suddenly increases to point B in the figure, as shown by the dotted line. On reducing $\dot{Q}$ the tip temperature retraces the boiling curve until

FIGURE 35

TIP HEAT FLUX DATA PLOTTED AS A FUNCTION OF ΔT_{SAT}

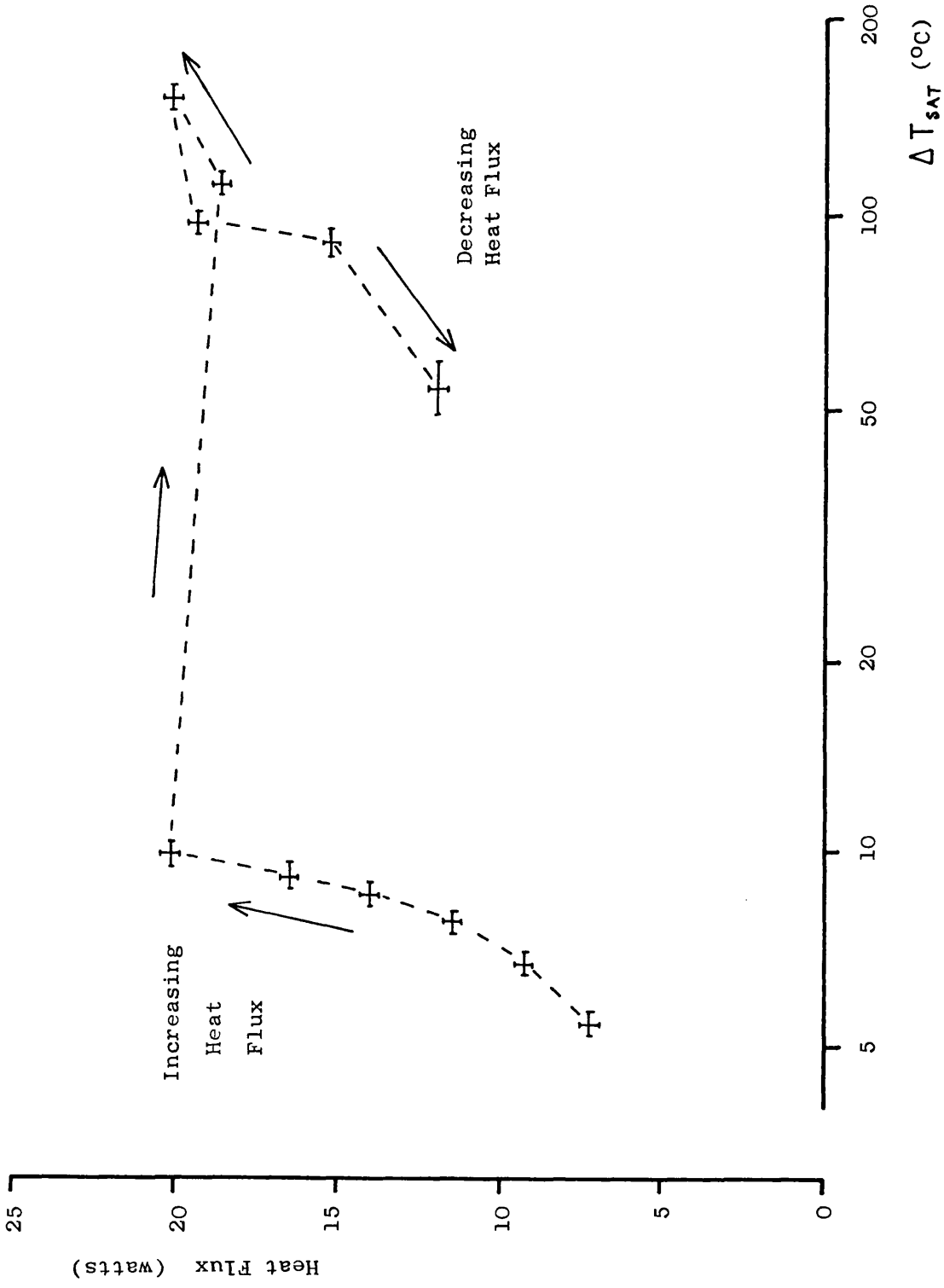

FIGURE 36

POSTULATED TIP BOILING CURVE BASED ON THE DATA SHOWN IN FIGURE 35

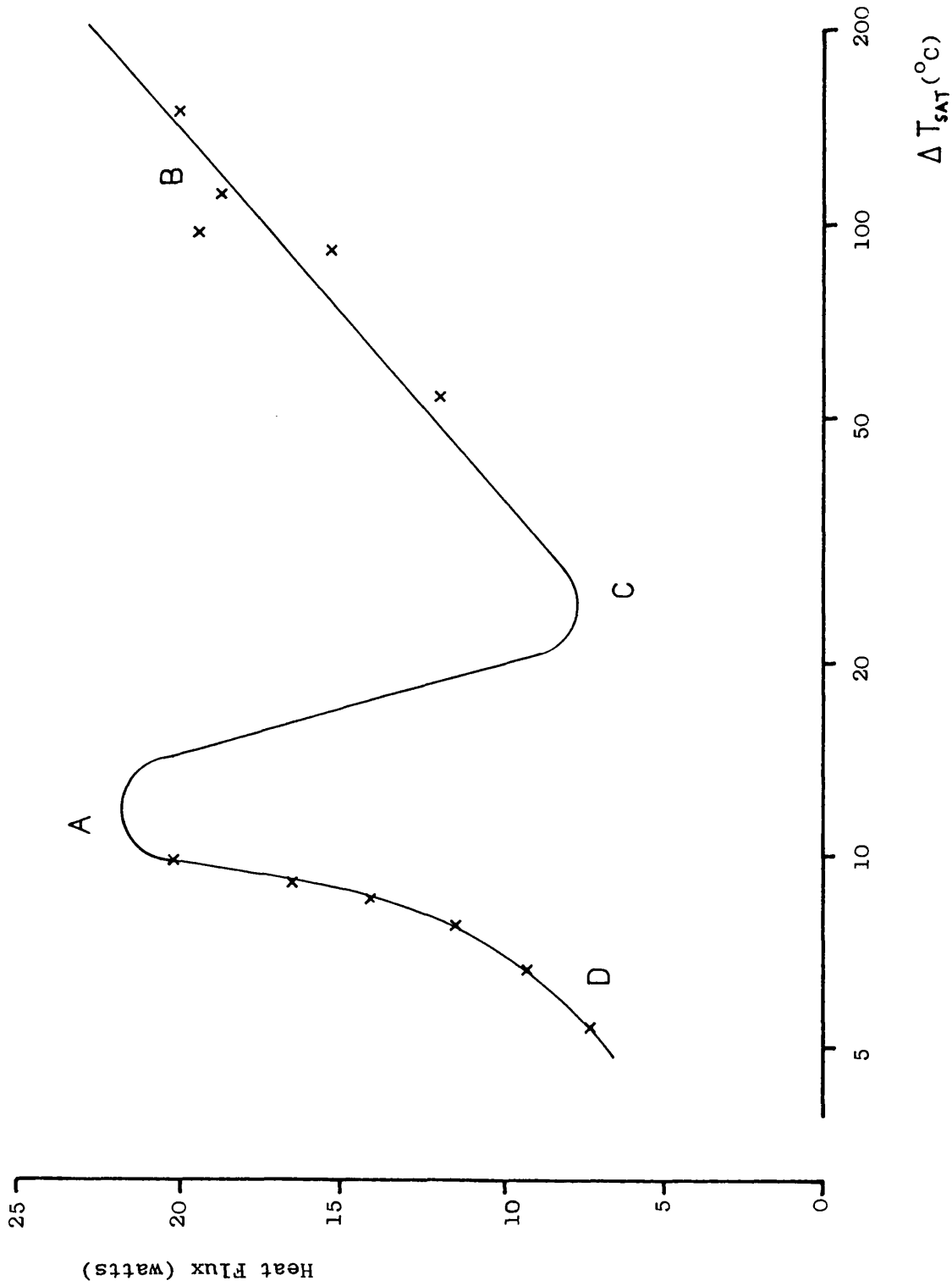

point C. Any further reductions in $\dot{Q}$ can now only be accommodated by a change from film boiling to nucleate boiling, resulting in a rapid drop in tip temperature to rejoin the boiling curve at point D in the figure.

5.5 Conclusions

The thermodynamic behaviour of typical cryoprobe tips has been investigated experimentally. The heat transferred to the boiling nitrogen has been shown to be strongly dependent on the tip temperature, as would be expected from the known nitrogen boiling curve. The heat flux measured during warming of the tip is different to that measured during cooling. This has been explained by again referring to the known boiling behaviour of nitrogen.

CHAPTER 6

Experimental Investigation of Tip Design

6.1 Introduction

This chapter describes how the tip design was derived empirically from tests on different tips. The aim of the experimental work was to find a tip design that ensured the heat flux to the nitrogen was sufficient to meet the performance specification derived in Chapter 3.

The boiling heat transfer process taking place within the tip is made even more complex by the abrupt changes in flow direction which occur . It was decided that an analytical investigation of such a complex process was beyond the scope of this project, and consequently the heat transfer performance of the tip was investigated experimentally. The test rig described in the last chapter was used to measure the effect of the major variables on the tip behaviour. Once the trends had been established, an optimised tip design could be defined.

6.2 Required Tip Heat Flux

6.2.1 Sources of heat

The heat extracted by the boiling liquid nitrogen within the cryoprobe tip must balance that externally transferred to the tip. The heat transferred to the tip comes from three main sources (see Figure 37).

FIGURE 37

SOURCES OF HEAT FOR CRYOPROBE IN BODY CAVITY

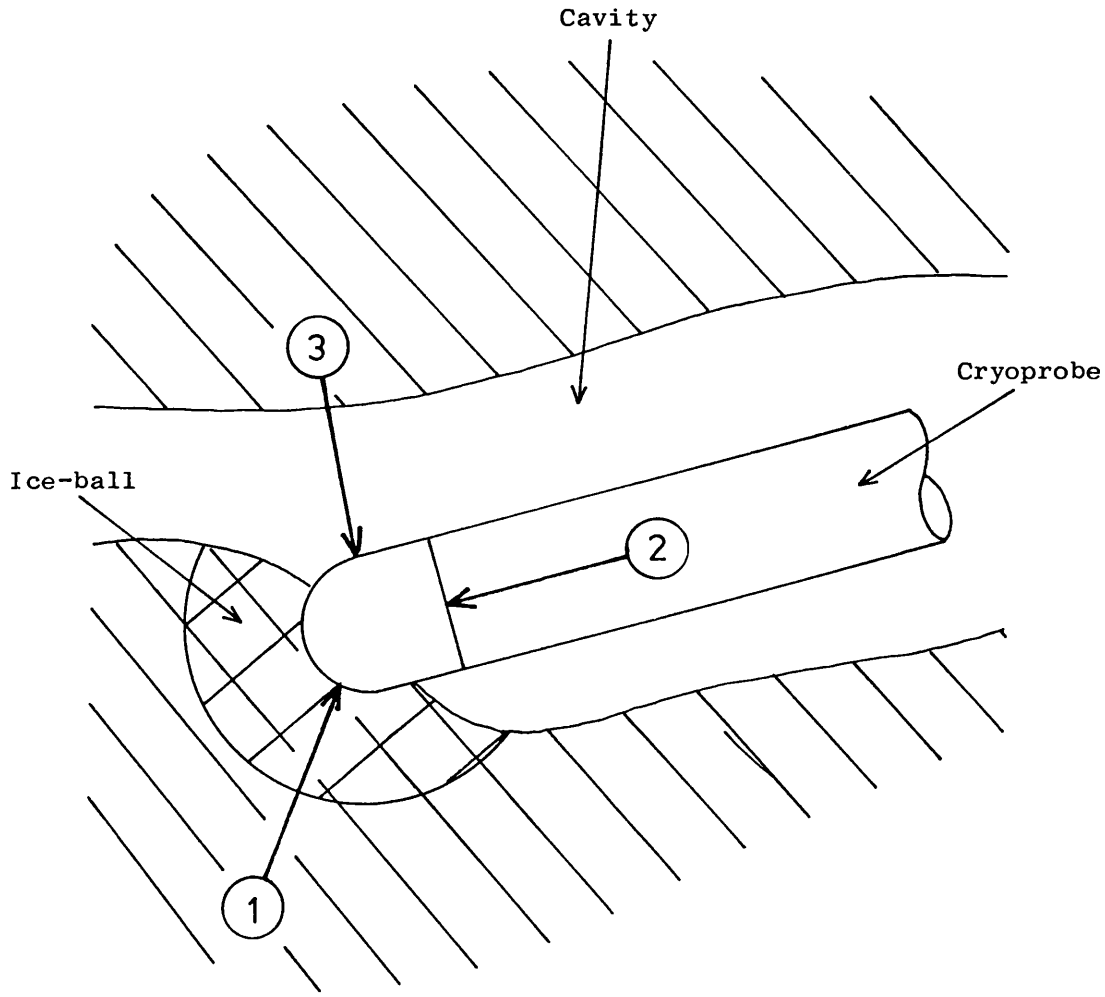

1. Heat conducted through growing ice-ball.

2. Heat conducted from cryoprobe shaft.

3. Heat transferred from surrounding tissues via air in cavity.

1. The sensible and latent heat conducted through the growing ice-ball.
2. The heat conducted from the cryoprobe shaft.
3. The heat transferred from the tissues via the air surrounding the tip (i.e. from the tissues not being frozen).

6.2.2 Sensible and latent heat from ice-ball

It was shown in Chapter 3 that in order for a 12mm diameter cryoprobe tip to remain below -160°C whilst freezing tissue, its tip would have to extract sensible and latent heat from the ice-ball at a rate of 14W.

6.2.3 Heat conducted from probe shaft

The shaft is assumed to be at +37°C (deep body temperature) and its interface with the tip to be a PTFE seal the same diameter as the tip (12mm), 3mm thick and 10mm bore.

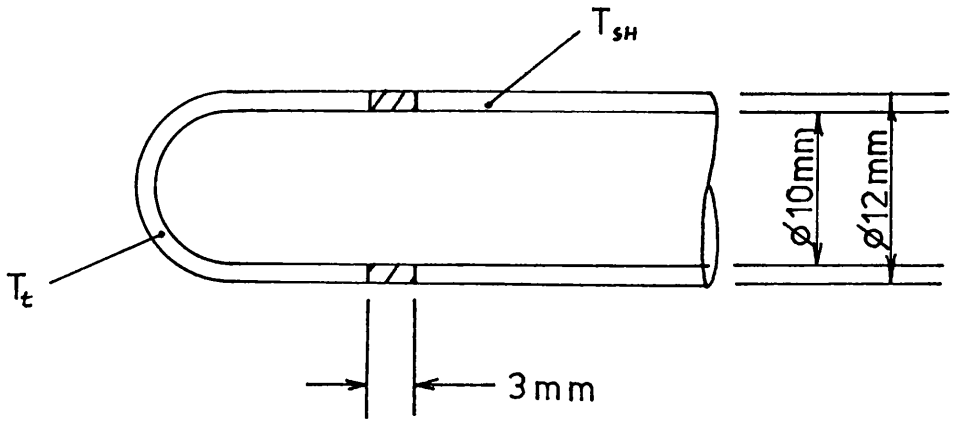

$$\dot{Q} = \frac{k A_s (T_{sh} - T_t)}{l_s} \qquad (23)$$

where $\dot{Q}$ = rate of heat transfer

k = thermal conductivity of PTFE = 0.25W/m.°C

A_s = area of seal = 34.56×10^{-6} m

l_s = length of seal = 3×10^{-3} m

T_{sh} = temperature of shaft = + 37°C

T_t = temperature of tip = -160°C

Therefore $\dot{Q}$ = 0.57W

6.2.4 Heat transferred from surrounding tissue

Heat is transferred from the surrounding tissue by conduction, convection and radiation. It is assumed from the performance specification derived in Chapter 3 that the tip is at -160°C, and is placed within a tissue cavity 20mm bore where the tissue is at +37°C.

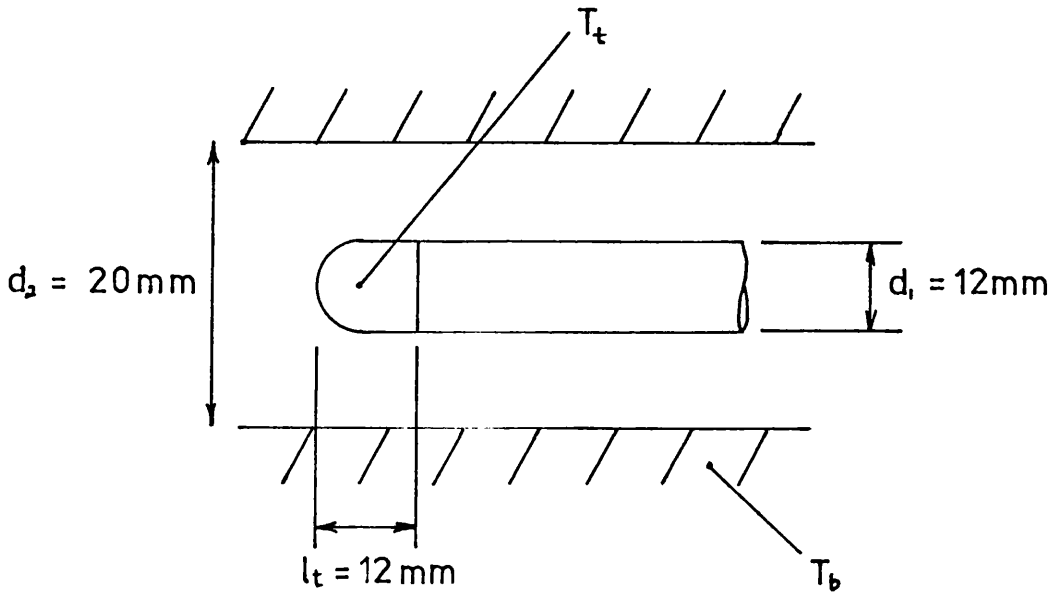

(a) Heat transferred by conduction = $\dot{Q}_{COND}$

$$\dot{Q}_{COND} = \frac{2\pi k l_t (T_b - T_t)}{\ln(d_2/d_1)} \quad (24)$$

where T_b = temperature of tissues

$$\therefore \dot{Q}_{COND} = 0.70W$$

(b) Heat transferred by convection = $\dot{Q}_{CONV}$

$$\dot{Q}_{CONV} = \pi d_1 l_t h (T_A - T_t) \quad (25)$$

where T_A = temperature of air = 37°C

h = heat transfer coefficient for tip/air boundary

$$= \frac{k Nu_d}{d}$$

Nu_d = $0.525 (Gr_d Pr)^{\frac{1}{4}}$ because $Ra < 10^9$ and air movement therefore laminar

$$\therefore \dot{Q}_{CONV} = 2.14W$$

(c) Heat transferred by radiation = $\dot{Q}_{RAD}$

$$\dot{Q}_{RAD} = E\sigma A_T (T_b^4 - T_t^4) \quad (26)$$

where E = emissivity = 0·05

σ = Stefans constant = $5.67 \times 10^{-8} W/m^2.°K^4$

A_T = area of tip = $0.942 \times 10^{-3} m^2$

$$\therefore \dot{Q}_{RAD} = 0.028W$$

The heat transferred is dominated by the natural convection taking place, with a total of 2.87W transferred altogether.

6.2.5 Total heat flux through tip

The total rate of heat transferred to the tip when generating the required ice-ball has been estimated above to be 14.0+0.57+2.87 = 17.44W.

6.3 Tests Used to Measure Tip Heat Flux

6.3.1 Aim of experimental investigations

The investigations of tip thermodynamic performance were carried out to evolve a tip design that met the performance specification. This was done by examining the effect of several variables on the tip heat flux. However each variable was only investigated until an insight had been gained into its effect on heat flux, and the trends had been established. A comprehensive study of cryoprobe tip heat transfer was beyond the scope of this project.

6.3.2 Test procedure

The test procedure followed was identical to that used for the tests described in Chapter 5. A large number of test tips were investigated, each one 12mm in diameter, and the main variables examined were as follows:

(a) flow rate of cryogen

(b) input pipe position

(c) input pipe design

(d) tip internal configuration

The main objective of the tests was to determine trends. Consequently the nucleate boiling region only of the boiling curve was examined rather than plotting the whole curve for each test. It was reasoned that if a given tip design led to an improved tip heat flux, this improvement would be present at all tip temperatures. Therefore readings of T_t, T_s, V and I were only taken for increasing power dissipation in the heating coil, and only until the tip temperature, T_t, suddenly increased, indicating the end of nucleate boiling.

6.4 Results Of Heat Flux Measurements

6.4.1 Effect of nitrogen mass flow rate

Figure 38 is a plot of heat flux versus tip temperature for several values of mass flow rate. All the curves are in the nucleate region of the boiling curve.

There is a minimum mass flow rate that must be exceeded to ensure that some liquid is present. If all the liquid is evaporated during its passage through the tip, then no more latent heat of vapourisation is available and the temperature of the nitrogen will rapidly rise. The tip will be unable to sustain any further increases in heat flux.

The critical mass flow rate can be estimated by

FIGURE 38

EFFECT OF NITROGEN MASS FLOW RATE ON TIP BOILING BEHAVIOUR

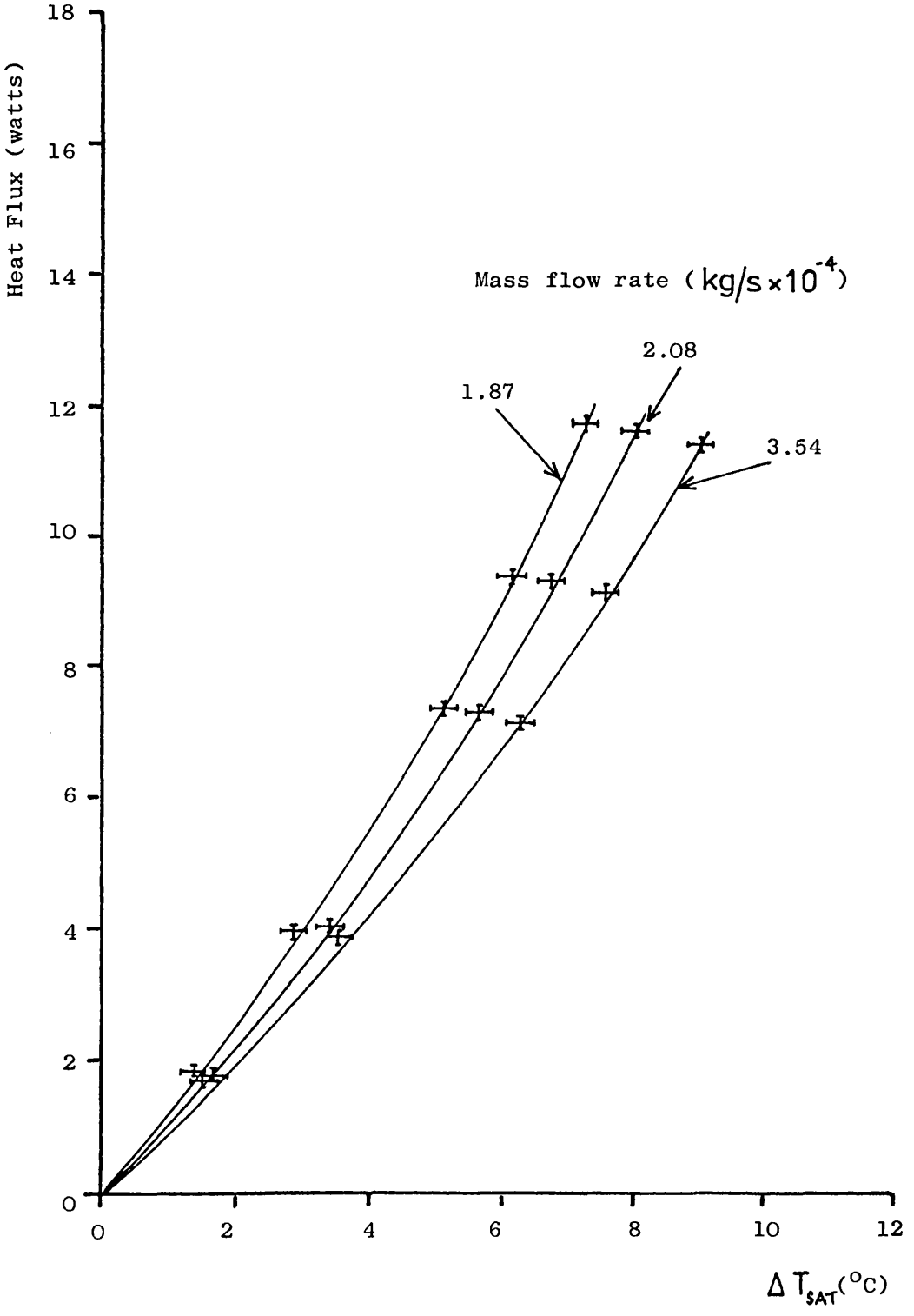

applying the Steady Flow Energy Equation to the nitrogen in the tip, as was done in equation 18.

$$\dot{Q} = \dot{m}\Delta h_e$$

where Δh_e is the latent heat of vapourisation,

$$\frac{\dot{Q}}{\dot{m}} > 20{\cdot}4 \times 10^4 \text{ J/kg} \qquad (27)$$

The experimental data are replotted in **Figure 39** in the form of $\dot{Q}$ versus $\dot{m}$. Included in this graph is the critical relationship expressed in equation 23. As can be seen, all the mass flow rates used in the experiments exceded the critical rate. Therefore, as would be expected, there is no obvious decrease in the curves at low mass flow rates. A rise in the heat flux might have been expected as the mass flow rate increased, due to the effect of increased velocity on the heat transfer coefficient. However this is not shown by the data.

It is concluded that the mass flow rate of nitrogen in the rectal probe should be above 1×10^{-4} kg/s.

6.4.2 Effect of input pipe position

The distance of the input pipe from the end of the tip is defined as l_p . **Figure 40** shows the boiling curves obtained for the two extreme values of l_p used in the investigation. It can be seen that there is only a small difference between them. In order to examine the trend, a plot of the heat flux obtained at $\Delta T_{SAT} = 8°C$ is

FIGURE 39

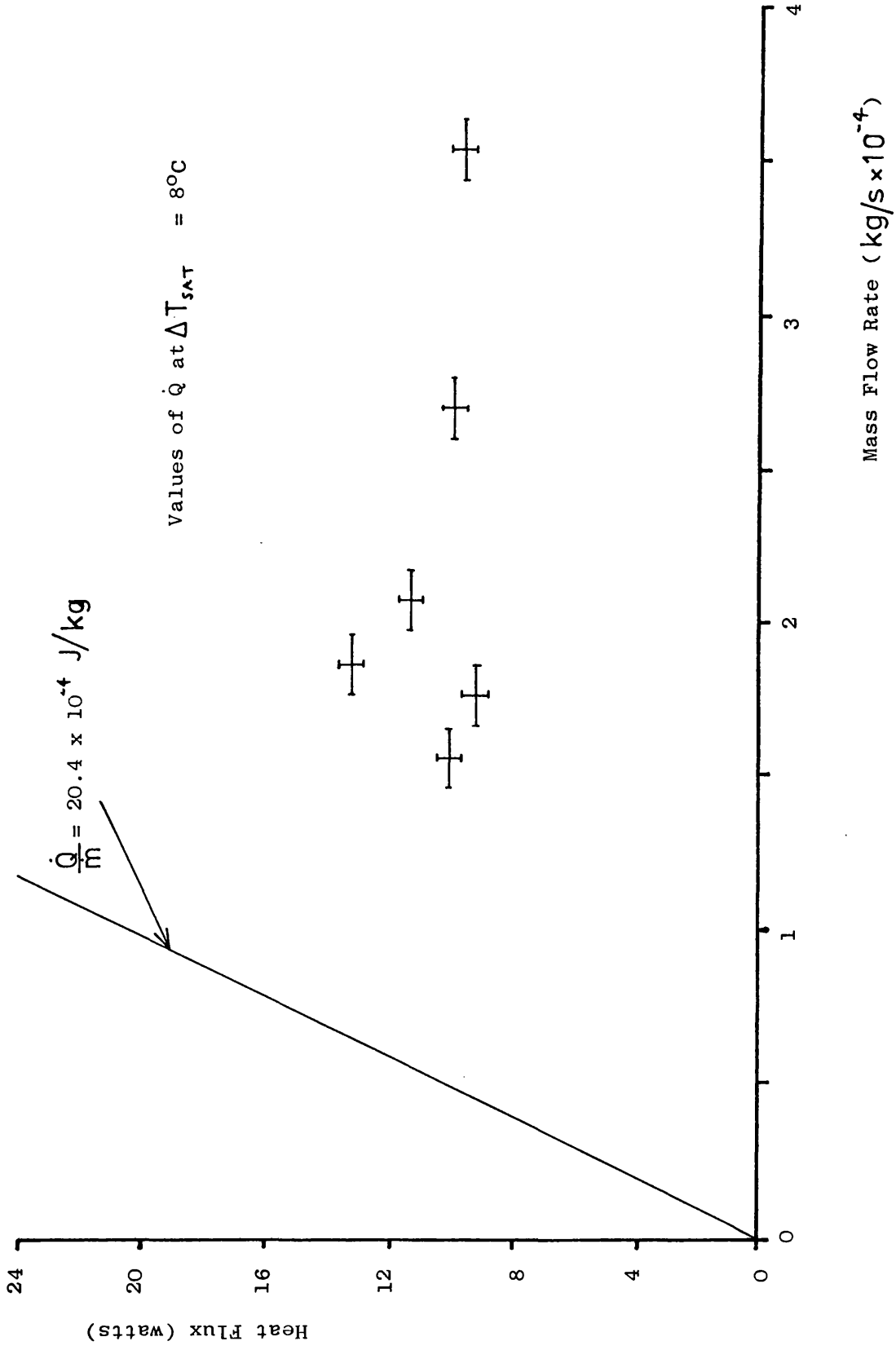

EFFECT OF MASS FLOW RATE OF NITROGEN ON TIP HEAT FLUX

FIGURE 40

EFFECT OF FEED PIPE POSITION ON TIP BOILING BEHAVIOUR

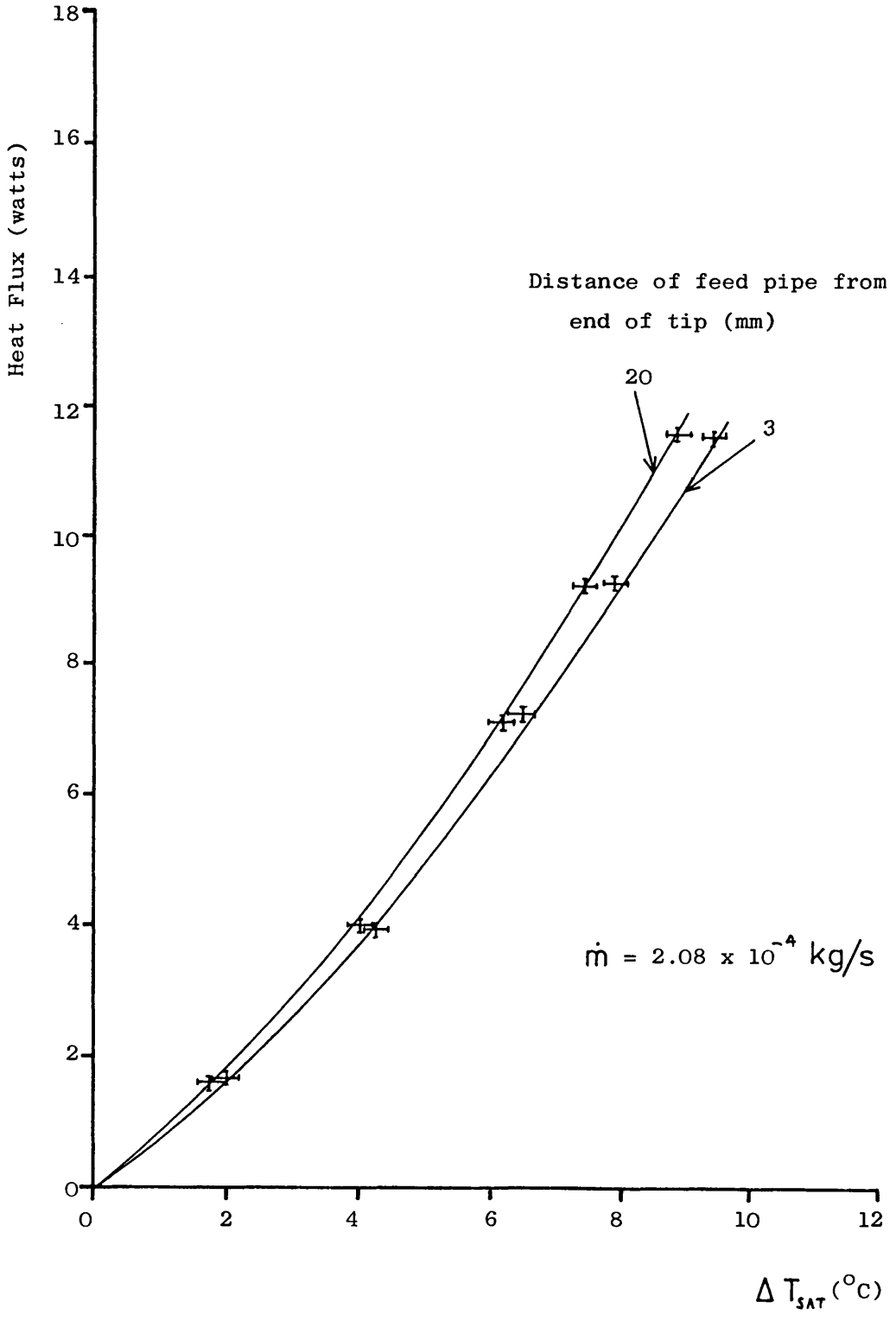

shown as a function of l_p in **Figure 41.** It is concluded from these tests that the input pipe position is not critical within the range $3mm \leqslant l_p \leqslant 20mm$.

6.4.3 Effect of input pipe design

A brief study was carried out on the effect of drilling small holes in the input pipe, with the aim of breaking up the incident nitrogen into several discrete discharges. Three different pipes were tried in this study and the results are illustrated in **Figure 42.** No trend can be established from these results. Two conclusions were drawn:

(1) There appears to be an enhancement of the heat transfer when multi-orificed pipes are used.

(2) From the tests carried out, the preferred pipe design has five holes, 1mm in diameter.

6.4.4 Effect of tip internal configuration

From the tests carried out it is possible to calculate the internal heat transfer coefficients and thereby estimate the heat fluxes that would occur for a tip with an increased internal surface area. However it was felt that the internal surface area and the heat transfer coefficient were not independent variables.

Within the tip there is an abrupt reversal in the direction of flow. This results in the heat transfer coefficient being dependent on both the nature of the two phase flow within the tip, and also the flow path. If the internal surface area is increased by

FIGURE 41

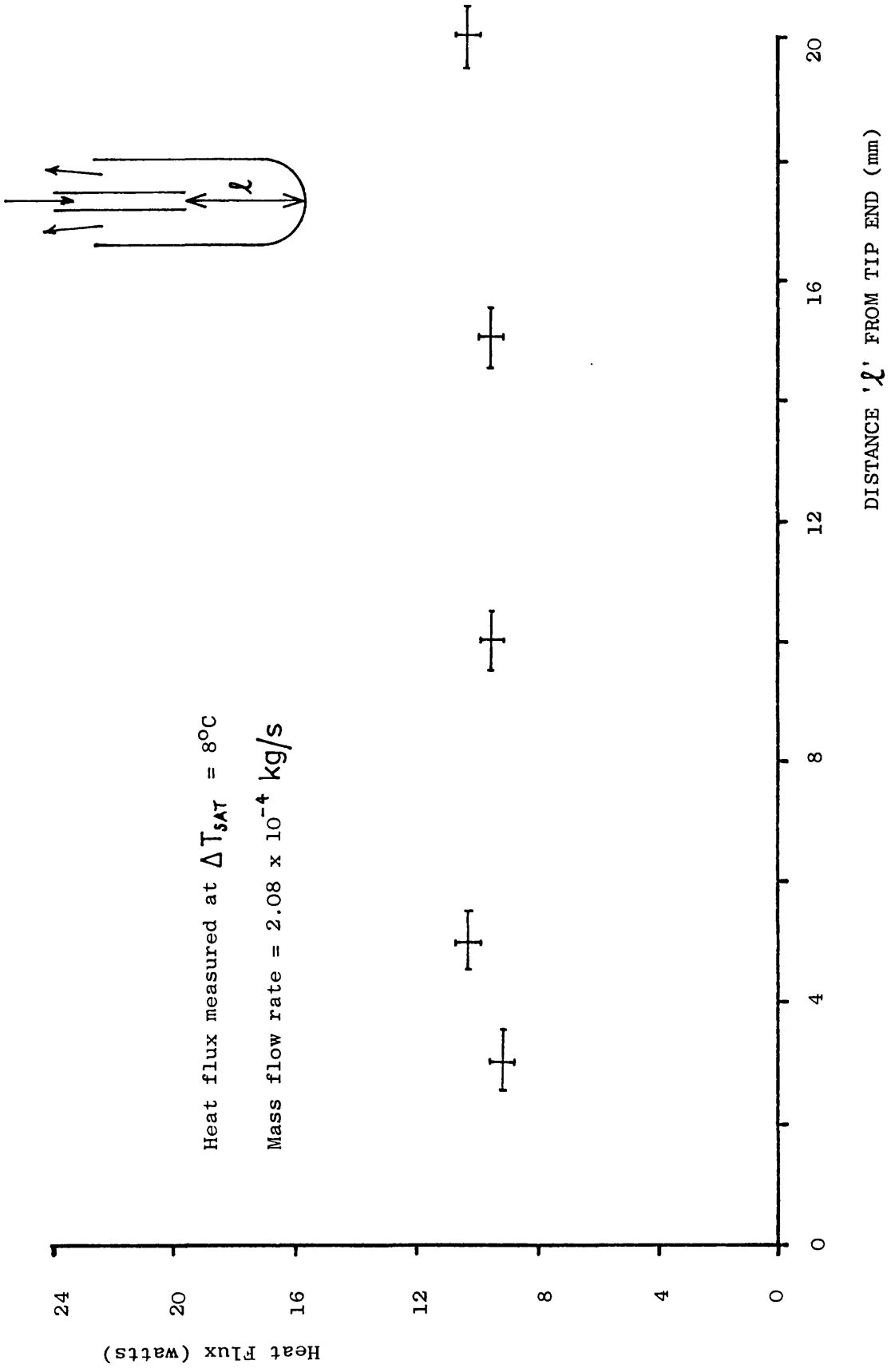

EFFECT OF INPUT PIPE POSITION ON TIP HEAT FLUX

FIGURE 42

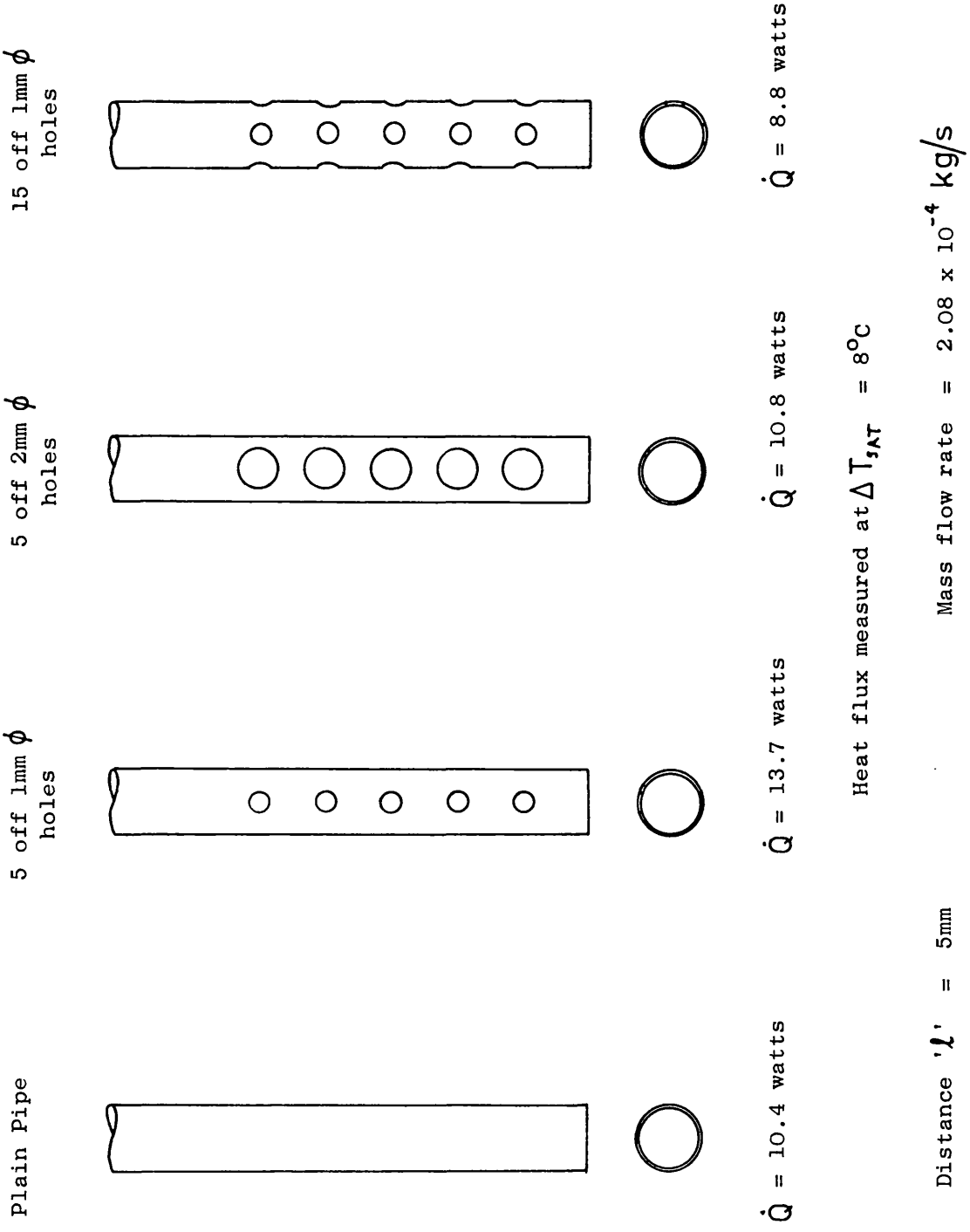

EFFECT OF FEED PIPE DESIGN ON TIP HEAT FLUX

convolutions, the pattern of flow through the tip will also change. The overall heat transfer within the tip will then change not only because of the increase in area, but also because the heat transfer coefficient will be affected by the changes in the flow path.

A test was therefore carried out in which the internal surface area was increased by cutting a $^{7}/_{16}$" UNC thread on the inside of a test tip. **Figure 43** shows a plot of the heat flux as a function of tip temperature for the tip described, together with the result obtained with a plain tip using the same flow rate and input pipe. As can be seen the increased surface area led to a much improved heat flux at a given temperature. **Figure 43** also shows the heat flux curve that would be expected for the increase in surface area, assuming the heat transfer coefficients were the same as those obtained with the plain tip. The modified tip produces a heat flux that is greater than that expected from the increase in surface area alone. For example, when ΔT_{SAT}=4° C,the increase is 2.3 times greater than would be expected.

The surface area and the internal heat transfer coefficients are not independent variables. However, it would require a large number of tests to relate the internal tip configuration to the heat fluxes obtained. As the values of $\dot{Q}$ that were measured satisfy the derived performance specification, this investigation was taken no further.

FIGURE 43

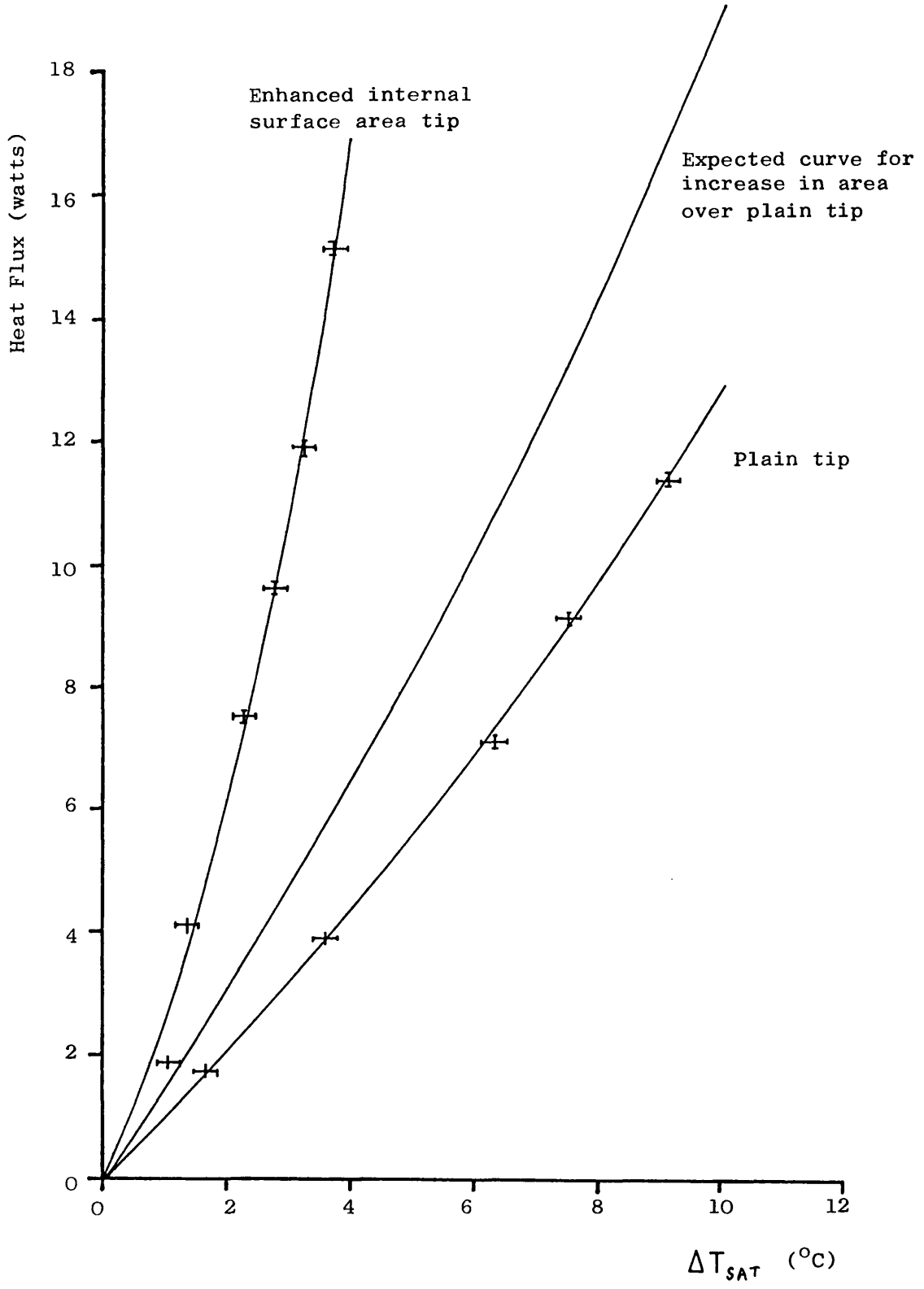

EFFECT OF INCREASE IN INTERNAL AREA ON TIP HEAT FLUX

6.5 The Boiling Curve and Tissue Cooling

6.5.1 Tip equilibrium temperature

In Chapter 3 the relationship between the tip temperature and the heat flux through the ice-ball was discussed. It was shown that the colder the tip, the greater the heat flux through the ice-ball. **Figure 13** showed that the heat flux was a linear function of tip temperature.

As nitrogen cools the tip, the heat flux through the tip wall varies with tip temperature according to the nitrogen boiling curves that have been measured. Let this heat flux be called the potential heat flux for the purposes of this discussion. The heat flux through the ice-ball at a given tip temperature can be compared to the potential heat flux that results from the boiling curve. The two relationships between heat flux and tip temperature are superimposed in **Figure 44**. The data for the heat flux through the ice-ball is taken from **Figure 13** for a 6mm radius tip and is non-linear in **Figure 44** because temperature is plotted on a log scale in this figure.

When the tip is placed into contact with the tissues its temperature will be about 37°C. When the liquid nitrogen is turned on, heat will be transferred from the surrounding tissues, through the tip to the nitrogen, and the tip will cool. The tip temperature will continue to drop until it reaches point P in **Figure 44**. At this point the heat extracted by the boiling nitrogen balances the heat supplied by the tissues.

FIGURE 44

GRAPH SHOWING TIP EQUILIBRIUM TEMPERATURE

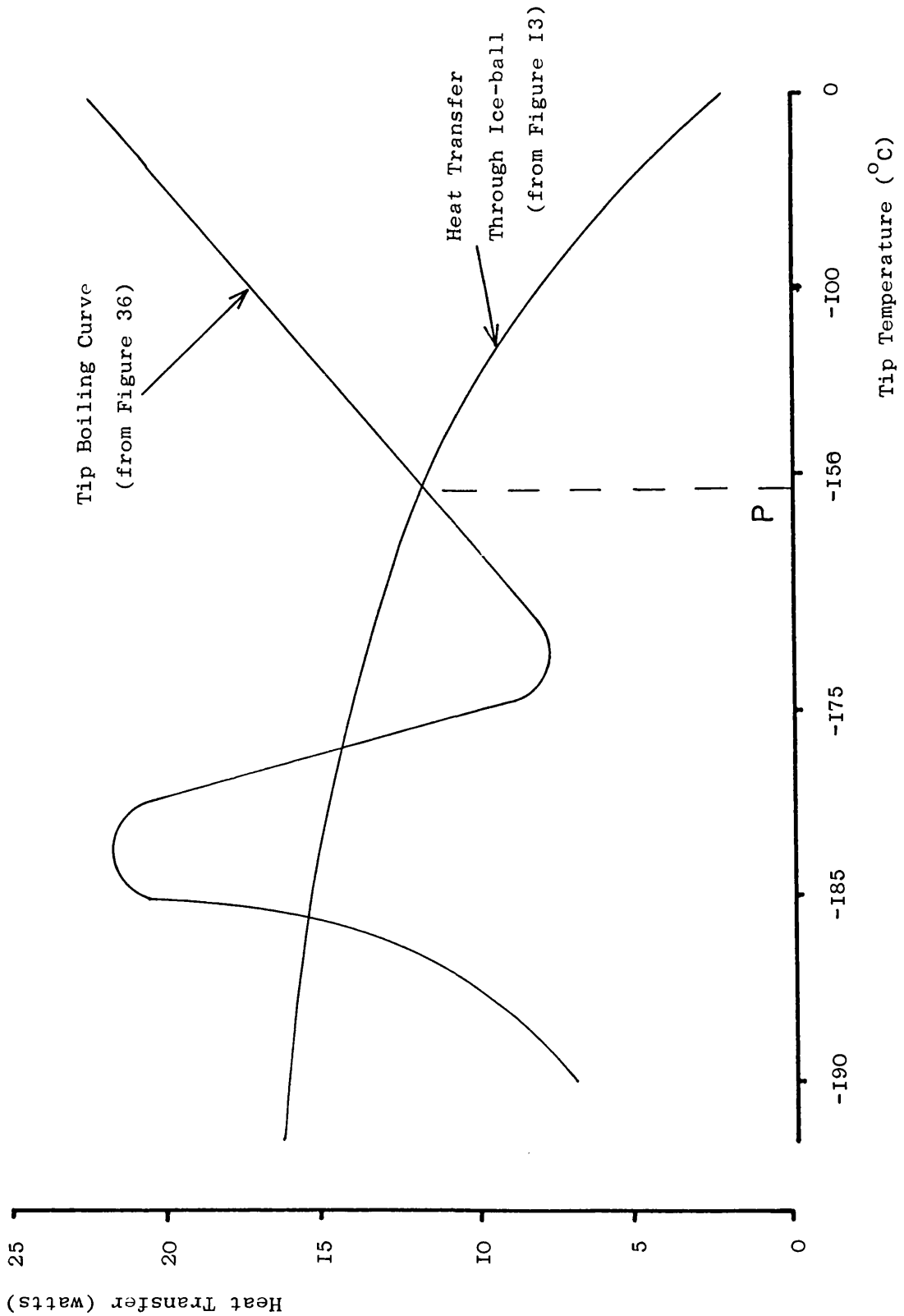

Figure 45 illustrates the effect of increasing the heat extracting capability of the tip by improving its design. As the heat extracting capability increases, so the equilibrium temperature, P, is reduced.

Once the tip design is such that curve C is possible, much lower equilibrium temperatures can be achieved because the two curves do not meet until the nucleate boiling region of the boiling curve is entered.

6.5.2 The importance of tip equilibrium temperature

The tip heat flux measurements described in this chapter have shown that the values of $\dot{Q}$ obtained can meet the requirements of the tip performance specification. However all the results were for nitrogen boiling in the nucleate boiling region. Although an adequate heat flux can be obtained with film boiling, the tip temperatures are very much higher ($> -50°C$). Tip temperatures as high as these would not meet the performance specification. A means of ensuring that the boiling in the tip is nucleate is needed. The remainder of this chapter discusses a solution to this problem.

6.6 Techniques of encouraging nucleate boiling in the tip

6.6.1 Breaking through the film barrier

To overcome the problem of film boiling during cooling, initial attempts were made to use the momentum

FIGURE 45

EFFECT OF IMPROVING TIP DESIGN ON TIP EQUILIBRIUM TEMPERATURE

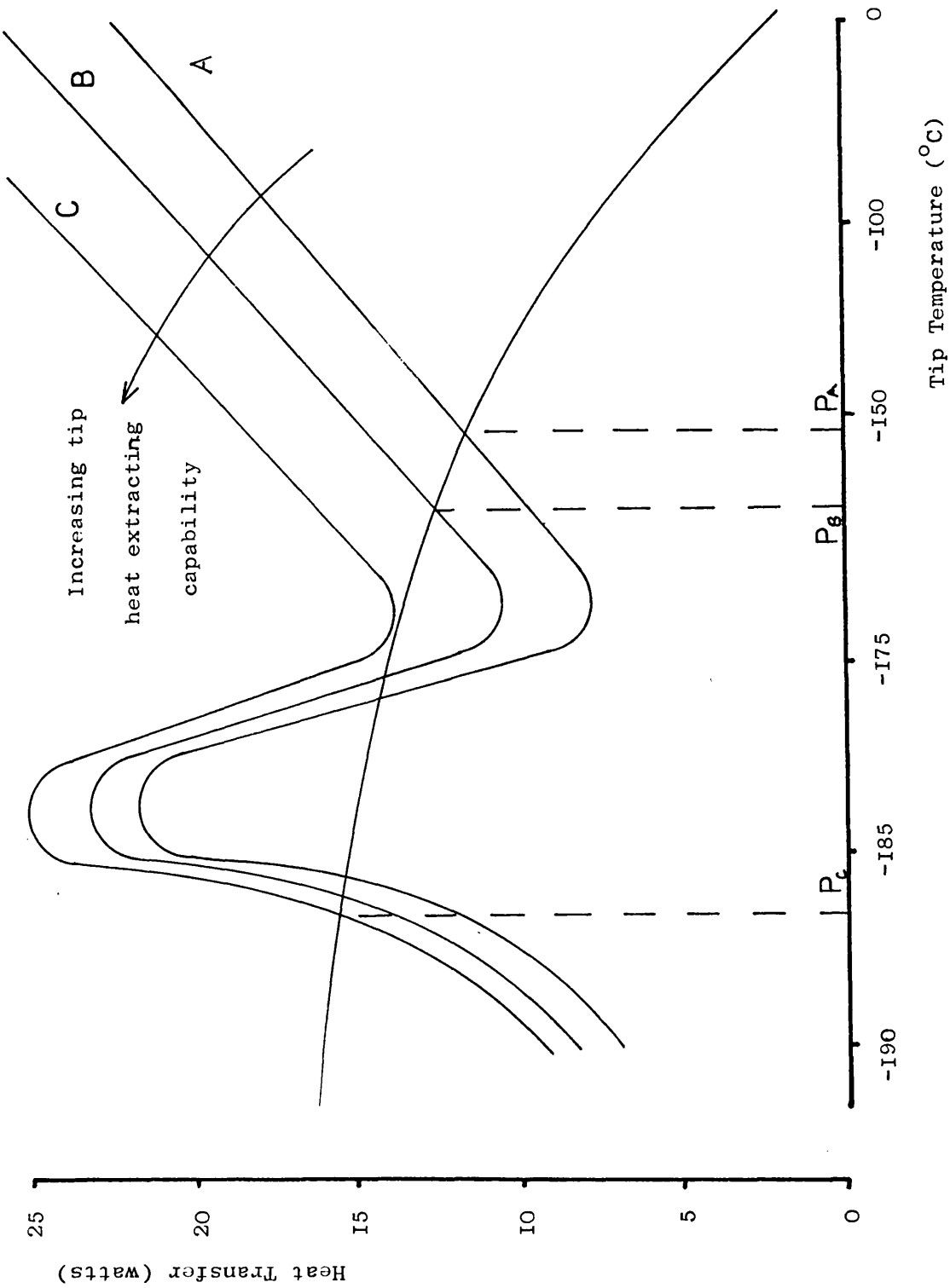

of the incident jet to break through the vapour film and wet a portion of the tip wall.

Several attempts were made to generate a series of incident jets in the hope that each one would produce its own wetted area. The total tip area in contact with the liquid would then be larger. However little improvement was achieved and a transparent model of the tip cavity was constructed in polycarbonate to try and observe flow conditions inside the tip. This model showed that the incident jet did indeed produce a wetted area but that the multi-orifice pipe behaved strangely. The liquid tended to only emerge from one of the orifices, the others simply vented vapour.

6.6.2 Generating a steep thermal gradient in the tip wall

Whilst the work on spray pipes was in progress, another approach was tried and proved to be very successful. It was argued that if the temperature of the inner wall of the tip could be cooled quickly below the critical temperature for nucleate boiling, even though the outer temperature was still warm, then a good heat transfer would result.

Initial attempts to establish a steep temperature gradient over the tip wall concentrated on trying to establish areas of the tip lining that would be remote from the rest of the tip and would cool more quickly.

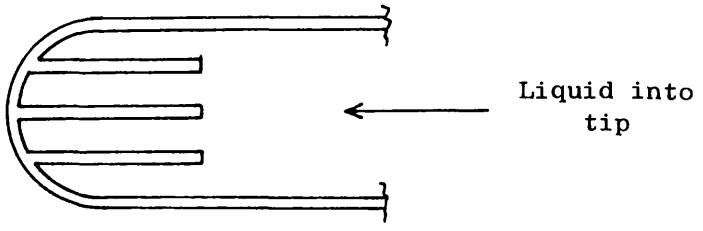

These ideas led to the possibility of incorporating a limited amount of thermal insulation in the tip wall so as to enable those areas to cool quickly and establish nucleate boiling there.

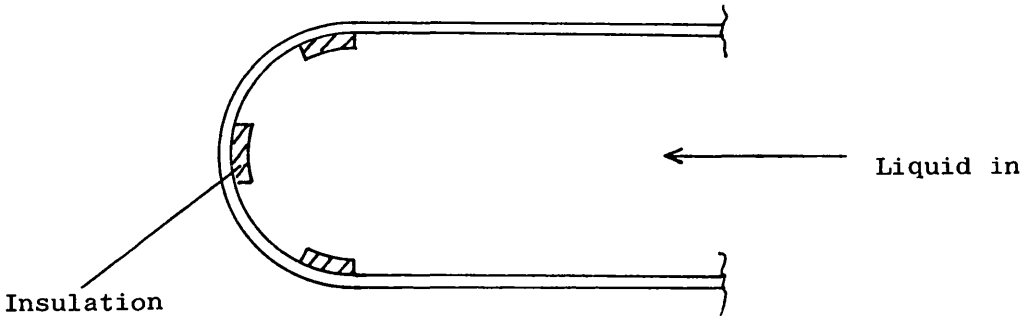

If this approach worked for a limited area then there was no reason why the whole tip should not be so lined to establish the necessary thermal gradients across the wall of the tip.

Some tips were constructed entirely out of polycarbonate and proved to cool to a low operating temperature very quickly. **Figure 46** plots the cooling curve obtained for two identical tips, one constructed from brass and the other from polycarbonate. The effectiveness of the plastic tip is clear.

6.7 Investigations of Plastic Tip Performances

6.7.1 The existence of an optimum wall thickness

There is an optimum wall thickness with which the tip will cool most rapidly. Consider a simplified overall thermal resistance, from the liquid nitrogen to

FIGURE 46

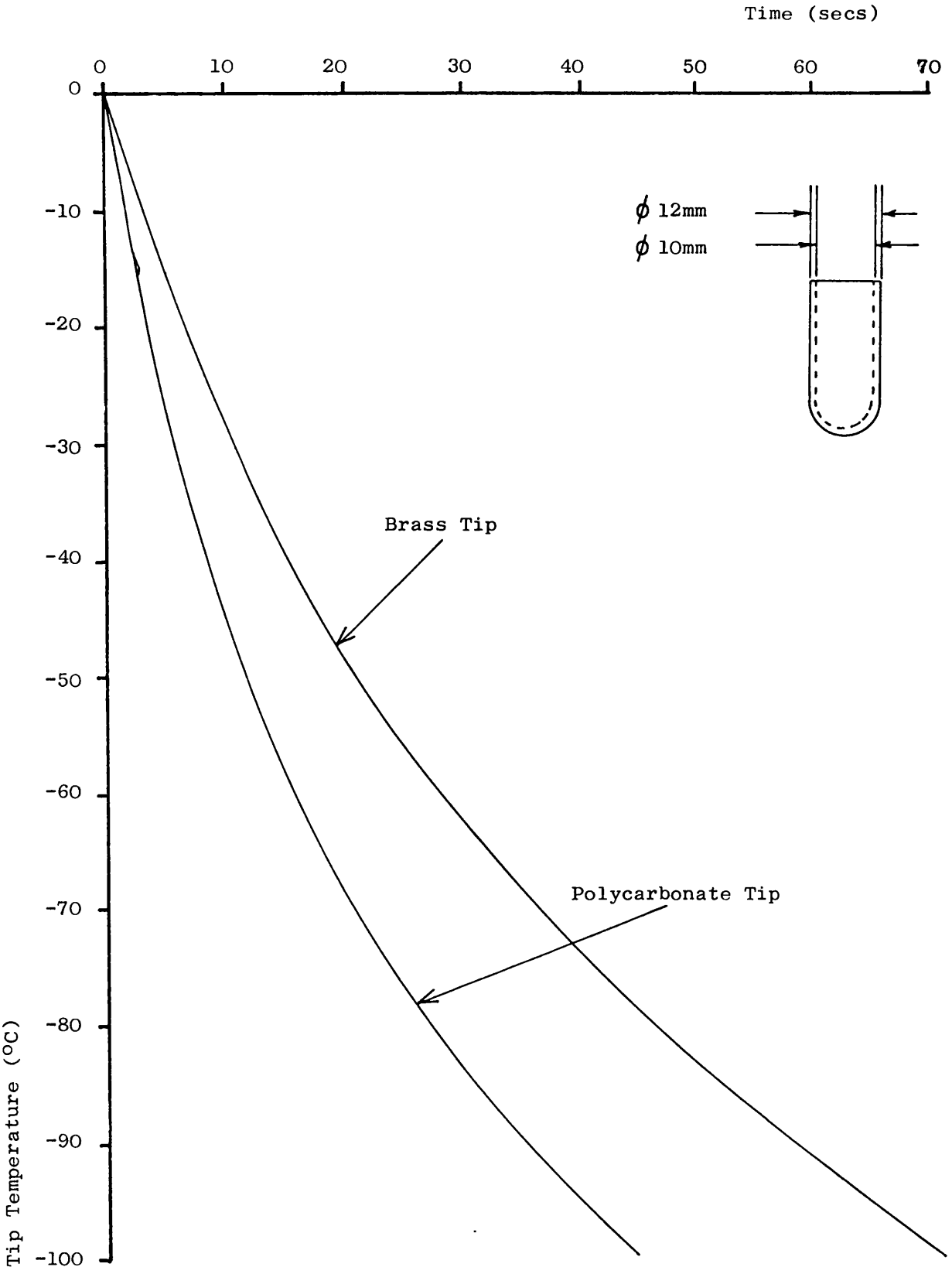

EFFECT OF TIP MATERIAL ON COOLING RATE

the outside of the tip wall. (Cartesean co-ordinates will be used and constant surface areas are assumed as the purpose of this argument is to demonstrate the existence of the optimum).

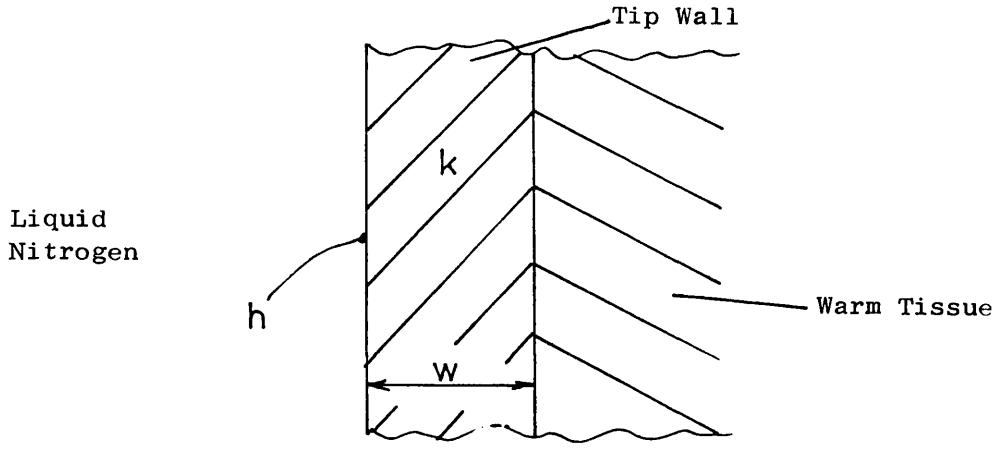

$$\text{Overall thermal resistance} = \frac{1}{U} = \frac{1}{h} + \frac{W}{k} \qquad (28)$$

Thermal Resistance of Boundary Film

Thermal Resistance of Wall

The overall thermal resistance should be as low as possible for optimum cooling.

When the thermal conductivity, k, of the wall is large, as it is with metal tips, the overall thermal resistance, $\frac{1}{U}$, is dominated by the thermal resistance of the boundary film, $\frac{1}{h}$.

When the thermal conductivity is small, as it is with plastic tips, the overall thermal resistance can be dominated by either thermal resistance term, depending on the wall thickness, W.

Consider initially the effect of variations in wall thickness on the internal heat transfer coefficient. When the wall is thin, only a small temperature

difference can be maintained across it. The entire wall is essentially at tissue temperature so the nitrogen will be undergoing film boiling and the heat transfer coefficient will be low. Alternatively with a thick wall, the inner wall temperature will quickly cool and establish the conditions necessary for nucleate boiling of the nitrogen, with a resulting high heat transfer coefficient.

Both the two terms of the thermal resistance equation **Equation 24**, are therefore dependant on the wall thickness. **Figure 47** shows a diagrammatic plot of the effect of wall thickness on these terms. As can be seen, there will be an optimum wall thickness where the overall thermal resistance will be a minimum.

6.7.2 Empirical investigation of optimum tip wall thickness

The optimum wall thickness was investigated empirically. A series of polycarbonate tips were constructed that had the same internal diameter and length but a different wall thickness. The outside tip temperature was monitored with a thermocouple and each tip in turn was cooled in an identical way. By measuring the cool-down time from 0°C to -100°C for each tip it was hoped to find the optimum value of wall thickness.

Figure 48 shows one series of results. The wall thickness that provided the fastest cool-down was consistently found to be the 0.25mm wall.

FIGURE 47

DIAGRAM SHOWING EXISTENCE OF OPTIMUM WALL THICKNESS FOR MINIMUM THERMAL RESISTANCE

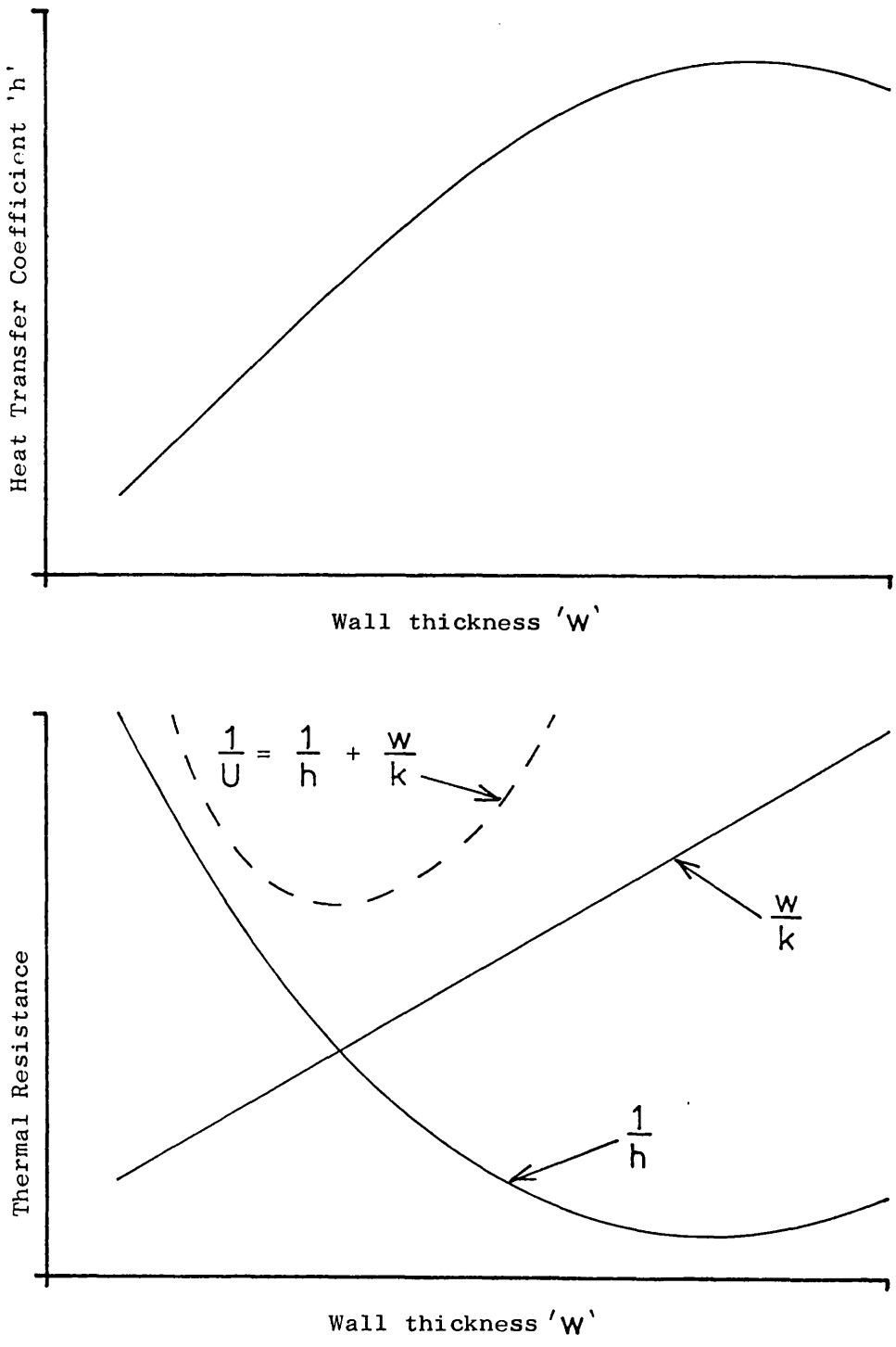

FIGURE 48

EFFECT OF PLASTIC TIP WALL THICKNESS ON COOLING RATE

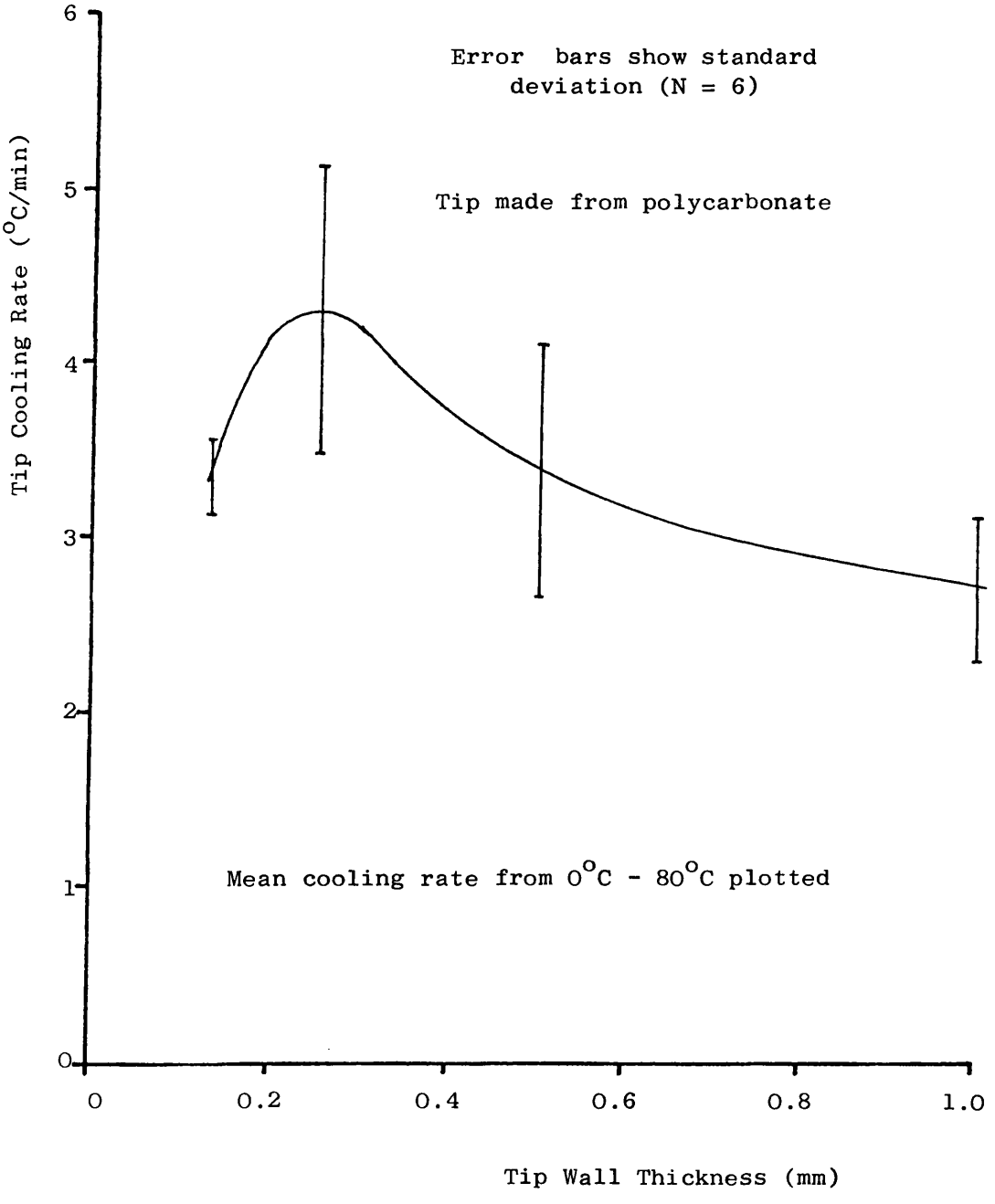

6.7.3 Effect of plastic tip on equilibrium temperature

Figure 49 shows a plot of heat flux versus T_t for a test on a plastic tip. The temperature differences plotted are based on the <u>outside</u> tip temperatures.

Also shown in **Figure 49** is the curve obtained with a metal tip that was geometrically identical to the plastic one. The curve for the plastic tip is similar in form to that obtained with the metal tip, but the various features occur at higher T_t's .

In **Figure 50** these two boiling curves are replotted together with the required heat flux through the ice-ball. The equilibrium temperature obtainable with the plastic tip is shown to be much lower than for the metal tip and within the performance specification.

If the curve for the plastic tip were replotted using temperature differences based on the <u>inside</u> tip temperatures, the curve would be expected to be almost identical to that illustrated for the metal tip. (Inside tip temperatures could unfortunately not be measured with the test rig used). The shift in the curve based on outside temperatures is due to the temperature gradient that exists over the plastic tip wall.

6.8 <u>Final tip design</u>

The optimised wall thickness of the plastic tip was rather thin to provide any scope for convoluting its internal surface. It was therefore decided that the

FIGURE 49

EFFECT OF TIP MATERIALS ON THE BOILING BEHAVIOUR

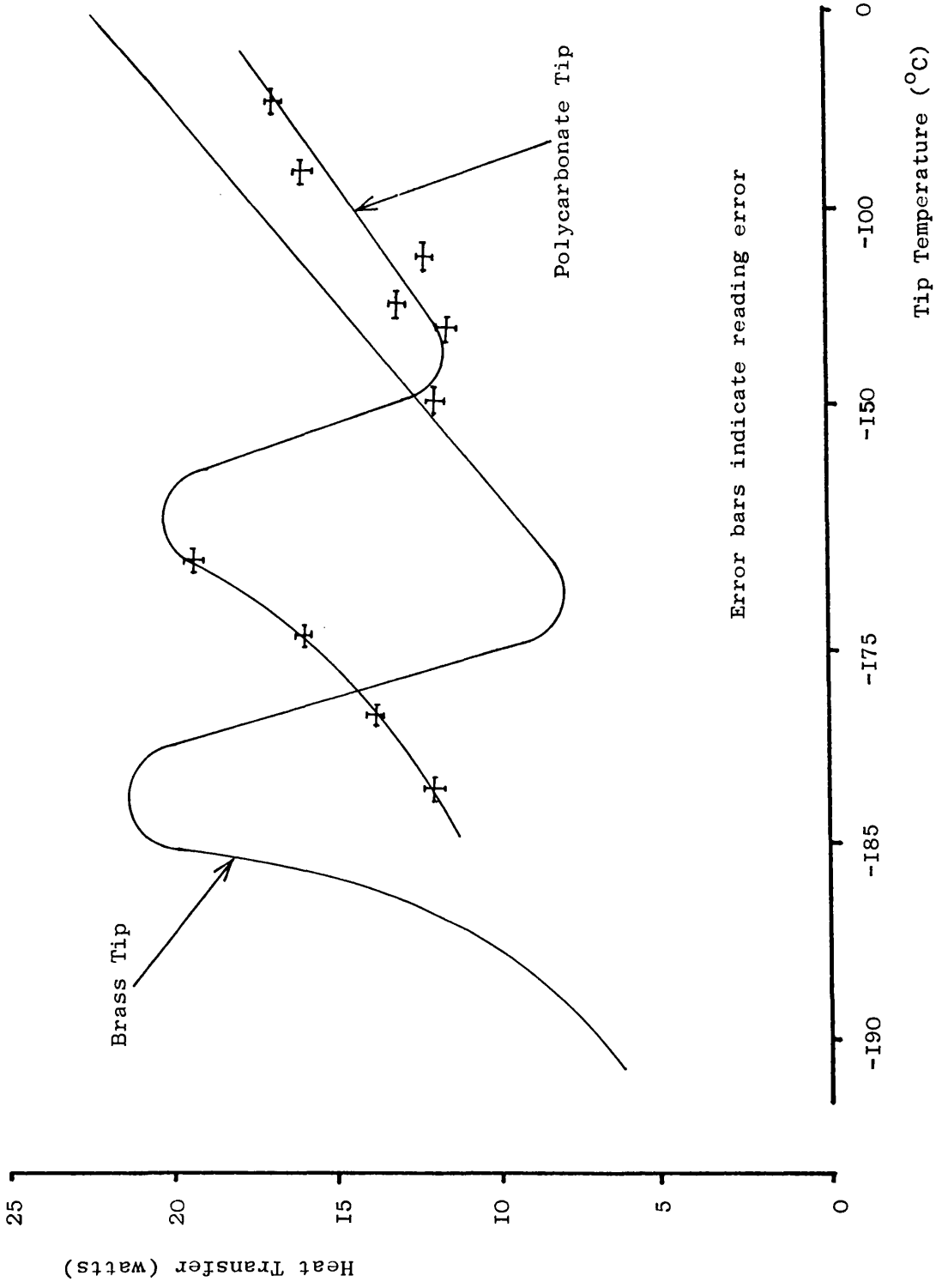

FIGURE 50

EFFECT OF TIP MATERIAL ON TIP EQUILIBRIUM TEMPERATURE

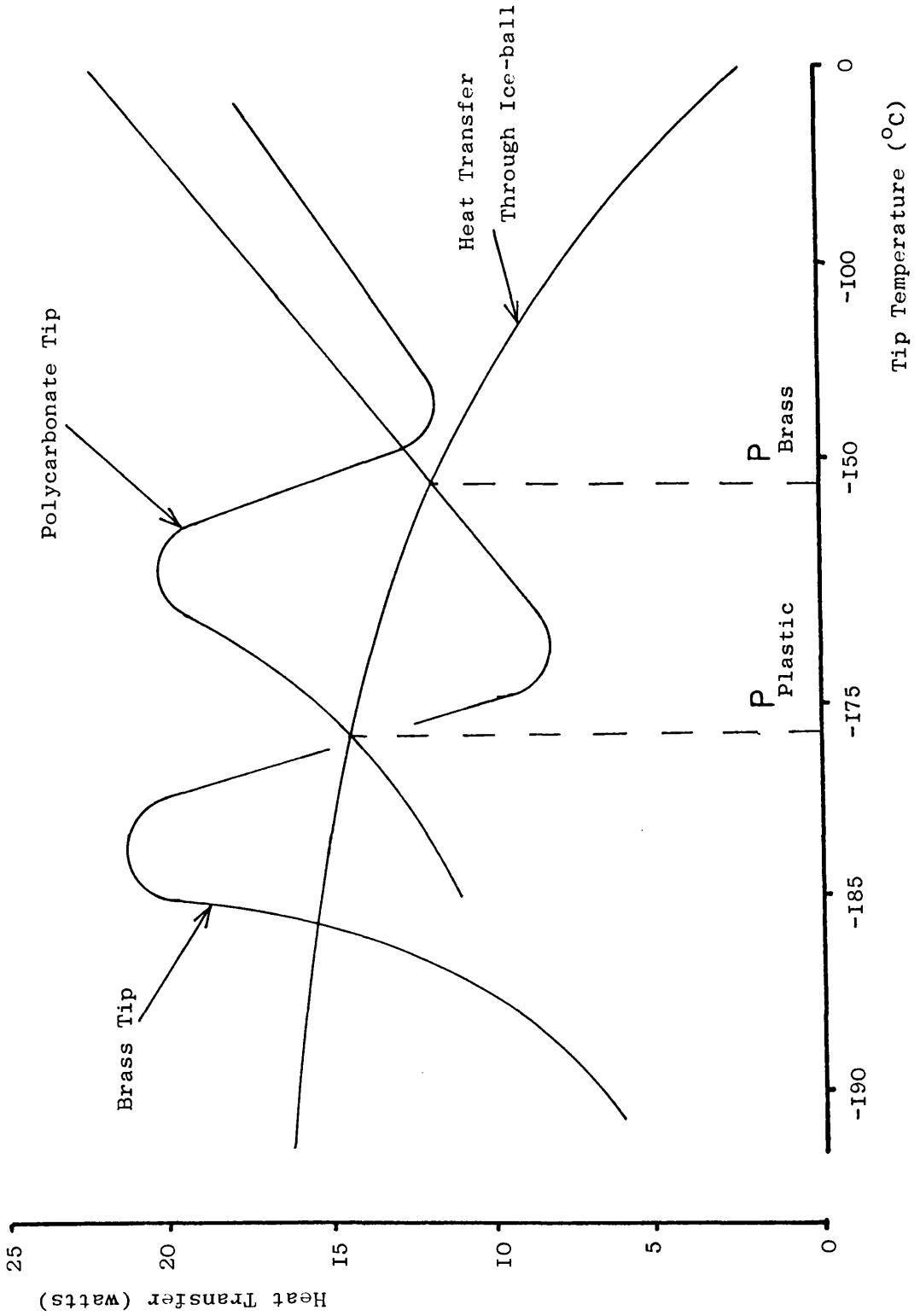

inner part of the tip would have be metal and include some convolutions, with a 0.25mm layer of plastic on the outside. However the tip would be thermally cycled between +37°C and -196°C and it was felt that a plastic coating may not withstand the loads imposed by the thermal expansions. The final design therefore was a composite structure as shown in **Figure 51.**

The composite tip had an inner metal lining to produce an increased surface area whilst the thermal insulation was to be a layer of silicone grease that would be sandwiched between the inner and outer metal cases. In this way it was felt that a good thermal contact could be maintained between the layers. This is the final tip design incorporated in the rectal cryoprobe.

6.9 Conclusions

1. The heat flux obtained during nucleate boiling can satisfy that required by the performance specification.
2. The mass flow rate of cryogen should be above 1×10^{-4} kg/s.
3. The input pipe should preferably contain five 1mm diameter holes and can be positioned anywhere between 3mm and 20mm from the tip end.
4. The incorporation of a $\frac{7}{16}$ " UNC thread within the tip improves the heat transferred at a given tip temperature.

FIGURE 51

FINAL TIP DESIGN

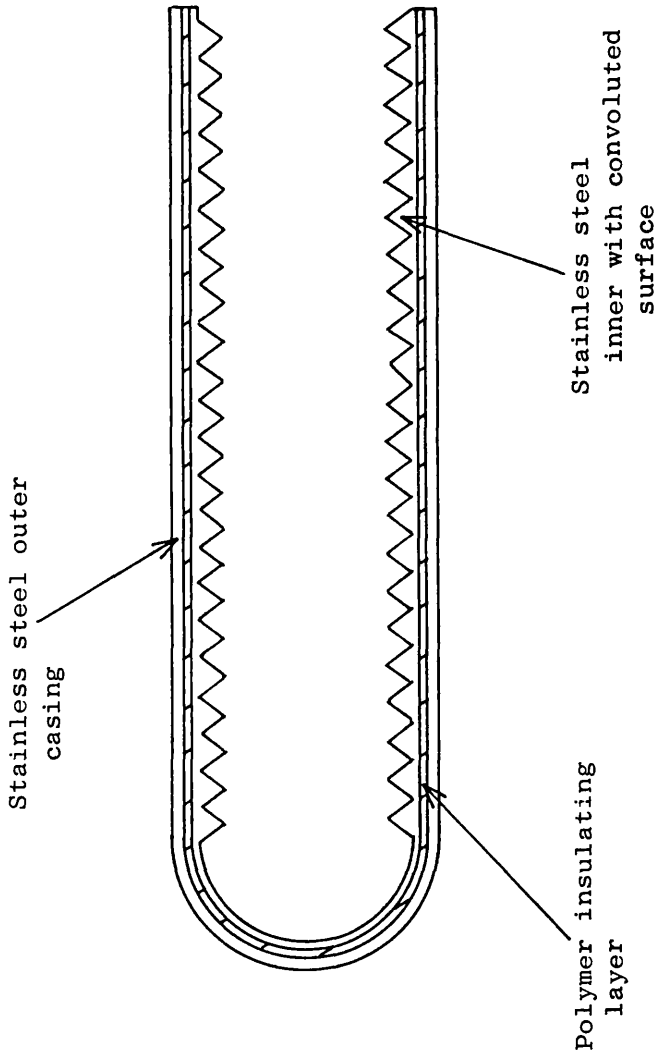

5. A layer of plastic, 0.25mm thick, incorporated in the wall of the tip, substantially increases the heat flux, and enables low tip equilibrium temperatures to be achieved when freezing tissue.
6. The tip design illustrated in **Figure 51** is preferred.

CHAPTER 7

Analysis of Tip Heat Transfer using Finite Difference Techniques

7.1 Introduction

In this chapter some of the work on tip cooling discussed in **Chapter 6** is analysed in more detail. In particular finite difference models of the cooling process are used to study the cooling rates achieved when transferring heat through different materials.

It was shown in **Chapter** 5 that when boiling takes place, the boundary heat transfer coefficient depends, in a rather complex manner, on the boundary temperature. As a consequence, the unsteady heat transfer from the material boundary to the boiling liquid is difficult, if not impossible, to model analytically. If, in addition the heat is transferred through a medium that consists of several materials, the unsteady heat transfer can only be studied numerically.

This chapter describes the use of finite difference models of the heat transfer through a cryo-tip wall to boiling liquid nitrogen. The finite difference equations are used to estimate temperatures in time and one-dimensional space. The work discussed explores the increased cooling rate that results from constructing the tip out of a poor thermal conductor. Three main areas are discussed:-

(1) The cooling rate of the inner surface of the sheet is calculated to demonstrate the basis of the phenomenon.

(2) The cooling rate at a distance from the cooled surface is calculated for sheets of different materials.

(3) Composite sheets are examined to see if a metal sheet coated in a thin layer of insulation can achieve the same result.

7.2 Major Assumptions

Two major assumptions were made.

7.2.1 Pool boiling heat transfer coefficients

All the studies described use heat transfer coefficients derived from the published pool boiling curve for liquid nitrogen. This data is well established and has been repeated by many authors.

However, when nitrogen is boiling within cryotips, the heat transfer coefficients could be different to those occuring for pool boiling. When liquid nitrogen is passed into a blunt ended cryoprobe tip it will possess considerable momentum. This momentum is likely to be sufficient for the liquid jet to break through a vapour film at the far end of the tip. Therefore, even if the boundary temperature difference is high, heat transfer coefficients higher than those occuring in pool film boiling might occur in this region.

7.2.2 One-dimensional heat transfer

In principle, to analyse the cooling performance of the cylindrical cryoprobe tip, the finite difference equations should have been formulated to cover the case of two-dimensional conduction using cylindrical co-ordinates. However the quantitative estimates discussed here were carried out using one-dimensional equations simply because of the speed of computation.

7.3 Structure of Finite Difference Models

7.3.1 Basis of models

In Appendix 3 a series of finite difference equations are derived. These equations describe the one-dimensional transient temperature distribution through a solid slab of material, of infinite extent normal to the direction of heat transfer. Figure 52 shows a series of points along this path, Δx metres apart, at which the temperature is to be calculated using the equations. The equations enable this temperature distribution to be recalculated at successive intervals of ΔT seconds, as shown in Figure 52. In this way, the manner in which the temperature distribution changes with time can be calculated.

7.3.2 The finite difference equations used

The temperature at any given point in the space/time grid is given the symbol, T_i^n. The subscript, i, refers to the position in space of the point and the superscript, n, refers to the position in time.

FIGURE 52

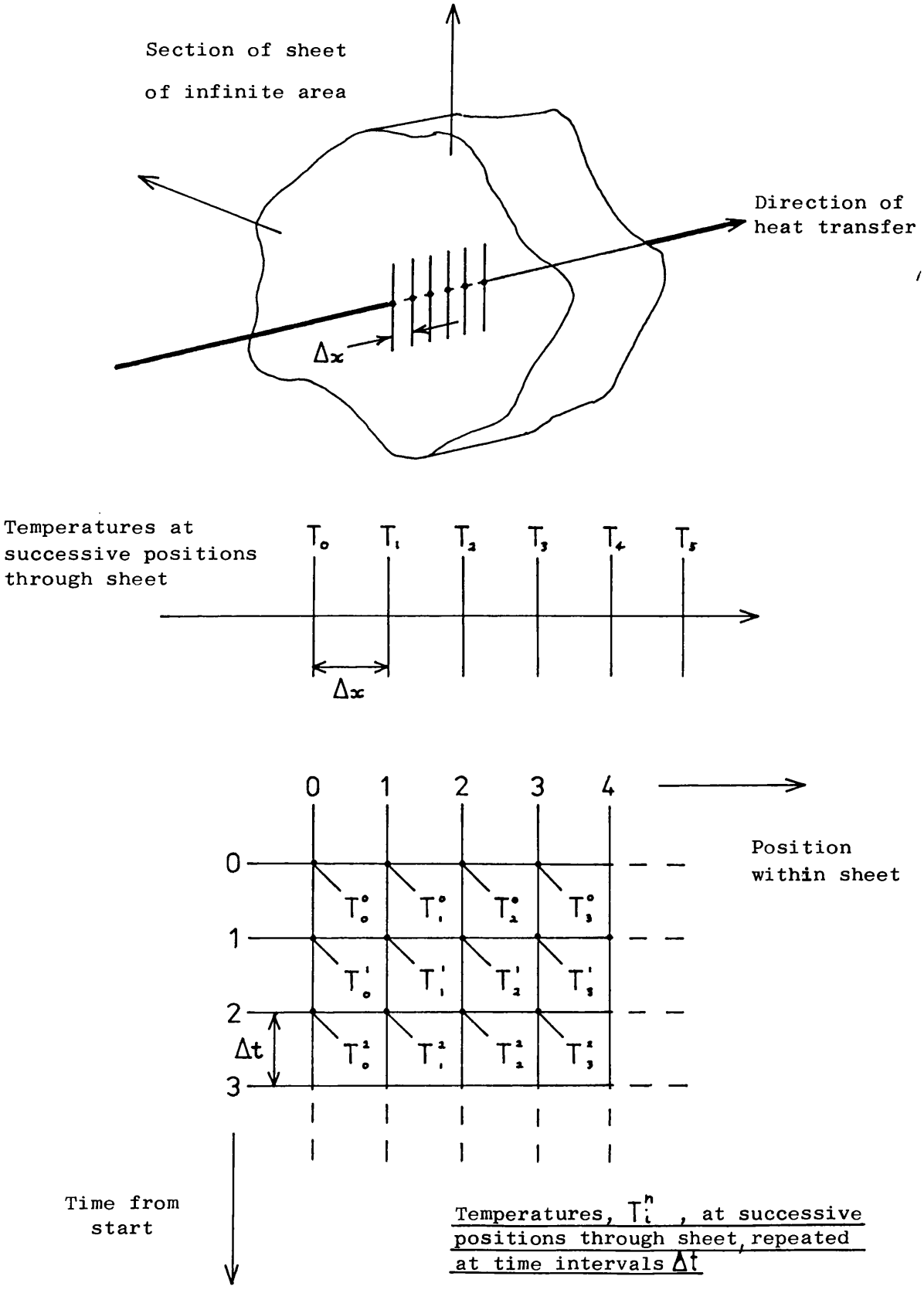
Section of sheet
of infinite area
Direction of
heat transfer
Δx
Temperatures at
successive positions
through sheet
T0 T1 T2 T3 T4 T5
Δx
0 1 2 3 4
Position
within sheet
0
1
2
3
Δt
Time from
start
Temperatures, Ti^n , at successive
positions through sheet, repeated
at time intervals Δt

Appendix 3 shows that the temperature at any point in a homogeneous medium away from a boundary is given by:-

$$T_i^{n+1} = Fo\left[T_{i-1}^n + T_{i+1}^n - 2T_i^n\right] + T_i^n \qquad (29)$$

Where $F_o = \frac{\alpha \Delta t}{(\Delta x)^2}$ = Fourier number

α = thermal diffusivity

Additional equations are also derived in **Appendix 3** that enable boundary conditions to be accommodated. When a boundary is in contact with a fluid and undergoing convective heat transfer, the following equation is derived for the temperature at the boundary:

$$T_o^{n+1} = 2Fo\left[T_1^n - (1 + Bi)T_o^n + Bi\,T_F^n\right] + T_o^n \qquad (30)$$

Where $Bi = \frac{h\Delta x}{k}$ = Biot Number

T_F = temperature of fluid

In the analysis of composite tips, a boundary exists at the junction of dissimilar materials. **Appendix 3** shows that the temperature at the junction is given by the following equation:-

$$T_i^{n+1} = \frac{2}{(1+\gamma)}\left[Fo_A\gamma\,T_{i-1}^n + Fo_B T_{i+1}^n - (Fo_A\gamma + Fo_B)T_i^n\right] + T_i^n \qquad (31)$$

where $\gamma = \frac{(\Delta x \rho c)_A}{(\Delta x \rho c)_B}$

$$Fo_A = \frac{\alpha_A \Delta t}{(\Delta x_A)^2} \qquad Fo_B = \frac{\alpha_B \Delta t}{(\Delta x_B)^2}$$

7.3.3 Stability criteria

In Appendix 3 it is shown that for each of the finite difference equations derived there is a stability criterion that must be satisfied. The stability criterion associated with Equation 29 (temperatures at points away from boundaries) is:-

$$Fo \leqslant 0{\cdot}5$$

For Equation 30 (temperature at connective boundary) the stability criterion is:-

$$\frac{Fo}{(1 + Bi)} \leqslant 0{\cdot}5$$

For Equation 31 (temperature at junction of dissimilar materials) the stability criterion is:-

$$\frac{\gamma Fo_A + Fo_B}{(1 + \gamma)} \leqslant 0{\cdot}5$$

If the stability criteria are not satisfied the calculated temperatures will oscillate wildly and to progressively higher amplitudes. Before a given case is analysed, therefore, the computer program checks the starting values of the variables to ensure the stability criteria are satisfied.

7.4 Computer Program Used to Calculate Temperature Distribution

7.4.1 Basic structure of program

The equations of **Appendix 3** are incorporated into a computer program. Once the initial temperature distribution within the slab is set up, the program will calculate the temperature at a time t seconds later for each of the space intervals through the slab. The calculations are continuously repeated at time intervals of Δt. A simplified flow chart is shown in **Figure 53** and a listing of the program is given in **Appendix 4.** All the investigations were carried out on either a PET or a BBC 'B' microcomputer.

7.4.2 Accommodating the cooled boundary heat transfer coefficient

In using the equations to describe the effect of heat transfer through the sheet, various boundary conditions are used. However, one boundary is always subject to heat transfer from the sheet through a convective boundary layer to boiling nitrogen. The heat transfer coefficient at that boundary is dependent on the boundary temperature. Therefore at each time interval, Δt , the heat transfer coefficient that corresponds to the current boundary temperature must be calculated.

7.4.3 Speed of computing

It was shown in **Appendix 3** that the stability

FIGURE 53

SIMPLIFIED OVERALL FLOW CHART FOR NUMERICAL ANALYSES PROGRAM

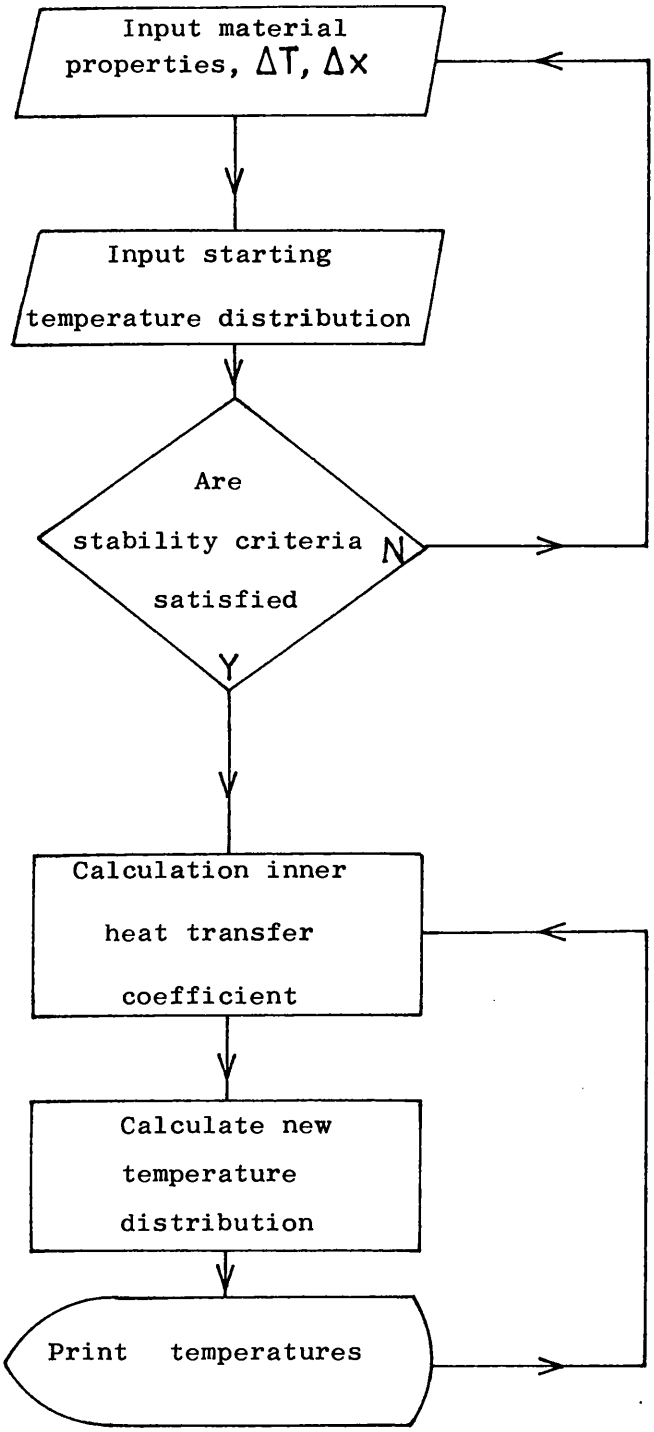

criterion for calculating temperatures away from boundaries was:-

$$Fo = \frac{\alpha \Delta t}{(\Delta x)^2} \ll 0.5$$

Δx was usually quite small because thin layers of material were being investigated. Consequently Δt had also to be small for stability. As the programmes were written in PET or BBC BASIC, which are rather slow in operation, computer runs to explore temperature changes towards equilibrium were rather protracted.

7.5 Pool Boiling Heat Transfer Coefficients

7.5.1 Access to heat transfer coefficients in the program

The heat transfer coefficient on the boiling nitrogen boundary will be called the inner heat transfer coefficient. In order to calculate its value for any given inner boundary temperature, a non-continuous heat transfer coefficient function, $h(\Delta T_{SAT})$ was defined. Most of the original analyses were carried out using inner heat transfer coefficients typical of nitrogen pool boiling. The coefficients were calculated from the pool boiling curve presented in "Heat Transfers at Low Temperatures" (Frost, 1975).

7.5.2 Division of the boiling curve into regions

When the boiling curve is plotted in the form of $\log(h)$ against $\log(\Delta T_{SAT})$, as shown in Figure 54,

FIGURE 54

HEAT TRANSFER COEFFICIENTS FOR LIQUID NITROGEN POOL BOILING AS A FUNCTION OF ΔT_{SAT}

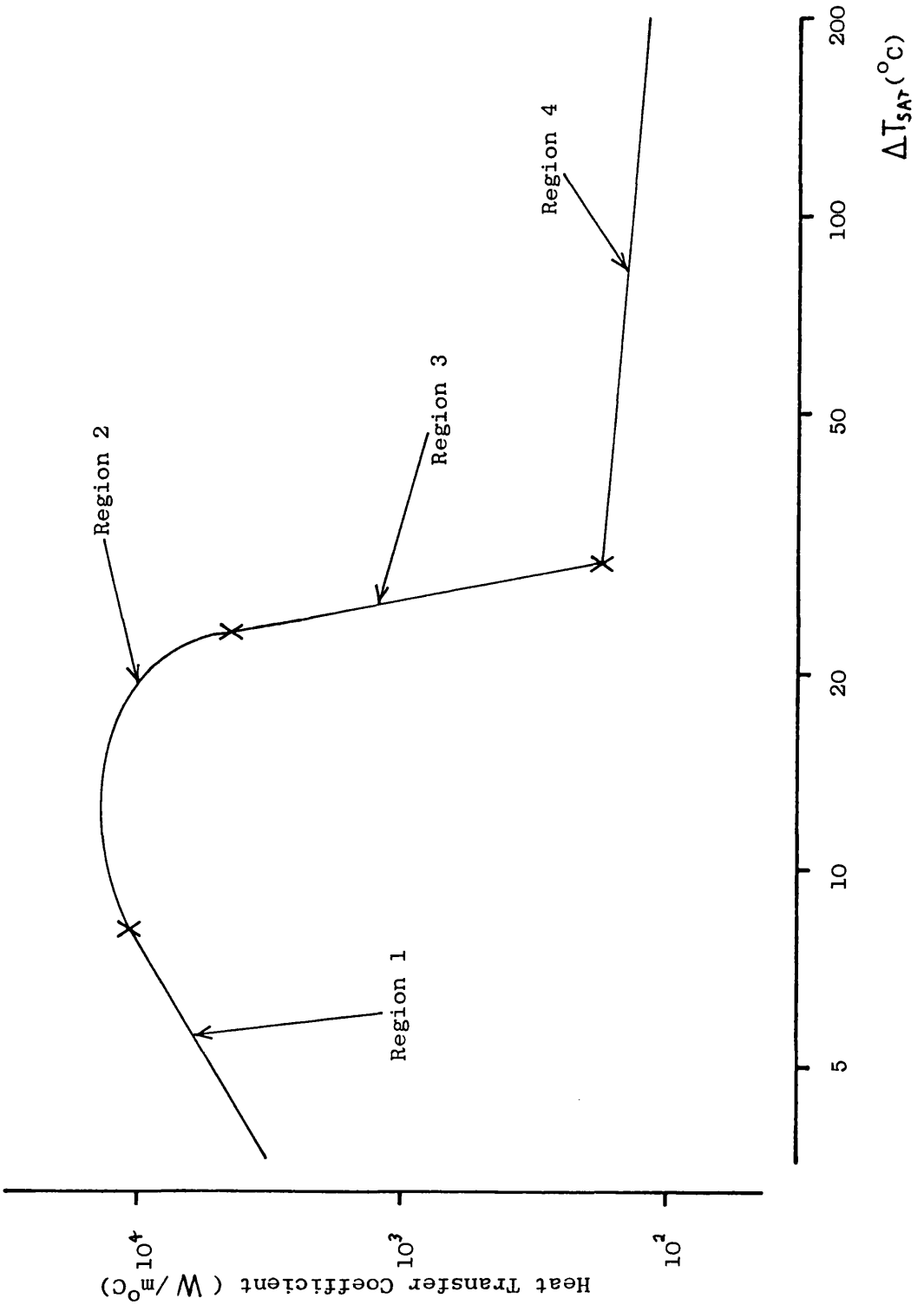

several regions of the curve are approximately linear. In order to include a heat transfer coefficient function in the computations, the curve was divided into four regions, as shown:

(1) $0 \leq \Delta T \leq 8.17°C$ (most of nucleate region)

(2) $8.17 < \Delta T \leq 23.34°C$ (peak around max. heat flux)

(3) $23.34 < \Delta T \leq 29.37°C$ (most of transition region)

(4) $29.37 < \Delta T °C$ (film boiling region)

7.5.3 Equations derived from boiling curve

All but the second of the four regions of the boiling curve can be simply represented by linear functions of $\log(h)$ and $\log(\Delta T_{SAT})$. The second region around the maximum heat flux point is less easily modelled. There are six conditions known for this portion of the curve and a polynomial can be derived from these. The six conditions are:-

(1) Co-ordinates for end of first linear section.

(2) Co-ordinates for start of second linear section.

(3) Co-ordinates for peak of curve.

(4) Gradient of first linear section.

(5) Gradient of second linear section.

(6) Gradient at peak (zero).

Six simultaneous equations could therefore be described. These were solved to find the co-ordinates of a polynomial by a straightforward matrix solving program based on the systematic Gauss elimination method.

In this way the heat transfer coefficient can be described as a function of temperature difference using four equations.

(1) $h=\exp(1.2095\log T+6.56)$ $\quad 0 \leq T \leq 8.17°C$

(2) $h=\exp -13.209(\log T)^5+163.30(\log T)^4-803.25(\log T)^3$
$+1963.6(\log T)^2-2383.9(\log T)+1158.1$

$8.17 < T \leq 23.34°C$

(3) $h=\exp(-10.0\log T+39.5)$ $\quad 23.34 < T \leq 29.37°C$

(4) $h=\exp(-0.214\log T+5.92)$ $\quad 29.37 < t°C$

7.6 Effect of Material on Cooled Surface Temperature

7.6.1 Description of case being modelled

The first series of studies were run with one boundary cooled by liquid nitrogen and the other held at a constant temperature. The thickness of the sheet was 2.5mm. The temperature of the cooled surface was recorded to show the effect of using different materials for the sheet.

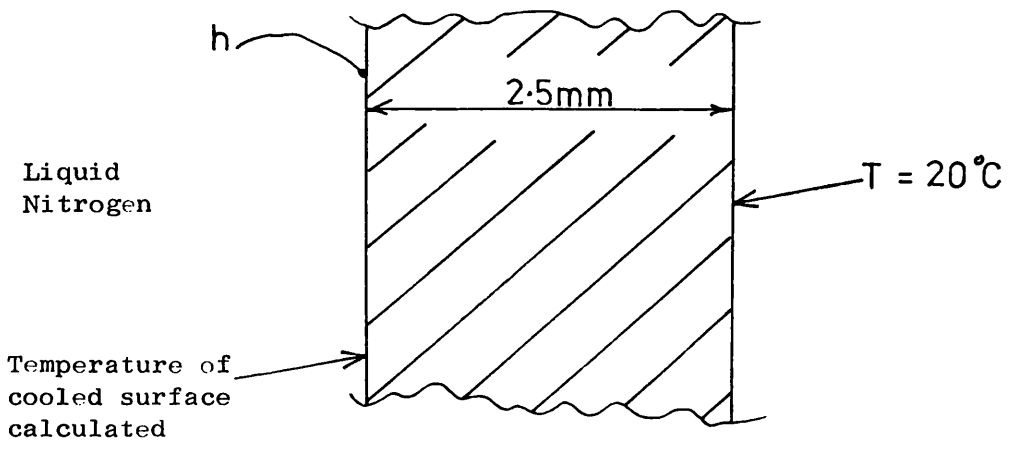

Two equations are needed for this situation, **Equation 29** for the internal points and **Equation 30** for the cooled boundary.

7.6.2 Results for boundary temperature

Figure 55 illustrates a plot of the cooled boundary temperature as a function of time, for different materials. The lower the thermal conductivity of the material, the more quickly the inner boundary was cooled. For the poorest conductor used, PTFE, it can be seen that the boundary temperature dropped below the minimum heat flux temperature during the time of the computer run. At this point the transition region of the boiling curve is entered and the heat transfer coefficient rapidly rises as the temperature falls lower. The result is a rapid cooling of the inner boundary as can be seen from **Figure 55.**

The rapid cooling of the boundary found with poorly conducting materials is exploited in the subsequent studies. The rapid cooling brings the nature of the boiling into the transition and nucleate regions of the boiling curve. The high heat transfer coefficients that result can lead to an overall higher heat transfer for the poor conductor compared to the good conductor.

7.7 Behaviour of an Infinite Sheet Cooled on Both Sides

7.7.1 Description of case being modelled

In this section the effect of the sheet material on

FIGURE 55

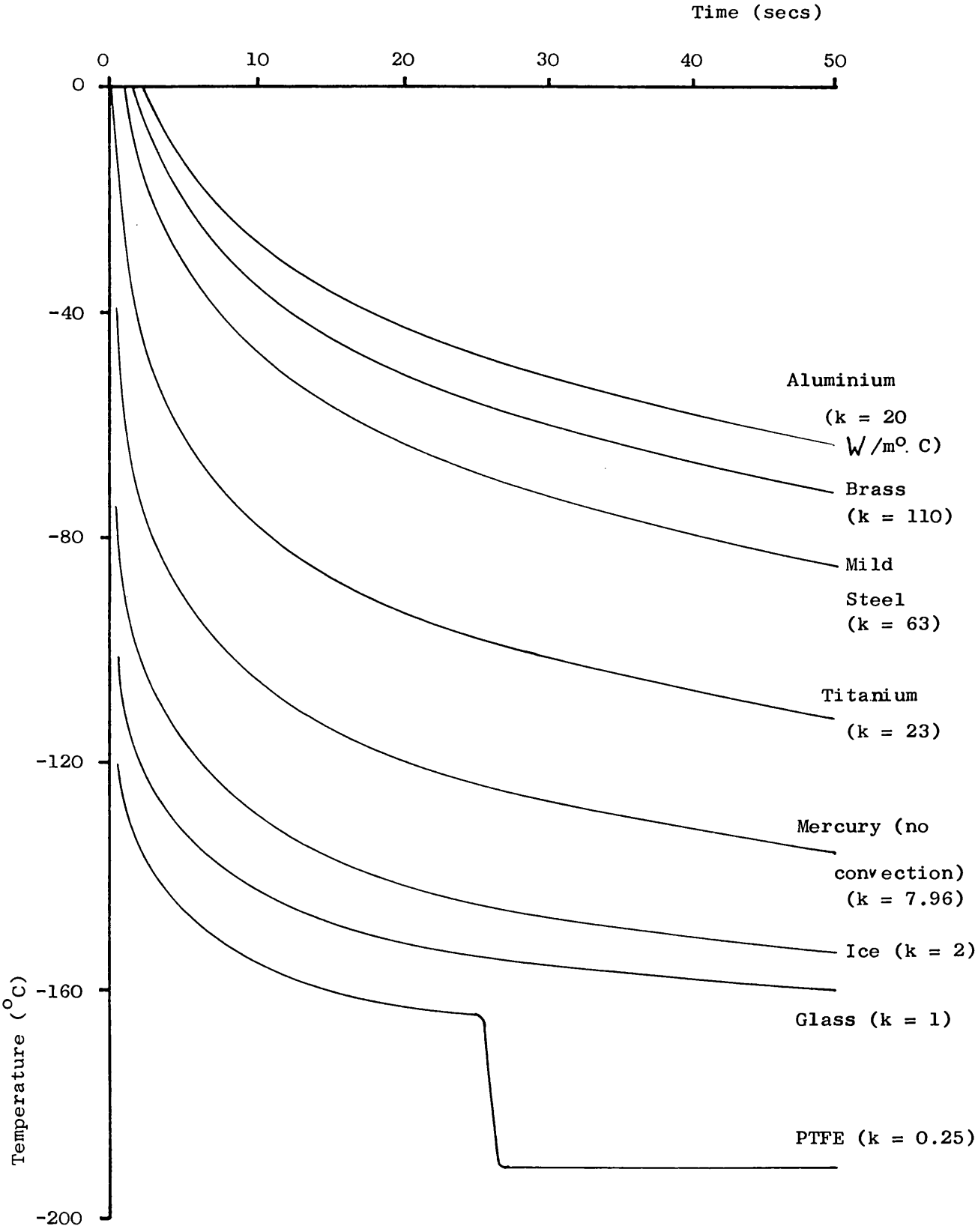

EFFECT OF MATERIAL ON INNER BOUNDARY COOLING CURVE

temperatures away from the cooled boundary is investigated. The case studied is that of an infinite sheet cooled on both sides by liquid nitrogen. This was done because it was felt that this situation could investigated experimentally by measuring temperatures in the middle of a large flat sheet.

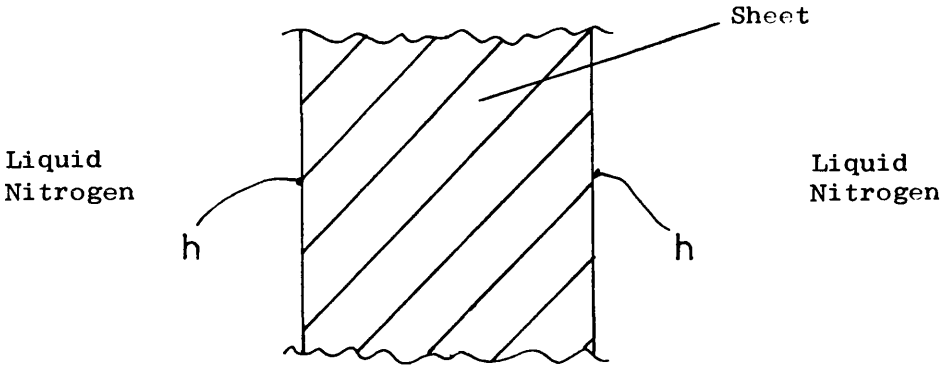

The midline is arranged to lie on the junction of two space intervals. The transient temperature distribution is assumed to be symmetrical about the midline. Consequently the midline temperature is given by the following equation:

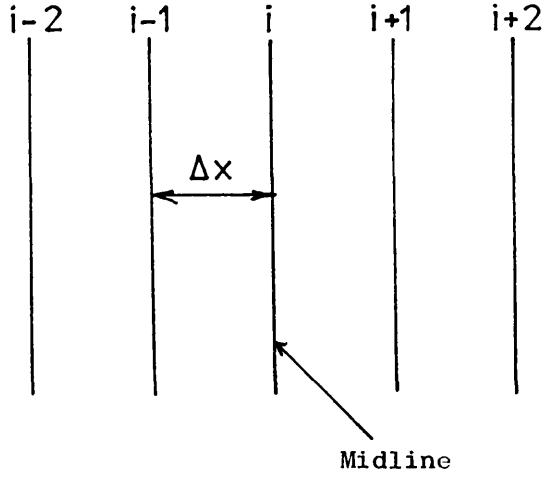

$i+1 = i-1$

$i+2 = i-2$ etc

$$\therefore \quad T_i^{n+1} = Fo(T_{i-1}^n + T_{i+1}^n - 2T_i^n) + T_i^n$$

$$= 2Fo(T_{i-1}^n - T_i^n) + T_i^n \qquad (32)$$

7.7.2 Results

Figure 56 illustrates a plot of the midline temperature for an infinite sheet of material 2.5mm thick, cooled on both sides by liquid nitrogen. Two materials are used, glass and steel. The boundary temperature for the glass quickly drops to low temperatures, as shown in the first series of experiments. Because the heat transfer coefficient is therefore higher for the glass at any given time, the midline temperature decreases faster than the steel, despite the fact that it is a much poorer thermal conductor.

This analysis was repeated for several different materials. Figure 57 illustrates a plot of the time taken for the midline temperature to decrease to -100°C for each of these materials. The infinite sheet modelled was again 2.5mm thick. For the set of variables used the optimum thermal conductivity would appear to be near that of glass.

7.8 Cooling Both Sides of a Sheet of Good Conductor Lined with a Layer of Poor Conductor

7.8.1 Outline of case being modelled

The previous computer runs demonstrated the effectiveness of using poorly conducting tips to increase the cooling rate. The next series of runs analyses the effect of using a good conductor for the tip material and covering it with a thin layer of poor conductor. Again both sides of the sheet are cooled

FIGURE 56

EFFECT OF MATERIAL ON MIDLINE COOLING CURVE

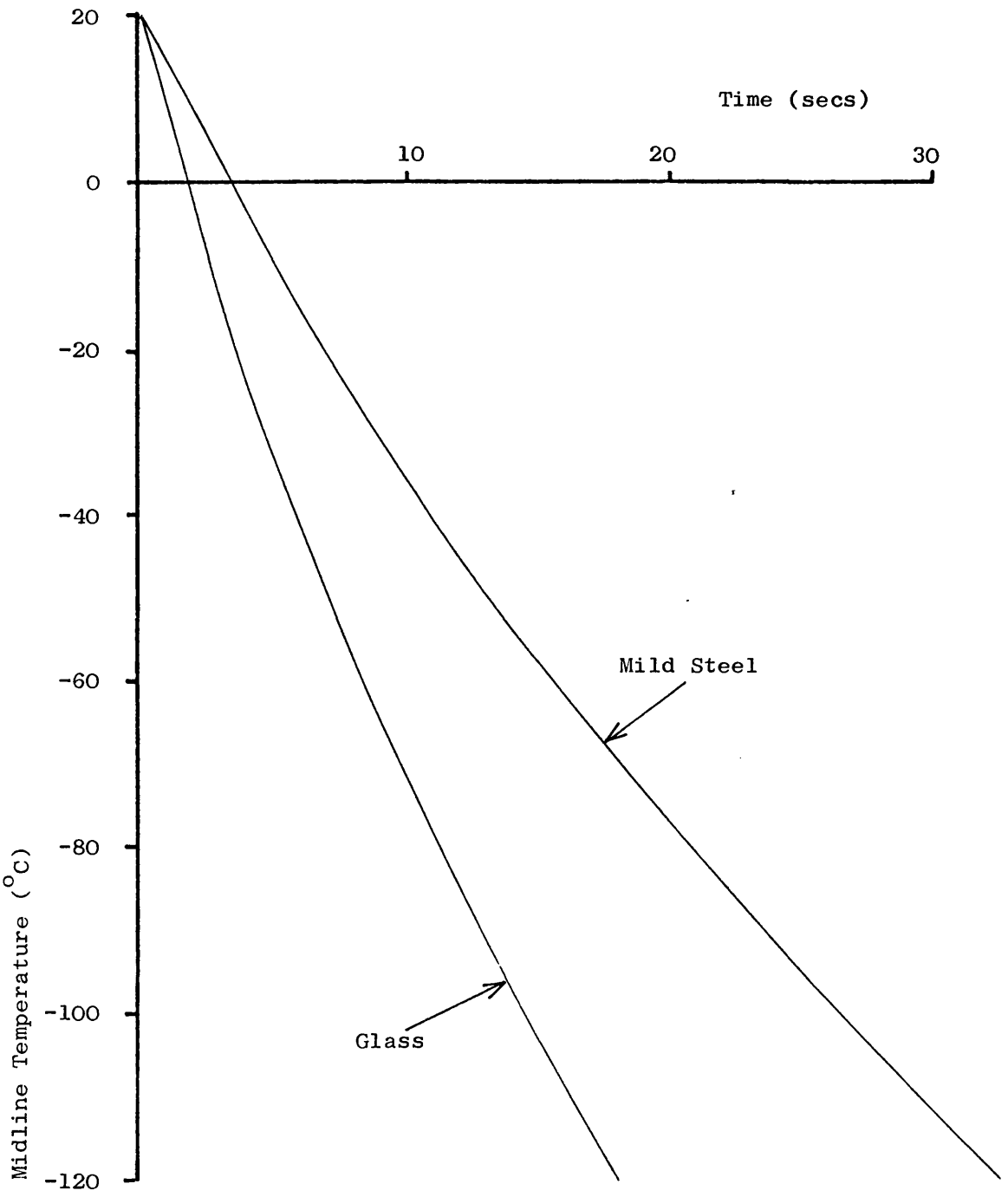

FIGURE 57

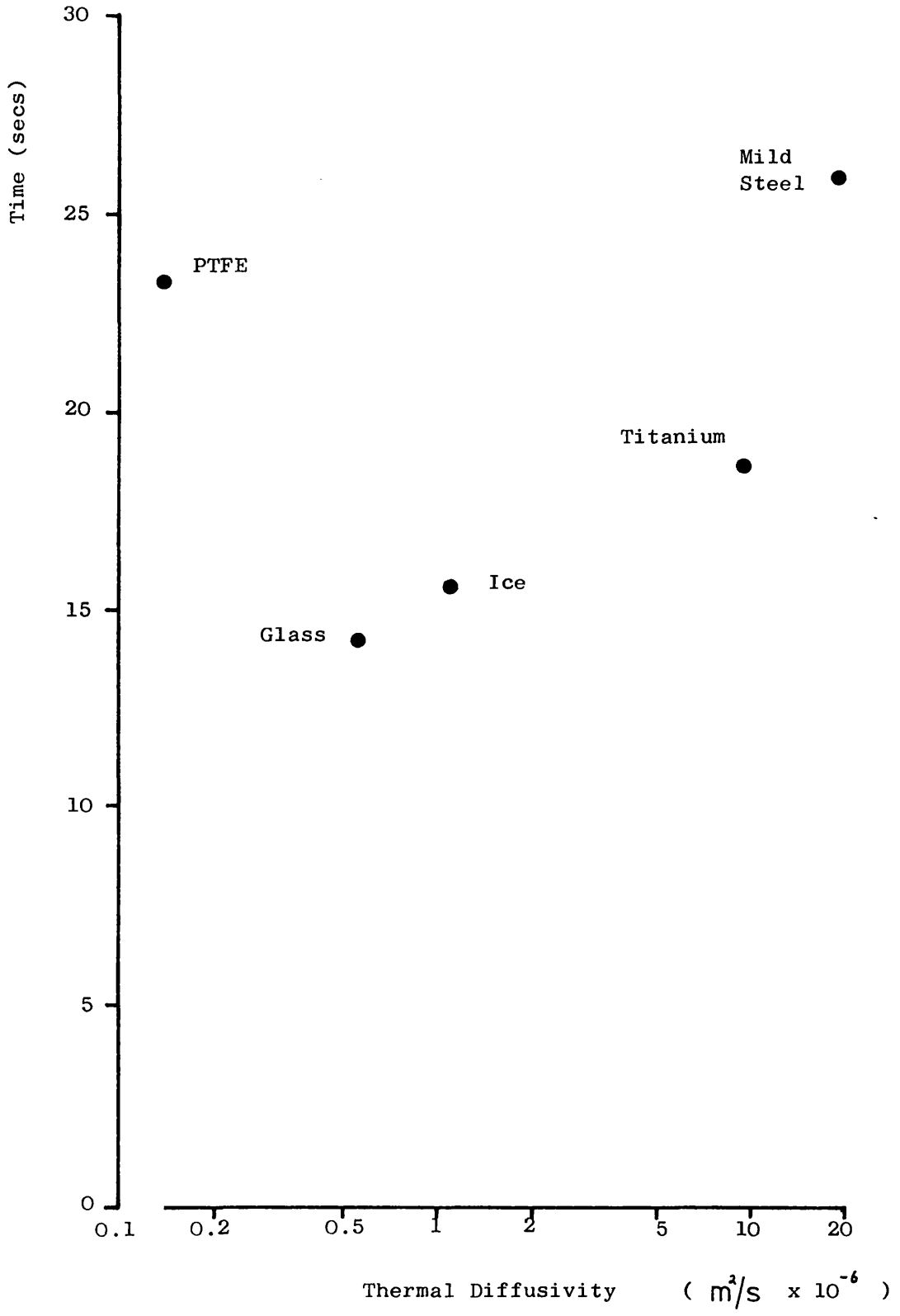

EFFECT OF MATERIAL ON TIME TAKEN TO COOL TO -100°C

AT MIDLINE OF SHEET 2.5mm THICK AND COOLED ON BOTH SIDES

and the midline temperatures are calculated.

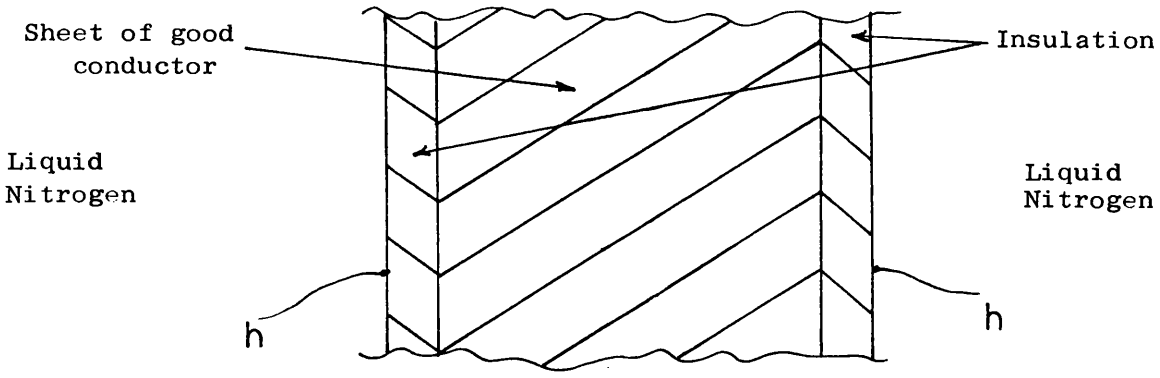

7.8.2 Results

Figure 58 illustrates a plot of the time taken for the midline temperature to decrease to -100°C for a sheet cooled on both sides. The sheet was again 2.5mm thick and results are shown for two situations. The first consists of mild steel alone but the second has a lining of PTFE that is 0.125mm thick, although the overall thickness is maintained at 2.5mm. As can be seen, the lined sheet cools more quickly.

A series of runs were carried out to investigate the optimum thickness of PTFE for the 2.5mm sheet. **Figure 59** illustrates a plot of the time taken for the midline temperature to decrease to -100°C for varying thicknesses of PTFE. The optimum thickness for speed of cooling to -100°C was the 0.125mm lining. For insulation thicknesses less or greater than this optimum, the cooling time increased.

The tests on polycarbonate cryoprobe tips discussed in **Chapter 6** showed a similar result. There was an optimum thickness of insulation to achieve the most rapid cool-down. For thicknesses greater than the

FIGURE 58

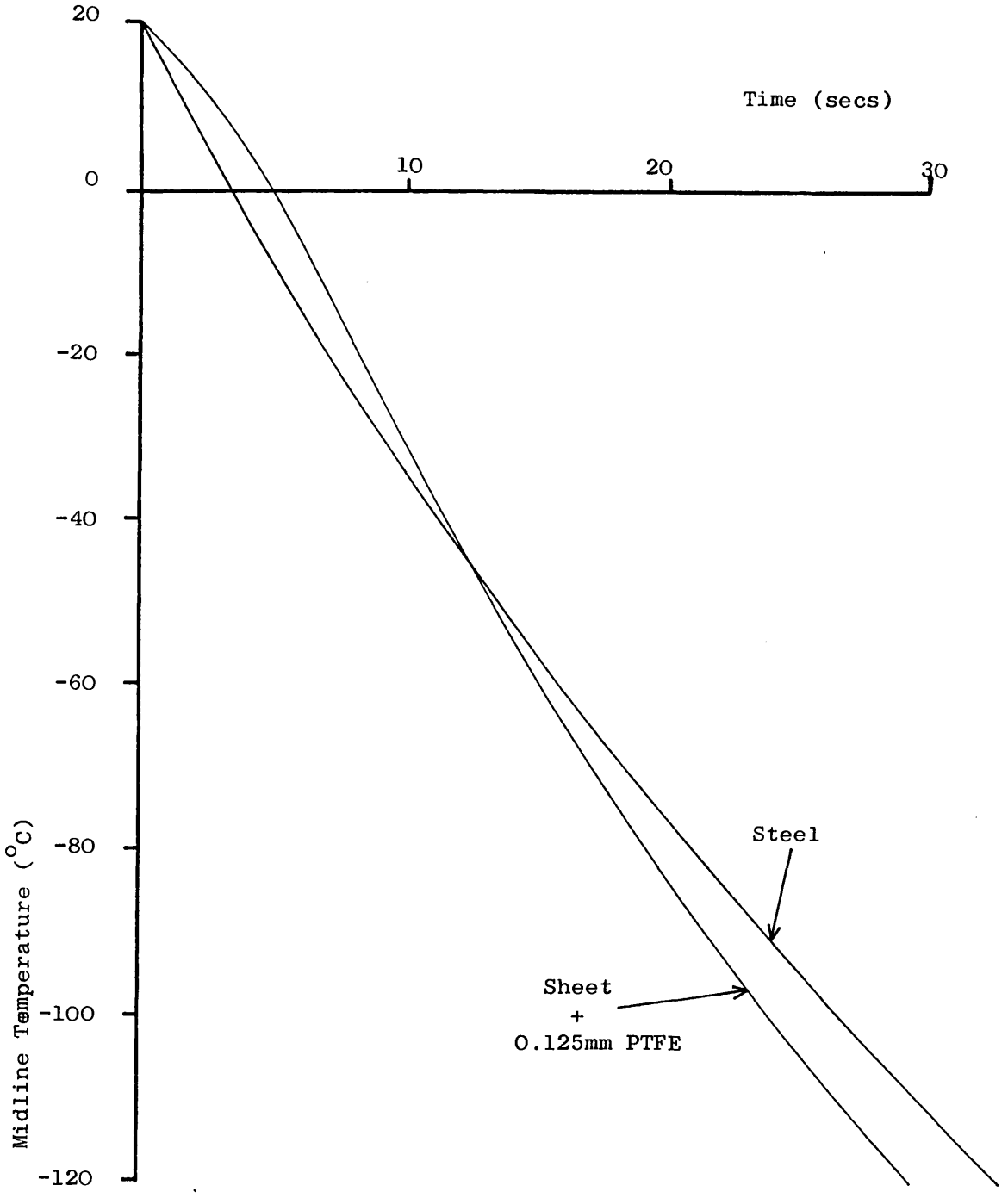

EFFECT OF THIN INSULATION LINING ON COOLING CURVE, FOR SHEET 2.5mm THICK, COOLED ON BOTH SIDES

FIGURE 59

EFFECT OF INSULATION THICKNESS ON COOLING RATE

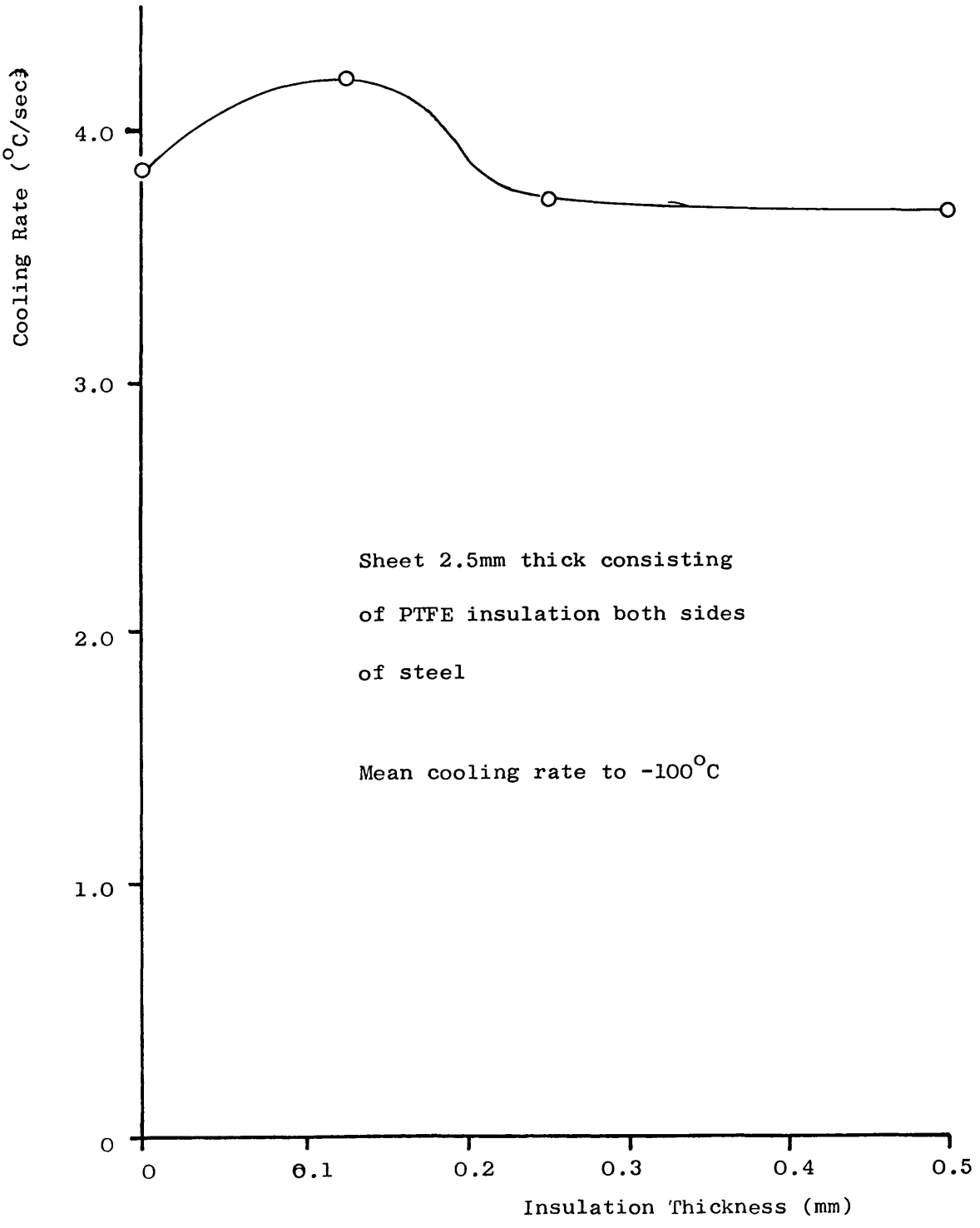

optimum, the thermal conductivity of the insulation dominated the heat transfer equation. For thicknesses less than the optimum, the inner boundary could not cool so rapidly and the poorer heat transfer coefficient dominated the heat transfer equation.

7.9 Conclusions

The studies described in this chapter have analysed the effect of transferring heat through poor conductors from boiling nitrogen by using finite difference equations. They have shown the increased cooling rate first demonstrated in the tip cooling tests described in Chapter 6, despite the two major assumptions that were made. Although the magnitude of the effect is not as large as that measured, the technique outlined has enabled the influence of variables to be explored. It should provide a good basis for further in-depth studies.

The numerical analysis of transient cooling by boiling liquid nitrogen shows several interesting results:

(1) A rapid decrease in the cooled boundary temperature is obtained with material of poor thermal conductivity.

(2) The rapid decrease can lead to a greater rate of heat transfer through a material with a poor thermal conductivity than for one with a large thermal conductivity, because much higher inner heat transfer coefficients are

operating.

(3) There is an optimum thickness of insulation for fastest cooling, all other variables being held constant.

CHAPTER 8

The Liquid Nitrogen Transfer System

8.1 Introduction

A design for the cryoprobe tip has been established that enables the surgical requirements of the rectal cryoprobe to be satisfied. This chapter describes the next stage of the cryoprobe design; the system to transfer liquid nitrogen from the storage vessel to the tip, and to transport the exhaust nitrogen back to the atmosphere.

The overall design of the transfer system is initially discussed and the major problems highlighted. It is shown that many of these problems can be overcome by operating the transfer system pipes in the stable film boiling region of the nitrogen boiling curve.

8.2 Overall Transfer System Design

8.2.1 Choice of system for the rectal probe

Chapter 4 contained a discussion of the problems of transporting liquid nitrogen from a storage dewar to a cryoprobe and reviewed several investigations aimed at overcoming these problems. Two main approaches have been tried:-

(1) Incorporate a small storage dewar on the probe itself.

(2) Use a separate storage dewar and connect it to the probe by means of a transfer hose.

The first solution leads to a compact overall system but the probe itself is rather unwieldly. In addition the probe cannot be turned upside down. The rectal probe must be able to freeze tumours both in the roof and the floor of the rectum, and therefore must be able to operate inverted.

If the cryoprobe was supplied with cryogen from a separate storage dewar it would need to be connected via a flexible transfer hose. The surgeon cannot be constrained in his positioning of the probe. However flexible transfer hoses for transporting liquid nitrogen require a sophisticated design. Corrugated stainless steel pipes are traditionally used although corrugated PTFE pipes are a less expensive alternative. In addition the hose requires substantial thermal insulation to prevent it being a hazard to operating theatre staff.

It was eventually decided that a separate supply dewar would be used, for the following reasons:-

(1) Several features are required that could not be mounted on the probe (e.g. light source, temperature monitors and rectal inflation system). The compact overall system possible by using a probe mounted dewar could not therefore be realised.

(2) It would be difficult to design the probe so that the dewar remained vertical when the freezing tip was turned upside down.

(3) The boiling of the nitrogen in the probe tip

generates large volumes of vapour which must be removed. It was decided that this vapour should be exhausted at a point well away from the patient and preferably back at the storage vessel.

8.2.2 The need for thermal insulation around the transfer pipes

The operating part of the cryoprobe is the tip of the instrument. This is the only component that should be at cryogenic temperatures, the rest of the device should be warm enough not to be dangerous to the surgeon or to cause damage to areas of the patient that are not in contact with the tip.

In the rectal cryoprobe there is an additional insulation problem. It will be shown in **Chapter 10** that a viewing system was incorporated in the cryoprobe for accurate placement of the tip and for monitoring ice-ball growth. The endoscope used is permanently damaged by temperatures below -30°C and must therefore be shielded from the low temperatures within the cryoprobe.

Some form of thermal insulation is needed around the liquid nitrogen transfer system, including the flexible transfer hose from the dewar to the cryoprobe.

8.2.3 Major problems of transfer system design

There are three major problems in designing a suitable transfer system:-

(1) As liquid nitrogen passes along the transfer pipes it continuously boils to vapour. This boiling must be minimised.

(2) Substantial amounts of thermal insulation are needed around the transfer pipes but space is limited in the probe.

(3) A flexible transfer hose is needed to carry the cryogen from the storage dewar to the probe.

A technique was found that solved all these three problems. This technique was to maintain the liquid nitrogen in Leidenfrost flow right from the storage dewar to the cryoprobe tip. The remainder of this chapter examines this solution.

8.3 The Operating Temperature of the Transfer System

8.3.1 The effect of pipe temperature on flow boiling behaviour

Chapter 5 contained a description of the liquid nitrogen boiling curve and showed how the heat flux to the nitrogen was a function of ΔT_{SAT} .

When the cryogen flow is initially turned on, the pipes will be at room temperature and film boiling of the cryogen will occur. At the low flow rates typical of cryoprobes the nitrogen will be undergoing Leidenfrost flow where the liquid is in the form of droplets, suspended in vapour. The heat flux to the nitrogen

causes the pipe to cool. When the pipe temperature reaches the minimum heat flux point of the boiling curve, the liquid boiling becomes transitional and then nucleate. The high heat fluxes that arise from these forms of boiling cause the pipe to rapidly cool to temperatures close to the saturation temperature.

8.3.2 Choice of operating temperature for the transfer pipes

As liquid nitrogen is transferred to the cryoprobe tip, it is continuously boiling. The liquid being lost in this way can be reduced to a minimum by operating in a part of the boiling curve where the heat flux to the cryogen is a minimum. The two minima occur at the boiling point of the cryogen, and at the lower temperature end of the film boiling region.

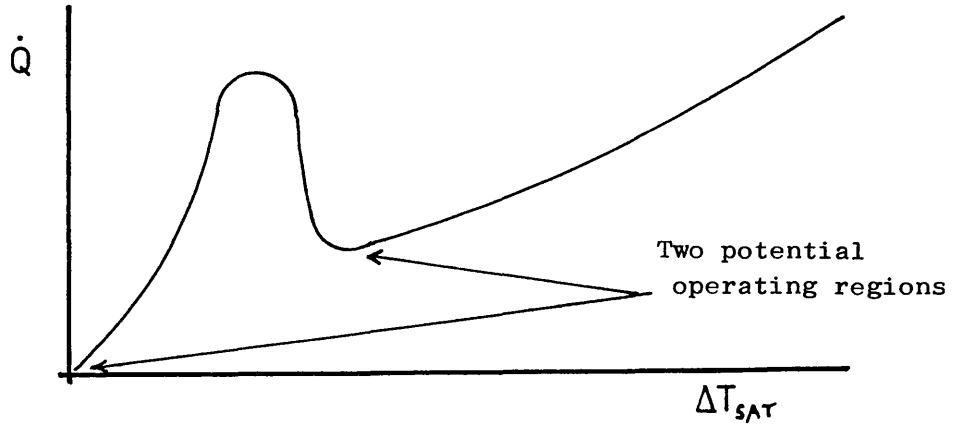

Traditionally liquid nitrogen transfer systems operate at temperatures close to the boiling point. The transfer system is allowed to cool after initiating the cryogen flow until low temperatures are reached. However, at the low flow rates used in cryoprobes, this pre-cool can take many minutes. With one of the

popular commercially available systems, 15 minutes have to be allowed for the transfer system to cool to its operating temperature.

The alternative operating region is the low temperature end of the stable film boiling region. Operating here can provide a major advantage for cryoprobes in that a pre-cool is not needed. As soon as the cryogen flow is turned on it will be undergoing film boiling. The major problem of minimising liquid nitrogen boiling during transfer can therefore be solved by operating in the film boiling region, without the need for long pre-cool times.

8.4 Advantages of Using Leidenfrost Flow

8.4.1 Overcoming the problem of transfer pipe insulation

Two techniques were explored to solve the problem of transfer pipe insulation:-

(1) Evacuated sheath around the cryoprobe with foam insulation of the hose.

(2) Heated transfer pipes.

An evacuated jacket was initially considered for the probe but was eventually abandoned because the second technique of using heated transfer pipes was found to be far superior. However, work on the vacuum insulation involved a substantial proportion of the time devoted to this aspect of the cryoprobe design and so some brief details of this work are given in **Appendix 2.**

In order to operate the transfer pipes in the

region of stable film boiling, the pipe temperature must be kept at least 30°C above the boiling point of liquid nitrogen. However, even if the pipes were kept as warm as room temperature the heat flux to the nitrogen would still be low. Consider the following table.

ΔT_{SAT}	5°C	216°C
$\dot{q}$	24.5×10^3 W/m²	22.1×10^3 W/m²

The heat flux for pipes at room temperature is about the same as if they were 5°C above the boiling point. But if the transfer pipes are kept as warm as 20°C there is no longer a need for thermal insulation. Therefore by operating the transfer pipes in the stable film boiling region, the problem of thermal insulation can be circum- vented.

8.4.2 Overcoming the problem of flexible transfer hose design

If flexible transfer hoses are designed to transport liquid nitrogen they need to be constructed out of materials such as corrugated stainless steel or PTFE. These materials are needed to enable the hose to withstand being cooled to -196°C and remain flexible. However if the hose is operated in the film boiling region of the nitrogen boiling curve its temperature can

be kept above the glass transition temperature of most plastics. A large number of materials therefore become possible for the hose construction (e.g. PVC, Silicone Rubber). The problem of hose materials is therefore also circumvented by not allowing the hose to cool to low temperatures.

8.5 Disadvantages of Using Leidenfrost Flow

During the transfer of the liquid nitrogen, the heat flux needed to evaporate the liquid will cool the pipe. The pipe temperature will eventually decrease beyond the film boiling region. Therefore a continuous and controlled heat source is needed to stabalise the operating temperature within the region required.

If the advantages of using Leidenfrost flow are compared to the disadvantages of needing heated transfer pipes, there is little doubt that the balance lies in favour of incorporating a Leidenfrost system. The problems associated with Leidenfrost flow and possible techniques for heating the transfer pipes are discussed in the next chapter.

8.6 Conclusions

(1) The cryogen transfer system should use a separate storage dewar connected to the cryoprobe via a flexible transfer hose.

(2) The transfer pipes should be operated in the stable film boiling region of the boiling curve. The Leidenfrost flow thereby

generated has several advantages for the transfer system.

(a) A minimum amount of liquid is evaporated during transfer without the need for a pre-cool of the pipes.

(b) The need for thermal insulation around the pipes is circumvented.

(c) The flexible transfer hose construction can be based on a large variety of flexible plastic pipes.

(3) Stable Leidenfrost flow requires the transfer pipes to be heated.

CHAPTER 9

Maintaining Leidenfrost Flow in the Transfer System

9.1 Introduction

This chapter discusses the problems of maintaining Leidenfrost flow throughout the transfer system from the storage dewar to the cryoprobe tip. Two main aspects are considered:

(1) The effect of pipe geometry and inclination on Leidenfrost flow.

(2) Methods of keeping the pipe warm.

The transfer system is divided into two parts; the transfer hose and the probe shaft. The heating requirements of these two components differ and their heating systems are described separately.

9.2 The Effect of Pipe Internal Geometry on Leidenfrost Flow

The low heat transfer coefficients of the film boiling region result from the physical separation of the liquid droplets from the pipe wall. Heat has to be conducted through the vapour film. The separation of the droplets from the wall can also be affected by the motion of the droplets.

When the two phase flow passes around a bend in the pipe, the droplets are forced towards the outside. If the centrifugal force acting on the droplets is greater

than the force generated by the vapour evolution, the liquid will be forced into contact with the pipe wall (**Figure 60**). In addition, if the flow passes through an abrupt reduction in pipe diameter, the momentum of the liquid droplets may project them into contact with the wall in the region of the reduction (**Figure 60**).

If through either of the two mechanisms just described the liquid droplets come into contact with the wall, the heat transfer coefficient increases dramatically. As the wall will be much warmer than the temperature of the droplets, a large amount of heat will be transferred to them and they will boil rapidly.

This process can be seen taking place if liquid nitrogen is caused to flow along a clear plastic pipe with an abrupt bend in it. The droplet flow can be clearly seen down the straight pipe but when the liquid traverses the bend the droplets vanish as they are forced into contact with the wall and are rapidly evaporated by the large heat transfer.

9.3 The Effect of Pipe Inclination on Leidenfrost Flow

Two phase flow in pipes is inevitably influenced by the inclination of the pipe relative to horizontal because of the large difference in density between the two phases. In the case of Leidenfrost flow the acceleration of the liquid droplets in the axial direction will mostly be dependent on two factors:-

(1) The drag force exerted on the droplets by the motion of the vapour phase.

FIGURE 60

TWO MAJOR CAUSES OF DROPLET EVAPORATION

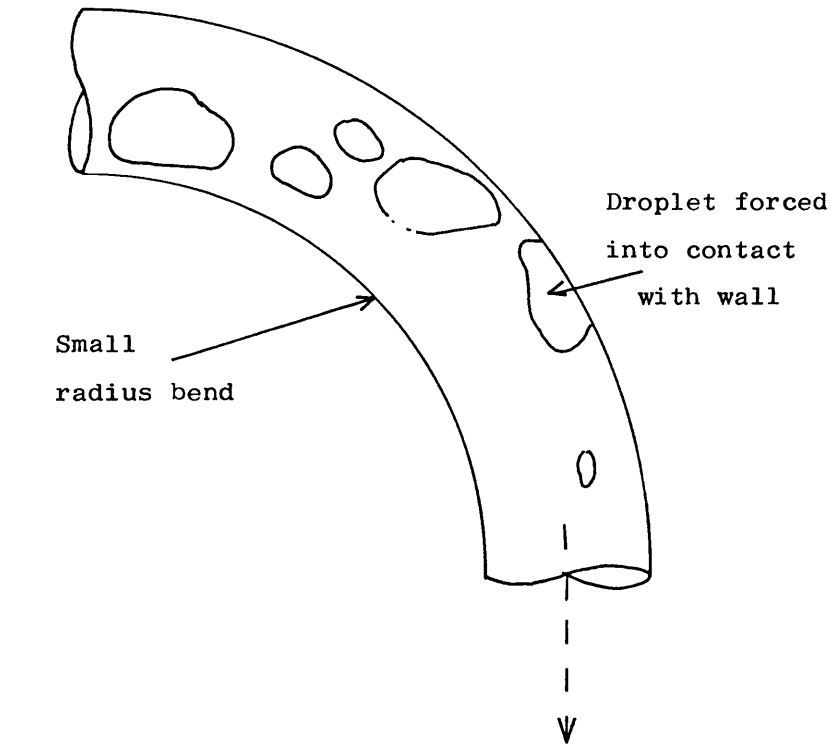

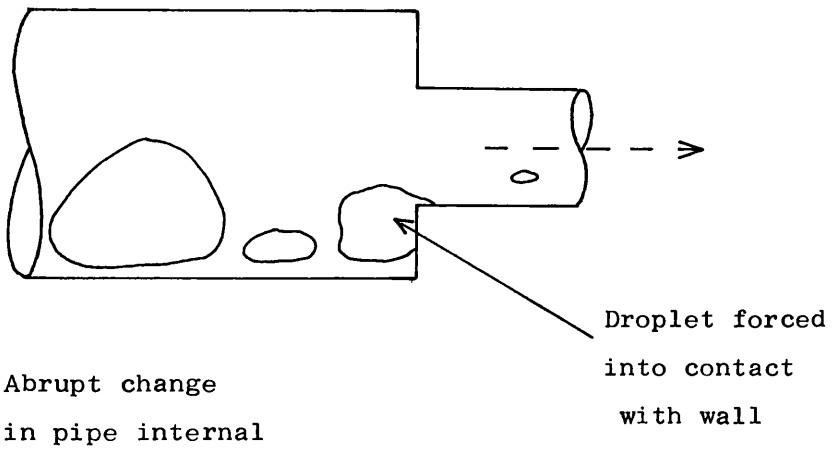

(2) The axial component of gravitational force.

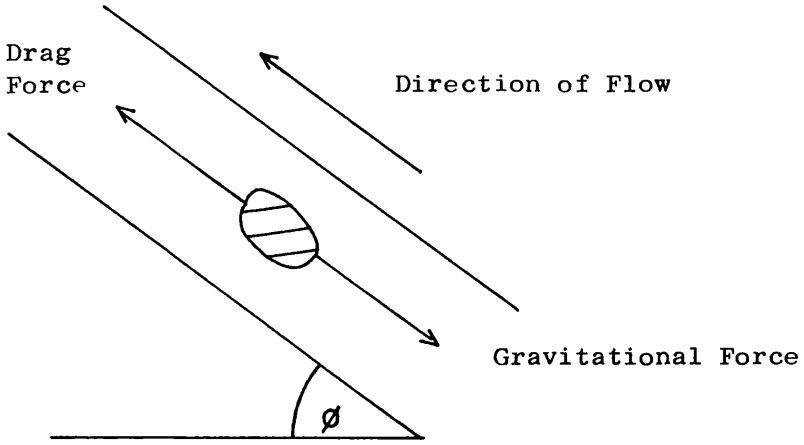

The resultant droplet acceleration is therefore

$$\frac{dU_D}{dz} = \text{acceleration due to drag} - \left(\text{acceleration due to gravity}\right) \times \sin\phi \qquad (33)$$

This resultant acceleration has been expressed by Hynek et al (1969) for flow in vertical pipes ($\phi = \frac{\pi}{2}$)

$$\frac{dU_D}{dz} = \frac{3C_D\rho_v(U_v - U_D)^2}{4\rho_L D_D} - g \qquad (34)$$

where U_D = droplet velocity

U_v = vapour velocity

D_D = droplet diameter

ρ_v & ρ_L = density of vapour and liquid respectively

C_D = drag coefficient (dependent on Re)

Two important conclusions result from these considerations:-

(1) The droplet flow is sensitive to pipe inclination.

(2) A critical condition exists in which droplets cannot flow along the pipe because the drag force on them is less than the axial component of the gravitational force.

The critical condition for flow depends on the pipe diameter. The smaller the pipe diameter the larger the vapour phase velocity for a given evaporation rate. In addition, the smaller the pipe diameter, the smaller the maximum size of droplet. If the droplet diameter is larger than a critical value the droplet will not flow until it is reduced in size by boiling.

These effects can quite clearly be seen by examining the flow behaviour of liquid nitrogen droplets within clear plastic pipes. As the inclination of the pipe is increased, the liquid droplets can be seen to slow down until a critical angle is reached when the larger droplets start to fall back down the pipe to the start of the inclined section. The collection of droplets in this region leads to a local cooling of the pipe, which will quite quickly, in the case of a plastic pipe, lead to the onset of nucleate boiling in that region with a concomitant reduction of the liquid fraction at the pipe exit. The larger the pipe the smaller the angle of inclination needed to induce this effect.

If the above test is repeated further downstream a larger angle of inclination of the pipe can be

tolerated. As the liquid flows along the pipe it is continuously evaporating and the vapour generated causes an increase in the mean velocity of the fluid. The increased momentum of the liquid droplets enables them to flow up steeper pipes, although only for a limited length.

Tests were carried out on different diameter pipes to find an optimum diameter for the cryoprobe transfer system. It would be expected from the discussion above that the smaller the pipe diameter the better. However, as the pipe diameter is reduced the pressure drop increases. In addition, with liquid nitrogen transport, the flow is rapidly accelerating due to the evaporation of liquid. Consequently the pressure drop, measured over a given length of pipe, becomes much larger the further downstream it is measured. Therefore the tests were carried out in two parts. The initial tests examined the section of pipe that climbs vertically out of the storage dewar. The optimum size for this section was found to be a 2.5mm bore pipe. Later tests examined the pipe used for the flexible transfer hose and a 5mm bore pipe was selected.

9.4 Acceleration of Flow Along Pipe

As the liquid phase evaporates to vapour the mean flow velocity increases. Consider a section of pipe as shown below.

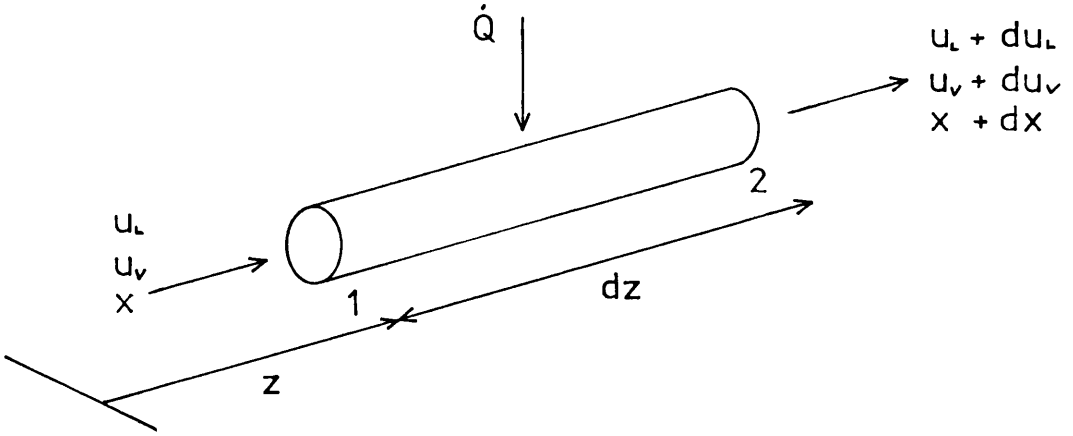

where u_L = liquid phase mean velocity

u_v = vapour phase mean velocity

x = vapour quality based on mass

(ie. x=1 for sat.vap., x=0 for sat.liq.)

Assume no slip between liquid and vapour phases

ie. $u_L = u_v = u$

For continuity:-

$$(A_L\rho_L + A_v\rho_v)_1 u = (A_L\rho_L + A_v\rho_v)_2 (u + du) \quad (35)$$

where A_L = cross-sectional area occupied by liquid

A_v = cross-sectional area occupied by vapour

The total cross-sectional area, $A = A_L + A_v$ (36)

By considering the mass flow rate at any point it can be shown that,

$$\frac{x}{1-x} = \frac{A_v\rho_v}{A_L\rho_L} \quad (37)$$

Combining Equations 35,36 and 37, and rearranging

$$\frac{du}{u} = \frac{dx\left(\frac{\rho_L}{\rho_v} - 1\right)}{1 + x\left(\frac{\rho_L}{\rho_v} - 1\right)} \quad (38)$$

Integrating and rearranging

$$\frac{u}{u_i} = \frac{1 + x\left(\frac{\rho_L}{\rho_v} - 1\right)}{1 + x_i\left(\frac{\rho_L}{\rho_v} - 1\right)} \quad (39)$$

where u_i = inlet mean velocity, x_i = inlet vapour quality

The change in vapour quality along the pipe depends on the heat input

$$\frac{dx}{dz} = \frac{\dot{q}}{\dot{m}L} \qquad (40)$$

where $\dot{q}$ = heat input per unit length of pipe

L = latent heat of evaporation

Integrating **Equation 40**, substituting in **Equation 39** and rearranging, incorporating the approximation, $\rho_L - \rho_V = \rho_L$

$$\frac{u}{u_i} = 1 + \frac{\dot{q}z}{\dot{m}L\left(\frac{\rho_V}{\rho_L} + x_i\right)} \qquad (41)$$

Figure 61 shows a plot of $\frac{u}{u_i}$ as a function of z, for typical hose variables. The velocity, u, is a linear function of distance along the pipe.

9.5 Energy Requirements to Maintain Leidenfrost Flow

The transfer pipes need to be heated in some way to stabalize their temperature in the film boiling region. Energy is needed to balance that transferred to the boiling nitrogen. The energy required to maintain a constant pipe temperature along its length was investigated experimentally by winding a heating coil around the pipe and measuring the pipe temperature for different levels of power dissipation. It was found that the energy required varied along the length of the pipe and the distribution was found by trial and error by varying the heater winding. **Figure 62** shows a plot of the required heat flux as a function of pipe length, for typical transfer hose variables.

FIGURE 61

ACCELERATION OF FLUID DUE TO EVAPORATION

(Equation 41)

$\dot{q}$ = 30 W/m

$\dot{m}$ = 4 x 10^{-4} kg/s

x_i = 0.1

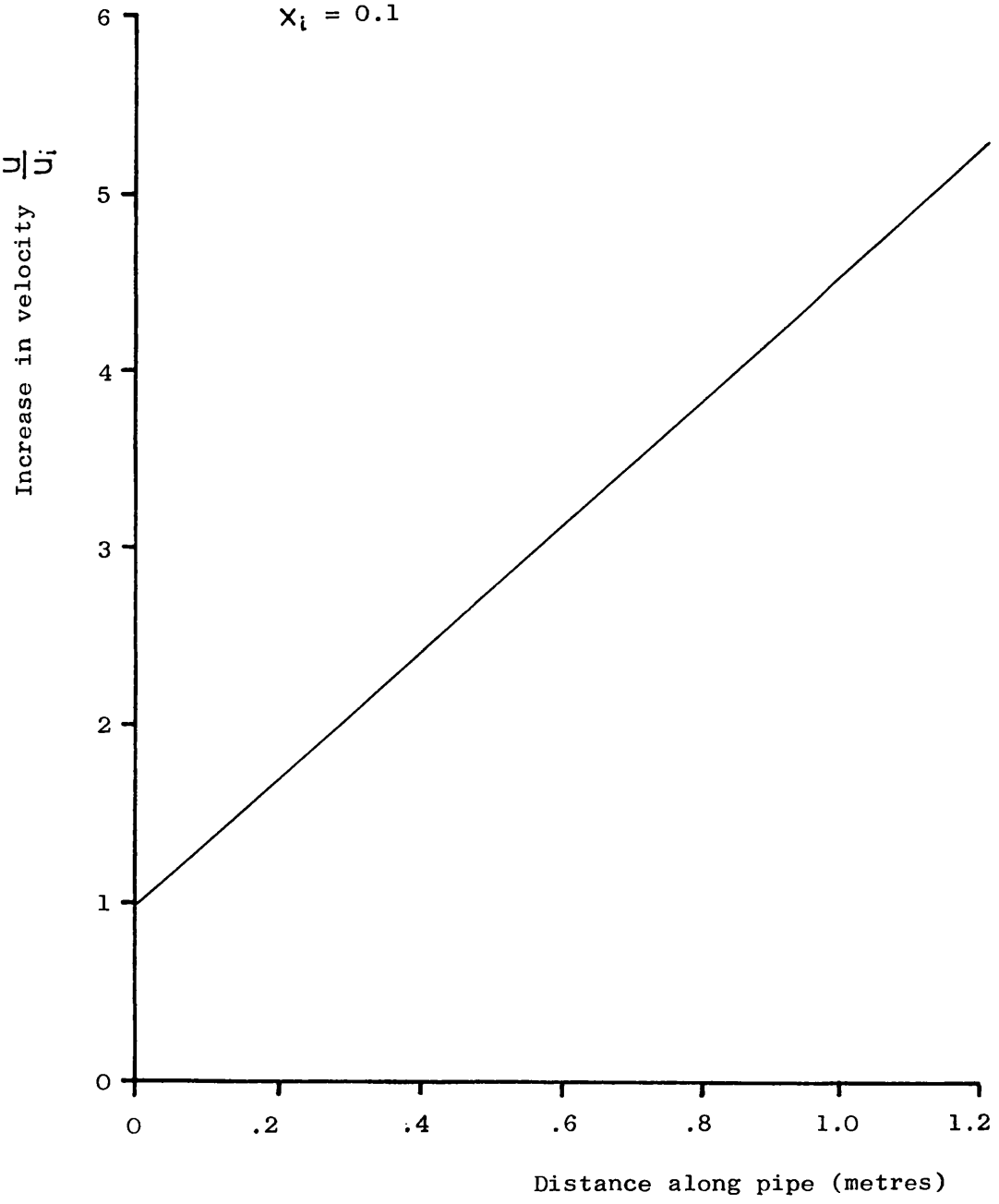

FIGURE 62

MEASURED DISTRIBUTION OF HEAT FLUX

REQUIRED TO MAINTAIN CONSTANT PIPE TEMPERATURE

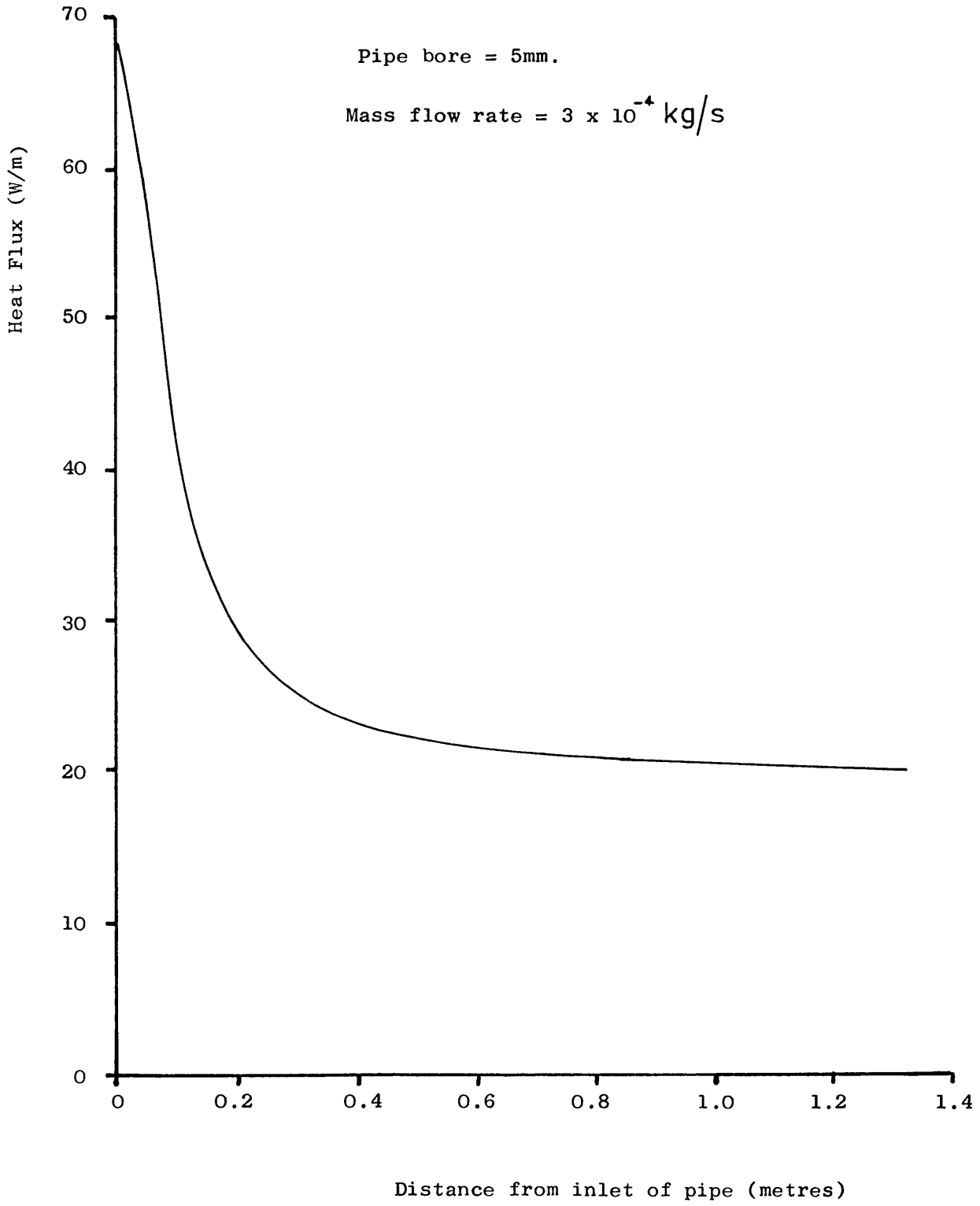

The heat flux is related to the other major variables as below.

$$\dot{q} = h(T_p - T_N)$$

where $\dot{q}$ = heat flux (W/m)

T_p = pipe wall temperature (°C)

T_N = liquid nitrogen temperature (°C)

h = heat transfer coefficient (W/m.°C)

If the temperatures are constant, the decrease in heat flux over the length of the pipe can only be explained by a reduction in the heat transfer coefficient. Two possible explainations for this behaviour are:-

1. As the vapour quality increases along the length of the pipe there is less chance of the liquid droplets contacting the pipe wall.
2. As the flow velocity increases along the length of the pipe, the liquid droplets are more confined to the axis of the pipe, as is the case with non-Newtonian flows of this kind.

9.6 Techniques used to Develop Heating Systems

9.6.1 The need for two separate heating systems

One problem with using heated transfer pipes is that the heat requirements of the probe and hose differ. When the probe is being used it will receive substantial heat inputs from the tissues in contact with it. The hose will be subjected to a far more constant thermal environment. Two separate heating and temperature control systems are therefore needed.

9.6.2 Methods used to monitor boiling behaviour

In all the tests described, it was necessary to know whether stable film boiling was being maintained. The nature of the boiling was monitored in three ways.

(1) Clear PVC tubes were used so that the flow behaviour could be observed.

(2) When Leidenfrost boiling is taking place, the flow pulses. There is a very noticeable change in the sound produced by the exhausting nitrogen as the boiling changes from pulsing Leidenfrost boiling to steady nucleate boiling.

(3) The liquid fraction at the exhaust end of the hose rapidly decreases as stable film boiling changes to nucleate boiling. This change can be detected by monitoring the liquid fraction.

9.6.3 Methods used to monitor liquid fraction

Knowledge of the liquid fraction at the exhaust end of a pipe being tested can provide information about the nature of the boiling in the pipe, and also about the efficiency of the pipe at transfering liquid nitrogen. Two techniques were used to monitor liquid fraction.

(1) The exhaust was directed at a sheet of paper. As the liquid was absorbed, the size of the wetted area of paper depended on the liquid fraction (see **Figure 63**).

FIGURE 63

TWO SIMPLE TECHNIQUES FOR COMPARATIVE LIQUID FRACTION ASSESSMENT

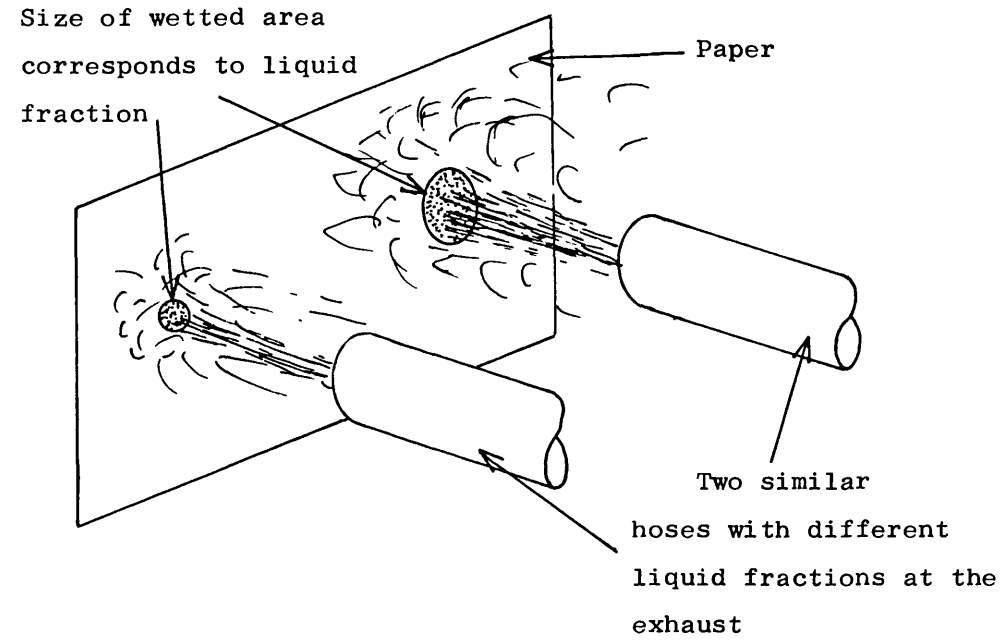

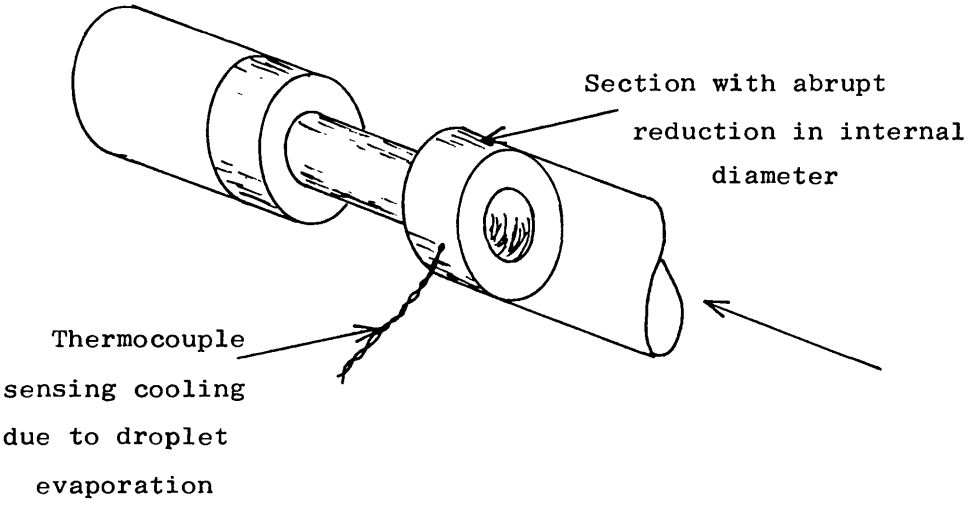

(2) The exhaust pipe incorporated an abrupt change in its internal diameter where the pipe temperature was monitored. Liquid droplets were forced into contact with the wall at this obstacle and low wall temperatures were generated. The greater the liquid fraction, the lower became the temperature at this point.

Both the above techniques indicated did not provide absolute measurements of liquid fraction. However they did enable a comparative assessment to be made of the effects of introducing changes to a given hose design. In this way trends could be established.

9.7 The Transfer Hose Heating System

9.7.1 The effect of pipe wall thickness

The flexible plastic hose is a poor heat conductor. A steep temperature gradient will exist across the pipe wall. The outside should ideally be around 20°C whereas the inside should be above the glass transition temperature of the material used or it may crack on the inside when bent. Such cracks would soon propogate through the wall.

To reduce the temperature difference across the pipe wall, thin walled pipes are needed. However excessive reduction in wall thickness must be avoided to prevent kinking. A wall thickness of 1mm was found necessary to prevent kinking of the 5mm bore PVC pipes which were used for most of the tests.

9.7.2 Warm vapour heating of flexible hose

In section 8.4 it was shown that to maintain Leidenfrost flow the pipe wall had to be heated. In particular, if the pipe were heated to near room temperature, Leidenfrost flow would be maintained but there would also be no need for thermal insulation. The use of warm vapour to heat the hose was an obvious first choice because this system would automatically provide a distributed heating. The larger the temperature difference between the pipe and the warm vapour, the more heat that would be transferred. As more heat would be required at the input of the hose it was sensible to try using a flow of warm vapour that was concurrent with the cryogen flow. This arrangement was achieved in the laboratory by taking the exhaust nitrogen from the exit of the hose, passing it through a loop of pipe in a warm water bath, and returning it to the input end of the outer hose (**Figure 64**).

When the arrangement described was tested it worked well as long as the gas was heated to at least 50°C. Stable film boiling was maintained and the droplets of liquid nitrogen could be clearly seen through the clear PVC wall.

Unfortunately, a practical hose needed the exhaust gas from the cryoprobe to be returned to the other end of the hose, heated, and then passed back to the cryoprobe again to be finally exhausted. A hose of this construction was tried but proved extremely difficult to

FIGURE 64

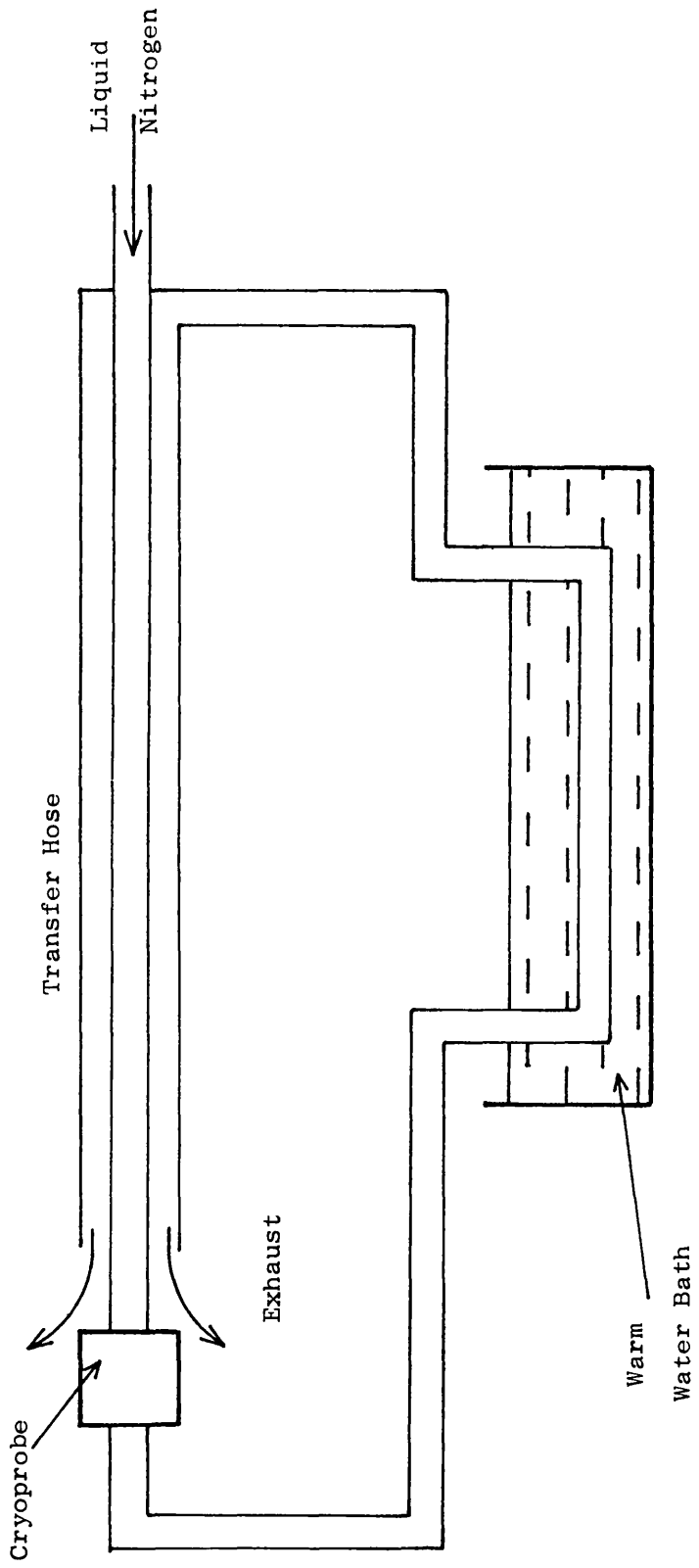

TRANSFER HOSE HEATED BY WARMED EXHAUST HOSE - CONCURRENT FLOW

make because of the multitude of pipes it contained. It was also difficult to achieve an adequate flow rate of nitrogen without using large pipes and producing a bulky hose. The hose that was eventually constructed had small pipes but could not maintain stable film boiling for more than 2 to 3 minutes.

A separate warm gas supply was tried as an alternative approach. **Figure 65** illustrates the arrangement used where nitrogen vapour from the dewar was passed through a heating bath and then to the outer hose. Unfortunately it was difficult to maintain the dewar pressure with the vapour flow rates that were necessary to keep the hose working.

Both the techniques described above resulted in large volumes of vapour being exhausted at the cryoprobe. This was not desirable, so a counter-current flow hose was tried. The exhaust vapour from the cryoprobe end of the hose was heated and then passed back along the hose (**Figure 66**). However, even with the vapour heated to 70°C this hose was unable to maintain stable film boiling for more than 1 to 1½ minutes.

9.7.3 Electrical heating of flexible hose

The problems encountered in trying to maintain a warm hose with heated vapour led to attempts to achieve the same end using electrical heating. A heating coil was wound around the hose and supplied from a variable 30V, 2A source. It was found to be very difficult to

FIGURE 65

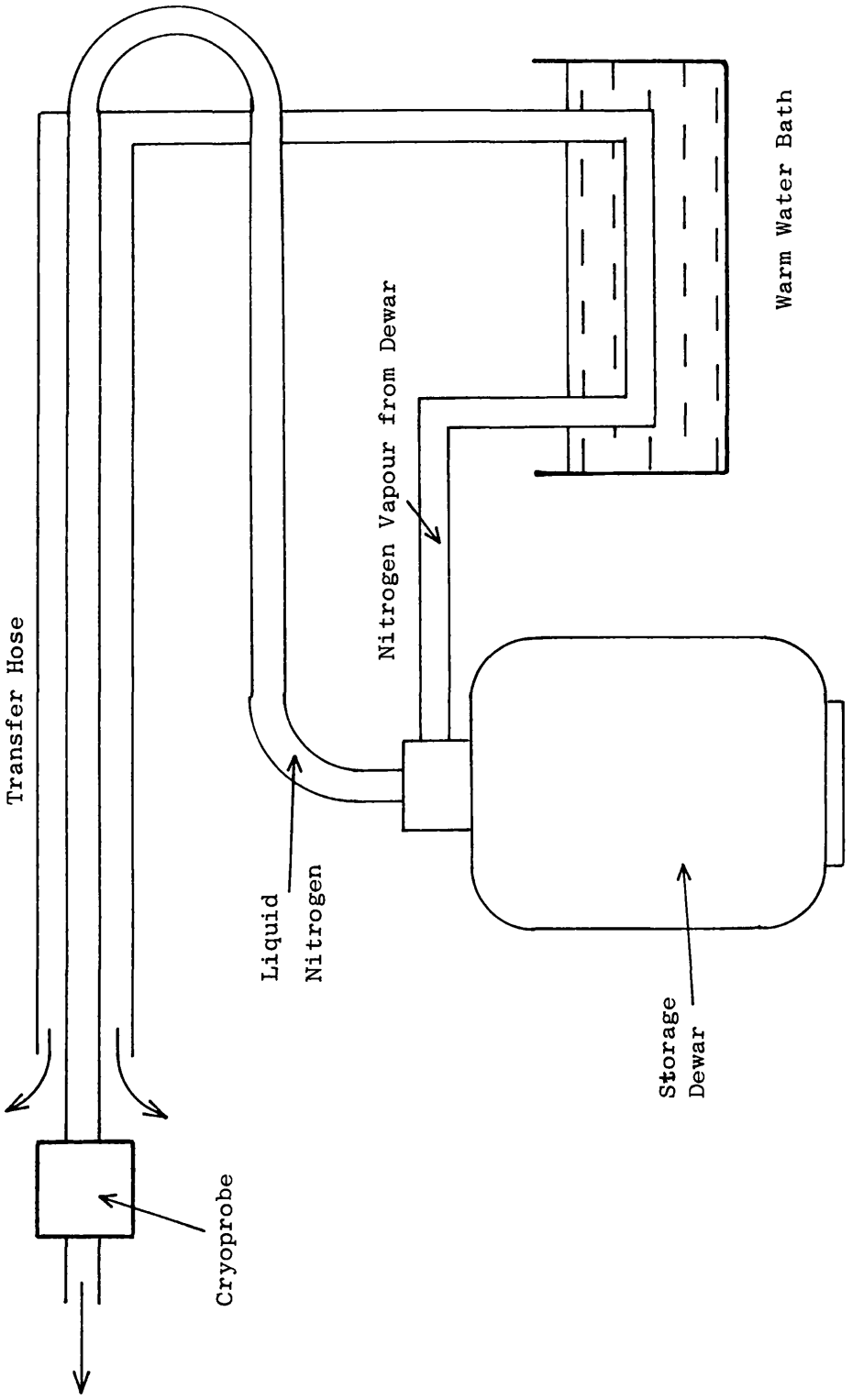

HOSE HEATED BY WARMED NITROGEN FROM VAPOUR PHASE OF DEWAR

FIGURE 66

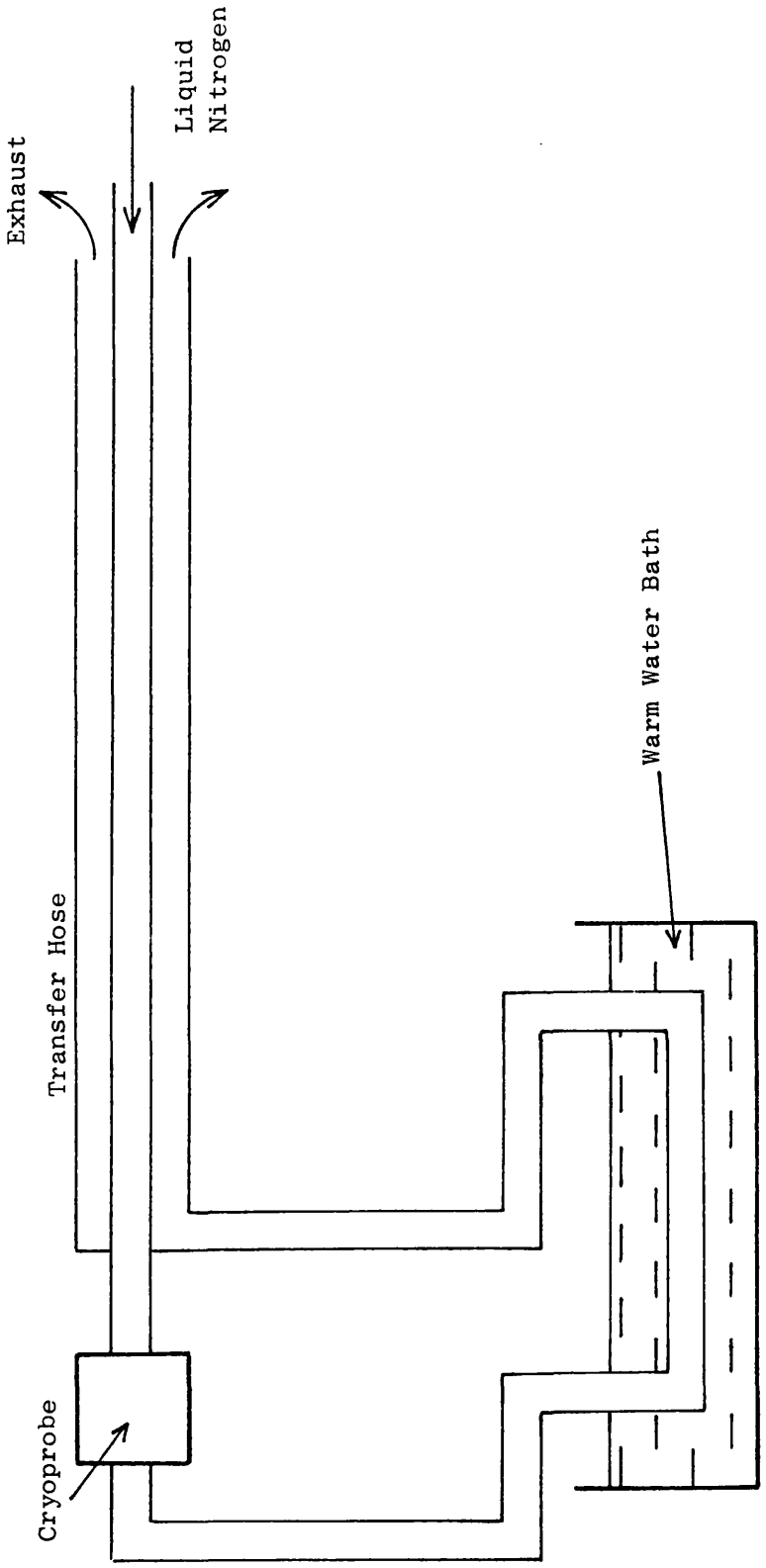

HOSE HEATED BY WARMED EXHAUST - COUNTER-CURRENT FLOW

achieve just the right winding distribution to maintain a constant pipe temperature along its length. Several hoses were melted in the process of trying to optimise the winding distribution by trial and error.

A solution to the problem was found by combining electrical heating with a gas flow. The heater winding used was the best distribution that had been tried in the previous test but the exhaust vapour from the cryoprobe end of the hose was then passed back over the windings (**Figure 67**). The vapour had the desired effect of preventing hot spots from occuring by acting as a heat distributing agent. Using this system, stable Leidenfrost boiling could be maintained indefinitely.

The details of the final hose design are given in **Chapter 13** where the complete rectal cryoprobe system is described.

9.8 The Probe Shaft Heating System

9.8.1 Procedure used to develop the probe heater

All the shaft heating tests used electrical heaters and in order to develop the necessary distributed heater winding, a test probe shaft was constructed as shown in **Figure 68.** The overall shaft size was the one that resulted from the viewing tests described in **Chapter 12.** Five thermocouples were positioned along the length of the shaft on the outside. The temperatures at these points were monitored as different test heaters were tried, until the external temperature distribution was acceptable.

FIGURE 67

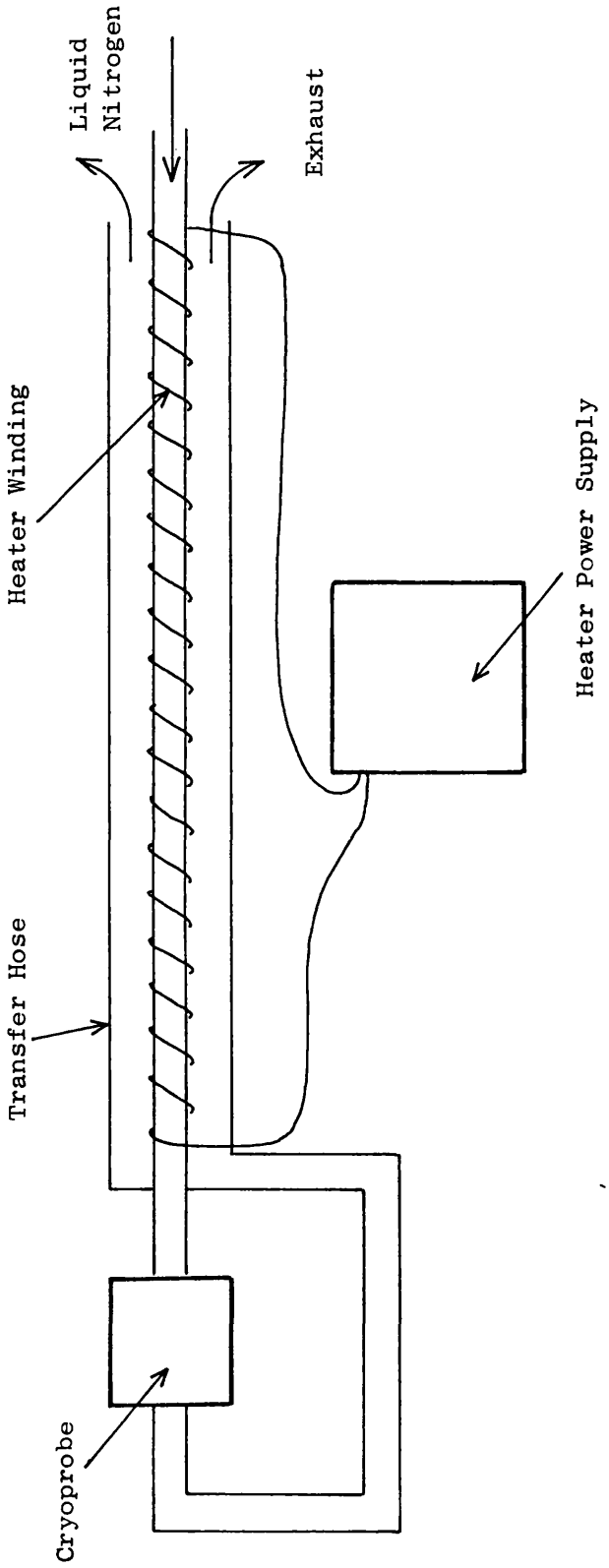

ELECTRICAL HEATING OF TRANSFER HOSE

FIGURE 68

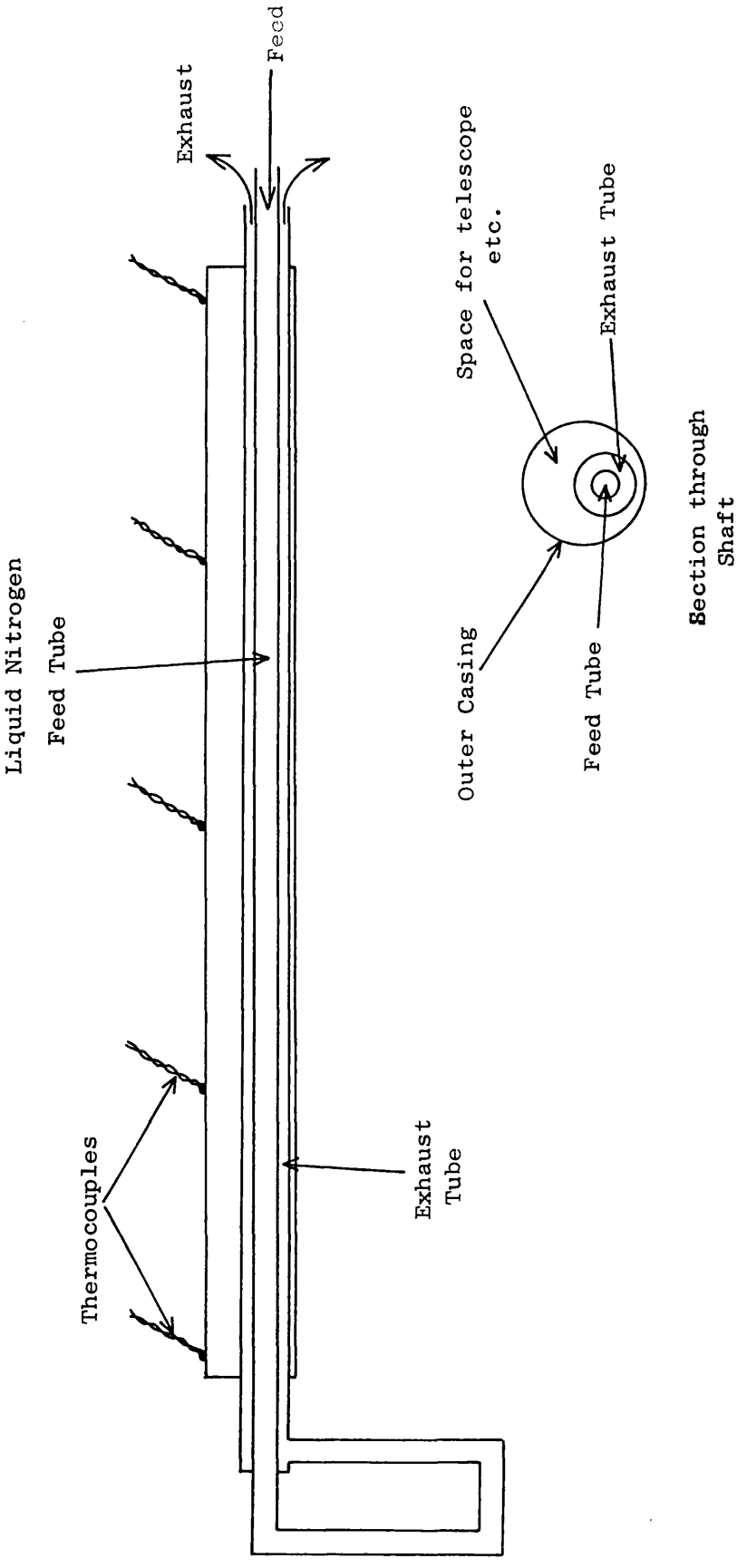

TEST PROBE SHAFT

Several techniques of electrically heating the probe shaft were explored. These techniques are now described.

9.8.2 The feed pipe used as a heating element

The feed pipe was made from stainless steel which is a metal of high resistivity. The pipe itself was used as the heating element. This approach led to an elegant design but it was difficult to provide distributed heating (**Figure 69a**).

9.8.3 Feed pipe immersed in a heated liquid

The feed pipe was immersed in a liquid into which were placed the heating elements. It was hoped that the liquid would distribute the heat. Methanol was used because of its thermal properties. However the heat distribution was not effective enough (**Figure 69b**).

9.8.4 Feed pipe heated by exhaust vapour

The feed pipe was heated indirectly through the exhaust vapour. The feed pipe was passed through a second pipe which transported the exhaust vapour back from the tip. An electrical heater was wound around the exhaust pipe. In this way the exhaust pipe (and therefore the probe shaft casing) could be kept at room temperature whilst allowing the feed pipe to be much cooler but still in the film boiling region (**Figure 69c**).

FIGURE 69

Figure 69a

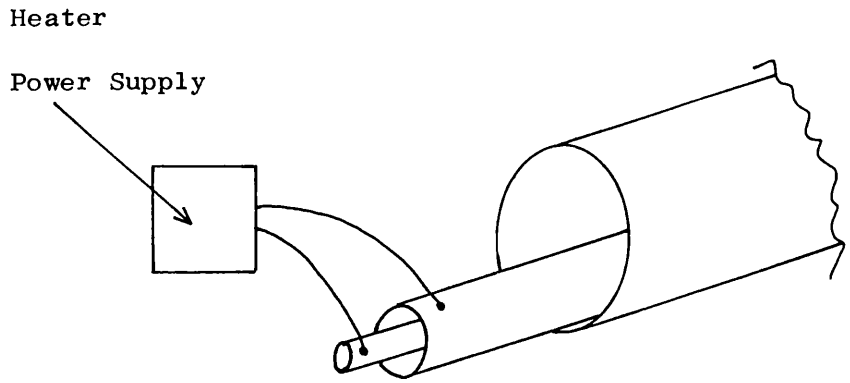

Figure 69b

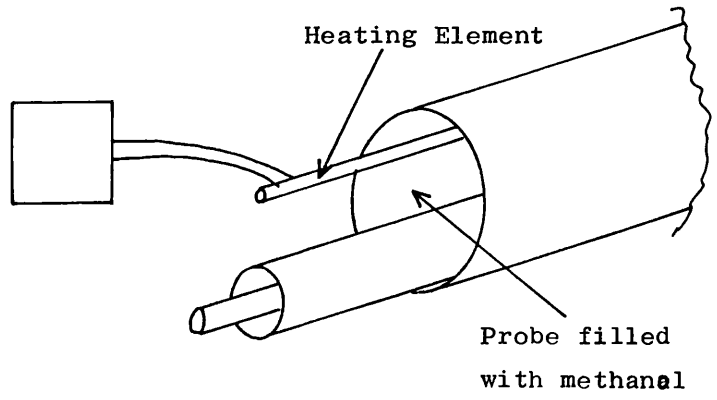

Figure 69c

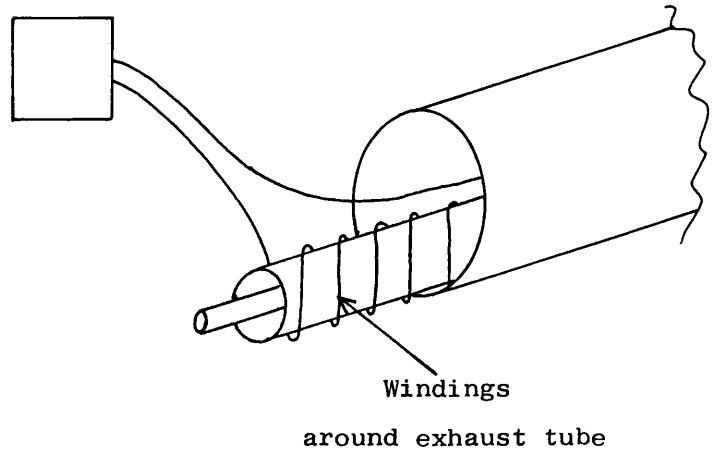

THREE MAIN EXPLORATORY TECHNIQUES OF PROBE SHAFT HEATING

The heater winding distribution was altered until the probe casing temperature was acceptably uniform. Figure 70 shows recordings from the five test thermocouples, for the final winding distribution. This is the solution adopted for the final rectal cryoprobe shaft.

9.9 Conclusions

1. Stable Leidenfrost flow is dependent on both the pipe internal geometry and its inclination relative to gravity.
2. Electrical heating should be used to keep the flexible transfer hose in the film boiling region. The heater should be wound around the feed pipe with the exhaust vapour passed over it as a heat distributing agent.
3. Electrical heating should also be used for the probe shaft feed pipe. The feed pipe should be heated indirectly via the exhaust vapour from the tip.

FIGURE 70

TEMPERATURE DISTRIBUTION ALONG TEST PROBE SHAFT FOR FINAL WINDING DISTRIBUTION

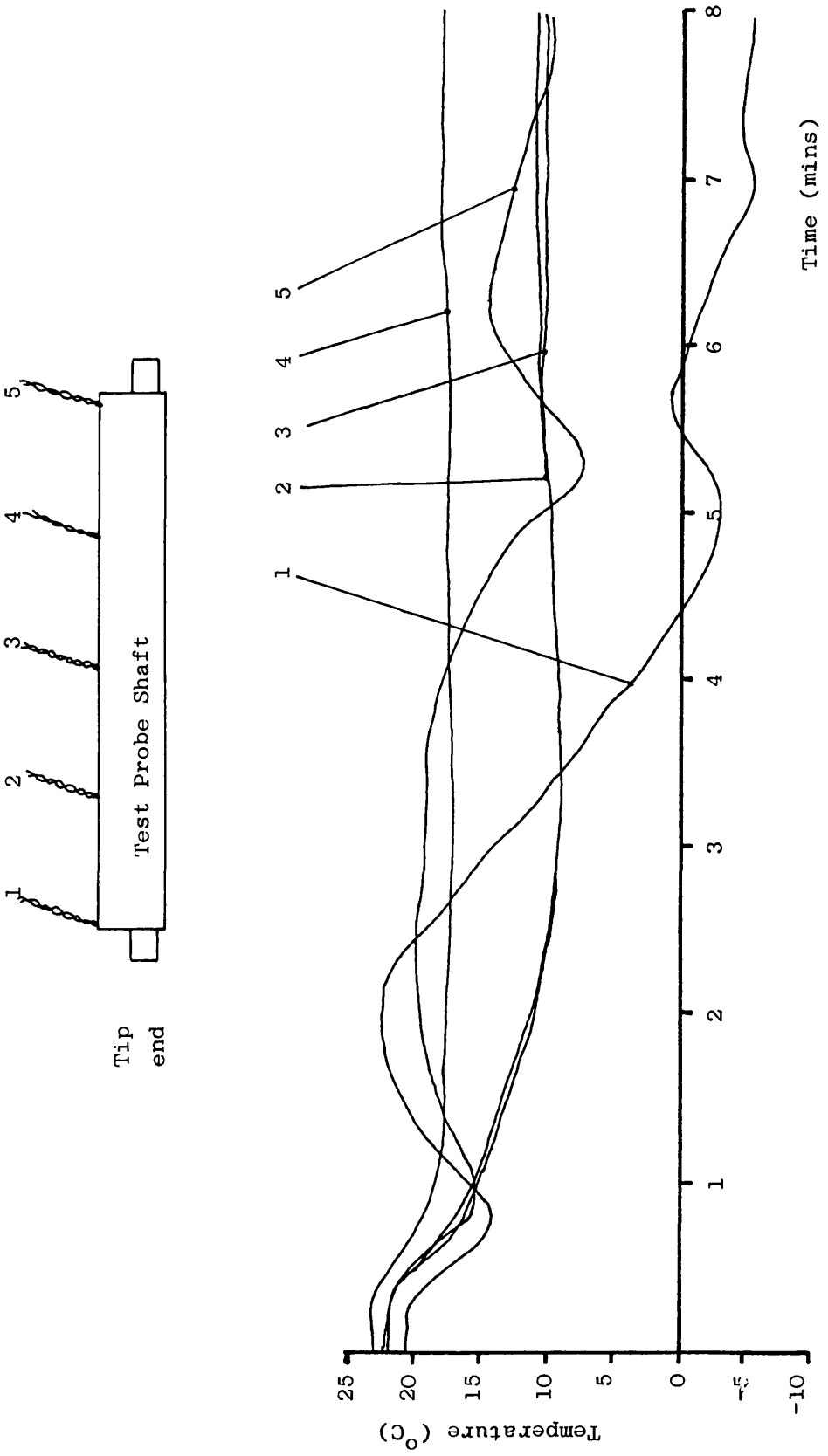

CHAPTER 10

Review of Cryosurgical Monitoring

10.1 Introduction

Whilst work was proceding on the cryogenic aspects of the rectal cryoprobe, the problem of designing a means of monitoring ice-ball growth within a body cavity was also being studied. Direct visual monitoring is usually used when freezing easily accessible tissues. The surgeon simply watches the white ice-mass growing until it appears to encompass the whole area he wishes to destroy. Direct visual monitoring is of course not possible within the rectum.

There are many other possible techniques for monitoring cryosurgery, some of them in practical use and others rather experimental. This chapter reviews these techniques and assesses them to see which would be the most suitable for an instrument that is being used inside a body cavity.

10.2 Indirect visual monitoring using endoscopes

If visual monitoring is to be used within body cavities, some kind of remote viewing is needed. Cryoprobes have been developed to enable cryosurgery inside the body by combining them with small telescopes, or endoscopes. Such instruments have been described for use in destroying the prostate gland. (Molnar et al

1969, Lymberpoulos 1972). Reuter (1971) has used a technique of bladder cryosurgery on several hundred patients, where the endoscope with its built in light source is inserted through the abdominal wall and the cryoprobe is inserted through the urethra.

Visual monitoring suffers from two main disadvantages.

(i) As shown in Chapter 3, the volume of destroyed tissue is less than the volume of tissue cooled below 0°C. The destroyed tissue usually lies within the -15°C isotherm.

(ii) The visual check is essentially only a two dimensional view. The depth of the lesion can only be estimated by assuming a hemispherical ice-ball shape.

10.3 Thermocouples

Probably the most common method of monitoring ice-ball growth other than direct vision or palpation is to use thermocouples. These transducers are usually mounted in hyperdermic needles and are placed on the outer border of the diseased tissue prior to cryosurgery. The freezing process is continued until the thermocouples register a temperature below zero (see Cahan 1971). The thermocouples themselves may change the thermal field around the cryoprobe because they introduce a heat source. The usefulness of this

technique depends on how accurately the thermocouples are placed. Accurate positioning can be quite difficult if the site is not accessible.

10.4 Tissue impedance measurements

Changes in tissue impedance have been monitored to provide information about ice-ball size. Measurement of tissue impedance is claimed to be superior to temperature measurements for monitoring the effects of cryosurgery because it gives information about the volume of tissue destroyed rather than just the volume of the ice-ball. The low frequency impedance of salt solutions increases slowly as the solution is frozen until the eutectic point is reached when the impedance rapidly rises to high values. The impedance of tissues has been shown to follow a similar pattern and it has been suggested that the sudden increase in impedance is associated with the formation of extracellular ice (le Pivert et al 1977, le Pivert and Binder 1975). As this process is understood to be a major cause of cell death from freezing, the sudden increase in impedance can be used to indicate when the boundary of tissue destruction has reached the recording electrode.

In this technique, exploratory electrodes are placed at the boundary of the region to be frozen and the impedance (typically at 1 k Hz) measured between these electrodes and a reference electrode. Freezing is continued until the impedance rises from that

characteristic of unfrozen tissue (approx. 2 kΩ) to 1 MΩ (le Pivert et al 1976, 1977). Gage (1979) has suggested that cryosurgery of malignant tumours should continue until higher critical impedances of 5-10 MΩ are achieved.

There seems to be some confusion in the literature over which electrode indicates the position of the eutectic region when making impedance measurements. When it is considered that only a small volume of high resistance tissue is needed to produce a high impedance reading, it seems preferable to use a double electrode with close spacing rather than several discrete ones.

10.5 Electrical current measurements

A similar approach to impedance measurements for assessing the extent of cryosurgical destruction is to measure the electrical current flowing between an active and a reference electrode in the frozen region (Torre 1979). The DC current used presumably gives rise to some polarisation problems, and in published tests arrived at correlating the current readings with the temperatures in the ice mass (Gage and Caruana 1980) there appears to be some confusion over what was actually being measured. The technique does not seem to offer any advantages over the impedance measurement technique.

10.6 Heat flux measurements

It has been suggested that a heat flux measurement could be used to provide an indication of ice-ball size after a certain freezing time (Harly and Aastrup 1972, Harly et al 1977). Since the latent heat of ice formation tends to dominate the cooling requirements of the probe, it is argued that a heat flow measurement would give an indication of ice mass formed. Harly and Aastrup (1972) found that the latent heat extracted by the cryoprobe was a fairly constant proportion of the total heat transferred to the tissues. However, this result can only hold for the initial stages of the freeze because as the ice-ball grows, the conduction terms of the heat transfer equation become more and more important compared with the latent heat term. When steady-state conditions are reached the latent heat extracted is zero. The monitoring of ice-ball growth by measuring the heat flux can therefore only be regarded as a reliable technique for short freezing times.

It has been suggested that heat flux measurements may indicate when an ice-ball has reached the limit of a tumour mass. Najjar et al (1979) measured the cooling curve in vivo for normal and malignant tissues and found different rates of ice-ball growth. However, considering the variable shape of the tumour mass compared with the ice-ball it would appear to be a technique that would be difficult to apply in practice.

10.7 Liquid crystals

Cholesteric liquid crystals have been used in experimental cryosurgery to determine the temperature fields and the ice-ball growth rate. This has usually been done by using a liquid crystal sheet that gives a two-dimensional picture of the temperature distribution around the probe. Temperatures are found by calibrating the colour changes and taking colour photographs at set intervals from the start of the freeze (Petrovic 1972, Cooper and Groff 1973, Cooper and Petrovic 1974). The lack of suitable crystals to produce colour changes at temperatures much below 0°C means that the temperature distribution within the ice-ball cannot be determined by this process. It is also a rather unwieldly technique for use in cryosurgery.

10.8 Thermography

Infra-red thermography has been investigated as a means of visualising the region frozen during cryosurgery (Bradley and Fisher 1975). It is a promising technique because the sensitivity level can be adjusted to give the operator information about a particular temperature band. Bradley (1977) was able to record a -15°C isotherm that gave the surgeon more relevant information about the destroyed volume than a simple measurement of ice-ball size. This author has also pointed out that thermography allows a photo-

graphic record of the cryogenic process to be obtained for later evaluation. The main probelm encountered was that of access for the infra-red sensor to the area requiring surgery.

10.9 Ultrasound

Some brief measurements were carried out by the author in conjunction with the Medical Physics Department of Bath Royal United Hospital to see if the growing ice-ball could be imaged using ultrasound. This proved to be possible although the image obtained was not very clear.

10.10 Standardised Cryosurgical Procedures

Some of the early work on mathematical models of ice-ball growth was intended to provide the surgeon with an accurate prediction of the effect of his freezing so that no monitoring was needed. To this end, Walder (1972) published plots of ice-ball size against tip temperature. Results with time as a variable have been published by Cooper and Trezek (1970, 1971a) in the form of sections through a brain, showing the increase in size of ice-ball expected with time.

The predictions of ice-ball size are not very reliable as an accurate guide to the surgeon because there are many variables which are difficult to take into account in the models. In an effort to make the freezing process more reproducible and thereby make the

theoretical predictions more useful to the surgeon, Rothenborg (1975) published a number of recommendations for standardised cryosurgical procedures. It proves to be quite difficult to achieve good reproducibility however and a number of the recommendations run counter to the ideal procedure for maximal cell death.

10.11 Choice of Technique for Monitoring Rectal Cryosurgery

In assessing the techniques that have been reviewed there is an important consideration. Irrespective of the techniques used to monitor ice-ball growth, the initial placement of the cryoprobe on the tumour will have to be done using indirect viewing. Only when the tumour is very close to the anal end of the rectum will it be possible to perform the initial placement using direct vision. Therefore it was decided that the cryoprobe would have to be designed around the need for a remote viewing facility. Initially the monitoring of ice-ball growth would be through indirect viewing by means of the same viewer. The problems of installing the necessary optics in a small instrument and subjecting them to very low temperatures would have to be tackled.

10.12 Conclusions

The rectal cryoprobe should incorporate a viewing system to enable both initial placement of the cold tip

on a tumour, and monitoring of ice-ball growth through indirect vision.

CHAPTER 11

An Evolutionary Design Technique

11.1 Introduction

This chapter is the first of two that describe the design of the viewer that is incorporated in the complete rectal cyroprobe. The viewer design is not straightforward because it involves the interface between the device and the patient, and also the interface between the device and the surgeon. The problems that the human/device interface pose for the designer are initially discussed in this chapter, and a solution is described that has been found to be very effective for problems of this type. The technique enables the design of devices that work well without the need for protracted development programmes

11.2 Outline of standard design technique

11.2.1 Problem definition

Figure 71 illustrates in diagramatic form a typical engineering design procedure. The initial step of defining the problem in general terms is an important part of all good design. This step involves trying to find the underlying roots of the problem rather than just accepting the problem as defined by the person requesting the design. This step is particularly important in medical engineering as most requests come from non-engineering personnel.

FIGURE 71

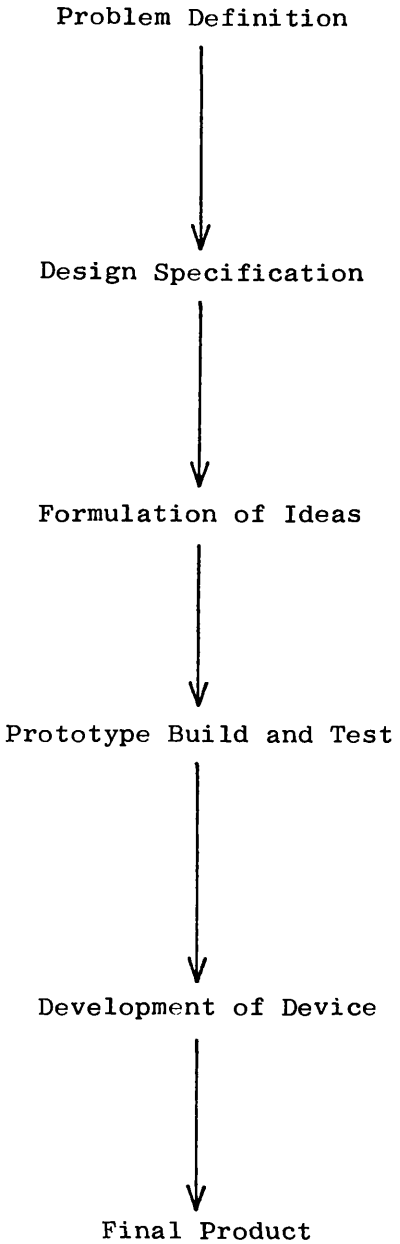

STANDARD ENGINEERING DESIGN PROCEDURE

11.2.2 Design Specification

The second step is to compile a design specification for the device. The specification is a description, both qualitative and quantitative, of all the features that the intended design must incorporate. These features can be uniquely defined variables or much more vague performance variables. For example, the specification for a simple device such as a box might include such things as the following.

a) length must be one metre (uniquely defined variable)

b) weight must be no more than 1kg (precise limit or constraint).

c) it must be able to be folded flat for storage (performance feature).

Design specifications typically include these three main features.

11.2.3 Creation of ideas for possible solutions

The third step in a typical design procedure is the creative task of generating possible solutions which will meet the requirements and constraints of the design specification. This is an extremely interesting area that is essentially an iterative exercise of matching a series of mental patterns. The exercise concludes when the designer is satisfied that his mental prediction of how his theoretical design(s) will behave is acceptably close to the behaviour outlined in the specification.

11.2.4 Construction and development of prototype

The fourth and fifth steps of the design procedure are the building of the prototype device and the testing of it.

11.2.5 Factors influencing the effectiveness of the prototype

There are two major factors which determine how close the behaviour of the prototype comes to the desired behaviour:-

1. The creative ability of the designer in finding solutions that match the specification.
2. The accuracy and completeness of the specification.

The second aspect is very important to the argument of this chapter. In many areas of engineering design the specification can be very comprehensive and can take into account nearly all the factors that may influence the functioning of the device. Given a comprehensive and accurate design specification a good designer can carry out the creative design activity in isolation from the problem itself. As long as all the requirements and constraints listed in the specification are satisfied, the engineer can be sure that the device he has designed will probably function reasonably well.

11.3 The effect of applying standard design procedures to devices with a human interface

11.3.1 The problem of compiling a complete specification

The main problem of applying standard design techniques to devices with a human interface is that it is extremely difficult to draw up a specification for such a device that is either complete or accurate. The functioning of the device will be influenced by a large number of anatomical, physiological and psychological variables. Many of these variables will be almost impossible to quantify and many will not even be at all obvious until after a device has been built and tested.

For example, the performance of even the simplest aid for the disabled can be extremely difficult to define precisely. Consider the problem of designing an aid to enable a child to put his socks on when he cannot reach any lower than his knees. Superficially the problem appears to be fairly simple. However the normal action of pulling on socks is a complex three dimensional movement with constant adjustments of the position of the foot and sock and of the direction of the forces used. The unravelling of the sock has to be coordinated with these movements. The movements of the sock are not fixed but depend on how the body tissues and joints react to the imposed loads. It is almost impossible to precisely define this action and to relate to to the anatomy of the child or his physical abilities.

Any design solution will invariably interact with other parts of the human body. Therefore the environmental constraints listed in the specification need to include many aspects of human anatomy and behaviour. In many areas of human interface design this kind of information is part of common experience and knowledge. When dealing with handicapped people however, this is often not the case.

11.3.2 The effect of designing for a human interface on the basis of a specification

If a design is attempted for a human interface on the basis of a specification, many problems arise. During the creative phase of design, the designer is constantly mentally comparing the expected behaviour of his theoretical design with the required behaviour as defined in the specification (see Orpwood 1984). He will be satisfied with his theoretical design when the expected behaviour is very close to the required behaviour. However if the device is not precisely defined in the specification, it is difficult to know when the expected behaviour is adequate. The end result of this difficulty is that the final design, when made up and tested, will inevitably not work very well and will need extensive development. Quite often, in an attempt to ease the mental evaluations of his designs, a designer will tend to concentrate on some aspects of the specification at the expense of the others.

The inevitable outcome of these problems is that when the prototype device is tried out it will not be very satisfactory. Extensive development in conjunction with patients, both of the human interface aspects and the supporting features, is usually then required.

11.3.3 A typical result of using standard design procedures

The effect of working in isolation from the human user was highlighted at the Bath Institute of Medical Engineering, (BIME) during the development of a lightweight leg caliper (Orpwood, 1977). The prototype caliper design was based on a specification that had been drawn up from the results of a detailed questionnaire completed by many caliper wearers.

However when the caliper was tried on patients it didn't work. Many problems were encountered that had not been anticipated. The knee joint release mechanism was too painful to operate. The anatomical problems of operating the mechanism had been too complex to define precisely. Some patients could not even put the caliper on for similar anatomical reasons. The caliper became extremely hot to wear after a short time because of unforseen physiological problems. Psychological problems also occured. The noise made by the caliper during walking reduced its acceptance by many patients. A period of extensive clinical development was needed to produce the final successful design.

11.4 The Evolutionary Design Technique

11.4.1 Aims of technique

The aim of the evolutionary design technique is to reduce development time by doing two things:-

(1) To separate the patient interface aspects of the design from the supporting features.

(2) To enable human interface aspects of designs to be evaluated at an early stage before the overall final form has been settled.

The second part is important because it enables the designer to augment his mental evaluations of a design approach with physical tests of components in their intended environment. **Figure 72** illustrates in diagrammatic form the evolutionary design technique and this is described in more detail. (Orpwood, 1983).

11.4.2 Initial stages of design.

The technique initially follows standard practice by carrying out problem definition and drawing up as comprehensive a specification as is practicable.

11.4.3 Define the human interface.

The technique is based on a recognition that the human interface aspects of the design will be the cause of most of the design difficulties. Therefore at an early stage, the human interface is defined. In other words the total device is studied and those aspects which are the supporting structure or mechanism are

FIGURE 72

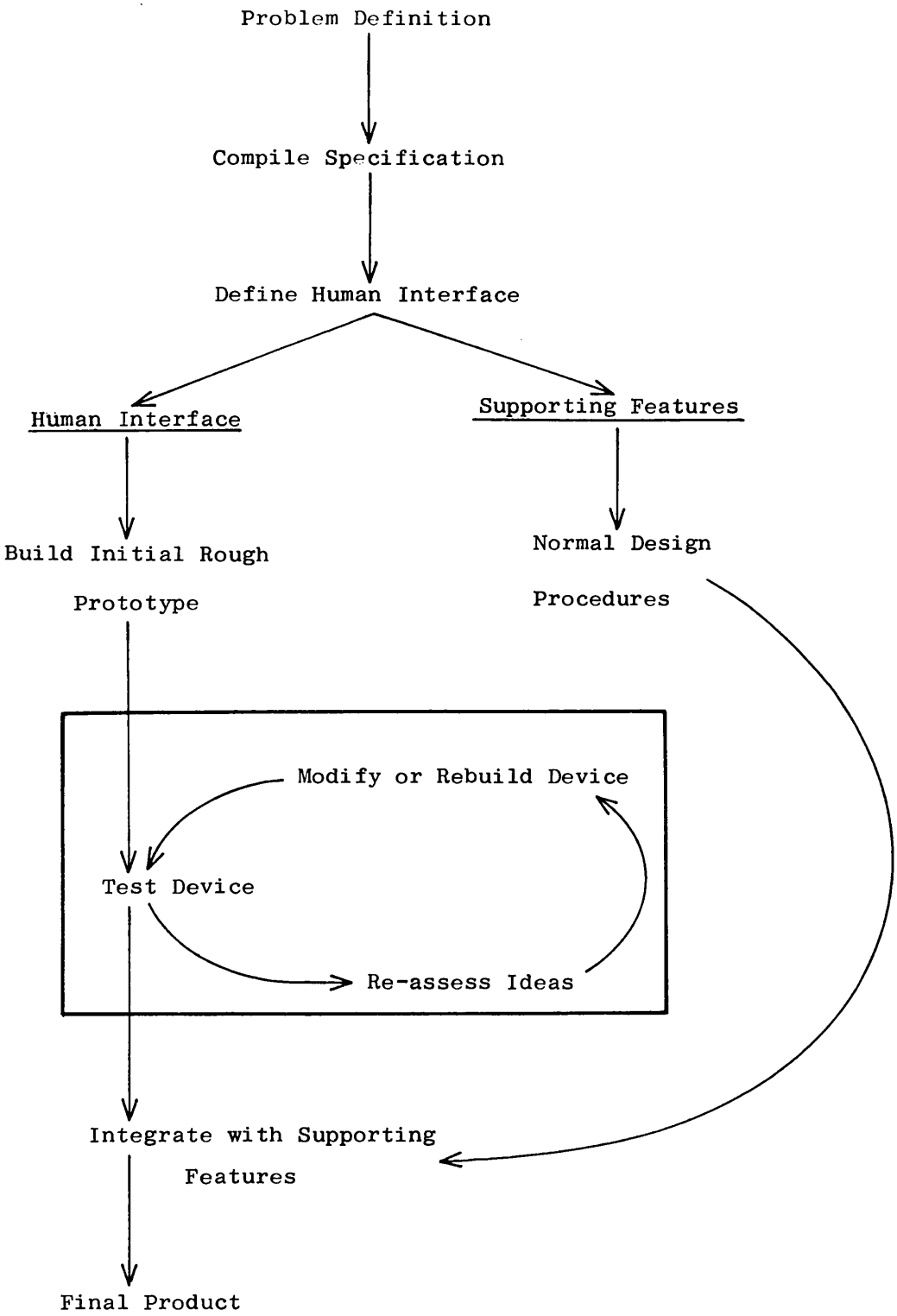

EVOLUTIONARY DESIGN PROCEDURE

differentiated from those aspects that form the interface with the patient or surgeon.

For example, a chair that was developed at BIME to enable elderly patients to get to their feet after sitting in it, can be subjected to this differention. The human interface is the nature of the cushion and the path it follows during the raising of the patient to a standing position. The supporting aspect of the design is the lifting mechanism itself, in other words those aspects of the design that are independant of the patient.

Having defined the human interface, the subsequent evolutionary method is applied just to the patient interface features of the design. The supporting aspects are usually more straightforward from a design point of view and can use standard design techniques to find an effective solution.

11.4.4 The First Rough Prototype

The evolutionary technique starts from a recognition that the specification is likely to be incomplete and innaccurate, and that the prototype device is unlikely to work. Consequently the first prototype is made as simple as possible and can be quite a rough and ready device. For example, with the lifting chair described above, the first prototype was a simple car hydraulic jack that was used to raise a hinged seat. It is not important that this simple first try should be very effective as long as it is a reasonable first

estimate at a possible solution and allows the human interface to be explored.

11.4.5 Trial of Prototype

The next step is to try the primitive device with the patient so that its potential and shortcomings can be examined, assessed and perhaps measured by both the engineer and the clinician. The patient should also be encouraged to comment on the device, if this is possible.

The initial evaluation of the rough prototype is an extremely important stage. The important variables become highlighted, many that were not considered in the original specification are exposed, and many that were considered are more precisely defined.

11.4.6 The Evolutionary Cycle

The next stage is to reconsider the design. However this time the task is both easier and more likely to lead to an effective solution. This is because the written specification will be more accurate and complete and also because the designer will have a much better "feel" for the problem

A second prototype is therefore made up on the basis of the reconsidered design, and again tried out. The second design is assessed with the patient and the process repeated. The design therefore goes through a series of evolutions where it is known and expected at each stage that there are likely to be problems and

shortcomings, but where these problems are progressively overcome.

Because the problems with the design, and their possible solutions, are indicated by applying the device to the patient, it is far less likely that some important patient variables will not be taken into account or that some variable is allowed to dominate one's thinking in producing a design.

11.4.7 Combine the patient interface aspects of the design with the supporting features.

Having obtained a satisfactory working solution to the human interface aspects of the device, the design of the supporting features can proceed. Standard design procedures are used for this phase of the work. It can be carried out in the sure knowledge that a complete redesign of the supporting features, caused by a failure of the patient interface, is most unlikely.

11.5 The Number of Evolutionary Cycles

11.5.1 The iteration followed in the evolutionary cycle.

The human interface design passes through a series of evolutions.

Let the design achieved at the nth evolution be DES_n

Let the behaviour of DES_n = BEH_n

Let the required behaviour of the device = BEH_r

Then the iteration followed is:-

$DES_{(n+1)}$ = DES_n modified by insight gained from BEH_r-BEH_n

This process is continued until BEH_r-BEH_n is acceptable.

11.5.2 The number of cycles needed.

The iterative scheme described above used the insight or understanding gained from studying BEH_r-BEH_n to modify the existing design. The number of evolutionary cycles that the design goes through depends strongly on this understanding. The more information gained, the smaller the number of cycles needed. During the trial of a design, it is therefore extremely important that as much information as possible is collected. Given thorough testing of designs, only a few cycles are needed before a satisfactory solution is found and often the second prototype will be the final version.

11.6 Conclusions

It is found that the use of standard design procedures for designing devices with a human interface can lead to the need for extensive prototype development. An alternative technique that tackles the human interface aspects of the design separately from the rest, and allows this part of the design to evolve in conjunction with the human user, can lead to effective designs much more quickly.

CHAPTER 12

Design of the Rectal Viewer

12.1 Introduction

This chapter describes the design of the viewing system that is incorporated in the rectal cryoprobe. This aspect of the design is not simple because it involves the interface between the device and the patient, and also the interface between the device and the surgeon. The evolutionary design technique discussed in the last chapter is used.

In the process of developing an effective viewer design, many different experimental devices were tested. Not all of these devices will be described. The chapter will concentrate on the designs that represent the major milestones of the evolving viewer.

12.2 Operating Requirements for Rectal Viewer

(1) The device must not damage the anal sphincter during insertion.

(2) The device must be capable of being inserted up to 200mm into the rectum without damaging the rectal walls. (The rectal wall can be easily damaged as it consists of sensitive tissue that is quite thin, and the rectal canal when empty is very contorted).

(3) The device must contend with any faecal remains or exudates in the rectal cavity.

(4) The surgeon must be able to identify structures such as polyps or tumours within the rectum.

12.3 The Telescope used for the Rectal Viewer

It was decided to use a Thackray urological endoscope as the basis of the viewer for the following major reasons:

(a) They are designed for clinical use.

(b) They are very compact.

(c) They incorporate their own light guide for illumination purposes.

(d) They are available in lengths appropriate to viewing in the rectum.

Figure 73 illustrates a cross section through the shaft of a Thackray telescope. The lenses are arranged up the centre of the instrument with the light guide in the form of an annular bundle just inside the outer casing. It can be seen from Figure 73 that the light guide fibres are connected to a separate input port. The tip of the telescope can be arranged either to view straight ahead (0°) or to view at 30° or 70° to the axis of the instrument. A 0° and a 30° telescope was obtained for the viewer tests and a 70° unit was also borrowed from the manufacturer.

FIGURE 73

THACKRAY TELESCOPE

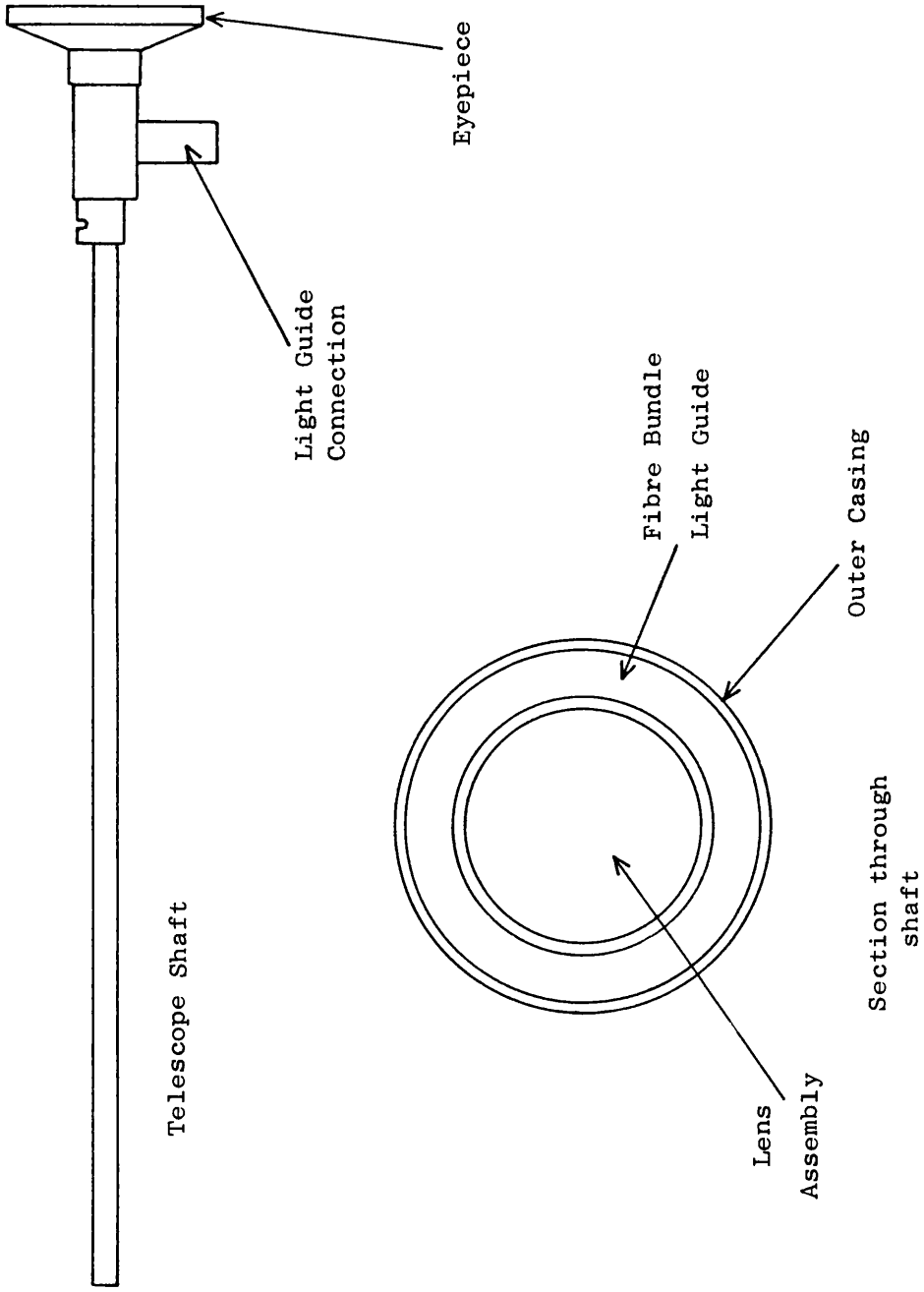

12.4 Study of Rectal Expansion

12.4.1 Reasons for study

It had been decided that the evolutionary design technique described in the last chapter would be used to produce a rectal viewer design. However, it was felt that one variable was sufficiently independent for it to be studied in isolation from the many others. This was the degree to which the rectum needed to be expanded.

The rectum needs to be dilated in order that an acceptable view of the cavity can be obtained. When there is nothing in the rectum it collapses down to an internal diameter of about 10mm. It was expected that a good view could only be obtained by expanding the cavity to a larger size.

12.4.2 Technique used to assess degree of expansion needed

A series of models of the rectal cavity were made (see **Figure 74**). Each of these consisted of a cylinder with an insert at one end to support the small telescope that was to be incorporated. The internal diameter of these tubes ranged from 12mm to 35mm and the internal surfaces were lined with $\frac{1}{4}$" square graph paper to give the operator some idea of the size of things he was looking at. A small tumour was also represented by a shaded area on the graph paper. The shaded area enabled the operator to see how close the telescope had to be to the tumour to give an acceptable view. It

FIGURE 75

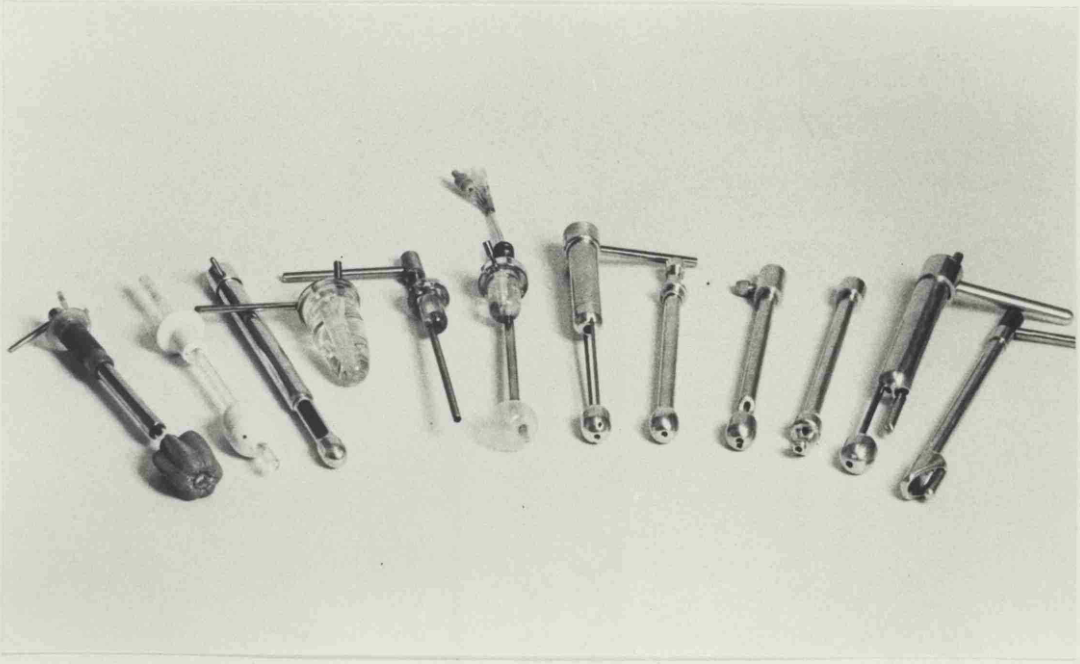

SEVERAL OF THE EXPERIMENTAL VIEWERS USED TO EVOLVE A RECTAL VIEWER DESIGN

FIGURE 74

MODEL OF RECTAL CAVITY

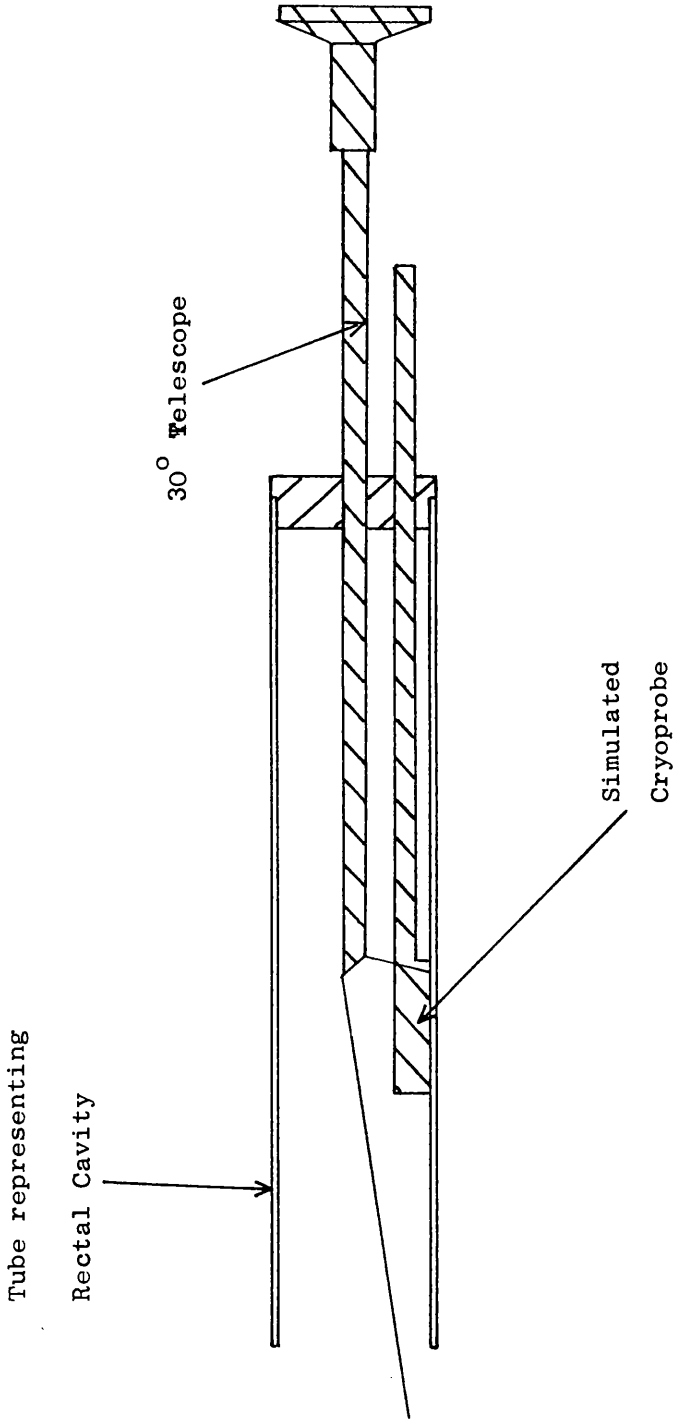

also indicated what minimum length of cavity had to be expanded, to give a high probability that something the size of a small tumour would be detected.

12.4.3 Results of expansion study

Despite the artificial nature of this test it did indicate important conclusions about the viewer design. The cavity needed to be expanded to an internal diameter of at least 20mm. The length of cavity in front of the telescope that needed to be expanded, was at least 25mm. These conclusions were reached without any theatre tests and were subsequently found to be valid conclusions for the real rectum.

12.5 Application of Evolutionary Design Technique to Rectal Viewer

12.5.1 Human interface identification

The human interface of the rectal cryoprobe is defined by three main requirements:

(a) The instrument needs to be inserted into the rectal cavity.

(b) The surgeon needs to be able to manipulate the device and to control its operation.

(c) The surgeon needs to be able to see both the rectal cavity and the freezing tip, and to be able to orientate himself within the view that he has of the cavity.

These requirements were extremely difficult to define precisely in order that a detailed specification could be produced. For example, this is particularly true of the structural properties of the rectal wall. The wall is almost able to emulate the properties of liquids in its ability to flow around and surround any objects placed in the rectum.

12.5.2 Isolation of the human interface

The human interface aspects of the device were isolated from the rest of the cryoprobe by constructing non-working models of the instrument. These included a non-working replica of the freezing tip and allowed the external geometry and the design of the viewer to be explored. Such devices could be made relatively quickly. A large number of these non-working models were made and tested. **Figure 75** is a photograph of most of them.

12.5.3 Problem of applying the evolutionary technique to the rectal cryoprobe

It was shown in **Section 11.5** that it is important to gain as much information as possible at each trial of a device. The more understanding that is gained, the smaller the number of evolutionary cycles that are needed to achieve an acceptable solution. Unfortunately it was difficult to thoroughly test each new version of the cryoprobe.

Each trial was carried out in the operating theatre just prior to an operation on a patient. The trial would be carried out by Mr. Lloyd-Williams, Consultant General Surgeon at the Bath Royal United Hospital, or one of his colleagues. The engineer was allowed to be present and make close observations himself. However, the amount of time available for evaluating a given design was inevitably limited. The patient was under a general anaesthetic and so time was very critical. The surgeon and his theatre support staff needed to get on with attending to the patient so that they could complete their lists for that theatre session.

In the rather delicate situation described above it was impossible for the engineer to gain as much information as he would have liked about the performance of the device being tested. As a consequence the design of the viewer tended to follow a number of blind alleys, using a large number of evolutionary cycles, before reaching effective solution.

12.6 Techniques of Rectal Expansion

The first series of trials explored techniques for expanding the rectum. Three methods of expansion were considered:

(1) The rectum could be expanded by means of an insertion which mechanically forced the cavity to a larger size. Viewing would be carried out between sections of the expander or the fingers or grid of the expanding

mechanism.

(2) A clear tube with an outside diameter large enough to form an expanded cavity could be inserted. Viewing would take place through the tube.

(3) A cavity would be generated by inserting a gas tight seal deep in the rectum and inflating the section between the seal and an airtight anal plug.

The mechanical expander did not work because the rectum simply wrapped itself around the expander. The clear tube did not work because when the tube was pressed against the rectal wall it flattened and distorted the appearance of the wall and made operating impossible. Most of the devices that are subsequently described, attempted to expand a section of the rectum by inflating it.

12.7 Viewer Designs that Attempted to Isolate a Rectal Cavity

12.7.1 Viewer using clear tube in cavity

Having found that gas inflation was the most suitable method for expanding the rectum, the initial viewer designs concentrated on attempting to isolate a gas tight section of the rectum.

Figure 76 illustrates the first device that was tried. It was attempted to isolate and enlarge a section of the rectum by inserting a latex seal into the far end of the rectum and inflating the section between

FIGURE 76

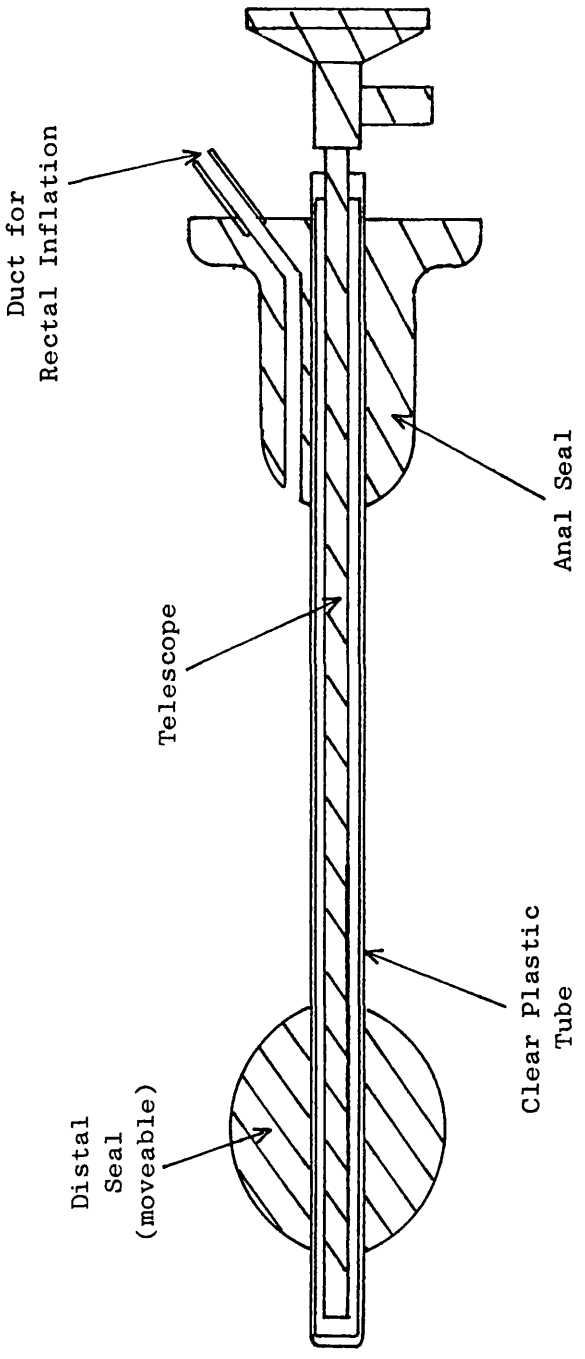

VIEWER USING CLEAR TUBE IN CAVITY

the seal and an air-tight anal plug. The seal and the anal plug were connected by a clear tube. A 0° telescope viewed out the end of the tube for safe insertion, and a 30° telescope would then be put in its place for viewing through the walls of the clear tube into the cavity inflated. It was expected that the cryoprobe would be inserted through the anal plug into the cavity.

Tests showed this to be a promising start but there were two main problems:

(1) The latex seal was not airtight.

(2) If the clear tube contacted the rectal wall, as it inevitably did during insertion, it became contaminated with mucus and was no longer transparent.

12.7.2 Viewer with integral balloon

The problem of mucus contaminating the tube, encountered with the initial prototype, was overcome in subsequent devices by having a metallic tube up the centre of the instrument. The telescope was placed in this tube whilst the device was inserted into the rectum but then removed and replaced through the anal plug and into the space outside the tube (**Figure 77**).

The problem of an airtight distal seal was not so easily overcome. One attempt which came close to working incorporated a balloon on the end of the inserting tube. The device was inserted with the balloon deflated and it was then pumped up once in place

FIGURE 77

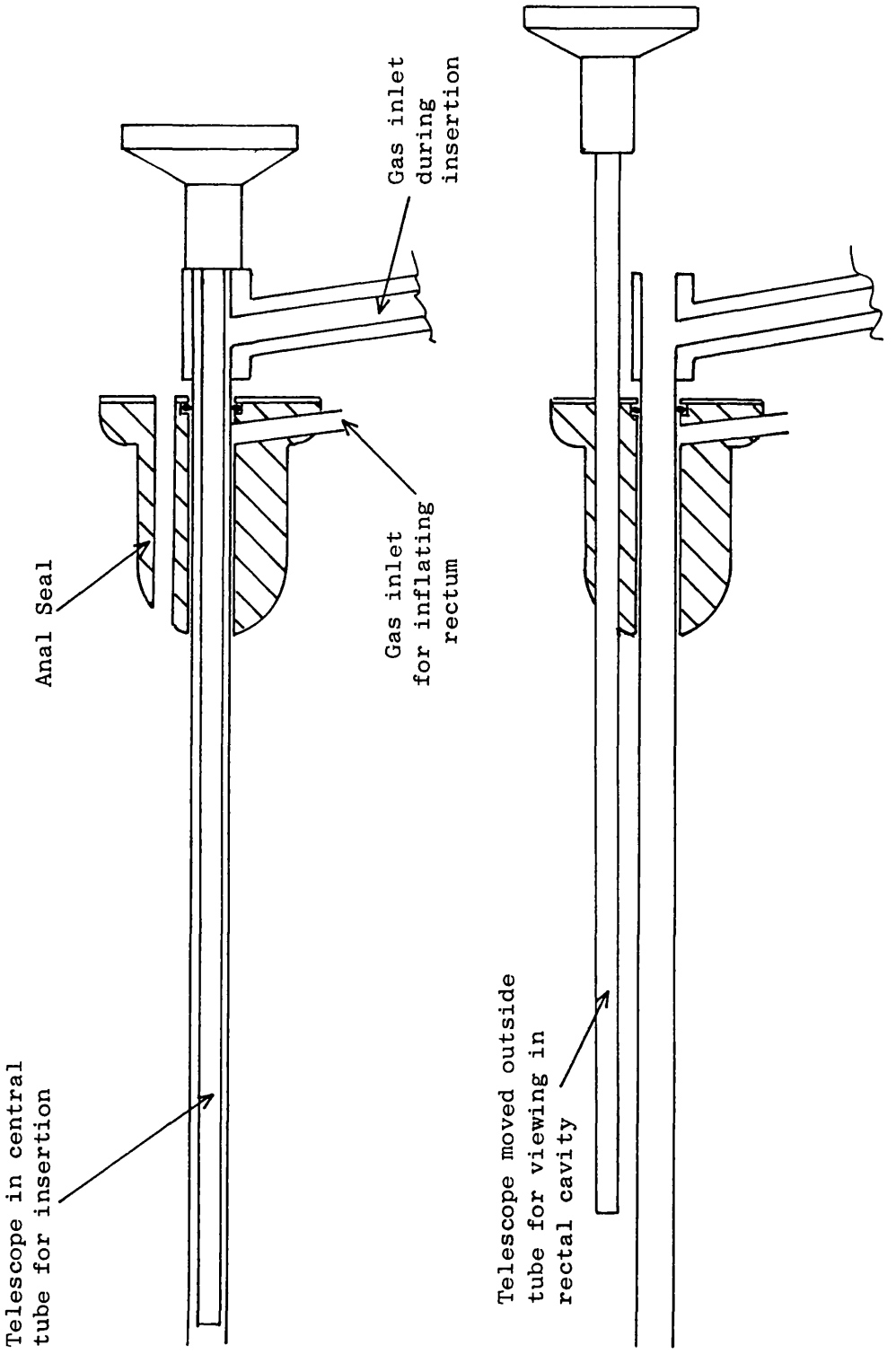

TECHNIQUE USED FOR USING THE SAME TELESCOPE FOR INSERTION AND VIEWING IN CAVITY

(see **Figure 78**).

The attachment between the tube and the balloon was unfortunately rather unreliable. Various other forms of expanding seal were explored using mechanical expansion but none proved to be very effective.

The introducing tube with its telescope proved to be an extremely useful device in its own right for inspecting the inside of the rectum and has since been developed as such.

12.7.3 Viewer using Foley catheter

In an attempt to introduce an inflatable seal into the far end of the rectum, a device was made that could insert a disposable Foley catheter. A Foley catheter is a tube for draining off various biological fluids. It incorporates a small balloon at the sampling end. The balloon has the function of sealing off the vessel in which the catheter is placed so that no fluid can escape past the sampling end of the tube.

The device shown in **Figure 79** was constructed initially to be inserted into the rectum under direct vision. Once in place the telescope was taken out of the central tube and a Foley catheter inserted. The balloon was pushed out of the far end of the tube and inflated, thus making an air tight seal. The telescope and the cryoprobe could then be inserted into the rectal cavity that had been generated by pushing them through seals in the anal plug.

This device worked very well but suffered from the

FIGURE 78

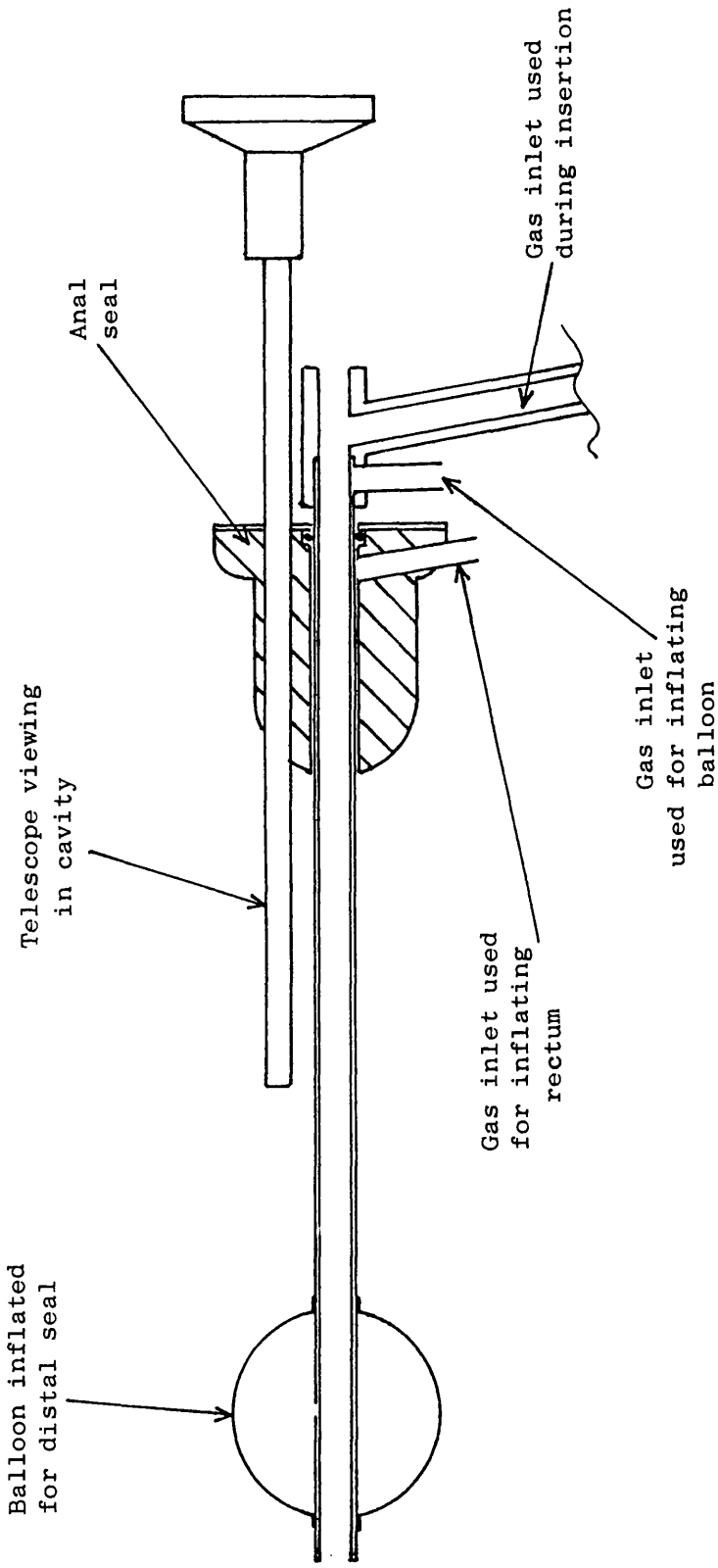

VIEWER USING INTEGRAL BALLOON FOR DISTAL SEAL

FIGURE 79

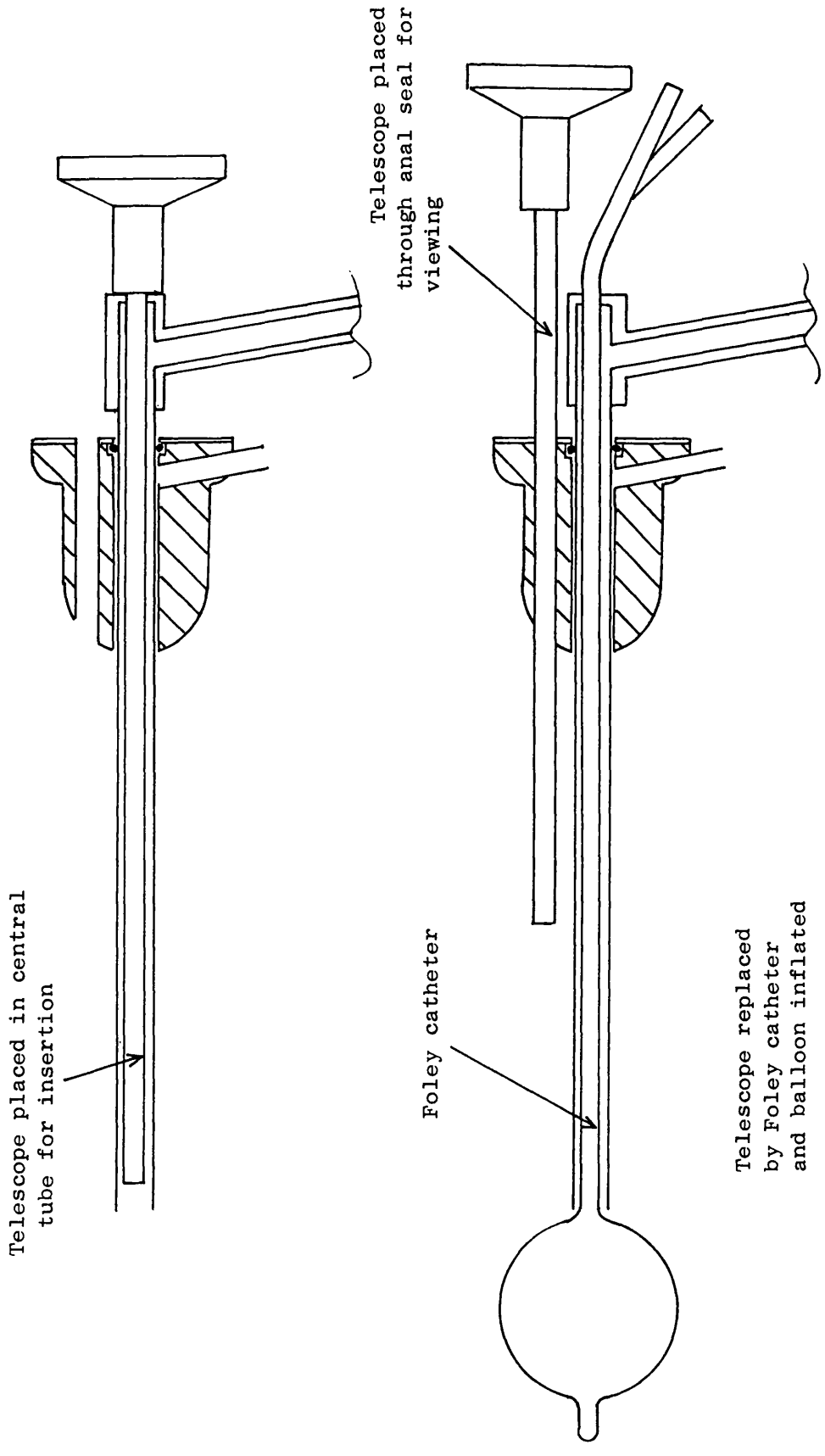

VIEWER USING FOLEY CATHETER

disadvantage of being extremely complicated to set up. Several pairs of hands were needed to achieve an inflated cavity with the seals in place and the probe and telescope in position. In particular the anal seal was continually being dislodged during the setting up procedure.

12.7.4 Device with fixed seals

In an attempt to simplify the technique of isolating and inflating the rectal cavity a further development was investigated (see **Figure 80**). The anal seal was made an integral part of the instrument so that once this region of the device was in the anus, the whole instrument could be moved without air escaping through the anal canal. The distal seal was also a rigidly formed component so that no balloons were required. The two seals were attached to each other so that no relative movement was possible.

This viewer was much easier to set up. Unfortunately the large anal seal made it difficult to manouver the device into the rectum and it also proved difficult to see areas of the rectal cavity near the anus.

12.8 Viewer Designs that did not confine Gas

12.8.1 Rationale behind alternative approach

A large number of viewers had been built in an attempt to isolate and inflate a rectal cavity. Progress towards a working solution was very slow and it

FIGURE 80

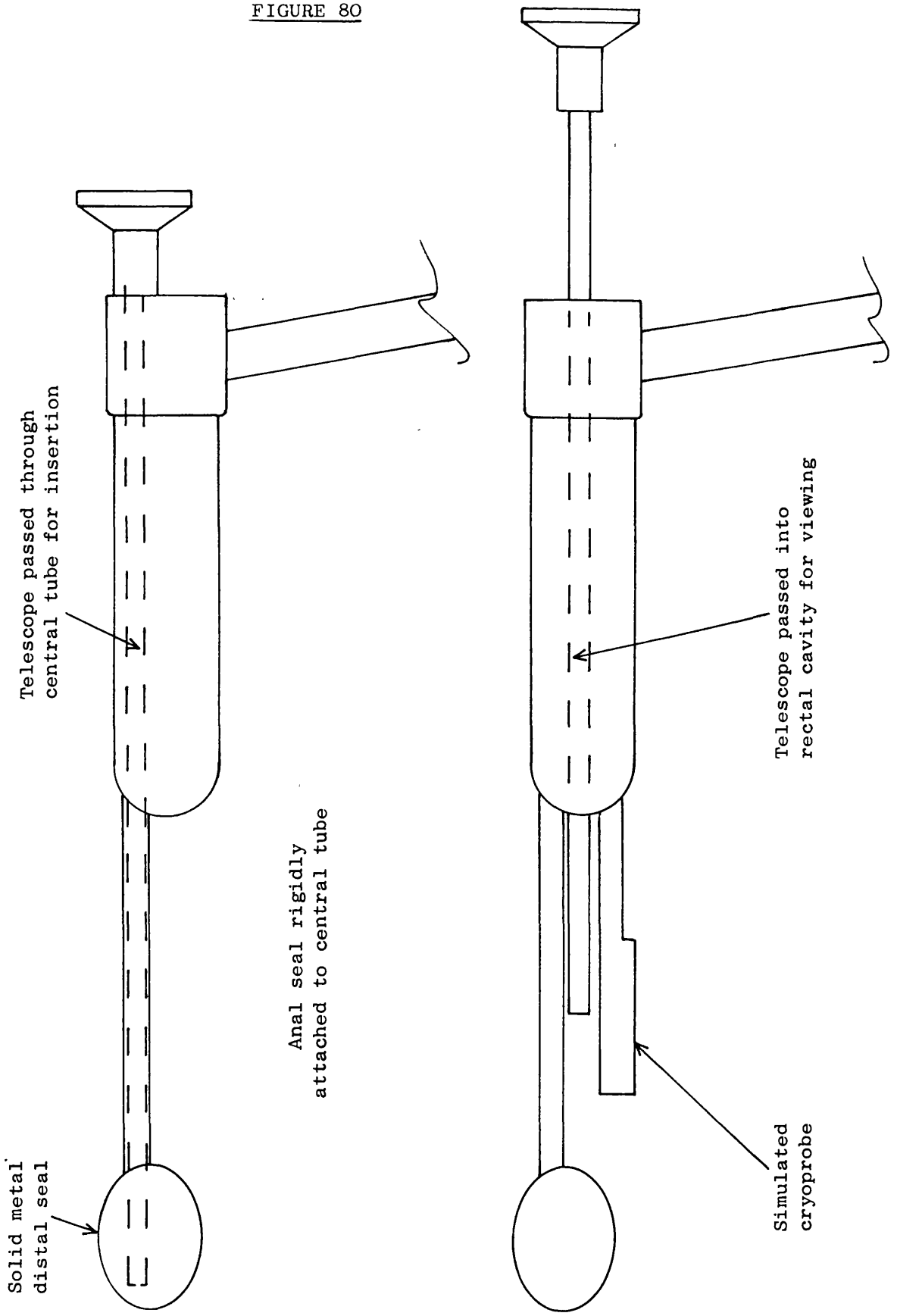

VIEWER WITH FIXED DISTAL AND ANAL SEALS

was difficult to make the devices simple to operate. An alternative approach was explored that did not confine the inflating gas within a cavity but allowed it to escape further into the intestines. Gas escaped quite slowly in this direction and could easily be bled out through a tube once the operation was complete.

12.8.2 Initial designs that allowed gas escape

Figure 81 shows a device that was partially successful. It was of a large enough diameter to provide an anal seal. It had an enlargement in diameter just behind the area where the telescope came out, to provide some distention of the rectum in the viewing area. The enlargement had a finger-like extension which passed down in front of the field of view. This extension represented the cryoprobe freezing tip.

Operation of this device was much simpler. However the view of the rectum was badly obscurred by the cryo-probe tip.

12.8.3 Final viewer design

The previous viewer was further developed so that the telescope looked down over the top of the cryoprobe tip. **Figure 82** illustrates the final viewer. A good view of the rectal cavity could be maintained with very little inflation. The cryoprobe tip could be seen clearly with a 30° telescope and did not obscure the view of the rectum. The enlarged hood helped generate

FIGURE 81

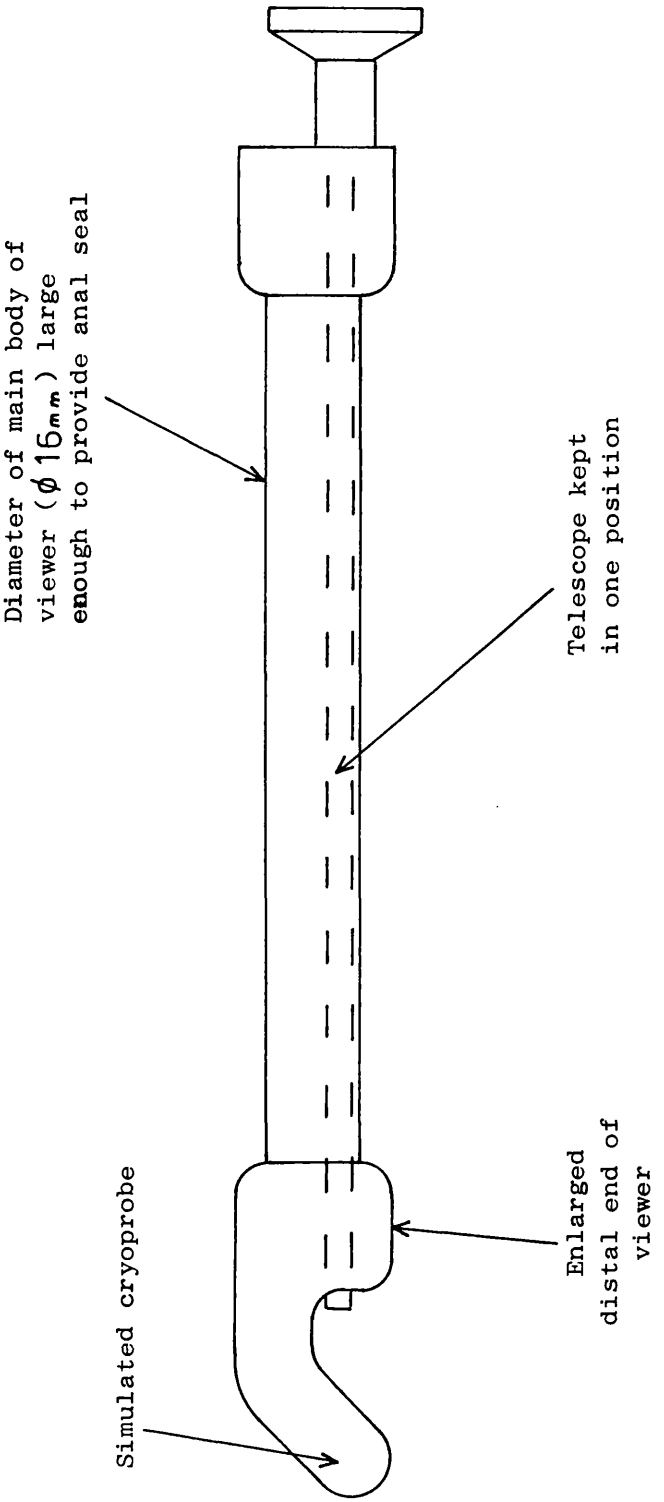

VIEWER THAT DOES NOT CONFINE GAS AND USES FINGER-LIKE CRYOPROBE TIP

FIGURE 82

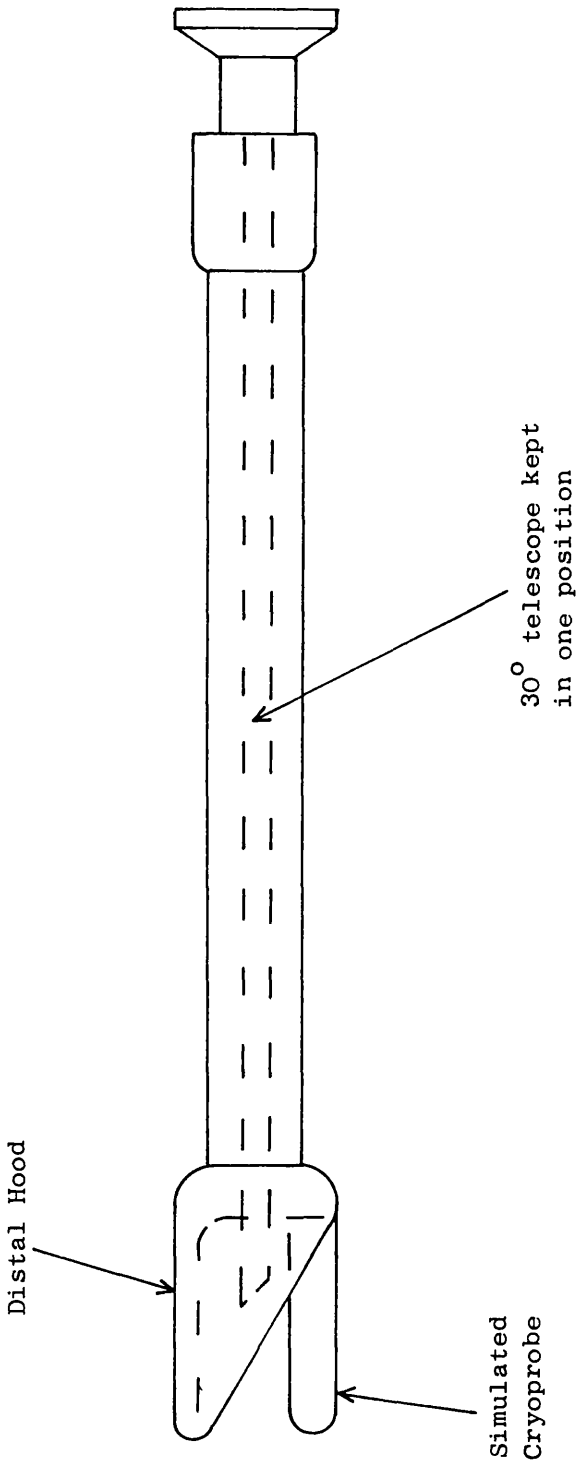

FINAL VIEWER DESIGN

an adequate cavity for viewing and also protected the telescope from coming into contact with the rectal wall. This device proved to be the best of all those tried, both because of its effectiveness and its simplicity. Although not perfect, the difference between its behaviour and the required behaviour ($BEH_r - BEH_n$) was acceptable. **Figure 83** is a photograph of the final viewer design with its support equipment.

12.9 Design of Anal Introducer for Viewer

The shape of the front end of the final viewer was not conducive to an easy passage through the anus. A special introducer had to be designed. The action of this introducer was to insert a metallic tube in the anal canal which guided the viewer into the much less constrained rectum. Further movement of the viewer into the rectum could be easily managed with the air inflator being used to clear a path. All movement was carried out under direct vision. The tubular introducer was removed once the viewer was in the rectum. This allowed the anus to form a gas tight seal around the viewer shaft. **Figure 84** is a drawing of the introducer and **Figure 85** illustrates its mode of operation.

12.10 Conclusions

1. The rectal viewer should be based on a Thackray urological endoscope.
2. The viewer should expand the rectum to a

FIGURE 83

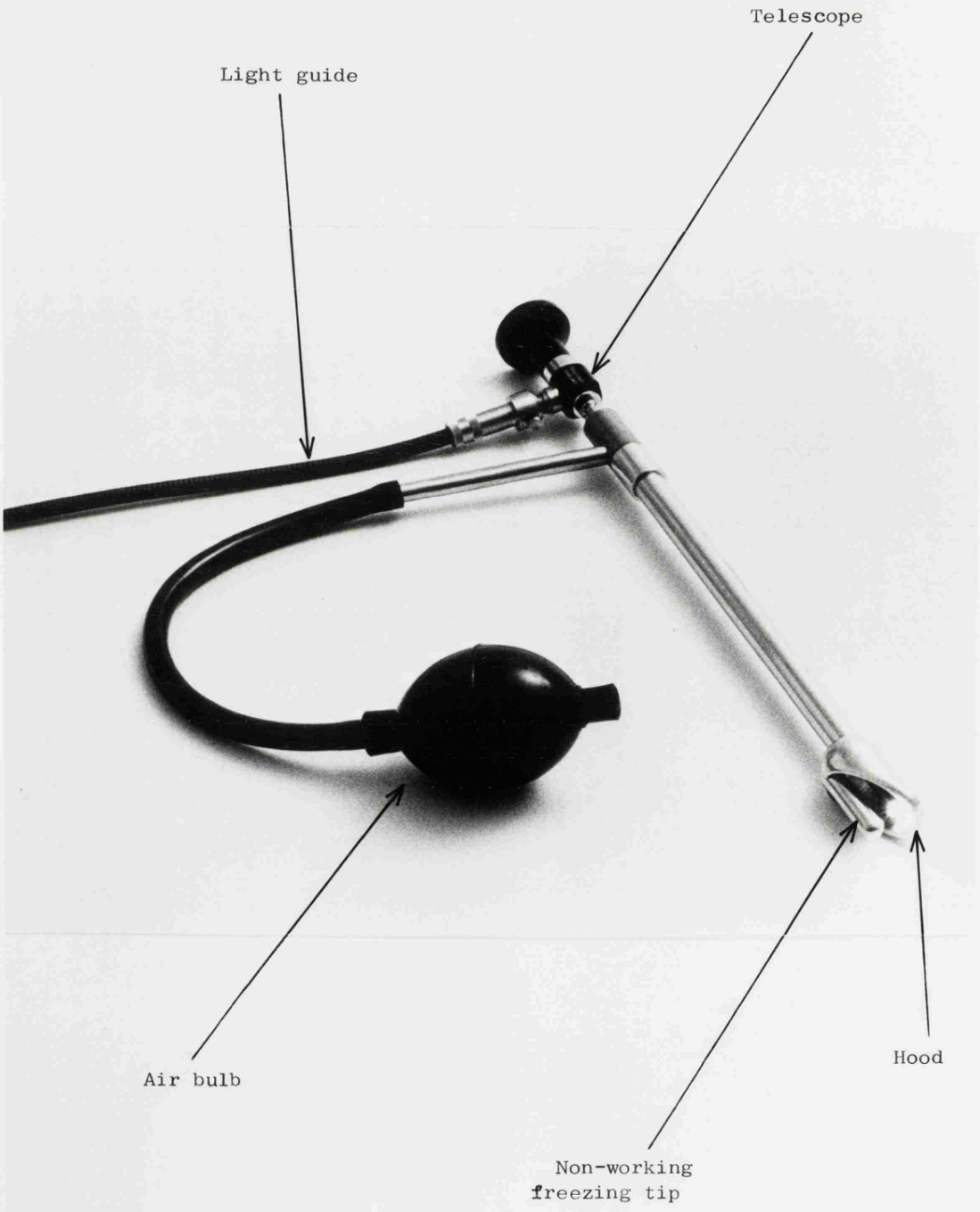

FINAL EXPERIMENTAL RECTAL VIEWER

FIGURE 84

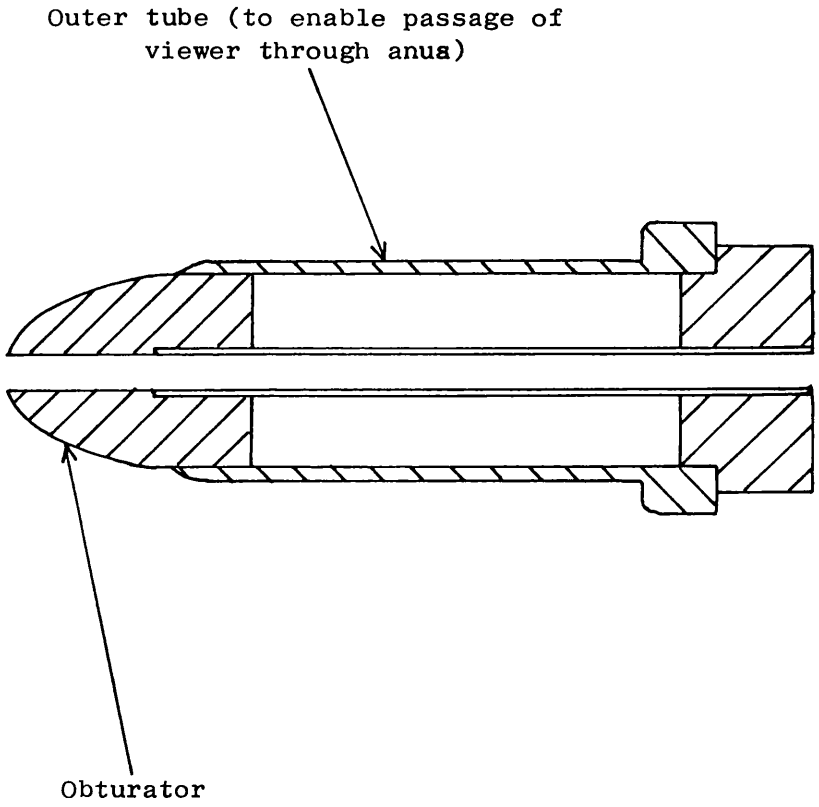

SECTION THROUGH ANAL INTRODUCER

FIGURE 85

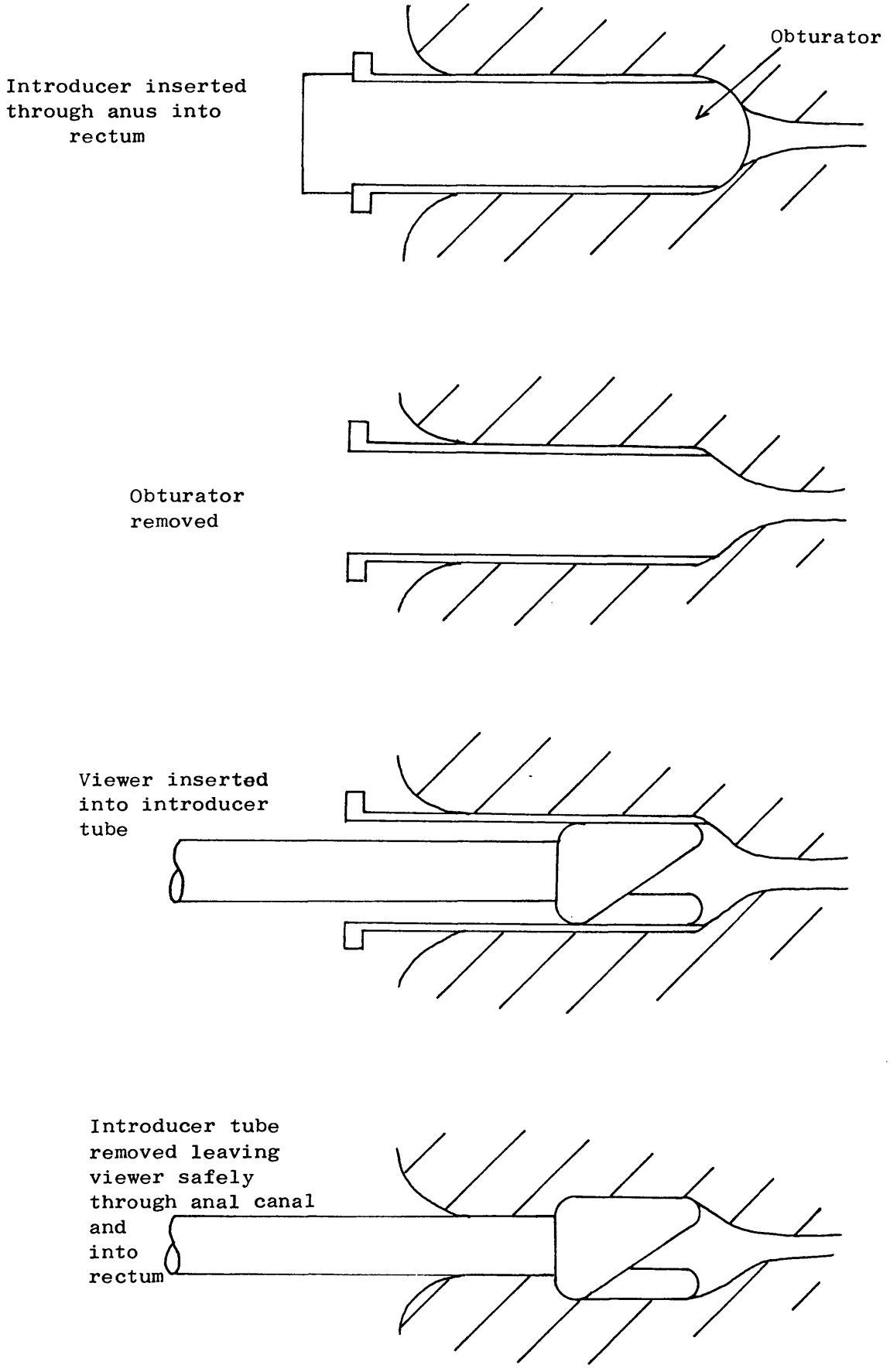

METHOD OF USING INTRODUCER

diameter of at least 20mm and this expansion should continue for at least 25mm in front of the telescope.

3. The rectum should be expanded using gas inflation.
4. The expansion can be simply effected without confining the inflating gas.
5. The viewer design illustrated in **Figure 82** and **83** is preferred together with the anal introducer illustrated in **Figure 84.**

CHAPTER 13

COMPLETE SYSTEM DESIGN

13.1 Introduction

Previous chapters have described work on both the cryogenic components of the cryoprobe and on the viewer. This chapter combines these two constituents and integrates them into the overall design of the rectal cryoprobe system.

The complete system is shown in **Figure 86** and consists of three main parts:-

(1) The cryoprobe itself, complete with viewer.

(2) The transfer hose.

(3) The support unit.

The support unit supplies the liquid nitrogen for the probe and houses the features that are necessary for the cryoprobes operation, such as the defrost system, the light source and the temperature control electronics.

The overall design of the cryoprobe is briefly examined. It is shown how the freezing tip design discussed in **Chapter 6** is combined with the cryogen supply system discussed in **Chapter 9**. Both these systems are then integrated with the viewer design discussed in **Chapter 12**.

The transfer hose design is also discussed. The final practical hose has not only to transfer nitrogen to the probe and return the exhaust gas, but also has to

FIGURE 86

COMPLETE RECTAL CRYOPROBE SYSTEM

provide a channel for rectal inflation and for the wiring loom.

The bulk of the chapter however is devoted to the design of the support unit. Standard design procedures were followed and a broad specification is outlined. Several sub-systems are needed in the support unit in order to satisfy the requirements and constraints of the specification and these are systematically discussed. These discussions include a summary of any development necessary to enable the prototype to function successfully.

13.2 Integrated Cryoprobe Design

13.2.1 Internal arrangement of components

The cryoprobe was designed as an assembly of four major components; the tip, the hood and shaft, the probe body and the handle. The division allowed a straightforward assembly and also provided acess for maintainance. **Figure 87** shows a general assembly diagram of the final design and the division into these four elements. The overall shape of the probe is the one concluded from the work presented in **Chapter 12.** A photograph of the complete cryoprobe is shown in the frontispiece and a close-up photograph of the operating end is shown in **Figure 88.**

The connection of the probe to the transfer hose is via the probe handle. Within its structure is the termination for the tubes of the transfer hose. It

FIGURE 87

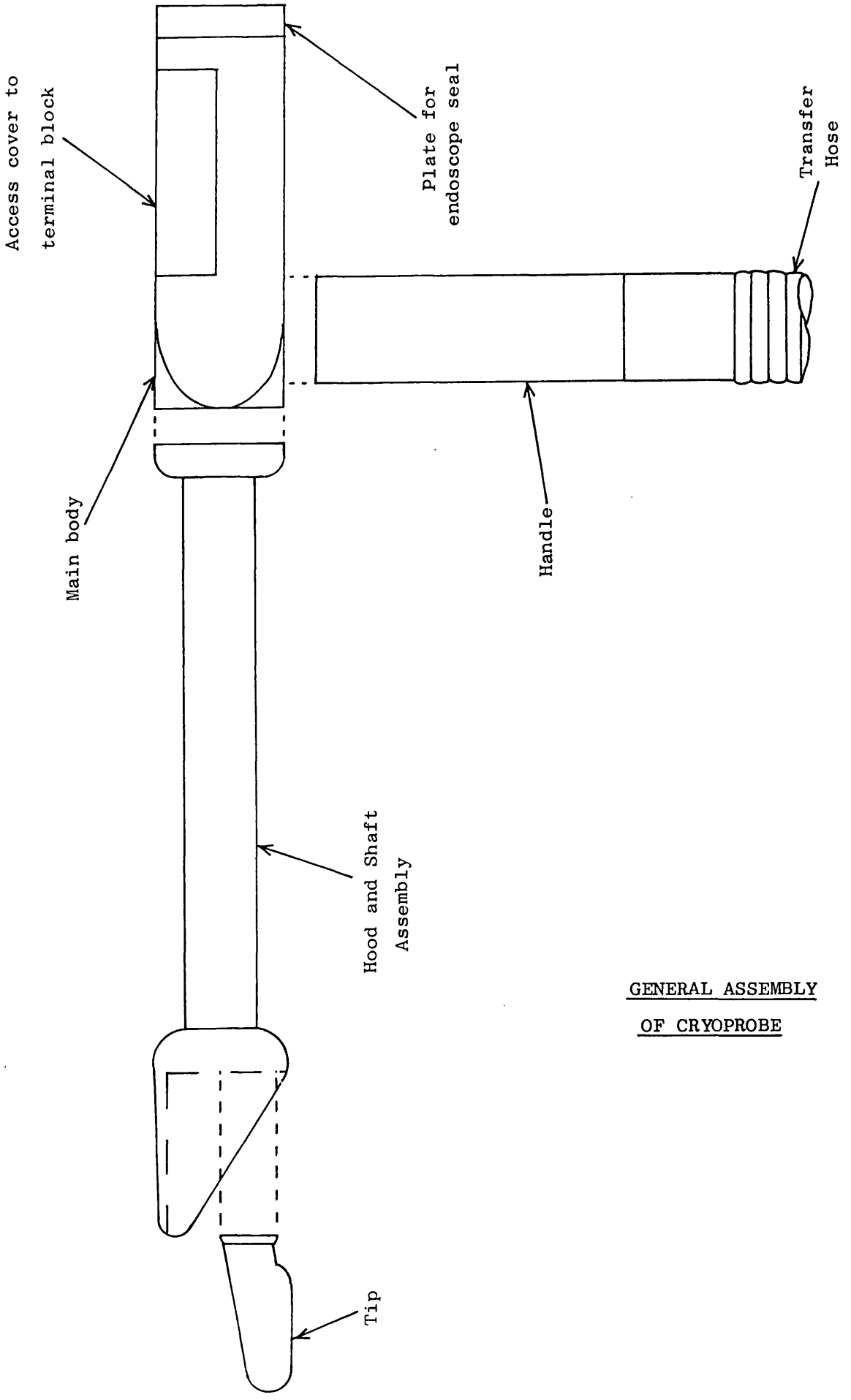

GENERAL ASSEMBLY OF CRYOPROBE

FIGURE 88

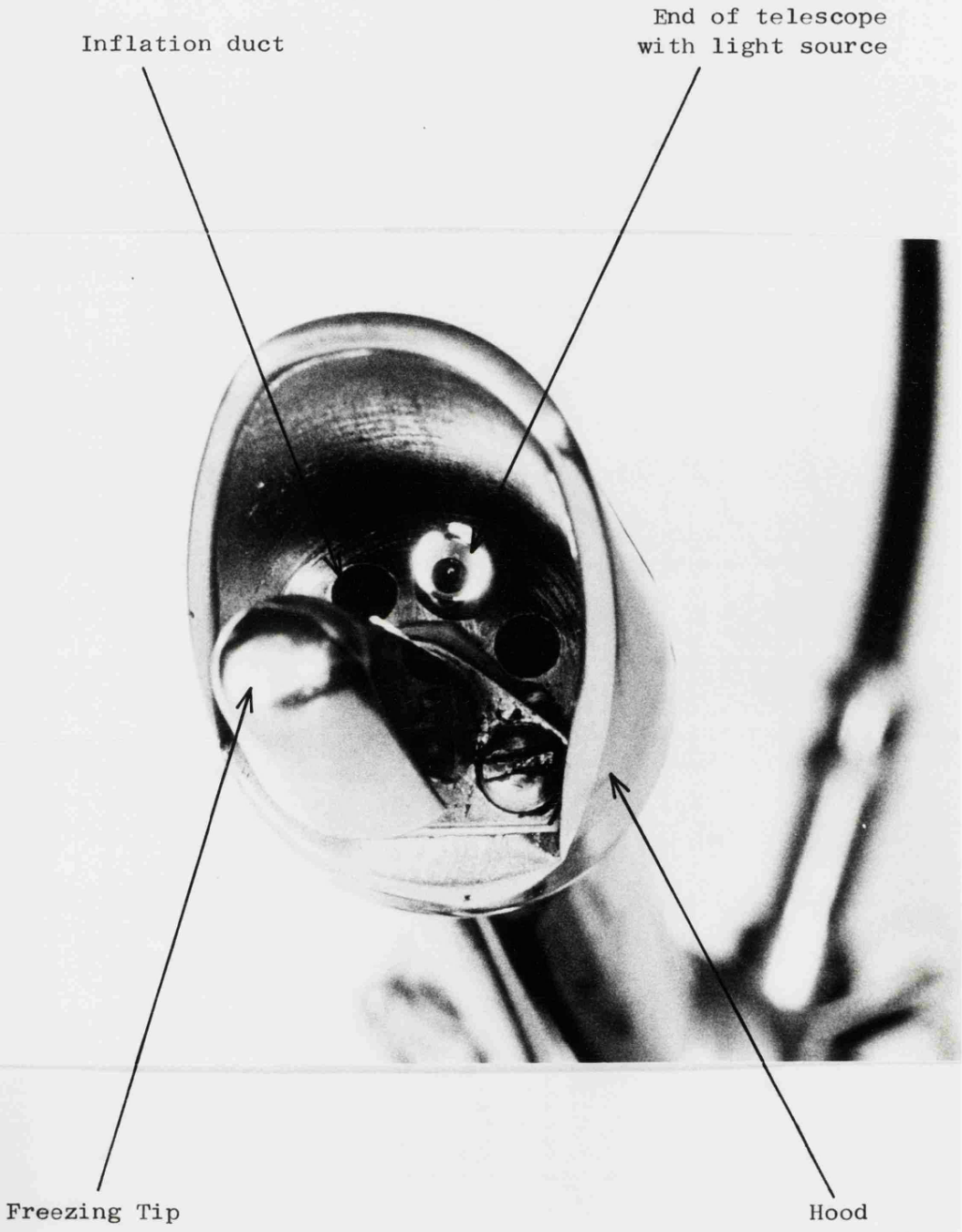

CLOSE UP OF OPERATING END OF CRYOPROBE

incorporates a tapered transition pipe to enable the liquid nitrogen to flow smoothly from the 5mm bore pipe of the transfer hose to the 2.8mm bore pipe in the cryoprobe.

Several wires for the heating coils and for temperature measurements have to be taken to the probe. A terminal block is incorporated in the probe body to provide a firm location for the wires and a test point. The terminal block consists of a PTFE machining pressed into the body with terminal pins incorporated in it. The probe wiring is shown in **Figure 89.**

13.2.2 Rectal inflation system within the cryoprobe

The rectum is inflated with dry nitrogen gas and this is done automatically in the final probe design. The rectal inflating gas serves a dual function.

(1) The gas expands the rectal cavity.

(2) The gas prevents "misting" of the telescope.

Gas within the rectum is saturated with water vapour and the water will condense onto objects placed in the cavity if they are cooler than the dew point. If this condensation occurred on the telescope it would cause severe viewing problems. Consequently the rectal inflating gas is passed into the cavity in such a way that it bathes the tip of the telescope in dry nitrogen. A slow continuous passage of gas through the cavity is encouraged by providing a gas bleed pipe in the probe. The inflation ducts can be seen in **Figure 88.**

FIGURE 89

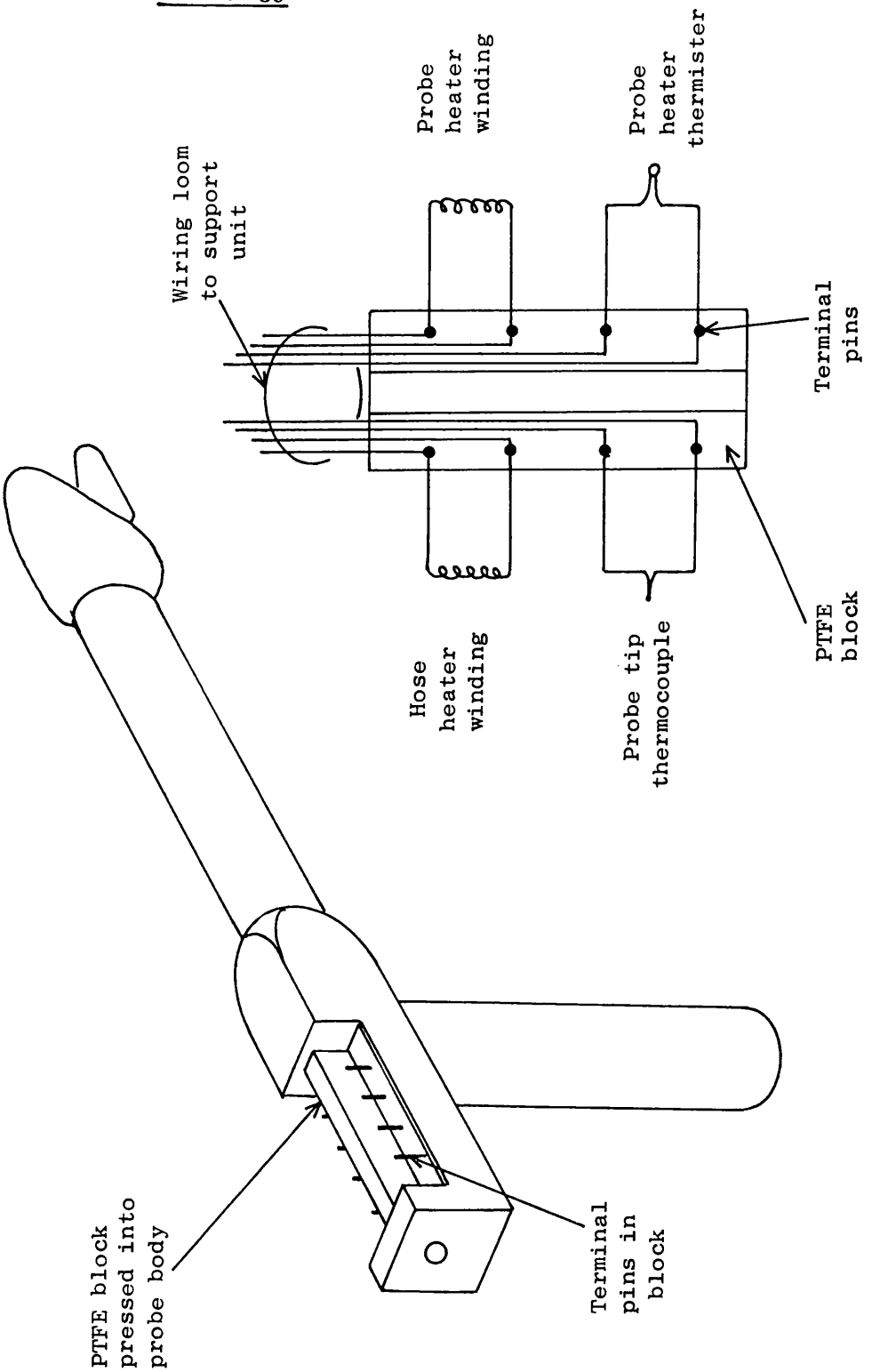

ELECTRICAL WIRING INSIDE PROBE

13.2.3 Materials used in the cryoprobe

There are two major concerns in choosing materials for the cryoprobe.

(1) The probe must be sterilizable.

(2) The probe must be biologically inert.

The usual technique for sterilizing surgical instruments is to subject the instrument to boiling water at 135°C in an autoclave. In order to satisfy the two constraints on materials, all metal parts in contact with tissues were made from 616 stainless steel, and all plastic parts from PTFE.

13.3 Complete Transfer Hose Design

13.3.1 The structure of the transfer hose

Having described the integrated cryoprobe design, the design of the final transfer hose will be examined. The basis of the design is the Leidenfrost transfer hose discussed in **Chapter 9**, but a third hose is added around the outside. The third hose has two functions:-

(1) It provides a path for gas to be passed to the probe for rectal inflation.

(2) It provides a sheath for the wiring loom.

Autoclavable material had again to be used. **Figure 90** is a diagram of the construction used in the final hose.

13.3.2 Problems caused by third hose

The original transfer hose had been tested without the outer third pipe. A 100 watt supply heater quite adequately maintained Leidenfrost flow indefinitely.

FIGURE 90

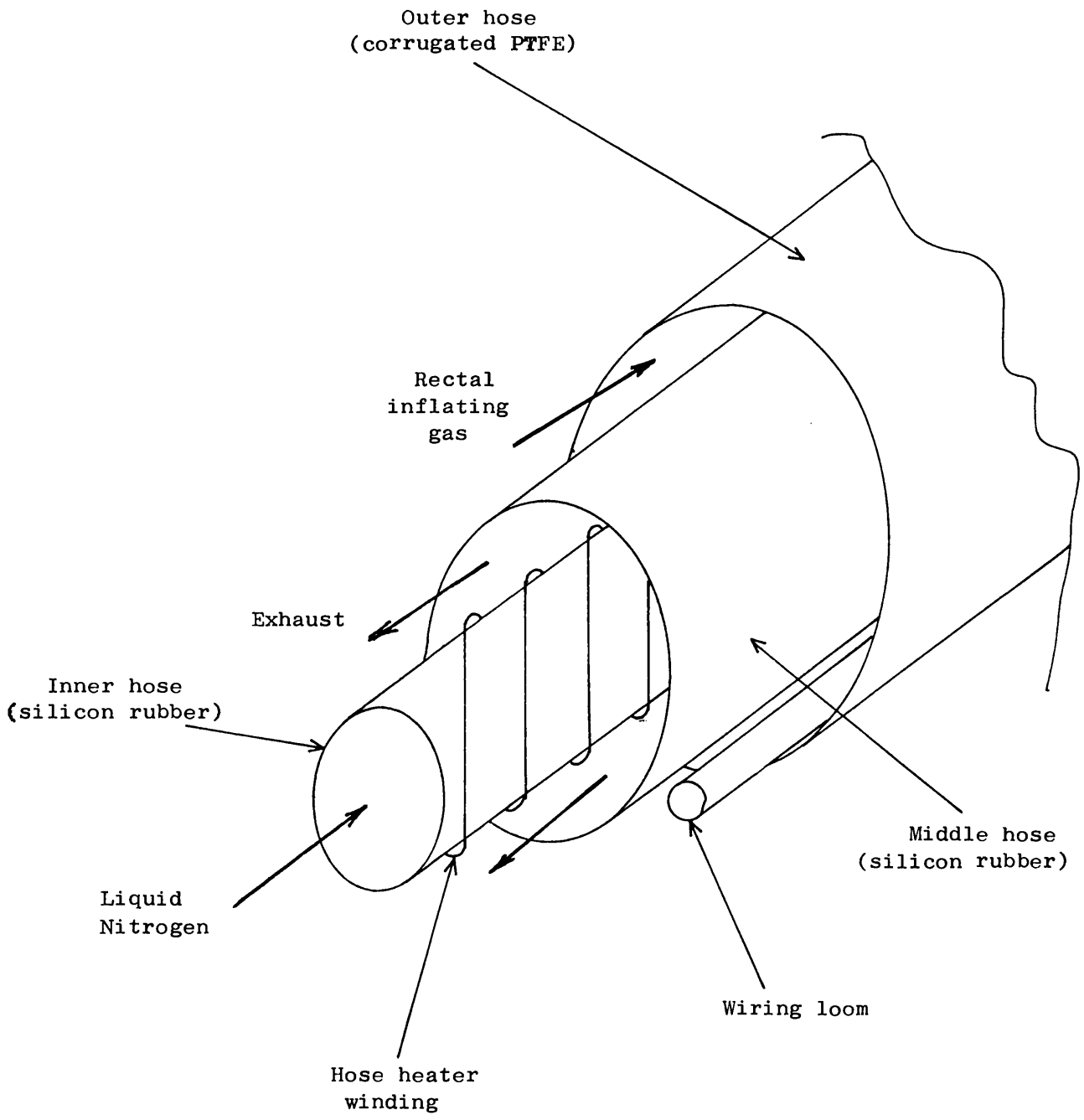

FINAL TRANSFER HOSE CONSTRUCTION

However when this hose was modified to include the third pipe problems arose. It was found that Leidenfrost flow could only be maintained for about one minute. The heater was unable to keep the feed pipe warm enough for film boiling to be maintained for longer than this time.

A test was carried out in which the original two-element hose was wrapped in thermal insulation. Again Leidenfrost flow could only be maintained for about one minute. It appeared that two-element hose on its own received substantial amounts of heat from the environment which supplemented that dissipated by the heating coil.

Many different hose designs were explored to try and enable the hose to work with a 100 watt heater. It was known that the exhaust nitrogen coming from the cryoprobe was much warmer than the critical temperature for film boiling, and was usually in the range -50°C to 0°C. A number of hoses were constructed to try and take advantage of this warm gas by increasing the thermal conductivity of the inner pipe or by reducing its thickness. Several flexible metal pipes were tested but none proved to be effective. Eventually a more powerful hose heater had to be used, and the space and weight penalties incurred from using a higher power transformer, had to be tolerated. A 200 watt heater was installed and this proved to be satisfactory.

13.3.3 Transfer hose connection to the supply unit

In order for the cryoprobe and transfer hose to be autoclaved they had to be deetachable from the supply unit. A connector had to be provided to enable this separation. As the hose contained three concentric tubes together with the wiring loom, the connector is inevitably rather complicated. The wiring loom was taken out from the main hose connector to a separate electrical connector. **Figure 91** is an assembly drawing of the connector design.

13.4 Specification of the Support Unit

The third major constituent of the complete system, and one that has not been discussed before, is the support unit. A specification for the support unit was drawn up following discussions with clinicians and from observations of cryosurgery in the operating theatre. The unit had to meet the following requirements and constraints:

(1) It must be easily moveable and such that it can be taken into the operating theatre.

(2) It should be free standing and stable.

(3) It should be reasonably pleasing to look at.

(4) It must be simple to operate by clinicians.

(5) There should be little delay in getting the unit ready for operation.

(6) It should store enough liquid nitrogen for a whole day's surgery assuming it is in use with

FIGURE 9I

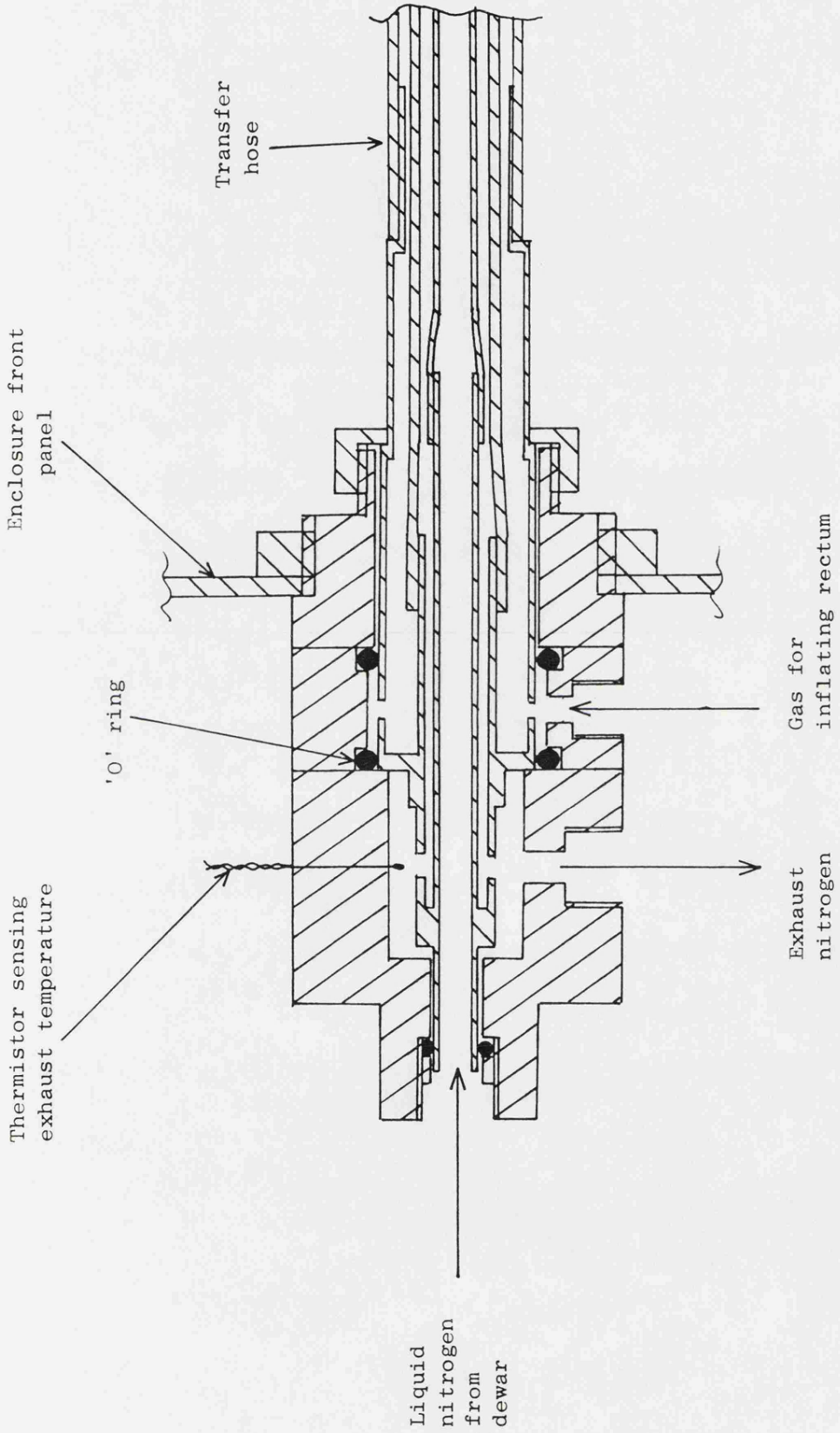

SECTION THROUGH TRANSFER HOSE CONNECTOR

every patient.

(7) It need not store liquid nitrogen between operating days.

(8) The storage dewar should be easily refillable without dismantling the unit.

(9) The liquid nitrogen should be supplied at pressure up to 15psi.

(10) Exhaust nitrogen from the probe should be safely exhausted at the unit.

(11) The unit should enable defrost of the cryoprobe to be effected.

(12) The unit should provide a means for automatically inflating the rectum.

(13) The unit should house a light source suitable for the Thackray endoscope.

(14) The unit should house all the control electronics.

(15) An indication of tip temperature should be provided.

(16) Auxillary outputs should be provided to enable the control temperatures to be monitored.

(17) The unit should be safe both mechanically and electrically, and should satisfy the requirements of BS5724.

The specification indicates a number of sub-systems and major design features needed in the support unit. These are systematically discussed in the remaining sections of this chapter.

13.5 Overall Design of the Unit Structure

It was estimaated that the various sub-systems of the support unit could be housed in an enclosure that was 6" high by 18" wide by 18" deep. To enable the controls to be at a convenient height for operating, the unit was mounted on its own frame so that it was 30" clear of the ground. (The surgeon is usually seated when carrying out operations in the anal region).

A liquid nitrogen storage vessel needed to be combined with the enclosure. From the specification it was decided that a 10 litre dewar would provide adequate liquid nitrogen without being too big and bulky. A Statebourne pressuriseable 10 litre dewar was bought.

The combination of enclosure, support legs and dewar was finally arranged as in **Figure 92.** It was felt that this design combined the functional and aesthetic needs of the unit. The frame was welded from 1" diameter stainless steel tube and was provided with castors with electrically conducting tyres to meet the requirements of operating theatre equipment. The dewar was supported in this frame. The enclosure was made from PVC faced aluminium and was arranged so that removal of the top panel allowed good access to the components inside.

13.6 The Liquid Nitrogen Supply System

13.6.1 Technique used to pump nitrogen

There are two main possibilities for pumping liquid

FIGURE 92

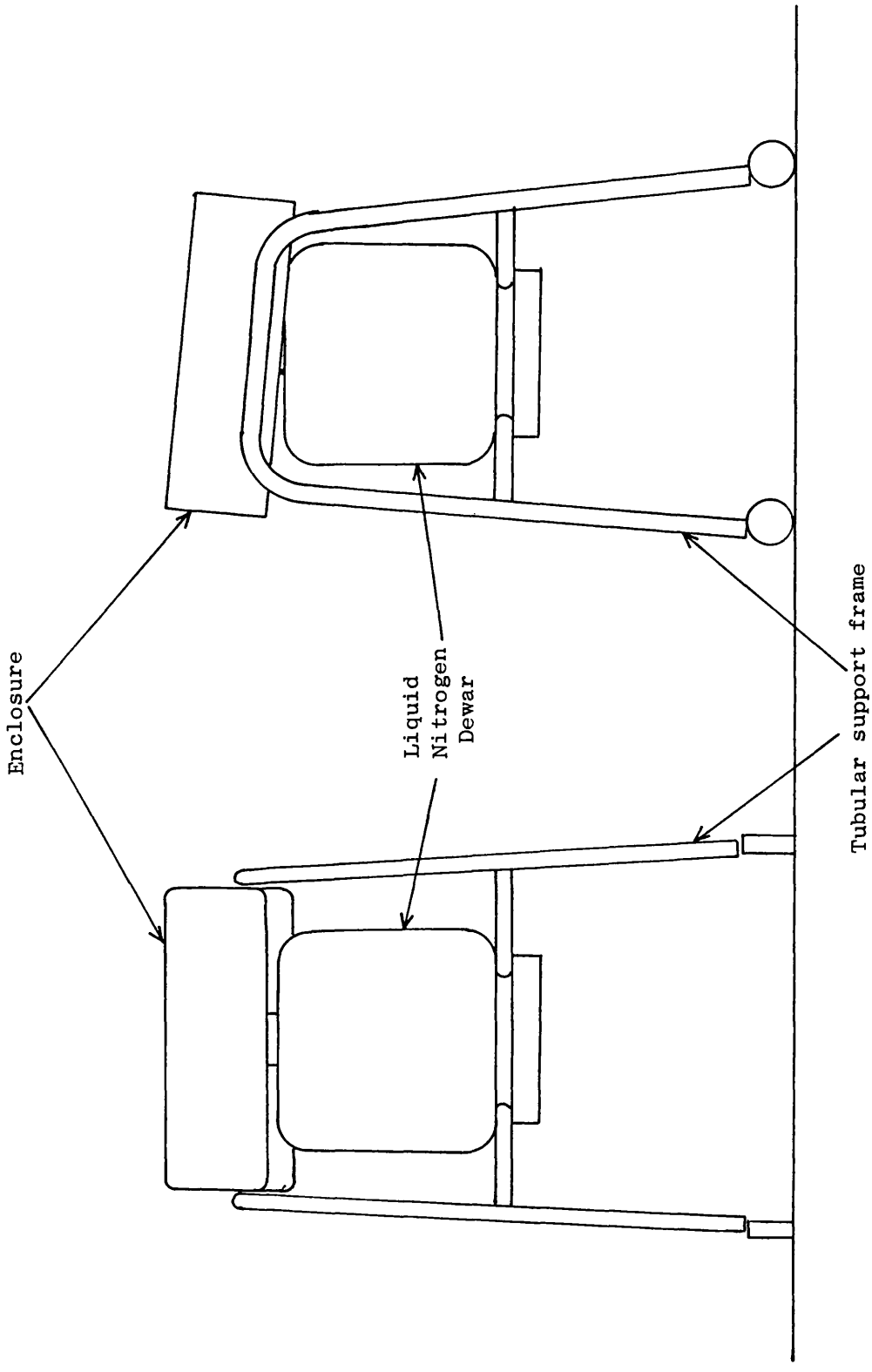

OVERALL CONFIGURATION OF SUPPORT SYSTEM

nitrogen from the storage dewar.

(1) Small electrical pumps.

(2) Boiling some liquid to vapour and using the pressure generated to force liquid out.

Unfortunately at the time the design was conceived, there were no suitable small electric pumps available for use with cryogenic liquids and so a pressurised dewar was needed. There are several ways to pressurise a dewar:

(1) Allow heat transferred from the environment to evaporate the cryogen and so pressurise the dewar.

(2) Use an additional external source of heat conduction path from the environment (Copper rod), to evaporate the liquid.

(3) Bleed off some liquid, allow it to evapourate outside the insulated dewar, and then pass the vapour back to pressurise the tank.

The last mentioned technique is very simple, and easy to control, but the smallest dewar available with a facility for bleeding off liquid at the base of the tank was 25 litres. Heat transferred from the environment pressurised the dewar too slowly and so an electrical heater was used. A 200 watt heating element was installed, controlled by a pressure switch sensing the vapour phase pressure in the dewar. **Figure 93** is a diagram of the pressurising system.

In order to provide a degree of safety a double pressure switch was used, with one switch set to operate

FIGURE 93

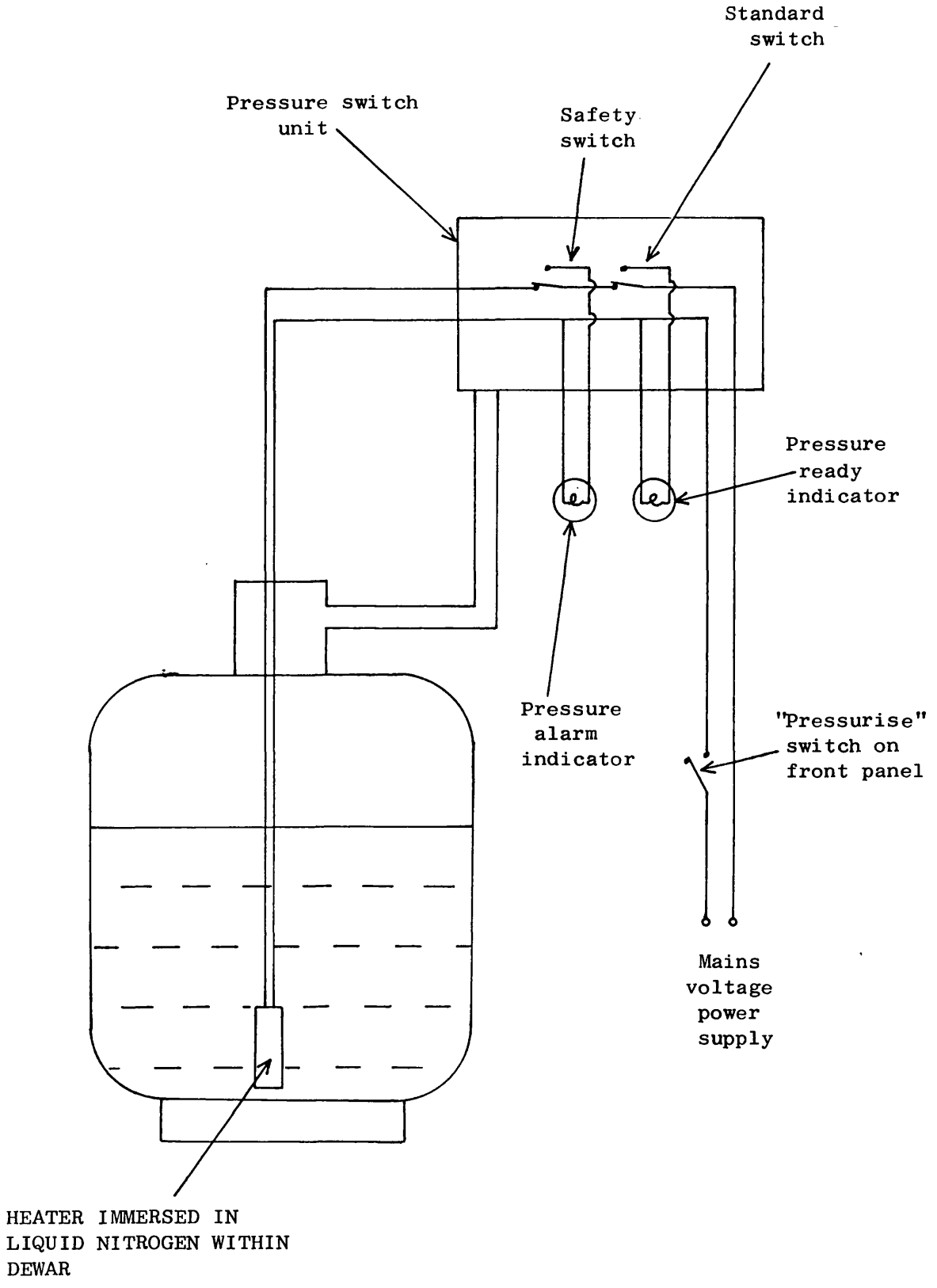

PRESSURISING SYSTEM

at a pressure slightly above the other. In this way if, for some reason, the first switch failed to operate, the second switch would make sure the heater was turned off. The two switches also operated indicators on the front panel. The first switch illuminated a green "pressure ready" light and the second a red "pressure alarm".

The dewar was fitted with a Statebourne manifold. This provided several vapour phase ports and was modified to enable two liquid phase pipes to be installed. One of these was used to fill the dewar. It consisted of a 12mm bore pipe and this diameter pipe was also used to connect the port to a "fill" valve on the back panel of the enclosure. The large diameter pipe enabled the dewar to be filled quickly. The "fill" valve is simply connected to a source of nitrogen without any dismantling of the unit being necessary.

The system described worked quite well but some development was necessary to enable it to completely meet the specification. This development is described in the next two sections.

13.6.2 Improving the heat transfer from the heater

The heating element suffered from the same problem as that initially occurring in the freezing tip when it is turned on. It ran at a higher temperature than the critical heat flux temperature. Therefore when the heater was turned on, the pressure initially rose rapidly but after 2-3 seconds the rate of the rise of

pressure slowed dramatically and the heating element became extremely hot (see **Figure 94**). When the heater was initially turned on it was cooler than the critical heat flux temperature and nucleate boiling ensued. A lot of vapour was generated and the pressure quickly rose. However the heater temperature continued to rise and once film boiling had started, the boiling rate was much reduced because of the insulating film of vapour around the heater.

The solution adopted was to increase the surface area of the heater rather than reduce its power. A finned housing was made for the heating element and this proved to solve the problem. **Figure 94** also shows the pressure time course achieved with the finned heater.

13.6.3 Problem of pressure switch control margin.

The driving pressure needed to provide the cryoprobe with the correct flow rate of cryogen was only 3.0 psi. If this pressure rose to 3.2 psi the flow rate was too excessive and Leidenfrost flow in the transfer hose could be lost. Unfortunately the pressure switches had a control margin at 3.0 psi of nearly 1.5 psi. In other words, if the switch was set to turn on when the pressure dropped to 2.9 psi, it wouldn't turn off again until the pressure had risen to nearly 4.4 psi.

The problem posed by the very large control margin was overcome by using a miniature solenoid valve. The pressure switch was connected to the vapour phase in

FIGURE 94

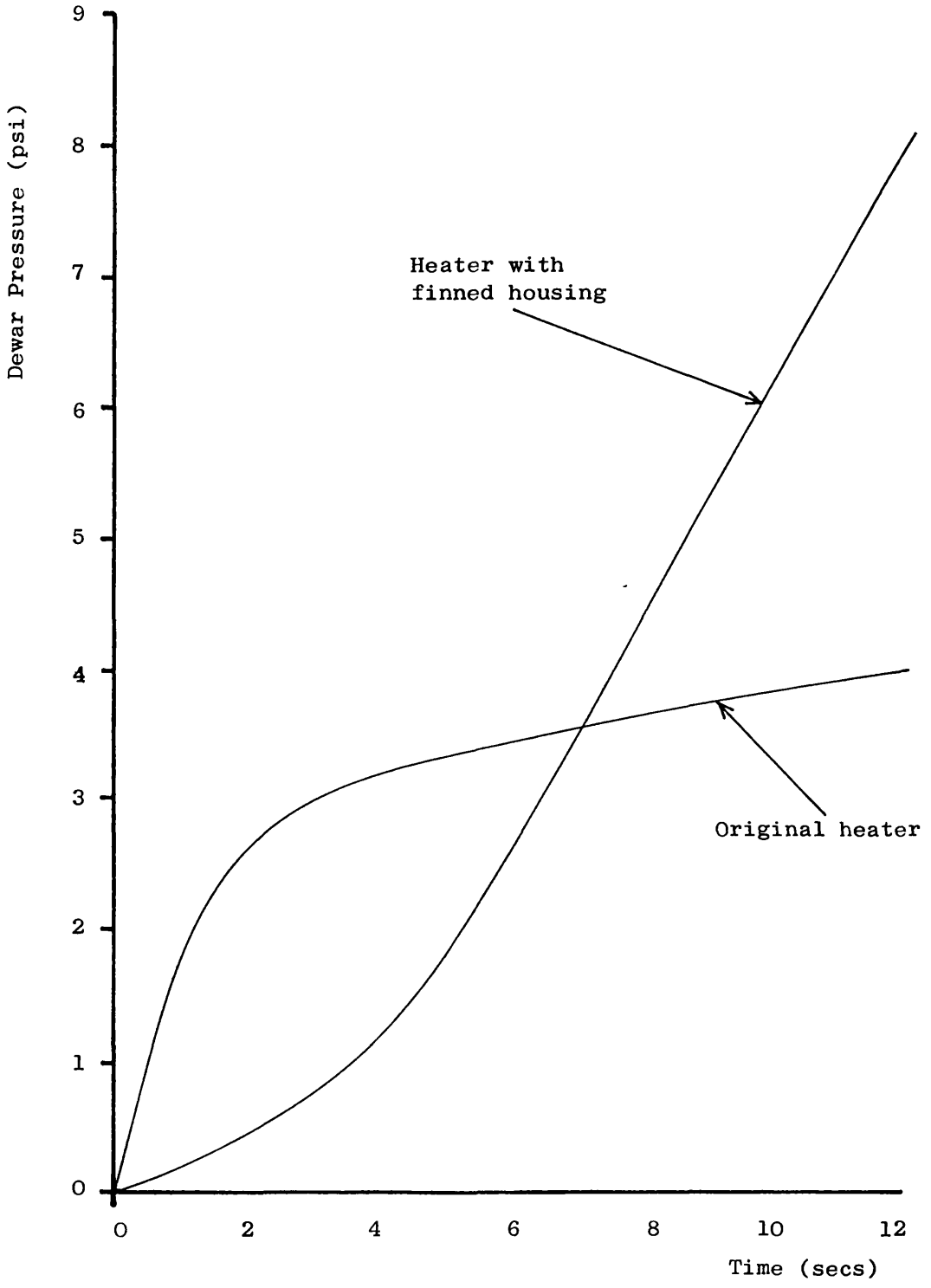

TIME COURSE OF DEWAR PRESSURE CHANGES

the dewar via the solenoid as shown in **Figure 95.** The valve was a normally-closed one and was supplied by the same electrical supply as the heater. When the heater was on and the pressure was rising, the valve would also be energised and the pressure switch sensed the dewar vapour pressure. When a pressure of 3.0 psi is achieved the heater electrical supply is turned off and the valve therefore closes. The pressure switch now senses the pressure of the vapour in the pipe downstream of the valve. This pipe is provided with a small gas bleed (a section of fine bore pipe) and so the pressure of the vapour within it dropped quite rapidly. The bleed was adjusted so that the pressure sensed by the pressure switch dropped to 1.5 psi (when the switch turns on again) in about 5 seconds. In this time the main dewar pressure would only drop to 2.9 psi. The time course of the pressure changes is shown in **Figure 96.**

13.7 Liquid Nitrogen Delivery System

13.7.1 Delivery system design

Figure 97 shows a diagram of the final liquid nitrogen delivery system. Leidenfrost flow is to be maintained throughout the delivery system from the dewar to the transfer hose connector. Three conditions have to be met to ensure this:-

(1) Metallic tubing must be used so that sufficient heat will be conducted through the tube wall to keep it above the critical temperature.

(2) All the bends in the pipe must have as large a

FIGURE 95

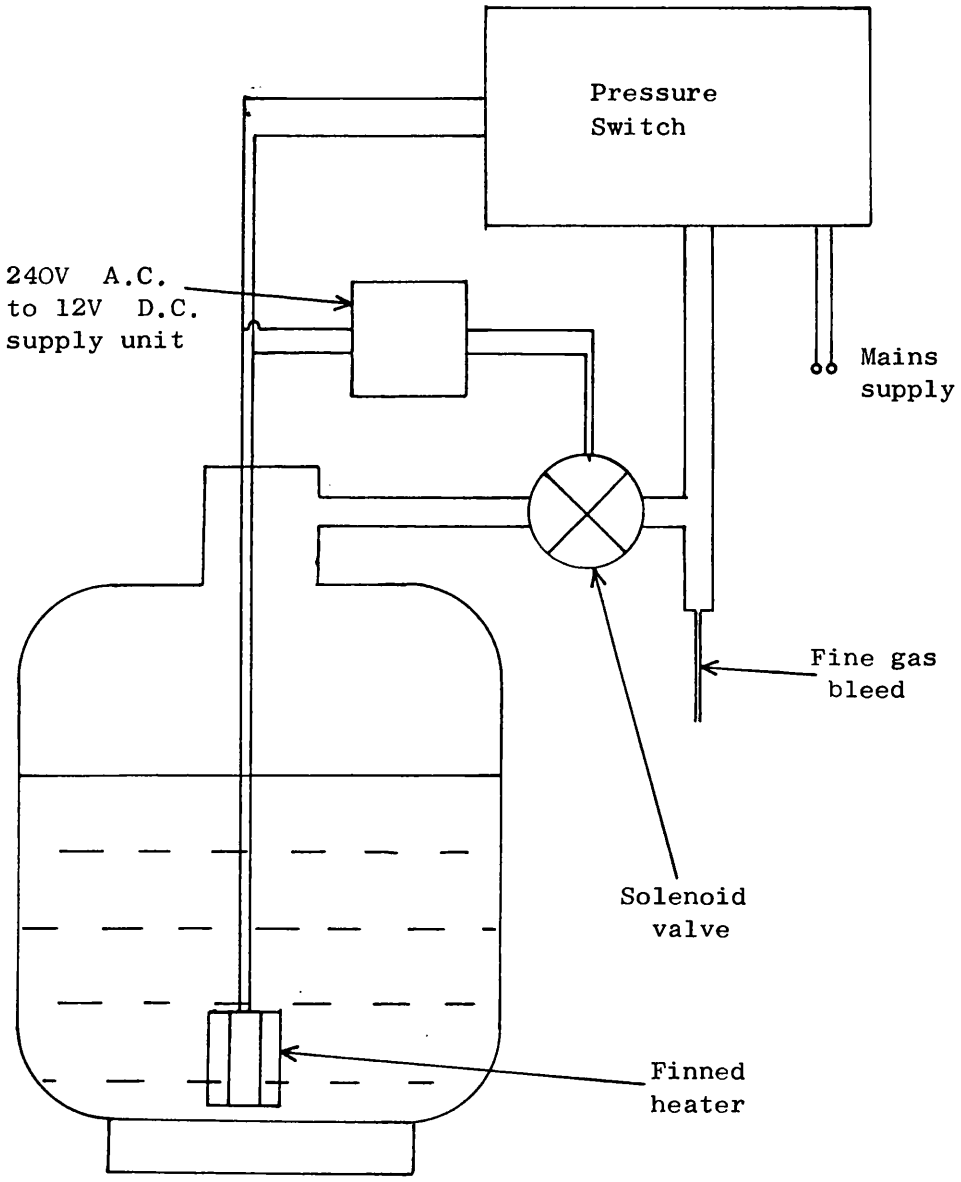

USE OF SOLENOID VALVE IN PRESSURISING SYSTEM

FIGURE 96

TIME COURSE OF PRESSURE CHANGES IN PRESSURISING SYSTEM

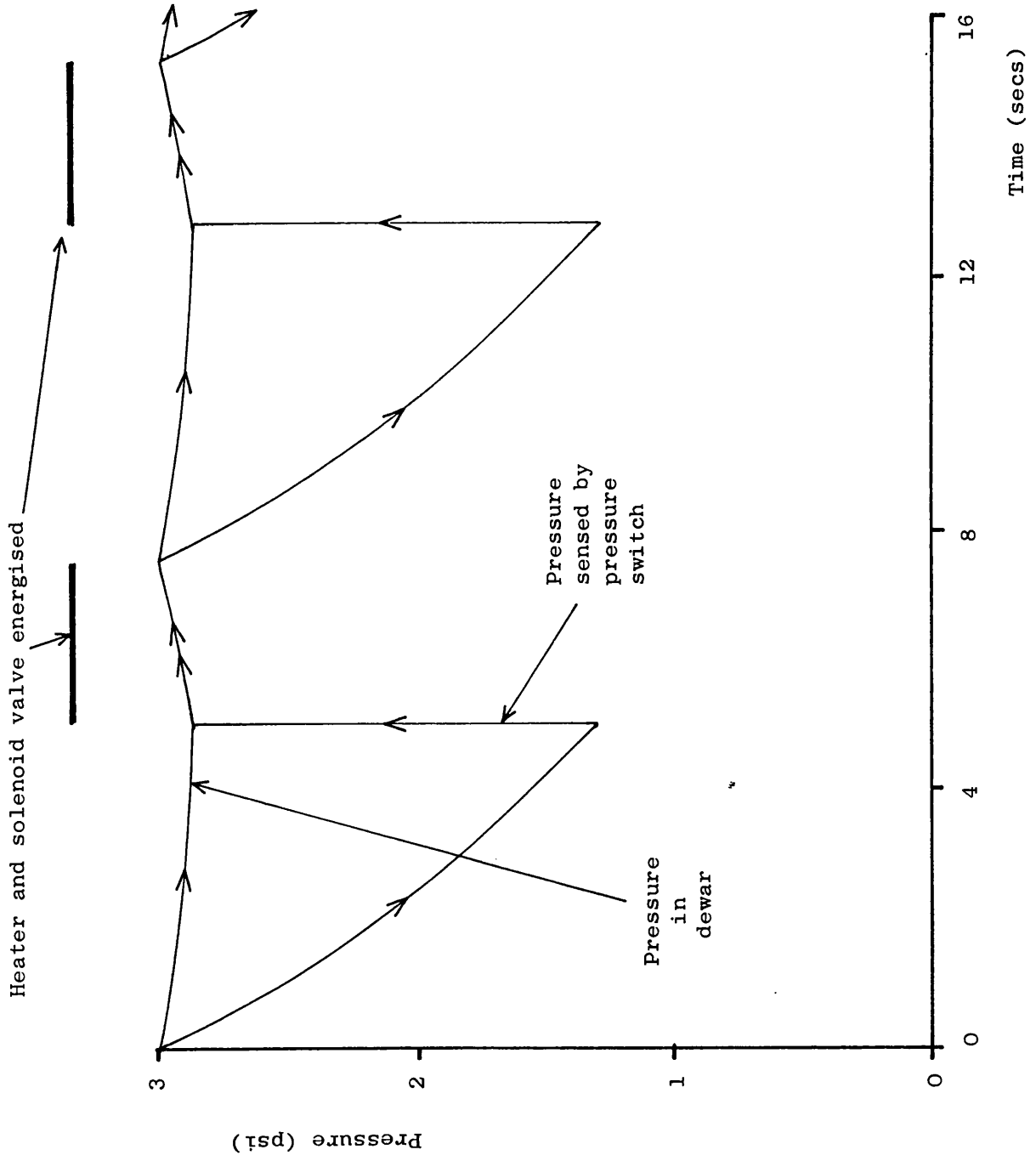

FIGURE 97

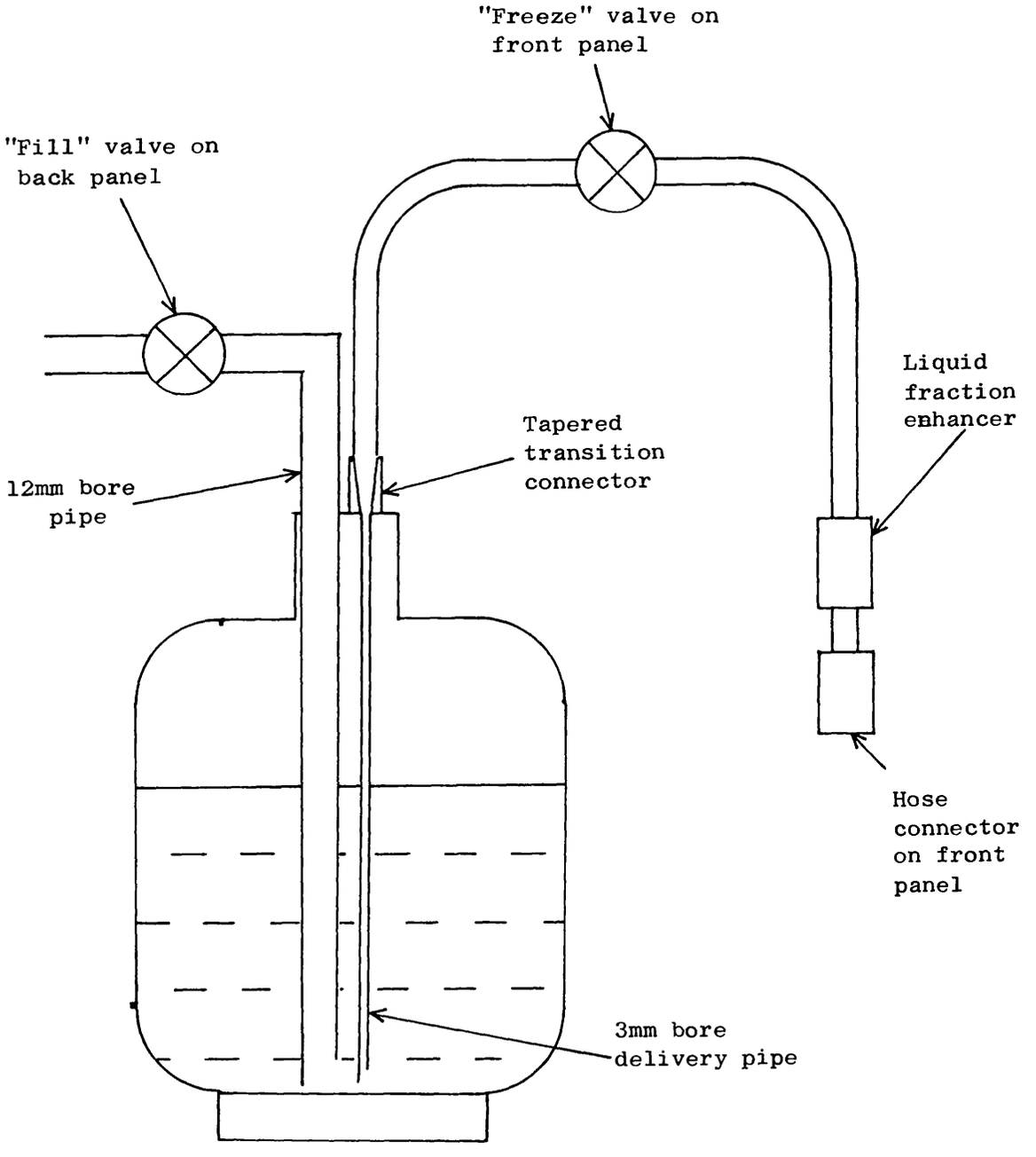

LIQUID NITROGEN DELIVERY SYSTEM

radius as possible.

(3) There must be no abrupt changes in pipe bore.

An on/off valve has to be incorporated in the delivery pipe and to maintain a constant pipe bore a ball valve was used which had a 5mm bore throughout when it was open. In the discussion in **Chapter 9** on Leidenfrost flow it was concluded that the vertical pipe used to pass liquid from the storage dewar should have a bore of 2.5mm. Such a pipe was incorporated in the design being discussed and to smooth the transition from a 2.5mm bore pipe to a 5mm one, a tapered transition pipe was incorporated in the output connection in the dewar manifold.

Despite the measures described, it was found that too much liquid was evaporating during its transfer within the enclosure. Two measures were taken to reduce this evaporation and these are now described.

13.7.2 Remote actuation of on/off valve

With the on/off valve mounted on the front panel, it was impossible to use large radius bends in the pipes connected to it. The valve was therefore moved to a position within the enclosure that enabled such bends to be used and it was connected to a remote actuator on the front panel via a flexible link.

13.7.3 Liquid fraction enhancing device

A liquid fraction enhancing device had been designed and built for earlier tests on Leidenfrost

flow and this was incorporated. **Figure 98** shows a diagram of this component. In film boiling flow, vapour tends to occur around the periphery of the pipe. This vapour is allowed to escape by using the device illustrated so that the fluid leaving has a higher liquid fraction than the incoming fluid. The device used enables the size of the vapour bleed to be adjusted so that an optimum setting could be found. In **Chapter 9** a technique was described that enabled comparative changes in liquid fraction to be estimated by measuring temperature changes at a sudden change in pipe diameter. This technique was used to find the optimum setting for the liquid fraction enhancing device. **Figure 99** shows some results obtained in finding the optimum.

13.8 The Defrost System

Figure 100 shows a diagram of the defrost system. When the surgeon has completed a freeze he will wish to remove the cryoprobe immediately. Unfortunately the ice will adhere to the probe tip and prevent the removal until the ice-ball has thawed. A means of quickly defrosting the tip is needed.

The initial defrost system considered used an electrical heater in the tip. However the eventual solution was much simpler and needed no additions to the cryoprobe. Nitrogen from the vapour phase in the dewar is passed to a coil of pipe within the enclosure to warm the vapour to around 0°C. The warmed gas is then passed via a defrost control valve on the front panel to

FIGURE 98

LIQUID FRACTION ENHANCEMENT DEVICE

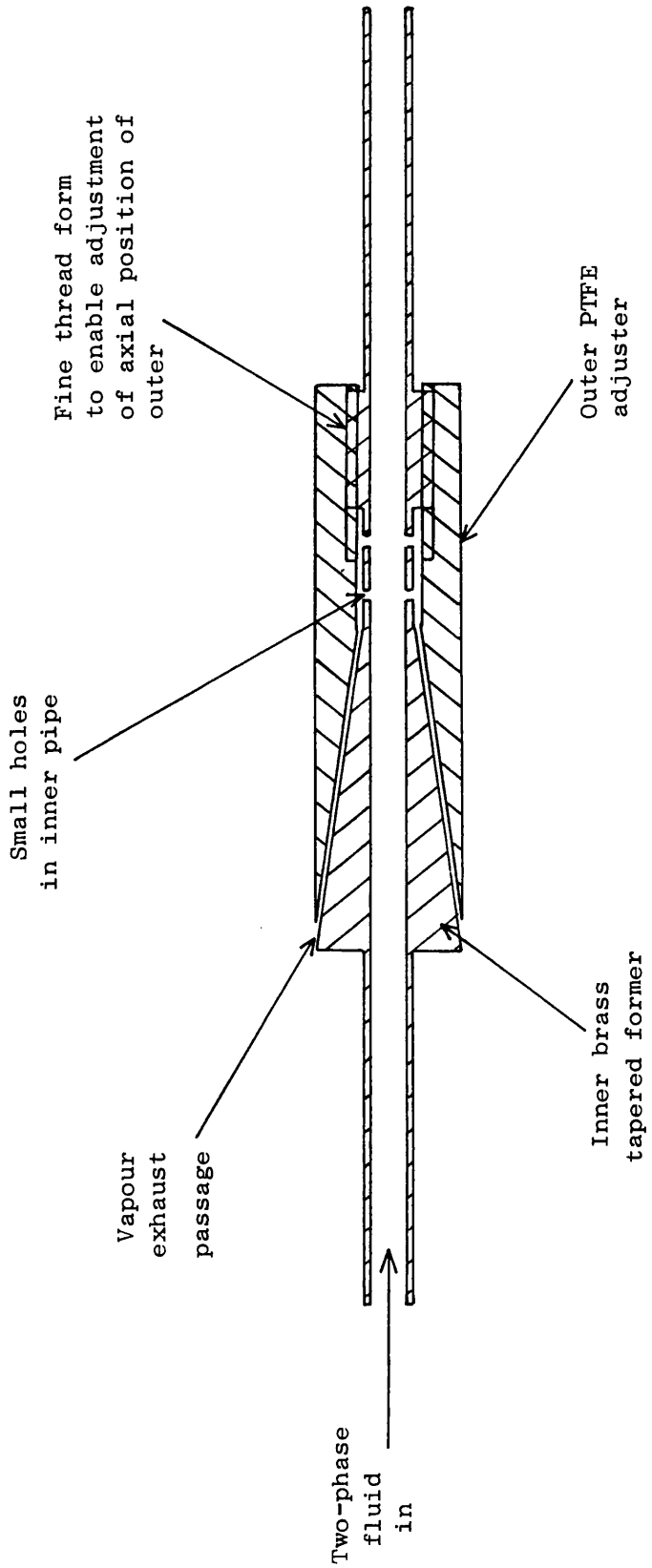

FIGURE 99

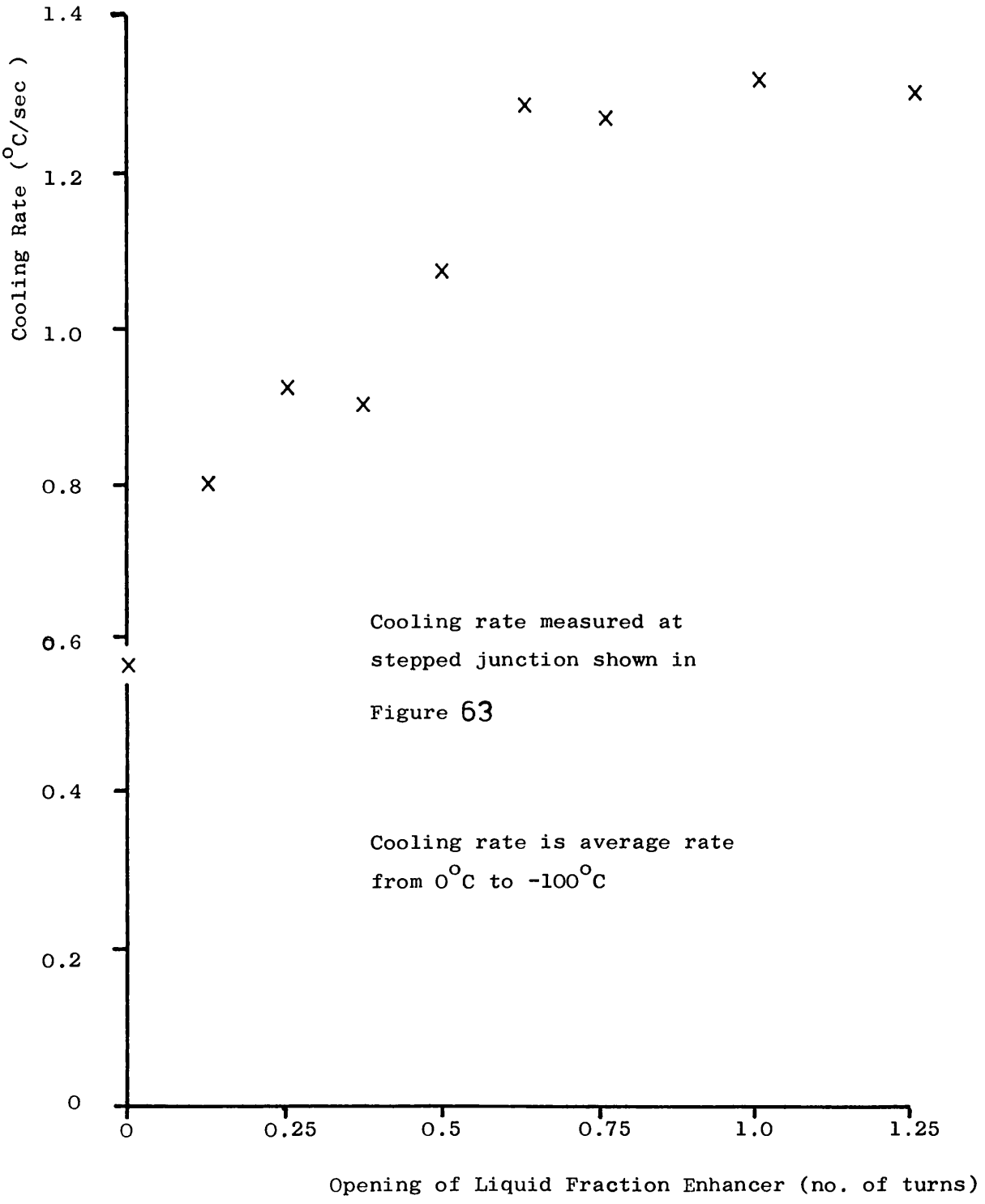

THE EFFECT OF THE LIQUID FRACTION ENHANCER

FIGURE IOO

DEFROST AND RECTAL INFLATION SYSTEMS

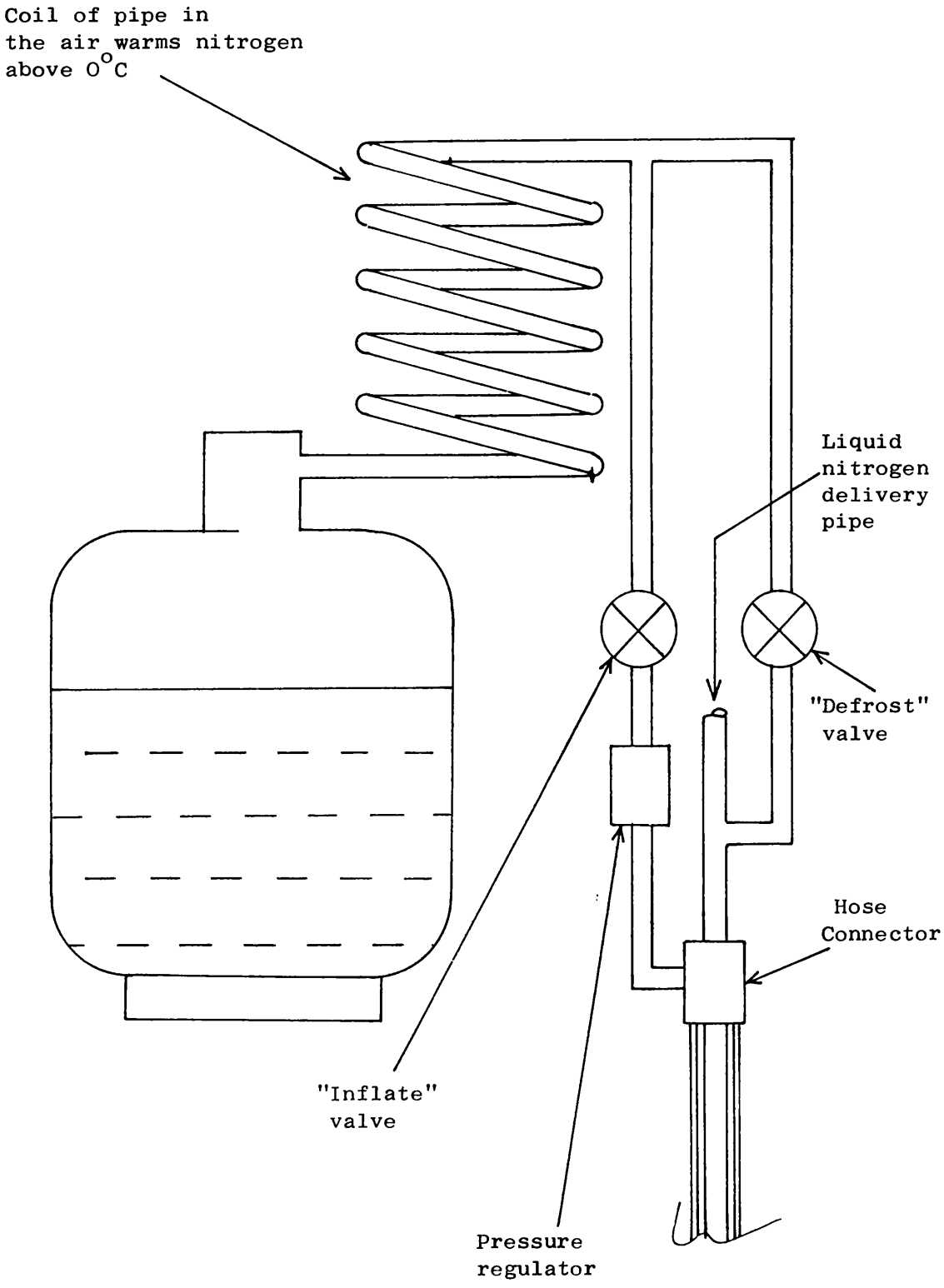

the main liquid nitrogen delivery pipe. When the defrost valve is opened, warmed gas is passed through to the cryoprobe. As will be described later in a brief outline of the electronics, when the defrost valve is actuated it also increases the controlled temperature of the transfer hose to +15°C. The nitrogen that arrives at the cryoprobe tip is therefore able to transfer heat to the tip wall to effect a defrost.

13.9 The Rectal Inflation System

13.9.1 Basic design of inflation system

During the viewer tests the rectum had been inflated by means of a hand bulb. It was felt that during cryosurgery, the operation would be easier if the inflation could be carried out automatically.

Figure 100 also shows a diagram of the automatic inflation system. It used vapour that had been warmed by passing it through a coil of pipe within the enclosure. The warmed vapour is passed to an inflate valve on the front panel and then to a sensitive pressure regulator. From the regulator the gas is taken to the transfer hose connector where it passes to the annular gap between the second and third pipes of the transfer hose. The pressure regulator is needed to reduce the dewar pressure to the low levels needed for rectal inflation.

13.9.2 Measurement of intra-rectal pressure

In order to know what pressures were needed for

rectal inflation, measurements were taken in the operating theatre during the examination of a patient. A sensitive pressure transducer was connected to the hand bulb of a sigmoidoscope (a rectal viewing instrument). The electrical output from the transducer was recorded on a chart recorder. While the surgeon was inflating the rectum and examining the patient, measurements of the intra-rectal pressure were recorded.

Figure 101 shows the recordings obtained. The pressure peaks occurred when the surgeon squeezed the hand bulb and represent the transient changaes occuring in the hand bulb as the inflation takes place. The much lower resting pressure was that needed to inflate the rectum for an acceptable view. As would be expected from the elasticity of the rectum, quite low pressures are needed to inflate it.

13.10 The Viewer Light Source

A light source for the Thackray endoscope was incorporated in the support unit. Components from a single output of a Thackray System 80 light source were installed on the front panel. A variable intensity control was provided. The bulb becomes very warm in use and a cooling fan was installed to blow air over the bulb when it was turned on. The warm air circulated within the enclosure had the added side effect of keeping the contents of the enclosure warm and preventing large quantities of ice forming when the

FIGURE IOI

TRACING OF PRESSURES RECORDED IN RECTUM DURING SIGMOIDOSCOPY

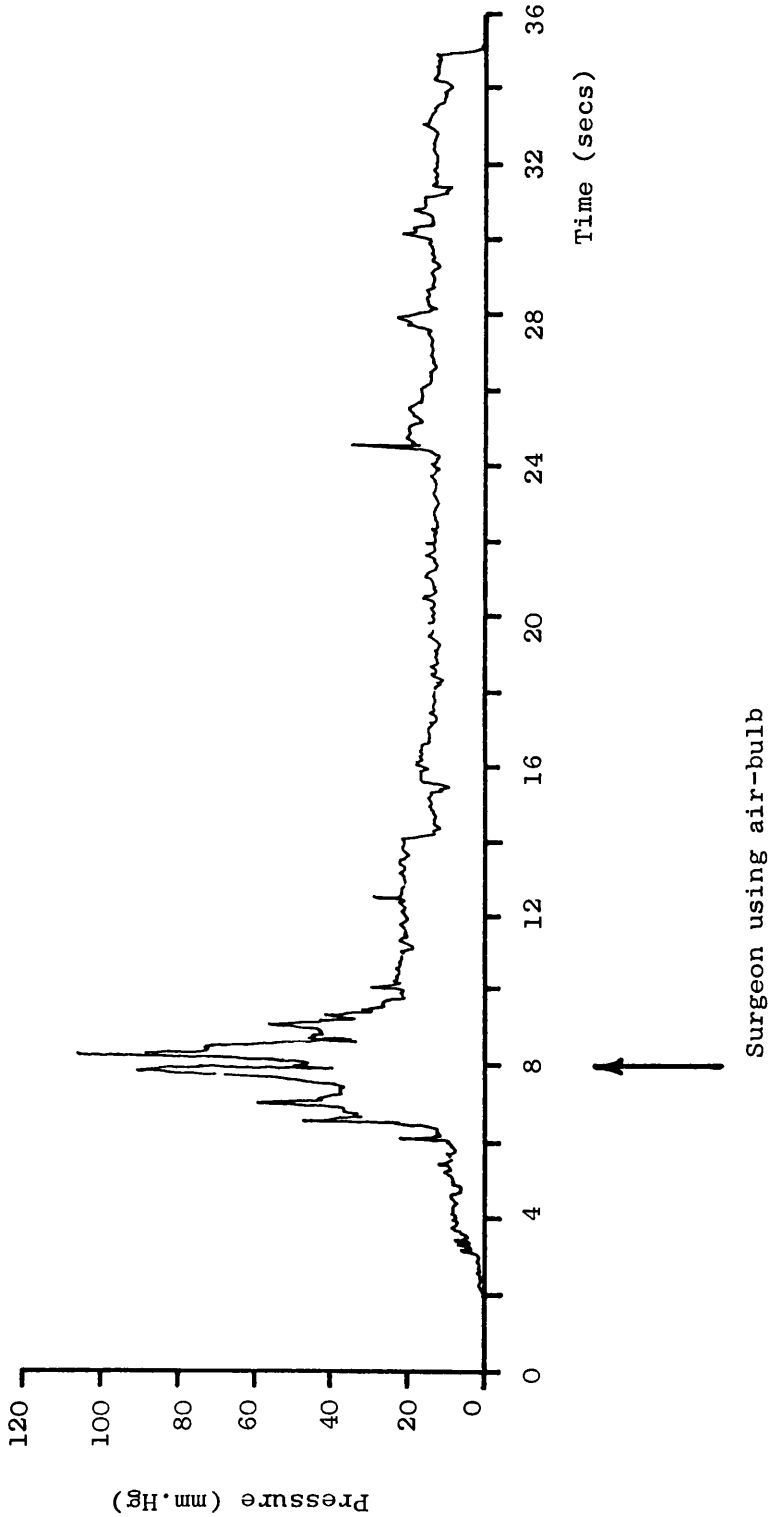

cryogen was flowing. A standard Thackray flexible light guide was used to pipe the light from the support unit to the endoscope in the cryoprobe.

13.11 Temperature Controllers

The temperature controllers were designed and constructed by electronics staff at BIME. They are proportional controllers with a 50 volt, 50 Hz output. The waveform is chopped to provide control of power. There are two controllers, one supplying the probe heater with a maximum of 100 watts, and the other supplying the transfer hose heater with a maximum of 200 watts.

The heater controllers used thermistors to provide a temperature input. The probe shaft heater had its thermistor attached to the outside of the probe heater windings. The hose heater used a thermistor mounted in the transfer hose connector in the support unit. This thermistor sensed the exhaust nitrogen temperature.

When the defrost valve was actuated the transfer hose was operated at a higher temperature. This was arranged by having two adjustable temperature settings in the hose heater controller. The lower setting was used normally but when the defrost valve was actuated the higher setting was selected. This was effected by mounting a microswitch behind the defrost valve so that the switch was operated when the valve was turned on.

Two indicator lamps were mounted on the front panel to provide information about the heaters. Each lamp

flashed on and off in sequence with the chopped output waveform of each heater controller. As well as indicating when the heaters were operating, it was possible to gain an impression of how much heat each heater was supplying by the length of time each lamp was staying on. Both controllers also had a separate output on the back panel of the support unit. These outputs provided an analogue voltage proportional to the temperatures of the two controlling thermistors. These outputs enabled temperature recordings to be taken during the cryoprobes operation.

13.12 Tip Temperature Display

The surgeon felt it was important that he should have some indication of tip temperature during an operation. Consequently, a thermocouple was attached to the cryoprobe tip and this was coupled, via the wiring loom, to a temperature monitor in the support unit. An analogue meter on the front panel provided the surgeon with the information he needed and a separate analogue signal was taken to a connector on the back panel so that tip temperature could be recorded during the operation.

13.13 Safety Considerations in the Design

13.13.1 Electrical safety

All the electrical systems installed were checked for compliance with BS5724 before being accepted. The heaters posed a particular problem. If no fluid flowed

along the transfer pipes when the heaters were turned on, heat would not be transferred away from the heaters. The overheating that would result could cause a breakdown of insulation in the cryoprobe and melting in the hose. Therefore overiding switches were incorporated in both the freeze and defrost valves to safeguard against this danger. Microswitches were mounted behind both the two valves such that they were operated when the valves were turned on. The heaters would only be in operation when one or the other valves were turned on.

13.13.2 Mechanical safety

The major mechanical danger arose from the pressurised dewar. The dewar was guaranteed to withstand 40 psi but a failure could generate pressures well in excess of this. A safety valve was installed that communicated directly with the vapour phase in the dewar and a bursting disc was incorporated in the dewar.

In an emergency it would be necessary to quickly depressurise the dewar. A depressurising valve was therefore installed on the front panel. The valve was selected using manufacturers data so that it had a low resistance to flow and was arranged so that there was as little resistance as possible for the vapour escaping to the atmosphere.

13.14 Performance of Complete System

The rectal cryoprobe system has only just started

clinical trials and so clinical performance data cannot be presented here. However the complete system has been tested in the laboratory and some results of its perfomance are included in this section.

A crucial test of the system is the tip cooling rate and tip temperatures achieved. **Figure 102** plots tip temperature as a function of time. It can be seen that the tip cooling starts as soon as the nitrogen is turned on. Very low tip temperatures are quickly achieved.

The major test of system performance that can be carried out in the laboratory is the rate of growth of the ice-ball. This was measured using the apparatus shown in **Figure 15** for freezing a gelatin solution, as described in **Section 3.7. Figure 103** plots the ice-ball radius as a function of time and it can be seen that after a 5 minute freeze, an ice-ball 17mm in radius was achieved. This result is well within the clinical performance specification.

13.15 Conclusions

This chapter has described the combination of the various constituents of the cryoprobe system. It is felt that the system it describes fulfills the functional and operational requirements of the total instrument and provides the surgeon with a device that is sufficiently developed for it to be clinically evaluated in safety.

FIGURE 102

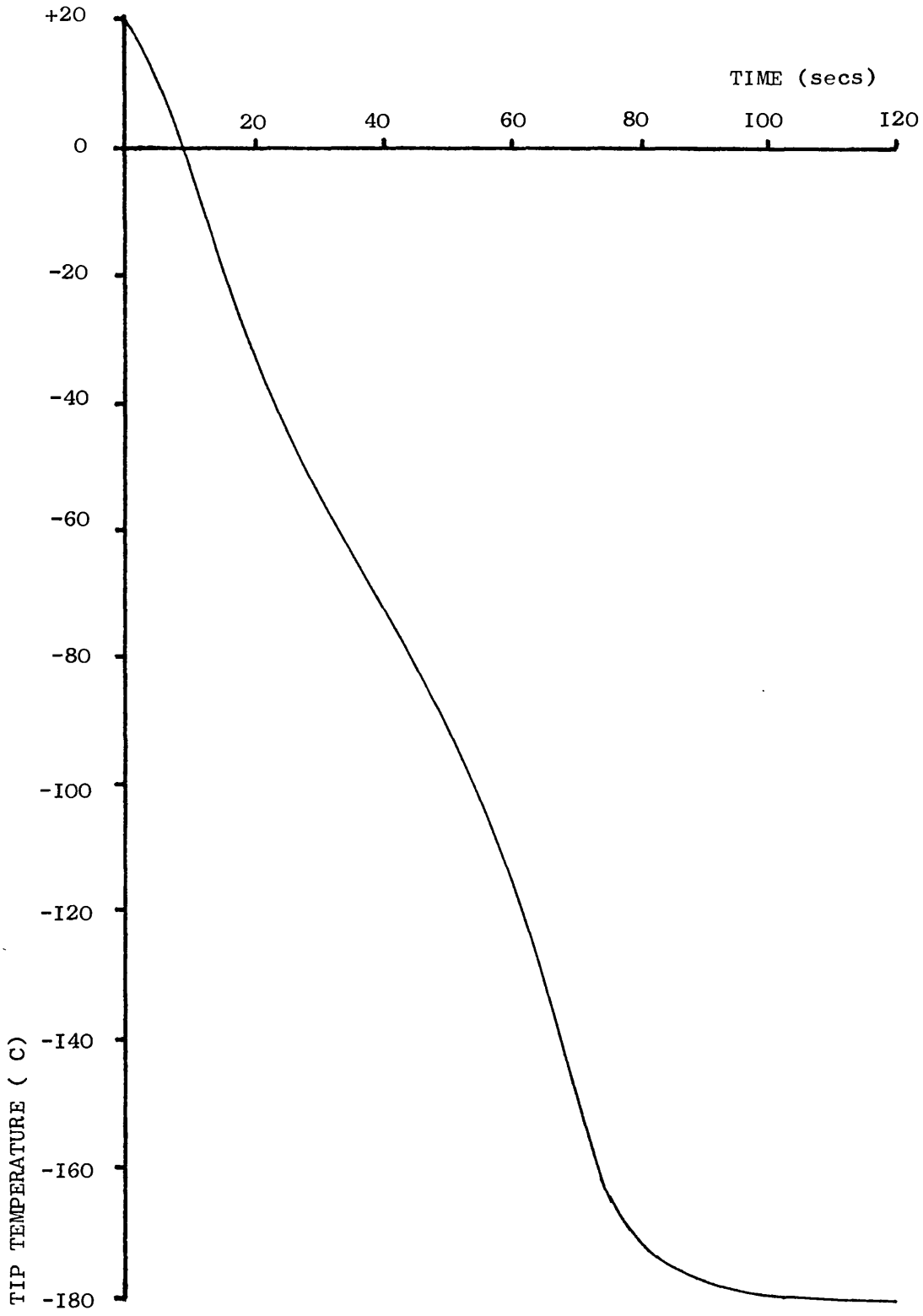

COOLING CURVE FOR COMPLETE SYSTEM (FREEZING GELATIN SOLUTION)

FIGURE 103

GROWTH OF ICE-BALL IN GELATIN USING COMPLETE CRYOPROBE SYSTEM

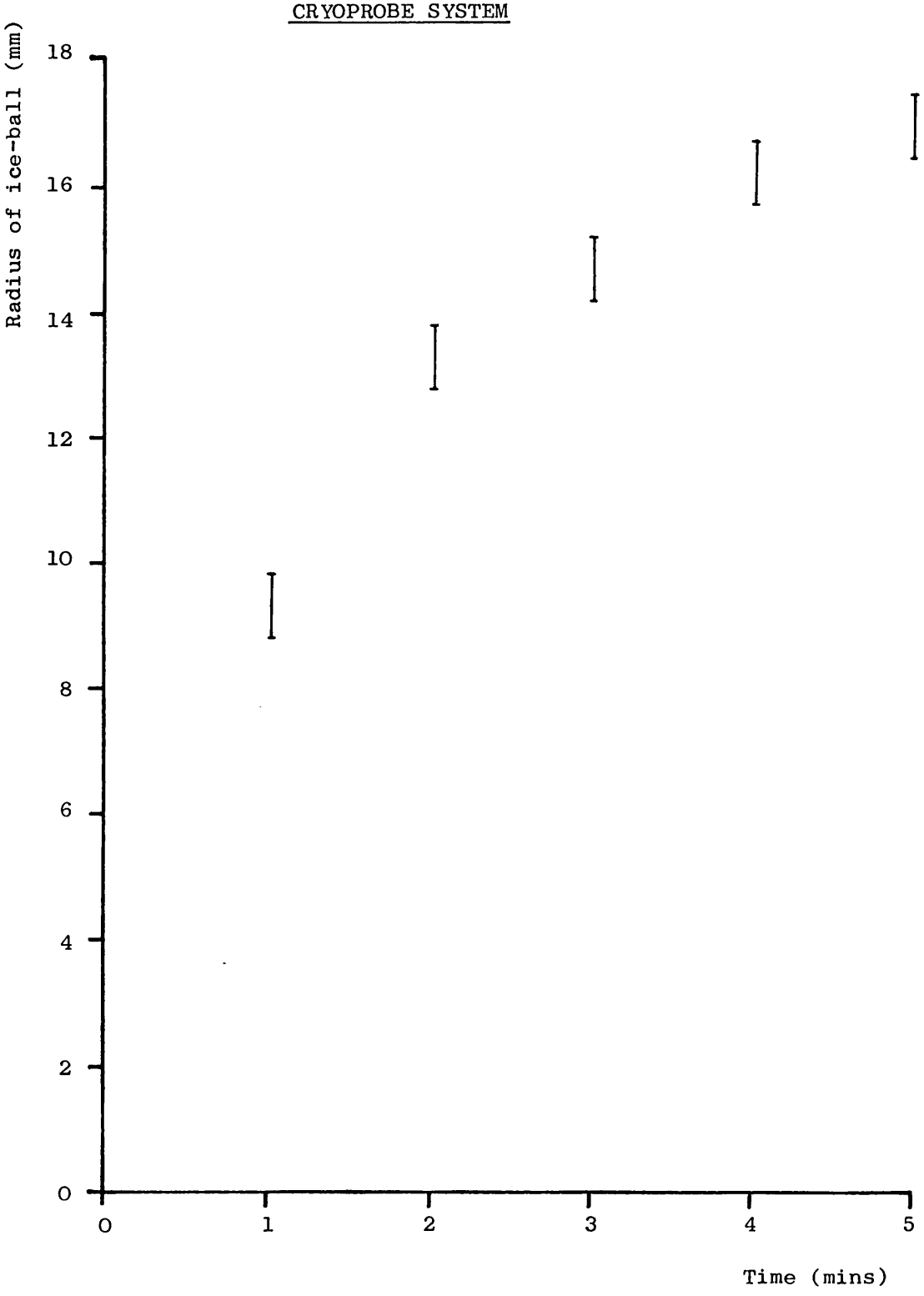

CHAPTER 14

CONCLUSIONS AND RECOMMENDATIONS

14.1 Introduction

At the end of each of the individual chapters of this thesis a conclusion is presented on the work that it contains. It is not intended to repeat these individual conclusions in this chapter but rather to reflect on the achievements and problems of the project and to recommend areas for further work and development.

14.2 Cryoprobe Performance and Cell Destruction

The early part of the project was concerned with deriving a thermodynamic performance specification for the freezing tip. The available models of ice-ball growth were quite adequate for this task. However, understanding of the process of cell destruction by freezing, both in vitro and in vivo, is still far from complete. Truly effective cryoprobe design will depend on further biological studies so that an optimum thermal environment for cell death can be defined. Relating that environment to cryoprobe performance, through the medium of ice-ball models, can then be done in confidence. It may well be the case that if the mechanism of cell death in vivo were fully understood, other additional procedures such as the local application of drugs could be defined to enhance the cryo-destructive process.

14.3 Analysis of Tip Thermodynamic Behaviour

The design of the freezing tip was a crucial aspect of the cooling system. Its analysis was carried out in two parts; the effect of nitrogen boiling behaviour on tip performance, and the effect of tip performance on ice-ball growth. A more comprehensive model that relates ice-ball growth to nitrogen boiling within the tip, would be extremely useful. The finite difference studies of **Chapter 7** could provide a good basis for such a model.

A start was made in **Chapter 7** to analyse tip cooling and the influence of tip materials on it. Much more work could be done in this area using finite difference techniques, especially by using heat transfer coefficients measured in experiments on cryoprobe tips . A more detailed understanding of the influence of the interface between a boiling cryogen and the object being cooled, would have useful application outside the limited field of cryoprobe design.

14.4 Liquid Nitrogen Transport

The nitrogen transfer system used in the cryoprobe and hose, also benefitted from studying the boiling behaviour of liquid nitrogen. The transfer pipes and hoses were very effective at providing quick and efficient transport of cryogen. The lack of a need for thermal insulation and the ability to produce simple flexible hoses using commonplace materials, were very attractive. However the technique of using electrical

heating in the hose with a distributed winding, would cause problems for commercially producing such hoses. Further work on means of hose heating would undoubtedly be useful.

14.5 Human Interface Design

When designing devices such as the cryoprobe the aspect that often causes difficulties is the human interface. An evolutionary design technique is discussed in this thesis which works very well when good feedback can be obtained during tests of prototypes. However, it was difficult to carry out comprehensive tests of the rectal viewer designs in this project. Because of this, further developments of the rectal probe are more probable in the area of the human interface rather than in the components of the cooling system.

There is no doubt that there is still much need for an effective design technique to cope with the problem of human interface design. Progress might well be made by applying CAD techniques to this aspect of design. So much of design relies on effective modelling (both mental and other- wise) and the potential that CAD provides for making modelling more realistic and for accommodating large numbers of complex variables, holds much promise for this awkward design area.

14.6 Further Development of System

It is felt that the rectal cryoprobe system is developed to a state where it can be evaluated in the operating theatre. The final performance tests carried out show that the original surgical requirements have been met. Inevitably during the evaluation, a number of areas which require further development will become apparent, but it is felt that these will be improvements of detail rather than fundamental changes.

14.7 Clinical Trials

The whole project has now reached the most interesting stage where clinical evaluation of the system is about to begin. The laboratory tests of the system indicate that the original clinical specification can be met but the device can only be properly evaluated in the operating theatre. The patient interface aspects of the design, the viewer and the overall configuration, have of course been thoroughly tested during their development. Many visits to the operating theatre have been made to assess the performance of these components and the final design worked very well. However the cryogenic aspects of the system have not yet been fully tested.

The author has previously developed surgical cryogenic devices and it is pertinent to present some procedures that will be used, based on this experience, during the rectal cryoprobes evaluation.

(1) It is absolutely essential that the engineer is present during the initial clinical evaluations of the probe. This requirement is not just to enable him to benefit from observing the systems behaviour, and thereby assessing the need for any further development, but also to ensure that there is no danger to the patient or clinical staff. The engineer is the person most able to see a dangerous situation developing and to know how to avert it quickly.

(2) When testing devices such as cryoprobes in the operating theatre it is important to have a record of the behaviour of the components of the system. To this end it is felt important to take a chart recorder into the operating theatre and record the time course of as many variables as possible.The rectal probe has been designed so that the tip temperature, hose exhaust temperature, probe shaft temperature, and the two heater power levels can all be monitored during its operation using a multichannel UV recorder.

(3) It is important to have a device evaluated by more than one surgeon. The rectal probe has mostly been developed in conjunction with one particular surgeon in Bath and he will carry out the initial evaluation. However arrangements were made at an early stage for the device to be tested elsewhere as well.

It is anticipated that the clinical evaluation of the instrument will take about 12 months. After that period it is hoped that the initial results can be

published and conclusions drawn about the instruments effectiveness.

14.8 Possible Areas for Future Work

The application of cryosurgery is of course strongly dependent on the kind of instruments available. It is hoped that the combination of viewing systems with cryoprobes will enable this useful technique to find application within body cavities. However other instruments are also made feasible by using controlled Leidenfrost flow. In **Chapter 3** it was concluded that a multi-tipped probe was the most suitable for freezing large tumours. Such a device could be constructed with small flexible hoses originating from a manifold and feeding each tip, thereby allowing their individual placement. A flexible cryoprobe for use with fibrescopes is also feasible. Flexible hoses only 4mm in diameter have been constructed. This size is approaching the diameter of the operating duct in fibrescopes. With a small freezing tip attached to the end of the flexible hose, the cryoprobe so formed would add a useful technique to the range available to the endoscopist.

A major drawback of cryosurgery is the lack of a monitoring technique that is both accurate and easy to use. It is felt that measuring the capacitance across the ice-mass, as discussed in **Chapter 3**, has potential as a clinical monitoring technique and is worthy of further study.

14.9 Concluding Remarks

The proof of any new development in biomedical engineering is its clinical usefulness. The rectal cryoprobe is only just starting its clinical evaluation and so its true potential can only be assumed at this stage. However its development has been soundly based and it is hoped that when the results of the clinical trials are published , it will be with the conclusion that the device provides an effective tool in the treatment of rectal cancer.

APPENDIX 1

DERIVATION OF MODEL OF ICE-BALL GROWTH

A.1.1 Introduction

This Appendix briefly outlines the derivation of the Equation 4 presented in Chapter 3, which provides a mathematical model of the rate of ice growth around a hemi-spherical cryoprobe tip. The derivataion is based on that published by Cooper and Trezek (1971b).

A.1.2 Starting point of Analysis

The derivation is started in Chapter 3 where the physical model and the assumptions used are described. Chapter 3 goes on to apply the basic partial differential equation of heat conduction in a solid to the frozen and unfrozen tissue. The two equations that result are expressed in radial co-ordinates as below:-

For the ice-ball

$$\frac{k_f}{r^2}\frac{\partial\left(r^2\frac{\partial T_f}{\partial r}\right)}{\partial r} = \rho c_f \frac{\partial T_f}{\partial t} \qquad (43)$$

For the unfrozen tissue

$$\frac{k}{r^2}\frac{\partial\left(r^2\frac{\partial T}{\partial r}\right)}{\partial r} + \dot{m}_b c_b (T_b - T) + \dot{q}'_m = \rho c \frac{\partial T}{\partial t} \qquad (44)$$

The boundary conditions are:-

$$T_f = T_t \quad \text{at} \quad r = r_t$$

$$T_f = T_o = T \quad \text{at} \quad r = r_o$$

$$k\frac{\partial T_f}{\partial r} = k\frac{\partial T}{\partial r} + \rho L\frac{\partial r_o}{\partial t} \quad \text{at} \quad r = r_o$$

$$T \longrightarrow T_b \quad \text{as} \quad r \longrightarrow \infty$$

A.1.2 Use of non-dimensional parameters

In Cooper and Trezeks analysis Equations 43 and 44 are re-expressed in non-dimensional form.

For the ice-ball

$$\frac{1}{R^2}\frac{\partial\left(R^2\frac{\partial\theta_f}{\partial R}\right)}{\partial R} = \frac{k c_f(T_\infty - T_o)}{k_f L}\frac{\partial\theta_f}{\partial\tau} \qquad (45)$$

For the unfrozen tissue

$$\frac{1}{R^2}\frac{\partial\left(R^2\frac{\partial\theta}{\partial R}\right)}{\partial R} - \beta\theta = \frac{c(T_\infty - T_o)}{L}\frac{\partial\theta}{\partial\tau} \qquad (46)$$

The non-dimensional groups used are as follows:-

$$\theta_f = \frac{T_f - T_\infty}{T_t - T_\infty} \qquad \theta = \frac{T - T_\infty}{T_t - T_\infty}$$

$$R = \frac{r}{r_t} \qquad R_o = \frac{r_o}{r_t}$$

$$\beta = \frac{\dot{m}_b c_b r_t^2}{k} \qquad \tau = \frac{k(T_\infty - T_o)t}{\rho L r_t^2}$$

The boundary conditions in non-dimensional form become:-

$$\theta_f = 1 \quad \text{at} \quad R = 1 \qquad (47)$$

$$\theta_f = \theta_o = 0 \quad \text{at} \quad R = R_o \qquad (48)$$

$$\frac{k_f}{k}\frac{\partial\theta_f}{\partial R} = \frac{\partial\theta}{\partial R} - \theta_o\frac{\partial R_o}{\partial\tau} \quad \text{at} \quad R = R_o \qquad (49)$$

$$\theta \longrightarrow 0 \quad \text{as} \quad R \longrightarrow \infty \qquad (50)$$

where $\theta_o = \frac{T_o - T_\infty}{T_t - T_\infty}$

A.1.4 Assumptions made to Solve Differential Equations

General solutions to Equations 46 and 47 which satisfy the boundary conditions are not known. However approximate solutions can be obtained if the heat capacity effects in both phases are assumed to be small compared to the latent heat effects.

ie. $$\frac{kc_f(T_\infty - T_o)}{k_f L} = 0$$

and $$\frac{c(T_\infty - T_o)}{L} = 0$$

Using these assumptions and the boundary conditions of Equations 47,48 and 50, quasi-static solutions to Equations 45 and 46 can be obtained.

$$\theta_f = 1 - \theta_o\left(\frac{T_o - T_f}{T_o - T_\infty}\right)\left(\frac{R_o}{R_o - 1}\right)\left(\frac{1 - R}{R}\right) \quad (51)$$

$$\theta = \theta_o \frac{R}{R} e^{-\sqrt{\beta}(R - R_o)} \quad (52)$$

Equations 51 and 52 express the non-dimensional temperature as a function of non-dimensional radius for both the ice-ball and the unfrozen tissue. These non-dimensional temperature profiles (Equations 51 and 52 are transient in nature because of the time dependance of R_o.

A.1.5 Combination of Temperature Profiles to Provide an Expression for Rate of Ice-growth

Equations 52 and 53 can be substituted into the

interface heat flux boundary condition (**Equation** 49) and differentiated.

$$\frac{\partial R_o}{\partial \tau} + \left(\frac{1 + \sqrt{\beta R_o}}{R_o}\right) + \frac{\theta}{R_o(1 - R_o)} = 0 \qquad (53)$$

Equation 53 can be evaluated to provide the following expression relating the ice-ball radius as a function of time,

$$\tau = \frac{1}{2a^2} \ln\left[\frac{(aR_o^2 + (1 - a)R_o + c)}{(1 + c)}\right] \qquad (54)$$

$$+ \frac{(1 - a(1 + 2c))}{2a^2 b} \ln\left[\frac{(a(2R_o - 1) + b + 1)(a - b + 1)}{(a(2R_o - 1) - b + 1)(a + b + 1)}\right] - \left(\frac{R_o - 1}{a}\right)$$

where $a = \sqrt{\beta}$ $\qquad b = \sqrt{(1 - a)^2 - 4ac}$

$$c = k_f\left(\frac{T_o - T_f}{T_\infty - T_o}\right) - 1$$

Equation 54 is used in **Chapter 3** to explore the effect of the cryoprobe variables on ice-ball growth.

APPENDIX 2

VACUUM INSULATION OF CRYOPROBE

A.2.1 Introduction

The original course followed to find a technique that would provide adequate thermal insulation around the cryoprobe shaft, was to investigate the use of vacuum insulation. This approach was eventually superceded by the use of heated transfer pipes but this Appendix briefly summarises the work completed on a vacuum insulated probe.

A.2.2 The Principle of Vacuum Insulation

Figure 104 shows a plot of the heat flux across a gas filled gap as a function of the gas pressure. As the pressure of the gas separating two surfaces is reduced, the conductive heat transfer remains constant until the pressure reaches about 10^{-1} torr. The heat transfer then drops to very low levels as the pressure is further reduced to around 10^{-3} torr. At these pressures the heat transfer is independent of the separation of the surfaces as long as they are further apart than the mean free path of the gas molecules.

A.2.3 The Effect of Powder Fillers on the Heat Transfer

The dramatic reduction in thermal conductivity as the pressure is reduced, occurs at higher pressures if

FIGURE 104

EFFECT OF PRESSURE ON HEAT TRANSFERRED ACROSS AIR GAP

(Data from Probert and Hub, 1968)

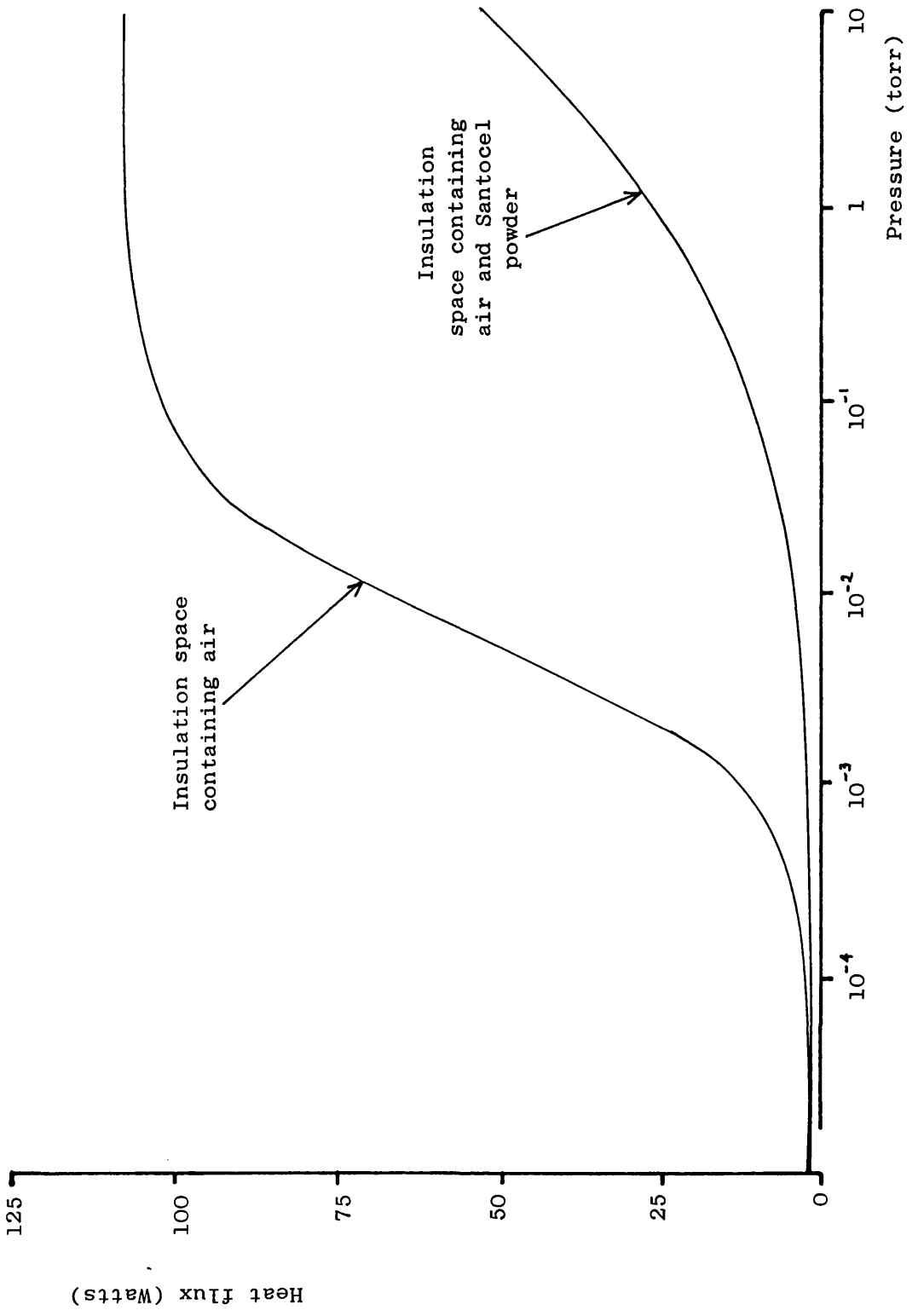

the gap separating the two surfaces is filled with a powder. **Figure 104** also illustrates the effect of including a powder in the gap. The powder illustrated is one typically used for this purpose, Santocel.

At reduced pressures most of the heat transferred is through radiation and this can be reduced by using a multiple layer of thermally insulated screens of low emissivity in the evacuated gap. Alternatively, fine aluminium powder can be mixed with the Santocel.

A.2.4 Tests to Measure Thermal Conductivity

It was planned to make use of these phenomena to insulate the cryoprobe shaft and handle. The available space was small and the evacuated gap not much larger than the mean free path length. It was decided to measure the heat transferred across gaps typical of those likely to be used in the probe and to assess the effect of using Santocel/Aluminium fillers. It was suspected that as the gap volume was small, the pressure would be strongly affected by outgassing of the materials exposed to the vacuum. Therefore it was also planned to measure the effect of increasing pressures on the conductivity.

The test rig shown in **Figure 105** was designed and constructed and the necessary pump and pressure monitoring equipment obtained. The thin radial gap could be altered by using different cylindrical inserts. The whole rig was immersed in a liquid nitrogen bath

FIGURE 105

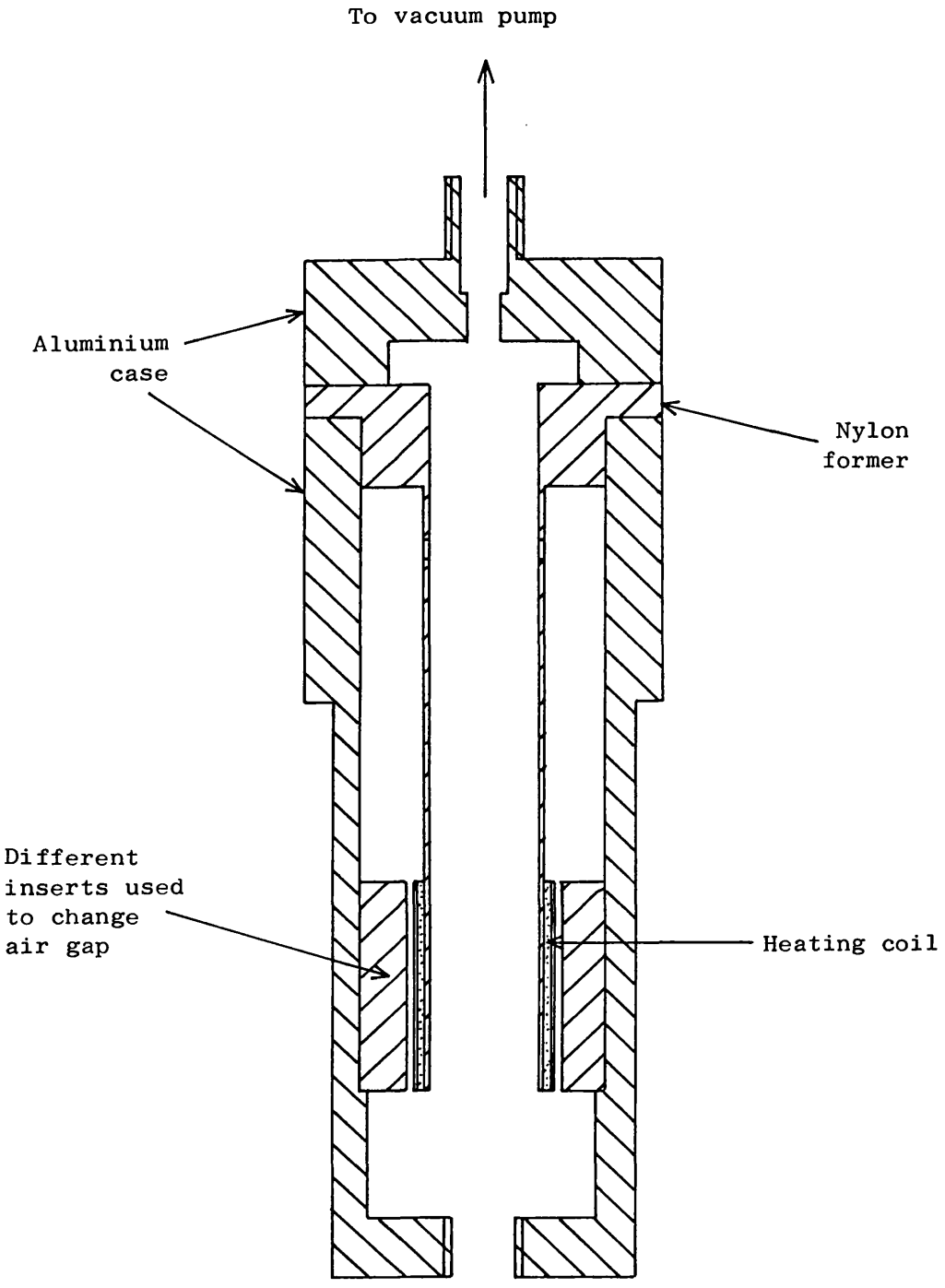

TEST RIG TO MEASURE EFFECTIVE THERMAL CONDUCTIVITY ACROSS SMALL AIR GAPS

and the temperatures either side of the gap monitored for different power dissipation from the heater.

From Fouriers equation:

$$\dot{Q} = \frac{-2\pi k l (T_2 - T_1)}{\ln\left(\frac{r_2}{r_1}\right)}$$

where $\dot{Q}$ = power dissipated by heater (watts)

k = effective thermal conductivity of gap

l = length of heated cylinder

T_2 = temperature of heated side of gap

T_1 = temperature of cooled side of gap

The thermal conductivity could be calculated from the gradient of a plot of ($\dot{Q} \times \ln\left(\frac{r_2}{r_1}\right)$) against $2\pi k l (T_2 - T_1)$.

APPENDIX 3

ONE-DIMENSIONAL FINITE DIFFERENCE EQUATIONS FOR TRANSIENT COOLING WITH VARIOUS BOUNDARY CONDITIONS

A.3.0 Introduction

This Appendix shows the derivation of the one-dimensional finite difference equations used in Chapter 7. The equations needed to deal with the various boundary conditions are included.

A.3.1 Finite difference approximations of partial derivatives

The numerical solution of the one-dimensional un-steady heat transfer through an infinite sheet of material uses finite difference approximations of the partial derivatives of the Fourier equation in one-dimension

$$\frac{\partial T}{\partial t} = \propto \frac{\partial^2 T}{\partial x^2}$$

The finite difference approximations can be derived from the Taylor series expansion of the function, T(t) about the point, t, and T(X) about point, X

Consider the function T(t)

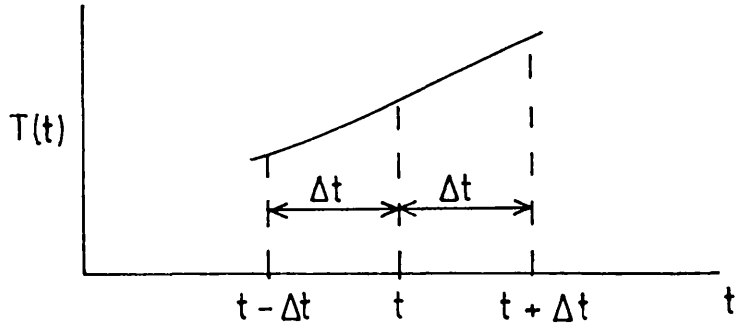

The Taylor series expansion gives

$$T(t+\Delta t) = T(t) + \Delta t\frac{dT}{dt} + \frac{(\Delta t)^2}{2!}\frac{d^2T}{dt^2} + \frac{(\Delta t)^3}{3!}\frac{d^3T}{dt^3} + \text{etc} \quad (55)$$

$$T(t-\Delta t) = T(t) - \Delta t\frac{dT}{dt} + \frac{(\Delta t)^2}{2!}\frac{d^2T}{dt^2} - \frac{(\Delta t)^3}{3!}\frac{d^3T}{dt^3} + \text{etc} \quad (56)$$

The forward difference approximation can be obtained from equation 55 to give

$$\frac{dT}{dt} = \frac{T(t+\Delta t) - T(t)}{\Delta t} \quad (57)$$

The second derivative of T(t) can be obtained by adding the expansions of equations 55 and 56 to give:-

$$\frac{d^2T}{dt^2} = \frac{T(t-\Delta t) + T(t+\Delta t) - 2T(t)}{(\Delta t)^2} \quad (58)$$

Similarly the function T(X) can be expanded about the point, X, to obtain the approximations

$$\frac{dT}{dx} = \frac{T(x+\Delta x) - T(x)}{\Delta x} \quad (59)$$

$$\frac{d^2T}{dx^2} = \frac{T(x-\Delta x) + T(x+\Delta x) - 2T(x)}{(\Delta x)^2} \quad (60)$$

A.3.3 Finite difference approximation of Fouriers equation in 1-D

Substituting the approximations given in equations 57 and 60 into the one- dimensional Fourier equation

$$\frac{T(t+\Delta t) - T(t)}{\Delta t} = \alpha\left(\frac{T(x-\Delta x) + T(x+\Delta x) - 2T(x)}{(\Delta x)^2}\right) \quad (61)$$

Let the temperature at any given point, X, and any given time, t, = T_i^n

Then the temperature at X after time $(t+\Delta t)$ = T_i^{n+1}

and the temperature at $(X+\Delta X)$ after time t = T_{i+1}^n

Equation 61 then becomes:-

$$\frac{T_i^{n+1} - T_i^n}{\Delta t} = \propto \frac{T_{i-1}^n + T_{i+1}^n - 2T_i^n}{(\Delta x)^2} \qquad (62)$$

$$\therefore T_i^{n+1} = Fo(T_{i-1}^n + T_{i+1}^n - 2T_i^n) + T_i^n \qquad (63)$$

where Fo = Fourier No. = $\propto \frac{\Delta t}{(\Delta x)^2}$

This equation enables the temperature at any point, i to be calculated at time n+1

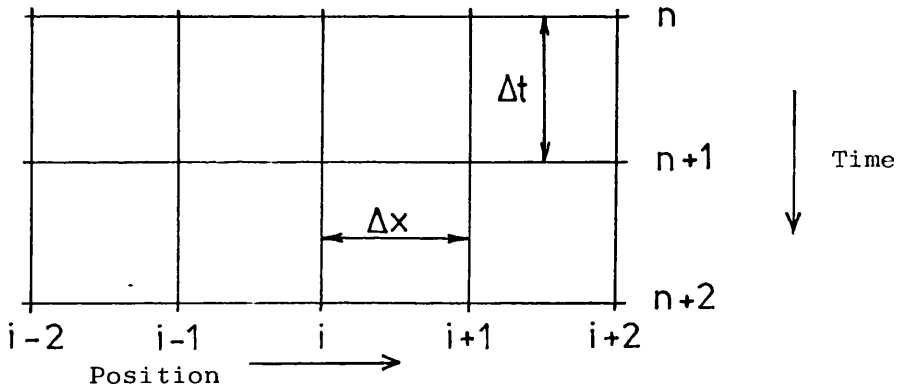

As long as the temperature distribution is known for $t = 0$ then at each time interval Δt later, the new temperature distriubtion can be estimated.

A.3.4 Stability

As the finite difference equation is applied at each time interval, the results for T_i^{n+1} will become unstable if the time interval, Δt is large compared to the space interval, Δx. It can be shown (e.g Richtmyer 1957) that the stability criterion for equation 63 is:-

$$Fo \leqslant 0{\cdot}5$$

For each finite difference equation derived there will always be a stability criterion that has to be satisfied.

A.3.5 Finite difference equation for the temperature at a boundary undergoing convective heat transfer

Equation 63 applies to the inner points in the material. When the point, i, being examined is at a boundary, the boundary heat transfer conditions have to be accomodated. If the boundary is being subjected to convective heat transfer (e.g. when exposed to boiling nitrogen) then a further finite difference equation is needed for the boundary temperature.

Consider such a boundary.

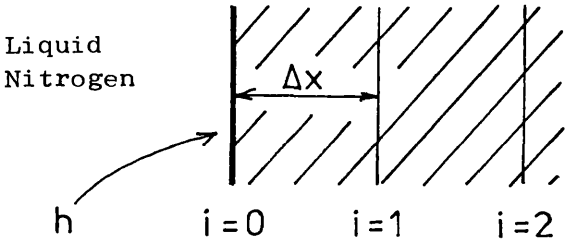

The partial differential equation describing the unsteady heat transfer at this boundary is:-

$$\rho c \frac{\Delta x}{2} \frac{\partial T}{\partial t} = k \frac{\partial T}{\partial x} + h(T_N - T_o) \qquad (64)$$

where T_N is temperature of boiling nitrogen

Substituting equations 57 and 59 into 64

$$\rho c \frac{\Delta x}{2} \left[\frac{T(t + \Delta t) - T(t)}{\Delta t} \right] = k \left[\frac{T(x + \Delta x) - T(x)}{\Delta x} \right] + h(T_N - T_o)$$

$$\rho c \frac{\Delta x}{2} \left[\frac{T_o^{n+1} - T_o^n}{\Delta t} \right] = k \left[\frac{T_1^n - T_o^n}{\Delta x} \right] + h(T_N^n - T_o^n)$$

rearranging gives

$$T_o^{n+1} = 2Fo \left[T_1^n - (1 + Bi) T_o^n + Bi T_N^n \right] + T_o^n \qquad (65)$$

where Bi = Biot No. = $\frac{h \Delta x}{k}$

The stability criterion associated with equation 65 is

$$Fo \leqslant 0{\cdot}5(1 + Bi)$$

A.3.6 Finite difference equation for the junction of two materials

When heat is being conducted across the junction of two different materials, a further finite difference equation is needed for the junction temperature.

Consider the junction between materials A and B

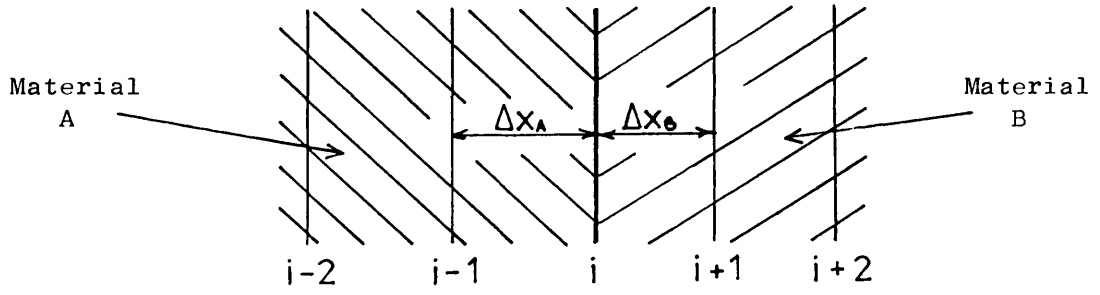

The difference equation that results is:-

$$T_i^{n+1} = \frac{2}{(1+\gamma)}\left[Fo_A \gamma T_{i-1}^n + Fo_B T_{i+1}^n - (Fo_A \gamma + Fo_B) T_i^n\right] + T_i^n \qquad (66)$$

where $$\gamma = \frac{(\Delta x \rho c)_A}{(\Delta x \rho c)_B}$$

$$Fo_A = \frac{\alpha_A \Delta t}{(\Delta x_A)^2} \qquad Fo_B = \frac{\alpha_B \Delta t}{(\Delta x_B)^2}$$

The stability criterion associated with equation 66 is:-

$$\frac{\gamma Fo_A + Fo_B}{(1+\gamma)} \leqslant 0{\cdot}5$$

APPENDIX 4

Computer Program used to Estimate Tip Cooling

This listing is of a typical program used to estimate tip cooling by means of finite difference equations.

```
>L.
   10  REM Plots plate outer temp
   20  REM and midline temp for
   30  REM infinite plate suddenly
   40  REM cooled by liquid nitrogen.
   50  ON ERROR GOTO 650
   60  CLS
   70  PROCintro
   80  FO=K*DT/(DX^2*P*C)
   90  IF FO>.5 THEN PRINT "UNSTABLE, FO>0.5, RE-ENTER VARIABLES":
GOTO 70:REM Checks stability criterion for inner points
  100  PROCinitialise
  110  REPEAT
  120    PROCincoefficient
  130    BI=H*DX/K
  140    IF FO>.5*(1+BI) THEN PRINT "UNSTABLE,FO>0.5*(1+BI),
RE-ENTER VARIABLES":GOTO 70:REM Checks stability criterion for
 boundary
  150    PROCtemps
  160    PROCresults
  170    D=D+DT
  180    FOR I%=0TOX%:T(I%)=TN(I%):NEXT
  190    UNTIL FALSE
  200  END
  210  DEF PROCintro
  220  REM Inputs values for variables
  230  PRINT "INPUT THERMAL CONDUCTIVITY, DENSITY AND  SPECIFIC
HEAT (SI UNITS)"
  240  INPUT K,P,C
  250  PRINT "INPUT PLATE THICKNESS (METERS)           NO. OF
SPACE INTERVALS (EVEN)"
  260  INPUT M,N%
  270  DX=M/N%
  280  X%=N%/2
  290  S = 0.5*DX^2*P*C/K
  300  PRINT "MAX. TIME INTERVAL FOR STABILITY IS ",S;" SECS"
  310  PRINT "WHAT TIME INTERVAL DO YOU WANT TO USE   FOR THE
CALCS (SECS)"
  320  INPUT DT
  330  PRINT "HOW OFTEN DO YOU WANT RESULTS PRINTED   (SECS)"
  340  INPUT L
  350  ENDPROC
  360  DEF PROCinitialise
  370  REM Sets up starting values for arrays,marker variables,etc
  380  DIM T(X%), TN(X%)
  390  FOR I%=0TOX%:T(I%)=20:NEXT
  400  D=DT:Z=0
  410  ENDPROC
```

```
  420  DEF PROCincoefficient
  430  REM Calculates value for internal heat transfer coefficient
  440  TF=T(0)+196
  450  IF TF<=0 THEN TF=.0001
  460  R=LN(TF)
  470  IF TF<8.166 THEN H=EXP(1.2095*R+6.56):ENDPROC
  480  IF TF<23.336 THEN H=EXP(-13.20904*R^5+163.2993*R^4-803.2488
*R^3+1963.628*R^2-2383.851*R+1158.086):ENDPROC
  490  IF TF<29.371 THEN H=EXP(-10*R+39.5):ENDPROC
  500  H=EXP(-0.2137*R+5.9223):ENDPROC
  510  DEF PROCtemps
  520  REM Uses finite difference equations to calculate
 temperature distribution at current time
  530  TN(0)=2*FO*(T(1)-(1+BI)*T(0)-BI*196)+T(0)
  540  IF TN(0)<-196 THEN TN(0)=-196
  550  FOR I%=1TO(X%-1):TN(I%)=FO*(T(I%+1)-2*T(I%)+T(I%-1))+T(I%):NEXT
  560  TN(X%)=2*FO*(T(X%-1)-T(X%))+T(X%)
  570  ENDPROC
  580  DEF PROCresults
  590  REM Prints results
  600  G=D-Z:IF G<L THEN ENDPROC
  610  @%=&20108
  620  PRINT D,TN(0),TN(X%)
  630  Z=Z+L
  640  ENDPROC
  650  IF ERR=17 THEN @%=10
  660  REPORT
>
```

REFERENCES

ABREU, O and KELLNER, K, 1974, Cryogenics, **19**:567-70.

AMOILS, S.P., 1967, Arch. Ophthalmol., **78**: 201-7.

AMOILS, S.P., 1968, Arch. Ophthalmol., **80**: 301-2.

ARNOTT, J., 1851 in The Treatment of Cancer by the Regulated Application of an Anaesthetic Temperature (London: J. Churchill).

ASAHINA, E., 1966 in Cryobiology, ed. H.T. Meryman (London: Academic Press) pp 451-86.

ASHWOOD-SMITH, M.J., 1965, Cryobiology, **2**: 39-43.

BARRON, R.F., 1966, Mach. Des., **38**: 184-9.

BARRON, R.F., 1968, J. Cryosurg., **1**: 316-25.

BARRON, R.F., 1971, in Cryogenics in Surgery, eds. H. Von Leden and W.G. Cahan (London: Lewis) pp 80-127.

BELLOWS, J.G., 1966, Am. J. Ophthalmol, **61**: 103.

BIETTI, G., 1935, Boll. d'Ocul, **94**: 349.

BORTHWICK, R., 1972, Vet. Rec., **90**: 446-8.

BOYARSKII, M.Y. and FILIPPOV, Y.P., 1978, Biomed. Eng. (N.Y.), **12**: 35-9.

BOYARSKII, M.Y. and FILIPPOV, Y.P., 1979, Cryobiology, **16**: 492-6.

BRADLEY, P.F., 1977, Acta. Therm., **2**: 83-9.

BRADLEY, P.F. and FISHER, A.D., 1975, Br. J. Oral Surg., **13**: 111-27.

CAHAN, W.G., 1971 in Cryogenics in Surgery, eds. H. Von Leden and W.G. Cahan (London: Lewis) pp 182-234.

COMINI, G. and DEL GUIDICE, S., 1976, J. Heat Transfer, 98: 543-9.

COOPER, I.S., 1964, Cryobiology, 1: 44-5.

COOPER, I.S., GRISSMAN, F. and JOHNSTON, R., 1962, St. Barnabus Hosp. Med. Bull. 1, 11.

COOPER, I.S., and LEE, A.S., 1961, J. Nerv. and Mental Disorders, 133-259.

COOPER, T.E. and GROFF, J.P., 1973, J. Heat Transfer, 95: 250-6.

COOPER, T.E. and PETROVIC, W.K., 1974, J. Heat Transfer, 96: 415-20.

COOPER, T.E. and TREZEK, G.J., 1970, Cryobiology, 7: 79-93.

COOPER, T.E. and TREZEK, G.J., 1971a in Cryogenics in Surgery, eds. H. Von Leden and W.G. Cahan (London: Lewis) pp 128-49.

COOPER, T.E. and TREZEK, G.J., 1971b Cryobiology, 7: 183-90.

CRAVALHO, E.G., 1971, Cryobiology, 8: 396.

CRUMP, R.E., 1967, Int. Ophthalmol. Clinics, 7: 309-23.

EICHLER, J. and LENZ, H., 1976, Cryobiology, 13: 185-90.

FARRANT, J., 1971 in Cryogenics in Surgery, eds. H. Von Leden and W.G. Cahan (London: Lewis) pp 15-41.

FARRANT, J., 1972 in Proc. Int. Congr. on Cryosurgery, pp 23-32.

FERRO, V. and FILIPPI, M., 1978, La Thermotecnica, 32: 487-90.

FRASER, J., 1979, Cryogenics, 19: 375-81.

FRASER, J. and GILL, W., 1967, Br. J. Surg., 54: 770-6.

FROST, W., 1975 in Heat Transfer at Low Temperatures (London: Plenum),pp 92-94

GAGE, A.A., 1979, Cryobiology, 16: 56-62.

GAGE, A.A. and CARUANA, J.A., 1980, Cryobiology, 17: 154-60.

GILL, W., da COSTA, J. and BEAZLES, R., 1970, Am. Surg., 38: 437-45.

GORLINA, A.A., ZINOVEV, U.S., POSEVIN, D.F. and NIKOLSKII, V.F., 1976, Biomed. Eng. (N.Y.), 10: 170-3.

GYE, W.E., BEGG, A.M., MANN, I. and CRAIGIE, J., 1949, Br. J. Cancer, 3: 259-67.

HARLY, S. and AASTRUP, J.E., 1972, Proc. Int. Congr. on Cryosurgery, pp 135-41.

HARLY, S., AASTRUP, J.E. and ELBROND, O., 1977 Cryobiology, 14: 609-13.

HOBBS, K.E.F., 1980 in Physical Techniques in Medecine Vol. 2, ed. J.T. McMullen (New York : Wiley) pp 97-131.

HRYCAK, P., LEVY, M.J. and WILCHINS, S.J., 1975, ASME Paper, 75-WA/Bio.-11 pp 1-5.

KOMAROV, B.A., 1974, Biomed. Eng. (N.Y.), 9: 362-5.

LANE, G.A., 1980, Science (N.Y.), 210: 899-901.

LEIBO, S.P., FARRANT, J., MAZUR, P., HANNA, M.G., and SMITH, L.H., 1970, Cryobiology, 6: 315-32.

LENTZ, C.P., 1961, Food Technol., 15: 243-7.

LENZ, H. and EICHLER, J., 1976, Cryobiology, 13: 37-46.

LOVELOCK, J.E., 1953, Biochem. Biophys. Acta, 10: 414-26.

LYMBERPOULOS, S., 1972 in Proc.Int.Congr.on Cryosurgery (Vienna:WMA) ppl51-5

MAZUR, P., 1963, J. Gen. Physiol., 47: 347-69.

MAZUR, P., 1968 in Cryosurgery, eds. R.W. Rand, A.P. Rinfret and H. Von Leden (Springfield: Thomas) pp 32-51.

MAZUR, P., FARRANT, J., LEIBO, S.P., and CHU, E.H.Y., 1969, Cryobiology, 6: 1-9.

MAZUR, P., LEIBO, S.P., FARRANT, J., CHU, E.H.Y., HANNA, M.G. Jr., and SMITH, L.H., 1970 in The Frozen Cell, eds. G.E.W. Wolstenholme and M. O'Connors (Ciba Symposium), (London: Churchill), pp 69-88.

MOLNAR, S., FLACHENECKER, G. and LANGE, K.P., 1969, Urol. Int., 24: 177-87.

MURINETS-MARKEVICH, B.N., NIKITIN, V.A., and NOSOV, M.E., 1975, Biomed. Eng. (N.Y.), 10: 154-5.

NAJJAR, T.A., WILCHINS, S., LEVY, M., HRYCAK, P., and NEWARK, N.J., 1979, Oral Surg., 47: 114-9.

OPENCHOWSKI, S., 1883, Compt. Rend. Soc. Biol., 5: 38.

ORPWOOD, R.D., 1977, presented at Inaugral Scien. Meet. of Oxford Orthopaedic Eng. Centre.

ORPWOOD, R.D., 1980 in Fibre Optics and Endoscopy, CRS 31, (London: HPA), pp 46-51.

ORPWOOD, R.D., 1981, Phys. Med. Biol., 26: 555-575.

ORPWOOD, R.D., 1983, Science, Care and Practice, 3: 24-26.

ORPWOOD, R.D., 1984, Proc. Design Research Soc. Meet., Bath.

ORPWOOD, R.D. and LILLICRAP, S.C., 1979, Abstracts HPA Ann. Conf. (Bristol).

OSBORNE, D.R., HIGGINS, A.F. and HOBBS, K.E.F., 1978, Br. J. Surg., 65: 859-61.

PERL, W., 1962, J. Theor. Biol., 2: 201-35.

PERL, W. and HIRSCH, R.L., 1966 in J. Theor. Biol., 10: 251-80.

PETROVIC, W.K., 1972, MSc Thesis, Naval Postgraduate School, Monterey, California.

Le PIVERT, P. and BINDER, P., 1975a, C.R. Acad. Sci. Paris, 281: 1191-4.

Le PIVERT, P., BINDER, P. and OUGIER, T., 1975b, Proc. 28th ALEMB, 307.

Le PIVERT, P., BINDER, P. and OUGIER, T., 1977, Cryobiology, 14: 245-50.

Le PIVERT, P., NICOLLET, B., CUILLERET, J., DUVERNE, J., MAZAURIC, F.X. and MAUGERY, J., 1976, Nouv. Presse Med., 5: 1259-60.

REUTER, H.J., 1971 in Cryogenics in Surgery, eds. H. Von Leden and W.G. Cahan (London: Lewis) pp 411-70.

ROTHENBORG, H.W., 1975, Cryogenics, 15: 4-7.

ROWBOTHAM, G.F., HAIGH, A.L. and LESLIE, W.G., 1959, Lancet, 1, 12

RUBINSKY, B. and SHITZER, A., 1976, J. Heat Transfer, 98: 514-9.

RUDNYA, P.G. and TARLYCHEVA,L.S., 1976, Biomed. Eng. (N.Y.), 10: 162-3.

SHALIMOV, A.A., SUKHAREV, I.I., KEISEVICH, L.V., YAGODIN, U.M., OSTAPENKO, I.V., NAUMENKO, I.P., NIKOLSKII, V.A., TOPIKIN, V.G. and MASAEV, A.S., 1976, Biomed. Eng. (N.Y.), 10: 158-60.

SMITH, J.J. and FRASER, J., 1974, Cryobiology, 11: 139-47.

SMITH, J.J., FRASER, J., and MACIVER, A.G., 1978, Cryobiology, 15: 426-32.

TORRE, D., 1979, Abstracts Ann. Meet. Am. Coll. Cryosurgery (Buffalo).

TREZEK, G.J. and JEWETT, D.L., 1970, IEEE Trans. Biomed. Eng., BME-17: 281-6.

VERKIN, B.I., MEDVEDEV, E.M., MURINETS-MARKEVICH, B.N., NOSOV, M.E., BEREZUTSKAYA, V.E. and LYSENKO, L.I., 1976b, Biomed.Eng. (N.Y), 10, 174-6

VERKIN, B.I., SIPITYI, V.I., MURINETS-MARKEVICH, B.N., ZANOSHNIKOV, V.N. and KRASNIKOV, A.R., 1977, Biomed.Eng.(N.Y), 11, 28-9

VERKIN, B.I., ZADOROZHNYI, B.A., MEDVEDEV, E.M., GEN, S.P., MURINETS-MARKEVICH, B.N., KUTASEVICH, Y.F., UTEMOV, T.V. and KRASNIKOV, A.R., 1976a, Biomed.Eng.(N.Y), 10, 176-7

WALDER, H.A.D., 1972 in Proc. Int. Congr. on Cryosurgery, pp 33-9.

WARREN, R.P., BINGHAM, P.E. and CARPENTER, J.D., 1974, ASME Paper, 74-WA/Bio-6, pp 1-9.

WHITE, A.C., 1899, Med. Rec, 56: 109.

WHITTACKER, D.K., 1975a, J. Pathol., 115: 131-9.

WHITTACKER, D.K., 1975b, J. Pathol., 115: 139-43.

WILD, D.E., 1975 in Practical Cryosurgery, ed. H.B. Holden (London: Pitman), pp 10-34.

WRIGHT, B.M., 1971, Lancet, 1: 951-2.

ZUBASHICH, V.F., REMENYAK, V.P., KHRIPUNOV, V.M., MALINKO, A.N. and KORNIENKO, V.P., 1976, Biomed. Eng. (N.Y.), 10: 168-70.